EXTENDING THE ABOVE- AND BELOWGROUND BARLEY PHENOTYPE

by

Erik Zachary Killian

A dissertation submitted in partial fulfillment
of the requirements for the degree

of

Doctor of Philosophy

in

Plant Science

MONTANA STATE UNIVERSITY
Bozeman, Montana

May 2025

©COPYRIGHT

by

Erik Zachary Killian

2025

All Rights Reserved

TABLE OF CONTENTS

TABLE OF CONTENTS CONTINUED

TABLE OF CONTENTS CONTINUED

LIST OF TABLES

Table Page

LIST OF FIGURES

Figure Page

LIST OF FIGURES CONTINUED

Figure Page

LIST OF FIGURES CONTINUED

Figure Page

LIST OF FIGURES CONTINUED

Figure Page

LIST OF FIGURES CONTINUED

Figure Page

ABSTRACT

Plant breeding is crucial for agricultural productivity by improving crop performance and resilience to deficient growing conditions. Soil microorganisms, particularly those in the rhizosphere, play a pivotal role in nutrient cycling, pathogen suppression, and overall plant performance. The composition and dynamics of these microbial communities are influenced by both plant genotype and environmental factors including soil chemistry, climate, and water availability. While plant-associated microbiomes vary across environments, the contribution of environment and plant genetics in microbiome recruitment, particularly across geographic regions, is not well understood. This research encompasses a large-scale, multi-location, and multi-year study across seven field trials to assess plant performance and microbial community composition in the barley rhizosphere. A core focus is understanding how plant genotypes and environmental factors such as soil chemistry and growing location influence microbial assembly. Results indicated that rhizosphere microbial communities are shaped by both plant genetics and environmental conditions, with distinct bacterial and fungal community patterns emerging in different environments. Specifically, while bacterial diversity remained largely consistent across barley-growing regions, fungal communities exhibited greater variability and were more strongly influenced by location-year and climatic factors. A Genome-wide association study (GWAS) identified many quantitative trait loci (QTL) associated with microbial traits, with some loci co-localizing with agronomic traits. This suggests potential genetic mechanisms underlying the interaction between plants and their microbiomes. These findings highlight the potential for genetic selection to optimize rhizosphere microbiomes, potentially improving crop productivity and resilience in variable environments. In addition to field studies, this dissertation introduces a novel, open-source workflow for the analysis of unoccupied aerial system (UAS) imagery in agriculture. This workflow uses a semi-automated approach for plant classification, plot delineation, spectral index calculation, and data extraction using QGIS software. By testing the workflow on barley UAS data collected over multiple flights, we show that spectral indices such as the Visible Atmospheric Resistant Index (VARI) correlate strongly with ground truth data, demonstrating the workflow's efficacy in agricultural monitoring. These studies provide a comprehensive survey of barley microbial community composition, offering valuable insights into improving agricultural sustainability through plant-microbe optimization and precision agriculture.

INTRODUCTION

In the last century, population growth and changing climate have highlighted the need for efficient and robust cropping systems to provide food security in the future. Plant breeding is important for crop performance and maintaining yield under variable environmental conditions. Using artificial selection and hybridization, humans have been breeding crops for increased efficiency and yield for thousands of years (Murphy, 2007). In recent decades, significant progress has been made in breeding for improved performance with an average 1% yield gain per year since 1963 in both rice and wheat, and 1.5% average increase in maize (Fischer, 2015). However, the rate of yield improvement for major crops will not meet future demand, even with advancements in breeding technologies (Cassman & Grassini, 2020; Ray et al., 2013). As a result, novel approaches are needed to alter factors influencing plant fitness, such as the soil microbiome, and refine existing technologies, like unoccupied aerial system crop monitoring, to optimize breeding programs and enhance yields. Current breeding approaches select traits for broad adaptation where plants perform well in many environments (Chapman et al., 2012). This could have negative effects on the maximum yield potential for many crops, as it ignores environmental variability. Extended plant phenotypes should be further studied to understand how effective broad adaptation or location-specific breeding approaches can be (Snowdon et al., 2021). Here, we review previous research on mechanisms and benefits of plant microbe interactions before briefly examining the need for novel remote sensing approaches to analyze plant imagery.

Soil microbes affect plant performance

The soil microbiome is critical to plant fitness, influencing survival and productivity. Microorganisms living in the soil support plant health in numerous ways, including mitigating abiotic stressors such as drought (Castrillo et al., 2017; Mayak et al., 2004; Poudel et al., 2021; J. Zhang et al., 2023), improving nutrient acquisition (Pii et al., 2015; Rosenblueth et al., 2018), and providing protection against pathogens (Mendes et al., 2011). Through plant breeding, plant-microbe interactions can be optimized to develop a beneficial rhizosphere microbiome capable of increasing plant performance and environmental robustness (Clouse & Wagner, 2021; Eduardo Contreras-Liza, 2021; Gopal & Gupta, 2016). Below, we explore the mechanisms and applications of these interactions, emphasizing their interdependence with environmental conditions.

Plants require at least 16 essential minerals to develop successfully, a vast majority of which are only available to uptake from the soil (Pandey, 2018). The abundance and availability of these nutrients vary by abiotic factors, including soil chemical and structural properties (Anderson, 1988), as well as biotic factors, including microbes, which can alter the concentration of nutrients available for plant root uptake (Miransari, 2013). Soil microbes mediate nitrogen (N) cycling, which benefits plants through direct and indirect interactions. Plants in the legume family (Fabaceae) have evolved to form a symbiosis with the bacterial genus *Rhizobium*, capable of converting atmospheric nitrogen (N_2) into plant available ammonia (NH_3). *Rhizobium* directly interact in the root endosphere, exchanging flavonoids from the plant host to induce N-fixation in the symbiotic bacteria (Yang et al., 2022). This mutualistic relationship with the belowground community allows legumes to tolerate N-deficient soils (Dong & Song, 2020; Masson-Boivin &

Sachs, 2018). It also has made legumes a staple crop that naturally fixes soil N, providing an alternative to N fertilizers (Garg & Geetanjali, 2009; Iannetta et al., 2016; Masson-Boivin & Sachs, 2018).

Phosphorus (P) is another essential macronutrient responsible for plant development. Availability of P can be limiting in semi-arid environments due to its low mobility in the soil relative to other macronutrients (Hedley & McLaughlin, 2015). A large pool of phosphate is bound to other minerals, making it unavailable to plants (Boitt et al., 2018). Acidification of the soil environment works to solubilize inorganic phosphates by destabilizing the bond between negatively charged phosphate and positively charged metal ions including iron, aluminum, and calcium (Yadav et al., 2020). Both plants and microbes participate in acidification. Certain plants such as *Lupinus* sp. produce and secrete organic acids including citrate and malate through the roots to lower soil pH in the rhizosphere, increasing phosphate solubility and consequently plant uptake (Braum & Helmke, 1995). Species of *Brassica napus* solubilize P bound by iron and aluminum through root exudation (Zhang et al., 2011). The ability to solubilize plant-available phosphate is extended by a variety of soil bacteria and fungi – known as phosphate-solubilizing microorganisms (PSM) – capable of converting insoluble P into plant-available forms (Rawat et al., 2021). PSMs create soluble, plant available phosphates through various methods to acidify their immediate soil environment. Parallel to plant roots, some PSM exude organic acids such as citric acid to solubilize bound P (Kishore et al., 2015). Acidification also occurs through cellular respiration in some microbes when proton-rich N sources like ammonium (NH_4^+) are reduced to ammonia (NH_3), resulting in excess H^+ ions (Gaind, 2016). Lastly, microbial lysis returns organic phosphate back to the soil in plant available form. Under soil drought stress and

subsequent rewetting, phosphate from lysed microbial cells is soluble, contributing to an increase in plant-available P (Butterly et al., 2009; Turner et al., 2003).

Plant-microbe relationships are critical for plant survival under environmental stresses. Drought conditions have widespread effects on plants at any stage of development. Seed germination, vegetative growth, reproductive development, and plant senescence are all affected by drought (Gontia-Mishra et al., 2020). Plants alter their growing strategies in response to drought to maximize survivability (Gupta et al., 2020). Aboveground, stomata closure helps reduce water loss by limiting transpiration, at the cost of decreased photosynthesis and growth (Okamoto et al., 2013). Belowground, plants focus on finding new water sources, extending root depth while slowing aboveground growth. These responses are associated with changes in abscisic acid (ABA) content, an early response to water stress in leaf and root tissues controlling many drought associated plant responses (Janiak et al., 2016). Phytohormone synthesis such as ABA in roots can be induced by soil microbes to improve plant stress tolerance (Lu et al., 2018). Multiple reports show that priming soil with specific bacterial genera significantly enhances plant drought tolerance later in development (Arshad et al., 2008; Mayak et al., 2004).

Microbes also augment the rhizosphere environment under drought stress to increase water holding capacity. Exopolysaccharides (EPS) created by bacteria in the rhizosphere form hydrophilic biofilms capable of protecting plant roots and rhizosphere soil from drought conditions (Rolli et al., 2015). Biofilms are exuded within and around roots, coating surfaces and increasing the available water holding capacity while the soil dries. Soil primed with such biofilms has shown significant effects in wheat (Ilyas et al., 2020) and maize (Naseem & Bano,

2014) when introduced to soil prior to drought stress, exemplifying how microbial taxa can improve the soil environment for plant development.

Microbes are also important for directly and indirectly suppressing plant pathogens in the soil. General suppression ability in the microbial community is the direct deterrent to pathogen caused by a diverse and competitive community leaving no niches for pathogens to establish. This provides a low level, broad suppression against multiple pathogen sources (Schlatter et al., 2017). Microbial biodiversity has been negatively correlated with pathogen establishment, showing the innate ability of a diverse community to repel novel pathogenic invasions (Van Elsas et al., 2012).

Soil microbiomes also provide pathogenic suppression (Weller et al., 2002) in which targeted interactions with specific species results in suppression of a specific pathogen (Schlatter et al., 2017). Importantly, these interactions have a significant effect on many soil-borne plant pathogens. Establishment of the common fungal plant disease *Fusarium oxysporum* can be diminished through microbial biocontrol including strains of *Pseudomonas spp.* and non-pathogenic strains of *F. oxysporum* (Alabouvette, 1999). These microbes compete with the *F. oxysporum* pathogen for the same space and nutrients and inhibit a persistent population from being established (Todorović et al., 2023). Disease-suppression through microbial interactions is important for reducing plant pathogens, however beneficial microbes also suppress plant pathogens by interacting directly with roots to induce a plant defense response.

Plant roots are sensitive to microbial taxa and recognize microbes through microbe associated molecular patterns (MAMPs) and pathogen associated molecular patterns (PAMPs). When a pathogen attack is identified, plants respond with systemic acquired resistance (SAR),

altering transcription factors and signaling molecules to induce morphological changes across leaf, shoot, and root tissue (Bigeard et al., 2015). Some beneficial soil microbes are able to sensitize plants to pathogens through induced systemic resistance (ISR), priming them for stronger and faster resistance responses (Yu et al., 2022).

Plant-microbe interactions support pathogen resistance through complex relationships. In a wheat study, plants were infected with the fungal pathogen *Fusarium pseudograminearum (Fp)*, causing a plant defense response through the jasmonic (JA) and salicylic (SA) signaling pathways. In the soil microbiome, *Stenotrophomonas rhizophilia (SR80)* bacteria was found abundantly in the root endosphere, correlating with fungal infection. While SR80 did not directly inhibit pathogen growth on agar plates or in the soil, multiple genes in the JA and SA signaling pathways were overexpressed in plant tissue when inoculated with SR80 (Liu et al., 2021). This exemplifies a plant-microbe-pathogen interaction where microbes indirectly improve plant-pathogen interactions by modulating plant gene expression.

Plant-promoting microbes interact directly or indirectly with roots in the soil to improve biotic and abiotic stress to plants. Plant roots also alter the soil microbes in their immediate environment. Below we explore how plant roots interact with their immediate surroundings to create a beneficial community of microbes distinct to the resident soil environment.

Plants recruit a beneficial rhizosphere microbiome

In the soil, plants and microbes interact in the rhizosphere, the region surrounding plant roots containing dynamic interactions among a diverse variety of microorganisms (Ahkami et al., 2024; Chepsergon & Moleleki, 2023). Plants release concentrated solutions of sugars and other organic compounds as root exudates to impact the rhizosphere. Up to 21% of the carbon fixed through photosynthesis can be delegated to exudates, highlighting the importance of belowground interactions to the overall health of the plant (Walker et al., 2003). Through these exudates, plants can assemble a microbiome distinct from the resident bulk soil microbial community (Bulgarelli et al., 2013; Zolti et al., 2020).

The extent and chemical composition of root exudates varies by environmental pressures and is capable of recruiting beneficial microbes that can improve nutrient availability (Zhao et al., 2021), drought stress tolerance (Tong et al., 2024), and pathogen resistance (Liu et al., 2021). There are multiple mechanisms that determine how plants condition the soil microbiome, including broad ecosystem-based community pressure (Bulgarelli et al., 2013) and specific taxa recruitment to drive the microbial community through microbe-microbe interactions (Agler et al., 2016).

Through rhizodeposition, root exudates flood the rhizosphere with sugars and organic compounds to spark microbial growth in the area. As a first selection step, microbes capable of utilizing root exudate compounds are recruited in the rhizosphere. Second, a selection step for recruiting beneficial microbes occurs in the endosphere, where root physiology promotes specific bacteria and fungi, different from the broader rhizosphere community. Expanding this model,

Reinhold-Hurek et al. proposed a three-step model in 2015 to differentiate specific selection pressures in the rhizosphere, the rhizoplane (area directly adjacent to and including the root), and the root endosphere (interior of plant root tissue) (Che et al., 2024; Corti et al., 2005). These models explain how the diverse community of soil microbes are selected for and against in the root zone. Decreasing diversity in microbial taxa between the root zone and bulk soil has been reported in multiple crop studies (Bulgarelli et al., 2013).

Alternatively, evidence found in the human microbiome suggested that the abundance of specific keystone microbes have disproportionately large effect on the microbial community structure, significantly altering the relative abundance of many other microbes (Hajishengallis et al., 2012). Since then possible keystone taxa have been reported in the plant phyllosphere (Agler et al., 2016) and rhizosphere (Banerjee et al., 2018) to explain rhizosphere functions.

Interestingly, both the selection model and keystone taxa hypotheses have reported a role for plant genotypic variability. Even in the root endosphere where microbial communities are less diverse, plant genotype was found to significantly affect relative abundance of bacterial taxa in the model organism *Arabidopsis thaliana* (Lundberg et al., 2012). Further evidence in tomato (French et al., 2020), maize (Peiffer et al., 2013), and soybean (Liu et al., 2019) report genotypic effects on the broader rhizosphere microbiome.

The plant genotype is the total combination of genes in any given plant, which influences observable traits including plant development and stress responses. Genes control soil microbial patterns through molecular signaling, regulating compounds used for root morphology and root exudate profiles (Liu et al., 2023). Under nutrient rich conditions, studies in wheat, cotton, and

soybean report changes in root exudate compounds in response to nutrient treatments. These changes also impacted the resulting rhizosphere microbial composition (Chen et al., 2019; Qiao et al., 2017; Shi et al., 2020). Similar gene-regulated belowground response patterns are reported to improve nutrient availability, disease pressure, and abiotic resistance (Liu et al., 2023).

Soil nutrients are critical for successful plant development and are primarily found in the soil. To improve nutrient uptake, plants have developed signaling pathways to control root morphology and in turn the rhizosphere. For example, in maize, *lateral rootless 1 (lrt1)* and *rootless with undetectable meristem 1 (rum1)* mutant plants do not grow lateral roots (Woll et al., 2005). These mutants were compared to wild type lines, where it was discovered that under N stress, flavonoid synthesis and root exudation increased. Wild type lines were compared to chalcone synthase-encoding gene (*C2*) mutant lines, which have reduced synthesis of apigenin-related flavonoids. Using an inbred population, researchers found that the highest biomass line under N stress had high expression of flavonoids and released the highest concentration of these as root exudates. This resulted in distinct differences between the rhizosphere microbiome in the *C2* mutant and wild type lines. Most notably was the recruitment of *Oxalobacteraceae* bacteria which increased N accumulation and stimulated lateral root growth even in *lrt1* mutant lines (Yu et al., 2021). In rice the NRT1.1B gene, a known nitrate transporter, was found to also be responsible for recruiting microbes involved in ammonification. Mutant lines were unable to access organic N as well as wild type, corresponding with their difference in microbiome (Zhang et al., 2019). These findings suggest that plant gene expression alters both root morphology and microbial community structure to improve nutrient uptake.

Environmental stressors like drought induce systemic plant responses through signaling pathways to modify shoot and root morphology (Gupta et al., 2020). The soil microbiome is also altered under drought stress due to less nutrient mobility and greater osmotic pressure. These factors often lead to decreasing microbial biomass (Naylor & Coleman-Derr, 2018). Microbial interactions are responsible for maintaining nutrient uptake and inducing drought-responsive genes in plants. A study in wheat reported that drought-resistant Yunhan 618 wheat had a more diverse microbial community in the rhizosphere than a drought-sensitive variety Chinese Spring. Specifically, fungal species *Mortierella alpine* and *Epicoccum nigrum* colonized Yunhan 618, inducing expression of two drought-response genes *calcineurin B-like-interacting protein kinase gene* (*CIPK9*) and *protein phosphatase 2C gene* (*PP2C30*) (Yue et al., 2024). These genes are critical to the mitogen-activated protein (MAP) kinase cascade, responsible for broad stress responses in cells including cell division, gene expression, and apoptosis (Pearson et al., 2001). In the model organism *Arabidopsis thaliana,* the rhizobacteria *Bacillus amyloliquefaciens* FZB42 was tested for its ability to improve plant drought tolerance. Rhizobacterial inoculation increased ROS scavenging enzymes and genes in the abscisic acid (ABA) signaling pathway. Highlighting the complex plant-microbe interactions, FZB42 drought mediation was lost in *epsC* mutant *A. thaliana* strains. This suggests that *epsC*, which encodes for exopolysaccharides, is responsible for recruiting FZB42 to mediate drought tolerance through ABA and ROS scavenging pathways (Lu et al., 2018).

Genotype and Environment influences microbiome assembly

In order to understand the effects of plant genetics on rhizosphere assembly, recent studies have conducted genetic mapping of root and rhizosphere microbiomes in crops, such as,

Arabidopsis (*Arabidopsis thaliana* L.) (Bergelson et al., 2019), tomato (*Solanum lycopersicum* L.) (Oyserman et al., 2022), and maize (*Zea mays* L.) (He et al., 2024). By growing crops in a controlled environment or providing a homogenous resident soil microbial community, the effects of plant genetics may be better understood. However, the influence of crucial gene by environment (GxE) interactions in shaping the rhizosphere community are often overlooked.

Given microbial communities are influenced by environmental factors like soil chemistry, temperature, and moisture, assessing the effects of environment is critical to understand how crop breeding can be used to recruit a beneficial rhizosphere microbiome and improve plant fitness (Babalola et al., 2021; Brown et al., 2020). Recent research in agricultural crops including maize (Peiffer et al., 2013), wheat (Schlatter et al., 2020), and rice (Edwards et al., 2015) have identified differences in the rhizosphere microbiome across growing locations. Soil microbes can alleviate environmental pressures, offering a novel approach to increase agriculture sustainability. Nutrient cycling improvement in the soil is able to decrease fertilizer needs, and improved drought tolerance through microbial associations can improve performance as growing regions become hotter and drier (Hunter, 2016). Optimizing the relationship between plants and microbes is only possible by mapping the microbe community across both environmental and genetic diversity (Clouse & Wagner, 2021). To integrate microbial associations into plant breeding, further research is needed to find loci in breeding populations that are variable for microbial recruitment traits. The plant-microbe interactions must then be tested across variable environmental gradients to understand how broadly applicable such a trait can be to improving plant performance.

Remote Sensing of Plant Phenotype

While research on GxE interactions and rhizosphere microbiome recruitment can inform breeding programs, emerging technologies, such as unmanned aerial system (UAS) also can contribute to crop improvement. Remote sensing techniques have been used to measure ground cover for decades (Rogan & Chen, 2004). Satellite imagery enabled growers and researchers to collect repeated measures of farm fields, collecting imagery in wavelengths beyond the visible spectrum that could be used to measure plant metrics including water stress and chlorophyll content (Brisco et al., 1998; Christopher et al., 2016; Jing et al., 2019; Khanal et al., 2020). For agricultural use, satellites lack image resolution to measure individual plants, and collect imagery on a set schedule, making it challenging to adapt to growing seasons and target specific data collection dates (Leinenkugel et al., 2013). Satellites are most useful in larger studies, commonly used to measure broader plant growing patterns across entire states or countries (Wu et al., 2014; Zhang et al., 2014).

Unoccupied aerial systems (UAS) are small remotely piloted aircraft with mounted sensors capable of collecting imagery directly over the field of interest. This allows for data to be collected more often, and at much higher resolution than satellites (Olson & Anderson, 2021). For agricultural study, UAS provides a remote sensing platform which can target specific plants and development stages to provide information critical to future decision making, including plant health (Sahoo et al., 2024), stand counts (Zortea et al., 2018), and invasive weeds (Rasmussen et al., 2019).

Collecting high resolution imagery using UAS is inexpensive and efficient, however, analyzing imagery is time-consuming and complicated, posing a barrier to expanding UAS

applications in agricultural research (Lachowiec et al., 2024). Building accessible and streamlined analysis workflows is essential to process the growing number of imagery datasets (Istiak et al., 2023) into actionable information for breeders and producers.

This dissertation consists of three research projects related to sustainable crop production. These projects investigate the plant rhizosphere microbiome in relation to both plant genetics and environmental variability. The first examines the barley genotypic effect on rhizosphere community assembly utilizing an elite population of barley breeding lines. Grown across three historical barley growing locations in Montana and South Dakota, specific microbial taxa colocalized with plant QTL, providing evidence for barley recruitment of its immediate bacterial microbiome. The second research project expands on the first project by exploring how the bacterial microbiome varies across environmental and plant factors. Bacterial community structure was highly consistent across locations and growing seasons, while fungal community members were more dependent on location, suggesting barley exerts a stronger influence on bacterial community assembly compared to the fungal community. The final project addresses a need for high resolution measurements of plant response to environmental conditions as a tool for developing superior varieties and addresses the lack of affordable and applicable workflows for research plot remote sensing analysis by introducing a novel workflow capable of extracting plot-level spectral data with minimal training time. This project aims to support further agricultural research and the broader agricultural industry by lowering financial costs and technical challenges to analyzing and interpreting imagery data. These three projects add to the body of knowledge on these topics and lay the groundwork for future investigations into remaining questions about the extended phenotype of barley and crops as a whole.

References

Agler, M. T., Ruhe, J., Kroll, S., Morhenn, C., Kim, S.-T., Weigel, D., & Kemen, E. M. (2016). Microbial hub taxa link host and abiotic factors to plant microbiome variation. *PLOS Biology*, *14*(1), e1002352. https://doi.org/10.1371/journal.pbio.1002352

Ahkami, A. H., Qafoku, O., Roose, T., Mou, Q., Lu, Y., Cardon, Z. G., Wu, Y., Chou, C., Fisher, J. B., Varga, T., Handakumbura, P., Aufrecht, J. A., Bhattacharjee, A., & Moran, J. J. (2024). Emerging sensing, imaging, and computational technologies to scale nano-to macroscale rhizosphere dynamics – Review and research perspectives. *Soil Biology and Biochemistry*, *189*, 109253. https://doi.org/10.1016/j.soilbio.2023.109253

Alabouvette, C. (1999). Fusarium wilt suppressive soils: An example of disease-suppressive soils. *Australasian Plant Pathology*, *28*(1), 57. https://doi.org/10.1071/AP99008

Anderson, D. W. (1988). The effect of parent material and soil development on nutrient cycling in temperate ecosystems. *Biogeochemistry*, *5*(1), 71–97. https://doi.org/10.1007/BF02180318

Arshad, M., Shaharoona, B., & Mahmood, T. (2008). Inoculation with pseudomonas spp. containing acc-deaminase partially eliminates the effects of drought stress on growth, yield, and ripening of pea (Pisum sativum L.). *Pedosphere*, *18*(5), 611–620. https://doi.org/10.1016/S1002-0160(08)60055-7

Babalola, O. O., Emmanuel, O. C., Adeleke, B. S., Odelade, K. A., Nwachukwu, B. C., Ayiti, O. E., Adegboyega, T. T., & Igiehon, N. O. (2021). Rhizosphere microbiome cooperations: strategies for sustainable crop production. *Current Microbiology*, *78*(4), 1069–1085. https://doi.org/10.1007/s00284-021-02375-2

Banerjee, S., Schlaeppi, K., & Van Der Heijden, M. G. A. (2018). Keystone taxa as drivers of microbiome structure and functioning. *Nature Reviews Microbiology*, *16*(9), 567–576. https://doi.org/10.1038/s41579-018-0024-1

Bergelson, J., Mittelstrass, J., & Horton, M. W. (2019). Characterizing both bacteria and fungi improves understanding of the Arabidopsis root microbiome. *Scientific Reports*, *9*(1), 24. https://doi.org/10.1038/s41598-018-37208-z

Bigeard, J., Colcombet, J., & Hirt, H. (2015). Signaling mechanisms in pattern-triggered immunity (PTI). *Molecular Plant*, *8*(4), 521–539. https://doi.org/10.1016/j.molp.2014.12.022

Boitt, G., Simpson, Z. P., Tian, J., Black, A., Wakelin, S. A., & Condron, L. M. (2018). Plant biomass management impacts on short-term soil phosphorus dynamics in a temperate grassland. *Biology and Fertility of Soils*, *54*(3), 397–409. https://doi.org/10.1007/s00374-018-1269-6

Braum, S. M., & Helmke, P. A. (1995). White lupin utilizes soil phosphorus that is unavailable to soybean. *Plant and Soil*, *176*(1), 95–100. https://doi.org/10.1007/BF00017679

Brisco, B., Brown, R. J., Hirose, T., McNairn, H., & Staenz, K. (1998). Precision agriculture and the role of remote sensing: a review. *Canadian Journal of Remote Sensing*, *24*(3), 315–327. https://doi.org/10.1080/07038992.1998.10855254

Brown, S. P., Grillo, M. A., Podowski, J. C., & Heath, K. D. (2020). Soil origin and plant genotype structure distinct microbiome compartments in the model legume Medicago truncatula. *Microbiome*, *8*(1), 139. https://doi.org/10.1186/s40168-020-00915-9

Brundrett, M. C., & Tedersoo, L. (2018). Evolutionary history of mycorrhizal symbioses and global host plant diversity. *New Phytologist*, *220*(4), 1108–1115. https://doi.org/10.1111/nph.14976

Bulgarelli, D., Schlaeppi, K., Spaepen, S., Van Themaat, E. V. L., & Schulze-Lefert, P. (2013). Structure and functions of the bacterial microbiota of plants. *Annual Review of Plant Biology*, *64*(1), 807–838. https://doi.org/10.1146/annurev-arplant-050312-120106

Butterly, C. R., Bünemann, E. K., McNeill, A. M., Baldock, J. A., & Marschner, P. (2009). Carbon pulses but not phosphorus pulses are related to decreases in microbial biomass during repeated drying and rewetting of soils. *Soil Biology and Biochemistry*, *41*(7), 1406–1416. https://doi.org/10.1016/j.soilbio.2009.03.018

Cassman, K. G., & Grassini, P. (2020). A global perspective on sustainable intensification research. *Nature Sustainability*, *3*(4), 262–268. https://doi.org/10.1038/s41893-020-0507-8

Castrillo, G., Teixeira, P. J. P. L., Paredes, S. H., Law, T. F., De Lorenzo, L., Feltcher, M. E., Finkel, O. M., Breakfield, N. W., Mieczkowski, P., Jones, C. D., Paz-Ares, J., & Dangl, J. L. (2017). Root microbiota drive direct integration of phosphate stress and immunity. *Nature*, *543*(7646), 513–518. https://doi.org/10.1038/nature21417

Chapman, S. C., Chakraborty, S., Dreccer, M. F., & Howden, S. M. (2012). Plant adaptation to climate change—Opportunities and priorities in breeding. *Crop and Pasture Science*, *63*(3), 251. https://doi.org/10.1071/CP11303

Che, J., Wu, Y., Yang, H., Wu, W., Lyu, L., Wang, X., & Li, W. (2024). Beneficial ecological networks dominate the dynamic root endosphere microbiome during long-term symbiosis with host plants. *Plant and Soil*, *501*(1–2), 289–305. https://doi.org/10.1007/s11104-024-06519-8

Chen, S., Waghmode, T. R., Sun, R., Kuramae, E. E., Hu, C., & Liu, B. (2019). Root-associated microbiomes of wheat under the combined effect of plant development and nitrogen fertilization. *Microbiome*, *7*(1), 136. https://doi.org/10.1186/s40168-019-0750-2

Chepsergon, J., & Moleleki, L. N. (2023). Rhizosphere bacterial interactions and impact on plant health. *Current Opinion in Microbiology*, *73*, 102297. https://doi.org/10.1016/j.mib.2023.102297

Christopher, J. T., Christopher, M. J., Borrell, A. K., Fletcher, S., & Chenu, K. (2016). Stay-green traits to improve wheat adaptation in well-watered and water-limited environments. *Journal of Experimental Botany*, *67*(17), 5159–5172. https://doi.org/10.1093/jxb/erw276

Clouse, K. M., & Wagner, M. R. (2021). Plant genetics as a tool for manipulating crop microbiomes: opportunities and challenges. *Frontiers in Bioengineering and Biotechnology*, *9*, 567548. https://doi.org/10.3389/fbioe.2021.567548

Corti, G., Agnelli, A., Cuniglio, R., Sanjurjo, M. F., & Cocco, S. (2005). Characteristics of rhizosphere soil from natural and agricultural environments. In *Biogeochemistry of Trace Elements in the Rhizosphere* (pp. 57–128). Elsevier. https://doi.org/10.1016/B978-044451997-9/50005-2

Dong, W., & Song, Y. (2020). The significance of flavonoids in the process of biological nitrogen fixation. *International Journal of Molecular Sciences*, *21*(16), 5926. https://doi.org/10.3390/ijms21165926

Eduardo Contreras-Liza, S. (2021). Plant breeding and microbiome. In I. Y. Abdurakhmonov (Ed.), *Plant Breeding—Current and Future Views*. IntechOpen. https://doi.org/10.5772/intechopen.94948

Edwards, J., Johnson, C., Santos-Medellín, C., Lurie, E., Podishetty, N. K., Bhatnagar, S., Eisen, J. A., & Sundaresan, V. (2015). Structure, variation, and assembly of the root-associated microbiomes of rice. *Proceedings of the National Academy of Sciences*, *112*(8). https://doi.org/10.1073/pnas.1414592112

Fischer, R. A. (2015). Definitions and determination of crop yield, yield gaps, and of rates of change. *Field Crops Research*, *182*, 9–18. https://doi.org/10.1016/j.fcr.2014.12.006

French, E., Tran, T., & Iyer-Pascuzzi, A. S. (2020). Tomato genotype modulates selection and responses to root microbiota. *Phytobiomes Journal*, *4*(4), 314–326. https://doi.org/10.1094/PBIOMES-02-20-0020-R

Gaind, S. (2016). Phosphate dissolving fungi: Mechanism and application in alleviation of salt stress in wheat. *Microbiological Research*, *193*, 94–102. https://doi.org/10.1016/j.micres.2016.09.005

Garg, N. & Geetanjali. (2009). Symbiotic nitrogen fixation in legume nodules: process and signaling: a review. In E. Lichtfouse, M. Navarrete, P. Debaeke, S. Véronique, & C. Alberola (Eds.), *Sustainable Agriculture* (pp. 519–531). Springer Netherlands. https://doi.org/10.1007/978-90-481-2666-8_32

Gontia-Mishra, I., Sapre, S., Deshmukh, R., Sikdar, S., & Tiwari, S. (2020). Microbe-mediated drought tolerance in plants: current developments and future challenges. In A. N. Yadav, J. Singh, A. A. Rastegari, & N. Yadav (Eds.), *Plant Microbiomes for Sustainable Agriculture* (Vol. 25, pp. 351–379). Springer International Publishing. https://doi.org/10.1007/978-3-030-38453-1_12

Gopal, M., & Gupta, A. (2016). Microbiome selection could spur next-generation plant breeding strategies. *Frontiers in Microbiology*, *7*. https://doi.org/10.3389/fmicb.2016.01971

Gupta, A., Rico-Medina, A., & Caño-Delgado, A. I. (2020). The physiology of plant responses to drought. *Science*, *368*(6488), 266–269. https://doi.org/10.1126/science.aaz7614

Gutjahr, C., & Paszkowski, U. (2013). Multiple control levels of root system remodeling in arbuscular mycorrhizal symbiosis. *Frontiers in Plant Science*, *4*. https://doi.org/10.3389/fpls.2013.00204

Hajishengallis, G., Darveau, R. P., & Curtis, M. A. (2012). The keystone-pathogen hypothesis. *Nature Reviews Microbiology*, *10*(10), 717–725. https://doi.org/10.1038/nrmicro2873

He, X., Wang, D., Jiang, Y., Li, M., Delgado-Baquerizo, M., McLaughlin, C., Marcon, C., Guo, L., Baer, M., Moya, Y. A. T., Von Wirén, N., Deichmann, M., Schaaf, G., Piepho, H.-P., Yang, Z., Yang, J., Yim, B., Smalla, K., Goormachtig, S., … Yu, P. (2024). Heritable microbiome variation is correlated with source environment in locally adapted maize varieties. *Nature Plants*. https://doi.org/10.1038/s41477-024-01654-7

Hedley, M., & McLaughlin, M. (2015). Reactions of phosphate fertilizers and by-products in soils. In J. Thomas Sims & A. N. Sharpley (Eds.), *Agronomy Monographs* (pp. 181–252). American Society of Agronomy, Crop Science Society of America, and Soil Science Society of America. https://doi.org/10.2134/agronmonogr46.c7

Herms, C. H., Hennessy, R. C., Bak, F., Dresbøll, D. B., & Nicolaisen, M. H. (2022). Back to our roots: Exploring the role of root morphology as a mediator of beneficial plant–

microbe interactions. *Environmental Microbiology*, *24*(8), 3264–3272. https://doi.org/10.1111/1462-2920.15926

Hunter, P. (2016). Plant microbiomes and sustainable agriculture: Deciphering the plant microbiome and its role in nutrient supply and plant immunity has great potential to reduce the use of fertilizers and biocides in agriculture. *EMBO Reports*, *17*(12), 1696–1699. https://doi.org/10.15252/embr.201643476

Iannetta, P. P. M., Young, M., Bachinger, J., Bergkvist, G., Doltra, J., Lopez-Bellido, R. J., Monti, M., Pappa, V. A., Reckling, M., Topp, C. F. E., Walker, R. L., Rees, R. M., Watson, C. A., James, E. K., Squire, G. R., & Begg, G. S. (2016). A comparative nitrogen balance and productivity analysis of legume and non-legume supported cropping systems: The potential role of biological nitrogen fixation. *Frontiers in Plant Science*, *7*. https://doi.org/10.3389/fpls.2016.01700

Ilyas, N., Mumtaz, K., Akhtar, N., Yasmin, H., Sayyed, R. Z., Khan, W., Enshasy, H. A. E., Dailin, D. J., Elsayed, E. A., & Ali, Z. (2020). Exopolysaccharides producing bacteria for the amelioration of drought stress in wheat. *Sustainability*, *12*(21), 8876. https://doi.org/10.3390/su12218876

Istiak, Md. A., Syeed, M. M. M., Hossain, M. S., Uddin, M. F., Hasan, M., Khan, R. H., & Azad, N. S. (2023). Adoption of unmanned aerial vehicle (UAV) imagery in agricultural management: A systematic literature review. *Ecological Informatics*, *78*, 102305. https://doi.org/10.1016/j.ecoinf.2023.102305

Janiak, A., Kwaśniewski, M., & Szarejko, I. (2016). Gene expression regulation in roots under drought. *Journal of Experimental Botany*, *67*(4), 1003–1014. https://doi.org/10.1093/jxb/erv512

Jing, Y., Zhang, Y., Hu, M., Chu, Q., & Ma, R. (2019). MODIS-satellite-based analysis of long-term temporal-spatial dynamics and drivers of algal blooms in a plateau lake Dianchi, China. *Remote Sensing*, *11*(21), 2582. https://doi.org/10.3390/rs11212582

Khanal, S., Kc, K., Fulton, J. P., Shearer, S., & Ozkan, E. (2020). Remote sensing in agriculture—accomplishments, limitations, and opportunities. *Remote Sensing*, *12*(22), 3783. https://doi.org/10.3390/rs12223783

Kishore, N., Pindi, P. K., & Ram Reddy, S. (2015). Phosphate-solubilizing microorganisms: a critical review. In B. Bahadur, M. Venkat Rajam, L. Sahijram, & K. V. Krishnamurthy (Eds.), *Plant Biology and Biotechnology* (pp. 307–333). Springer India. https://doi.org/10.1007/978-81-322-2286-6_12

Kun Yuan, Zhang, H., Yu, C., Luo, N., Yan, J., Zheng, S., Hu, Q., Zhang, D., Kou, L., Meng, X., Jing, Y., Chen, M., Ban, X., Yan, Z., Lu, Z., Wu, J., Zhao, Y., Liang, Y., Wang, Y., … Wang, B. (2023). Low phosphorus promotes NSP1–NSP2 heterodimerization to enhance strigolactone biosynthesis and regulate shoot and root architecture in rice. *Molecular Plant*, *16*(11), 1811–1831. https://doi.org/10.1016/j.molp.2023.09.022

Lachowiec, J., Feldman, M. J., Matias, F. I., LeBauer, D., & Gregory, A. (2024). Adoption of unoccupied aerial systems in agricultural research. *The Plant Phenome Journal*, *7*(1), e20098. https://doi.org/10.1002/ppj2.20098

Leinenkugel, P., Kuenzer, C., Oppelt, N., & Dech, S. (2013). Characterisation of land surface phenology and land cover based on moderate resolution satellite data in cloud prone

areas—A novel product for the Mekong Basin. *Remote Sensing of Environment*, *136*, 180–198. https://doi.org/10.1016/j.rse.2013.05.004

Liang, L., Liu, B., Huang, D., Kuang, Q., An, T., Liu, S., Liu, R., Xu, B., Zhang, S., Deng, X., Macrae, A., & Chen, Y. (2022). Arbuscular mycorrhizal fungi alleviate low phosphorus stress in maize genotypes with contrasting root systems. *Plants*, *11*(22), 3105. https://doi.org/10.3390/plants11223105

Liu, F., Hewezi, T., Lebeis, S. L., Pantalone, V., Grewal, P. S., & Staton, M. E. (2019). Soil indigenous microbiome and plant genotypes cooperatively modify soybean rhizosphere microbiome assembly. *BMC Microbiology*, *19*(1), 201. https://doi.org/10.1186/s12866-019-1572-x

Liu, H., Li, J., Carvalhais, L. C., Percy, C. D., Prakash Verma, J., Schenk, P. M., & Singh, B. K. (2021). Evidence for the plant recruitment of beneficial microbes to suppress soil-borne pathogens. *New Phytologist*, *229*(5), 2873–2885. https://doi.org/10.1111/nph.17057

Liu, Q., Cheng, L., Nian, H., Jin, J., & Lian, T. (2023). Linking plant functional genes to rhizosphere microbes: A review. *Plant Biotechnology Journal*, *21*(5), 902–917. https://doi.org/10.1111/pbi.13950

López-Bucio, J., Cruz-Ramírez, A., & Herrera-Estrella, L. (2003). The role of nutrient availability in regulating root architecture. *Current Opinion in Plant Biology*, *6*(3), 280–287. https://doi.org/10.1016/S1369-5266(03)00035-9

Lu, X., Liu, S.-F., Yue, L., Zhao, X., Zhang, Y.-B., Xie, Z.-K., & Wang, R.-Y. (2018). Epsc involved in the encoding of exopolysaccharides produced by bacillus amyloliquefaciens FZB42 act to boost the drought tolerance of Arabidopsis thaliana. *International Journal of Molecular Sciences*, *19*(12), 3795. https://doi.org/10.3390/ijms19123795

Lundberg, D. S., Lebeis, S. L., Paredes, S. H., Yourstone, S., Gehring, J., Malfatti, S., Tremblay, J., Engelbrektson, A., Kunin, V., Rio, T. G. D., Edgar, R. C., Eickhorst, T., Ley, R. E., Hugenholtz, P., Tringe, S. G., & Dangl, J. L. (2012). Defining the core Arabidopsis thaliana root microbiome. *Nature*, *488*(7409), 86–90. https://doi.org/10.1038/nature11237

Masson-Boivin, C., & Sachs, J. L. (2018). Symbiotic nitrogen fixation by rhizobia—The roots of a success story. *Current Opinion in Plant Biology*, *44*, 7–15. https://doi.org/10.1016/j.pbi.2017.12.001

Mayak, S., Tirosh, T., & Glick, B. R. (2004). Plant growth-promoting bacteria that confer resistance to water stress in tomatoes and peppers. *Plant Science*, *166*(2), 525–530. https://doi.org/10.1016/j.plantsci.2003.10.025

Mendes, R., Kruijt, M., De Bruijn, I., Dekkers, E., Van Der Voort, M., Schneider, J. H. M., Piceno, Y. M., DeSantis, T. Z., Andersen, G. L., Bakker, P. A. H. M., & Raaijmakers, J. M. (2011). Deciphering the rhizosphere microbiome for disease-suppressive bacteria. *Science*, *332*(6033), 1097–1100. https://doi.org/10.1126/science.1203980

Miransari, M. (2013). Soil microbes and the availability of soil nutrients. *Acta Physiologiae Plantarum*, *35*(11), 3075–3084. https://doi.org/10.1007/s11738-013-1338-2

Murphy, D. J. (2007). *People, Plants and Genes: The Story of Crops and Humanity* (1st ed.). Oxford University PressOxford. https://doi.org/10.1093/acprof:oso/9780199207145.001.0001

Naseem, H., & Bano, A. (2014). Role of plant growth-promoting rhizobacteria and their exopolysaccharide in drought tolerance of maize. *Journal of Plant Interactions*, *9*(1), 689–701. https://doi.org/10.1080/17429145.2014.902125

Naylor, D., & Coleman-Derr, D. (2018). Drought stress and root-associated bacterial communities. *Frontiers in Plant Science*, *8*, 2223. https://doi.org/10.3389/fpls.2017.02223

Okamoto, M., Peterson, F. C., Defries, A., Park, S.-Y., Endo, A., Nambara, E., Volkman, B. F., & Cutler, S. R. (2013). Activation of dimeric ABA receptors elicits guard cell closure, ABA-regulated gene expression, and drought tolerance. *Proceedings of the National Academy of Sciences*, *110*(29), 12132–12137. https://doi.org/10.1073/pnas.1305919110

Olson, D., & Anderson, J. (2021). Review on unmanned aerial vehicles, remote sensors, imagery processing, and their applications in agriculture. *Agronomy Journal*, *113*(2), 971–992. https://doi.org/10.1002/agj2.20595

Oyserman, B. O., Flores, S. S., Griffioen, T., Pan, X., Van Der Wijk, E., Pronk, L., Lokhorst, W., Nurfikari, A., Paulson, J. N., Movassagh, M., Stopnisek, N., Kupczok, A., Cordovez, V., Carrión, V. J., Ligterink, W., Snoek, B. L., Medema, M. H., & Raaijmakers, J. M. (2022). Disentangling the genetic basis of rhizosphere microbiome assembly in tomato. *Nature Communications*, *13*(1), 3228. https://doi.org/10.1038/s41467-022-30849-9

Pandey, N. (2018). Role of plant nutrients in plant growth and physiology. In M. Hasanuzzaman, M. Fujita, H. Oku, K. Nahar, & B. Hawrylak-Nowak (Eds.), *Plant Nutrients and Abiotic Stress Tolerance* (pp. 51–93). Springer Singapore. https://doi.org/10.1007/978-981-10-9044-8_2

Pearson, G., Robinson, F., Beers Gibson, T., Xu, B., Karandikar, M., Berman, K., & Cobb, M. H. (2001). Mitogen-activated protein (MAP) kinase pathways: Regulation and physiological functions*. *Endocrine Reviews*, *22*(2), 153–183. https://doi.org/10.1210/edrv.22.2.0428

Peiffer, J. A., Spor, A., Koren, O., Jin, Z., Tringe, S. G., Dangl, J. L., Buckler, E. S., & Ley, R. E. (2013). Diversity and heritability of the maize rhizosphere microbiome under field conditions. *Proceedings of the National Academy of Sciences*, *110*(16), 6548–6553. https://doi.org/10.1073/pnas.1302837110

Pérez-Torres, C.-A., López-Bucio, J., Cruz-Ramírez, A., Ibarra-Laclette, E., Dharmasiri, S., Estelle, M., & Herrera-Estrella, L. (2009). Phosphate availability alters lateral root development in *arabidopsis* by modulating auxin sensitivity via a mechanism involving the TIR1 auxin receptor. *The Plant Cell*, *20*(12), 3258–3272. https://doi.org/10.1105/tpc.108.058719

Pervaiz, Z. H., Contreras, J., Hupp, B. M., Lindenberger, J. H., Chen, D., Zhang, Q., Wang, C., Twigg, P., & Saleem, M. (2020). Root microbiome changes with root branching order and root chemistry in peach rhizosphere soil. *Rhizosphere*, *16*, 100249. https://doi.org/10.1016/j.rhisph.2020.100249

Pii, Y., Mimmo, T., Tomasi, N., Terzano, R., Cesco, S., & Crecchio, C. (2015). Microbial interactions in the rhizosphere: Beneficial influences of plant growth-promoting rhizobacteria on nutrient acquisition process. A review. *Biology and Fertility of Soils*, *51*(4), 403–415. https://doi.org/10.1007/s00374-015-0996-1

Poudel, M., Mendes, R., Costa, L. A. S., Bueno, C. G., Meng, Y., Folimonova, S. Y., Garrett, K. A., & Martins, S. J. (2021). The role of plant-associated bacteria, fungi, and viruses in drought stress mitigation. *Frontiers in Microbiology, 12*, 743512. https://doi.org/10.3389/fmicb.2021.743512

Qiao, Q., Wang, F., Zhang, J., Chen, Y., Zhang, C., Liu, G., Zhang, H., Ma, C., & Zhang, J. (2017). The variation in the rhizosphere microbiome of cotton with soil type, genotype and developmental stage. *Scientific Reports, 7*(1), 3940. https://doi.org/10.1038/s41598-017-04213-7

Rajamanickam, V., Vinod, K. K., Vengavasi, K., Kumar, T., Chinnusamy, V., & Pandey, R. (2024). Root architectural adaptations to phosphorus deficiency: Unraveling genotypic variability in wheat seedlings. *Agriculture, 14*(3), 447. https://doi.org/10.3390/agriculture14030447

Rasmussen, J., Nielsen, J., Streibig, J. C., Jensen, J. E., Pedersen, K. S., & Olsen, S. I. (2019). Pre-harvest weed mapping of Cirsium arvense in wheat and barley with off-the-shelf UAVs. *Precision Agriculture, 20*(5), 983–999. https://doi.org/10.1007/s11119-018-09625-7

Rawat, P., Das, S., Shankhdhar, D., & Shankhdhar, S. C. (2021). Phosphate-solubilizing microorganisms: Mechanism and their role in phosphate solubilization and uptake. *Journal of Soil Science and Plant Nutrition, 21*(1), 49–68. https://doi.org/10.1007/s42729-020-00342-7

Ray, D. K., Mueller, N. D., West, P. C., & Foley, J. A. (2013). Yield trends are insufficient to double global crop production by 2050. *PLoS ONE, 8*(6), e66428. https://doi.org/10.1371/journal.pone.0066428

Rogan, J., & Chen, D. (2004). Remote sensing technology for mapping and monitoring land-cover and land-use change. *Progress in Planning, 61*(4), 301–325. https://doi.org/10.1016/S0305-9006(03)00066-7

Rolli, E., Marasco, R., Vigani, G., Ettoumi, B., Mapelli, F., Deangelis, M. L., Gandolfi, C., Casati, E., Previtali, F., Gerbino, R., Pierotti Cei, F., Borin, S., Sorlini, C., Zocchi, G., & Daffonchio, D. (2015). Improved plant resistance to drought is promoted by the root-associated microbiome as a water stress-dependent trait. *Environmental Microbiology, 17*(2), 316–331. https://doi.org/10.1111/1462-2920.12439

Rosenblueth, M., Ormeño-Orrillo, E., López-López, A., Rogel, M. A., Reyes-Hernández, B. J., Martínez-Romero, J. C., Reddy, P. M., & Martínez-Romero, E. (2018). Nitrogen fixation in cereals. *Frontiers in Microbiology, 9*, 1794. https://doi.org/10.3389/fmicb.2018.01794

Sahoo, R. N., Rejith, R. G., Gakhar, S., Ranjan, R., Meena, M. C., Dey, A., Mukherjee, J., Dhakar, R., Meena, A., Daas, A., Babu, S., Upadhyay, P. K., Sekhawat, K., Kumar, S., Kumar, M., Chinnusamy, V., & Khanna, M. (2024). Drone remote sensing of wheat N using hyperspectral sensor and machine learning. *Precision Agriculture, 25*(2), 704–728. https://doi.org/10.1007/s11119-023-10089-7

Sánchez-Calderón, L., López-Bucio, J., Chacón-López, A., Cruz-Ramírez, A., Nieto-Jacobo, F., Dubrovsky, J. G., & Herrera-Estrella, L. (2005). Phosphate starvation induces a determinate developmental program in the roots of Arabidopsis thaliana. *Plant and Cell Physiology, 46*(1), 174–184. https://doi.org/10.1093/pcp/pci011

Schlatter, D. C., Yin, C., Hulbert, S., & Paulitz, T. C. (2020). Core rhizosphere microbiomes of dryland wheat are influenced by location and land use history. *Applied and Environmental Microbiology*, *86*(5), e02135-19. https://doi.org/10.1128/AEM.02135-19

Schlatter, D., Kinkel, L., Thomashow, L., Weller, D., & Paulitz, T. (2017). Disease suppressive soils: new insights from the soil microbiome. *Phytopathology®*, *107*(11), 1284–1297. https://doi.org/10.1094/PHYTO-03-17-0111-RVW

Shi, Q., Liu, Y., Shi, A., Cai, Z., Nian, H., Hartmann, M., & Lian, T. (2020). Rhizosphere soil fungal communities of aluminum-tolerant and -sensitive soybean genotypes respond differently to aluminum stress in an acid soil. *Frontiers in Microbiology*, *11*, 1177. https://doi.org/10.3389/fmicb.2020.01177

Smith, S. E., Smith, F. A., & Jakobsen, I. (2003). Mycorrhizal fungi can dominate phosphate supply to plants irrespective of growth responses. *Plant Physiology*, *133*(1), 16–20. https://doi.org/10.1104/pp.103.024380

Snowdon, R. J., Wittkop, B., Chen, T.-W., & Stahl, A. (2021). Crop adaptation to climate change as a consequence of long-term breeding. *Theoretical and Applied Genetics*, *134*(6), 1613–1623. https://doi.org/10.1007/s00122-020-03729-3

Todorović, I., Moënne-Loccoz, Y., Raičević, V., Jovičić-Petrović, J., & Muller, D. (2023). Microbial diversity in soils suppressive to Fusarium diseases. *Frontiers in Plant Science*, *14*, 1228749. https://doi.org/10.3389/fpls.2023.1228749

Tong, Y., Zheng, X., Hu, Y., Wu, J., Liu, H., Deng, Y., Lv, W., Yao, H., Chen, J., & Ge, T. (2024). Root exudate-mediated plant–microbiome interactions determine plant health during disease infection. *Agriculture, Ecosystems & Environment*, *370*, 109056. https://doi.org/10.1016/j.agee.2024.109056

Turner, B. L., Driessen, J. P., Haygarth, P. M., & Mckelvie, I. D. (2003). Potential contribution of lysed bacterial cells to phosphorus solubilisation in two rewetted Australian pasture soils. *Soil Biology and Biochemistry*, *35*(1), 187–189. https://doi.org/10.1016/S0038-0717(02)00244-4

Van Elsas, J. D., Chiurazzi, M., Mallon, C. A., Elhottovā, D., Krištůfek, V., & Salles, J. F. (2012). Microbial diversity determines the invasion of soil by a bacterial pathogen. *Proceedings of the National Academy of Sciences*, *109*(4), 1159–1164. https://doi.org/10.1073/pnas.1109326109

Walder, F., Niemann, H., Natarajan, M., Lehmann, M. F., Boller, T., & Wiemken, A. (2012). Mycorrhizal networks: Common goods of plants shared under unequal terms of trade. *Plant Physiology*, *159*(2), 789–797. https://doi.org/10.1104/pp.112.195727

Walker, T. S., Bais, H. P., Grotewold, E., & Vivanco, J. M. (2003). Root exudation and rhizosphere biology. *Plant Physiology*, *132*(1), 44–51. https://doi.org/10.1104/pp.102.019661

Wang, B., & Qiu, Y.-L. (2006). Phylogenetic distribution and evolution of mycorrhizas in land plants. *Mycorrhiza*, *16*(5), 299–363. https://doi.org/10.1007/s00572-005-0033-6

Weller, D. M., Raaijmakers, J. M., Gardener, B. B. M., & Thomashow, L. S. (2002). Microbial populations responsible for specific soil suppressiveness to plant pathogens. *Annual Review of Phytopathology*, *40*(1), 309–348. https://doi.org/10.1146/annurev.phyto.40.030402.110010

Williamson, L. C., Ribrioux, S. P. C. P., Fitter, A. H., & Leyser, H. M. O. (2001). Phosphate availability regulates root system architecture in Arabidopsis. *Plant Physiology*, *126*(2), 875–882. https://doi.org/10.1104/pp.126.2.875

Woll, K., Borsuk, L. A., Stransky, H., Nettleton, D., Schnable, P. S., & Hochholdinger, F. (2005). Isolation, characterization, and pericycle-specific transcriptome analyses of the novel maize lateral and seminal root initiation mutant *rum1*. *Plant Physiology*, *139*(3), 1255–1267. https://doi.org/10.1104/pp.105.067330

Wu, B., Meng, J., Li, Q., Yan, N., Du, X., & Zhang, M. (2014). Remote sensing-based global crop monitoring: Experiences with China's CropWatch system. *International Journal of Digital Earth*, *7*(2), 113–137. https://doi.org/10.1080/17538947.2013.821185

Yadav, D. S., Jaiswal, B., Gautam, M., & Agrawal, M. (2020). Soil acidification and its impact on plants. In P. Singh, S. K. Singh, & S. M. Prasad (Eds.), *Plant Responses to Soil Pollution* (pp. 1–26). Springer Singapore. https://doi.org/10.1007/978-981-15-4964-9_1

Yang, J., Lan, L., Jin, Y., Yu, N., Wang, D., & Wang, E. (2022). Mechanisms underlying legume–rhizobium symbioses. *Journal of Integrative Plant Biology*, *64*(2), 244–267. https://doi.org/10.1111/jipb.13207

Yu, P., He, X., Baer, M., Beirinckx, S., Tian, T., Moya, Y. A. T., Zhang, X., Deichmann, M., Frey, F. P., Bresgen, V., Li, C., Razavi, B. S., Schaaf, G., Von Wirén, N., Su, Z., Bucher, M., Tsuda, K., Goormachtig, S., Chen, X., & Hochholdinger, F. (2021). Plant flavones enrich rhizosphere Oxalobacteraceae to improve maize performance under nitrogen deprivation. *Nature Plants*, *7*(4), 481–499. https://doi.org/10.1038/s41477-021-00897-y

Yu, Y., Gui, Y., Li, Z., Jiang, C., Guo, J., & Niu, D. (2022). Induced systemic resistance for improving plant immunity by beneficial microbes. *Plants*, *11*(3), 386. https://doi.org/10.3390/plants11030386

Yue, H., Sun, X., Wang, T., Zhang, A., Han, D., Wei, G., Song, W., & Shu, D. (2024). Host genotype-specific rhizosphere fungus enhances drought resistance in wheat. *Microbiome*, *12*(1), 44. https://doi.org/10.1186/s40168-024-01770-8

Zhang, H., Huang, Y., Ye, X., & Xu, F. (2011). Genotypic variation in phosphorus acquisition from sparingly soluble P sources is related to root morphology and root exudates in Brassica napus. *Science China Life Sciences*, *54*(12), 1134–1142. https://doi.org/10.1007/s11427-011-4254-y

Zhang, J., Liu, W., Bu, J., Lin, Y., & Bai, Y. (2023). Host genetics regulate the plant microbiome. *Current Opinion in Microbiology*, *72*, 102268. https://doi.org/10.1016/j.mib.2023.102268

Zhang, J., Liu, Y.-X., Zhang, N., Hu, B., Jin, T., Xu, H., Qin, Y., Yan, P., Zhang, X., Guo, X., Hui, J., Cao, S., Wang, X., Wang, C., Wang, H., Qu, B., Fan, G., Yuan, L., Garrido-Oter, R., … Bai, Y. (2019). NRT1.1B is associated with root microbiota composition and nitrogen use in field-grown rice. *Nature Biotechnology*, *37*(6), 676–684. https://doi.org/10.1038/s41587-019-0104-4

Zhang, M., Wu, B., Yu, M., Zou, W., & Zheng, Y. (2014). Crop condition assessment with adjusted NDVI using the uncropped arable land ratio. *Remote Sensing*, *6*(6), 5774–5794. https://doi.org/10.3390/rs6065774

Zhao, M., Zhao, J., Yuan, J., Hale, L., Wen, T., Huang, Q., Vivanco, J. M., Zhou, J., Kowalchuk, G. A., & Shen, Q. (2021). Root exudates drive soil-microbe-nutrient feedbacks in

response to plant growth. *Plant, Cell & Environment*, *44*(2), 613–628. https://doi.org/10.1111/pce.13928

Zolti, A., Green, S. J., Sela, N., Hadar, Y., & Minz, D. (2020). The microbiome as a biosensor: Functional profiles elucidate hidden stress in hosts. *Microbiome*, *8*(1), 71. https://doi.org/10.1186/s40168-020-00850-9

Zortea, M., Nery, M., Ruga, B., Carvalho, L. B., & Bastos, A. C. (2018). Oil-palm tree detection in aerial images combining deep learning classifiers. *IGARSS 2018 - 2018 IEEE International Geoscience and Remote Sensing Symposium*, 657–660. https://doi.org/10.1109/IGARSS.2018.8519239

CHAPTER TWO

UNCOVERING GENETIC LINKAGE IN THE RHIZOSPHERE CONTRIBUTING TO ADAPTATION

Contribution of Authors and Co-Authors

Manuscript in Chapter 2

Author: Jessica L. Williams*

Contributions: performing experiments, analysis, writing.

Co-Author: Erik Z. Killian*

Contributions: performing experiments, analysis, writing.

Co-Author: Anna Halpin-McCormick

Contributions: performing experiments, analysis, writing.

Co-Author: Michael B. Kantar

Contributions: conceptualization, writing.

Co-Author: Jamie D. Sherman

Contributions: conceptualization, analysis, writing.

Co-Author: Patrick E. Ewing

Contributions: conceptualization, performing experiments, writing.

Co-Author: Jed O. Eberly

Contributions: funding, conceptualization, analysis, writing.

Co-Author: Jennifer Lachowiec

Contributions: conceptualization, analysis, writing.
* Equal contribution

Manuscript Information

Status of Manuscript:
☐ Prepared for submission to a peer-reviewed journal
☒ Officially submitted to a peer-reviewed journal
☐ Accepted by a peer-reviewed journal
☐ Published in a peer-reviewed journal

Abstract

Microorganisms assembled into the plant rhizosphere from the surrounding soil can benefit the fitness of their host. Variation in plant genetics is associated with variation in rhizosphere microbial community composition leading to increased fitness and crop production and reducing reliance on synthetic agricultural inputs through selection. However, what impact the abiotic environment has on connections between microbes and host genetics, and whether those connections in turn impact crop performance in realistic agricultural scenarios is still unclear. We assessed agronomic performance and 16S sequence-based rhizosphere bacterial community composition on a large diverse barley population grown in seven field trials across four locations and two years. Within adapted regions, we observed consistent rhizosphere compositions across diverse soils, whereas in unadapted environments, distinct microbial communities were recruited, indicating environmental specificity in microbial assembly. Greenhouse trials further revealed that abiotic soil properties and microbial inoculants together interact to modulate rhizosphere composition and plant growth. Genome-wide association studies identified hundreds of quantitative trait loci (QTL) for microbial traits, with thirty of those loci co-localizing with agronomic traits, suggesting interspecies pleiotropy or genetic linkage. At specific loci, candidate genes associated with root-microbe interactions, including those related to pathogen response and root exudate production, suggest mechanisms that enable adaptation to local environments. These findings support the idea that genetic manipulation of rhizosphere microbiomes via selection of crops could enhance adaptation (i.e., yield, quality) across variable environments, advancing breeding strategies for improved crop resilience and productivity.

Key Words: microbiome, genome wide association, barley, plant breeding, agriculture

Introduction

Rhizosphere microbiomes contribute critically to plant survival and productivity. Soil-borne microbes benefit plant health by facilitating the acquisition of nitrogen, phosphorus, and other nutrients[1,2], stimulating hormonal pathways to promote plant growth[3], protecting against pathogens[4] and mitigating abiotic stressors such as drought[5-8]. The development of microbial inoculants as a biological solution to environmental degradation due to agricultural practices is an active area of research producing mixed results[9]. Large scale production, distribution, application, and establishment of these products pose hurdles to their efficacy[10]. A different tactic that has received attention more recently is breeding crop varieties for an enhanced ability to recruit beneficial microorganisms[11-13]. To do this, a detailed understanding of the interactions between plants and microbiomes and how this is altered by varying environmental conditions is needed. Thus, large knowledge gaps remain to be filled before microbial communities can be predictably manipulated via host genetic selection to benefit crop performance.

A critical zone ripe for microbial manipulation is the rhizosphere—the region surrounding plant roots that is characterized by dynamic interactions among a diverse variety of microorganisms and is considered one of the most complex biological habitats on earth[14,15]. Soil factors and plant traits are the main drivers governing rhizosphere assembly[16]. The genetic basis regulating plant control of rhizosphere microbiome assembly remains poorly understood[17,18]. While soil microbial communities are driven by local climates and soil factors, the rhizosphere harbors a unique microbiome that is assembled from the soil microbiome and influenced by plant traits[19].

Only traits under the influence of plant genetics can be targeted by selection in plant breeding. Some rhizosphere microbiome variation is attributed to plant genotype, which shows heritability of these extended phenotypes[20,21], suggesting breeding may be possible. Recent research has begun to uncover some of these loci through genetic mapping of root and rhizosphere microbiome extended phenotypes in domesticated and wild monocots and dicots, including Arabidopsis (*Arabidopsis thaliana* L.)[22], switchgrass (*Panicum virgatum* L.)[23], tomato (*Solanum lycopersicum* L.)[24], and maize (*Zea mays* L.)[17]. These studies have minimized variation in the plants' abiotic and biotic environment by providing a uniform starting soil microbial community, growing in a controlled environment, or examining a single field location and time point. This may aid in detecting the effects of plant genetics but overlooks the effects of important gene by environment (GxE) interactions.

Recent studies incorporating the examination of GxE on plant rhizospheres reveal the need to assess context to exploit the microbiome. Microbial communities are sensitive to a plethora of environmental factors such as water and nutrient availability, so the success of manipulating the rhizosphere microbiome for agricultural systems through crop breeding depends on incorporating plant-microbe-environment interactions[25]. For example, the heritability of the rhizosphere microbiome is dependent on variation in local microbiota, variation in soil type and fertility[26,27].

To understand GxE interactions shaping the rhizosphere microbiome we used a barley (*Hordeum vulgare* L.) population representative of five different breeding programs based in Minnesota, North Dakota, Montana, Idaho and Washington: The Spring Two-Row Multi-Environment Trial panel (S2MET[28]). We grew this population in field trials within and far

outside of the adapted range of barley to investigate connections between barley genetics, rhizosphere bacterial community characteristics, and local adaptation. Due to its history of selection, this population contains both lines that are locally adapted and lines that are more generally adapted across the growing regions[29]. We further explore the colocalization of microbiome associations with fitness related phenotypic traits. We discuss how the current research informs the long-term goal of breeding for plant microbe interactions that improve local adaptation.

Results

Environmental variation shapes rhizosphere microbiomes and agronomic traits in barley's adapted and unadapted ranges

We investigated the effect of location, within and outside the adapted barley range to uncover the interaction between host genetics and environmental variation in shaping rhizosphere bacterial microbiomes. We conducted field trials containing the 237 S2MET genotypes for two years in locations representing the adapted range of barley in the United States including southwest Montana (swMT), central Montana (cntrMT), and Brookings, South Dakota (SD). We also conducted a trial for one year in Kunia, Hawaii (HI) which represents an unadapted region where barley is not grown. The field locations had distinct climates and soil physical and chemical properties (Table A2.1).

Within the adapted range, rhizosphere bacterial community composition was relatively similar, suggesting a broad adaptation of the barley rhizosphere microbiome to conditions across barley's adapted range (Fig. 2.1A, B). Actinobacteriota, Bacterioidota, and Proteobacteria were the dominant phyla associated with the barley rhizosphere and represented around 80% of the

relative abundance at the adapted locations, which is consistent with other plant rhizosphere studies[30-32]. In contrast, lines grown in the Hawaii environment recruited a distinct rhizosphere microbiome relative to adapted regions (Fig. 2.1A). While rhizosphere compositions were broadly similar in the adapted locations, they also had key differences in both taxonomic and predicted functional compositions (Fig. 2.1C, D). Five genera belonging to the phylum Actinomycetota, *Arthrobacter*, *Gaiella*, *Microlunatus*, *Pseudoarthrobacter*, and *Rhodococcus*, were enriched in the drier cntrMT environment relative to the other adapted environments. Communities in all locations were dominated by functions associated with chemoheterotrophy (Fig. 2.1D), reflecting the carbon rich environment of the rhizosphere[33,34].

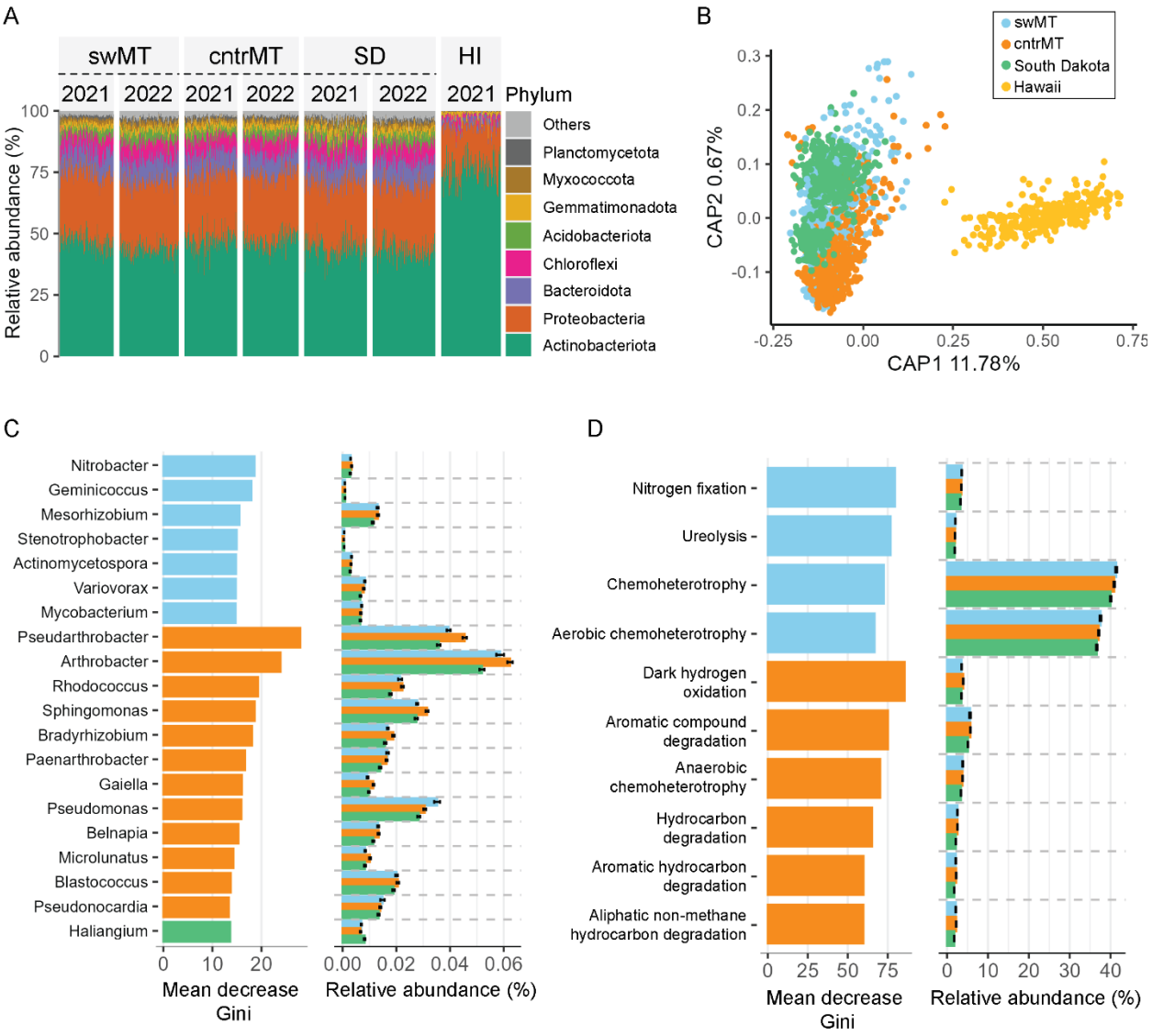

Figure 2.1: Location-Specific Variation in Rhizosphere Microbiomes Across Barley Field Trials (A). Relative abundance of microbial phyla are shown for each site-year. (B) Constrained analysis of principal coordinates (CAP) of the weighted unifrac distances of the rhizosphere bacterial communities among location-years (PERMANOVA, $r^2 = 0.13$, $p < 0.001$) are shown. Differentially abundant genera (C) and functions (D) predicted by a random forest model with a Mean Decrease Gini (MDA) threshold of 10. Functions were predicted from 16S sequences using the functional annotation of prokaryotic taxa (FAPROTAX) database. swMT: southwest Montana shown in light blue, cntrMT: central Montana shown in orange, SD: Brookings, South Dakota shown in green, HI: Kunia, Hawaii shown in yellow.

In addition to the differences in rhizosphere microbiome, we observed large differences in plant traits among the field trials, including phenology, shoot and grain morphology, and yield (Fig. A2.1). The photoperiod in Hawaii prevented flowering of any of the lines and thus agronomic assessment, consistent with the lack of barley adaptation to the location.

The interaction of soil and rhizosphere influences plant growth

To partition the effects of the physicochemical characteristics of soils from microbial communities on plant growth, we performed a greenhouse experiment using soils from locations with contrasting yield potentials (Fig. A2.1), microbial community composition, and predicted microbial function (central Montana 2022 [cntrMT] and southwest Montana 2022 [swMT], Fig. 2.1C-D). We created four combinations of base pasteurized soils and inoculum from the two locations (Fig. 2.2A, e.g. swMT/cntrMT refers to a base soil from swMT combined with inoculant from cntrMT). We assessed the barley rhizosphere communities, as in the field, from a subset of 10 S2MET lines. Results demonstrated the distinct roles of the base soil and the locally available soil microbiome in shaping rhizosphere communities.

Rhizosphere compositions shifted in response to the base soil but also remained distinct depending on inoculum source (Fig. 2.2B). These differences were indicated by distinct indicator taxa and functions (Fig. 2.2C-D). Functions associated with nitrogen fixation, cellulolysis, and aromatic hydrocarbon degradation were more abundant in swMT/swMT relative to the other treatments (Fig. 2.2D). Chitinolysis and functions related to arsenate including arsenate detoxification and dissimilatory arsenate reduction were more abundant with cntrMT inoculum compared to swMT. We also detected soil source effects on functions in the rhizosphere

community with greater abundance of functions related to nitrogen cycling, fermentation, and anaerobic chemoheterotrophy in cntrMT soil.

We examined whether these microbiome-shaping contexts of base soil and inoculum interact to drive differences in plant growth. Plant growth varied most strongly due to inoculant within the context of base soil (Fig. 2.2E-F). The cntrMT base soil with swMT inoculant resulted in the greatest biomass (Fig. 2.2E) and manganese oxidation was more abundant in this treatment (Fig. 2.2D). Field soil tests showed that manganese was >2.5-fold higher in cntrMT than swMT, revealing a potential base soil-inoculum interaction resulting in greater abundance of manganese oxidation functions with cntrMT soil regardless of inoculum source. These results align with the concept of optimizing the rhizosphere microbial environment for improved plant performance.

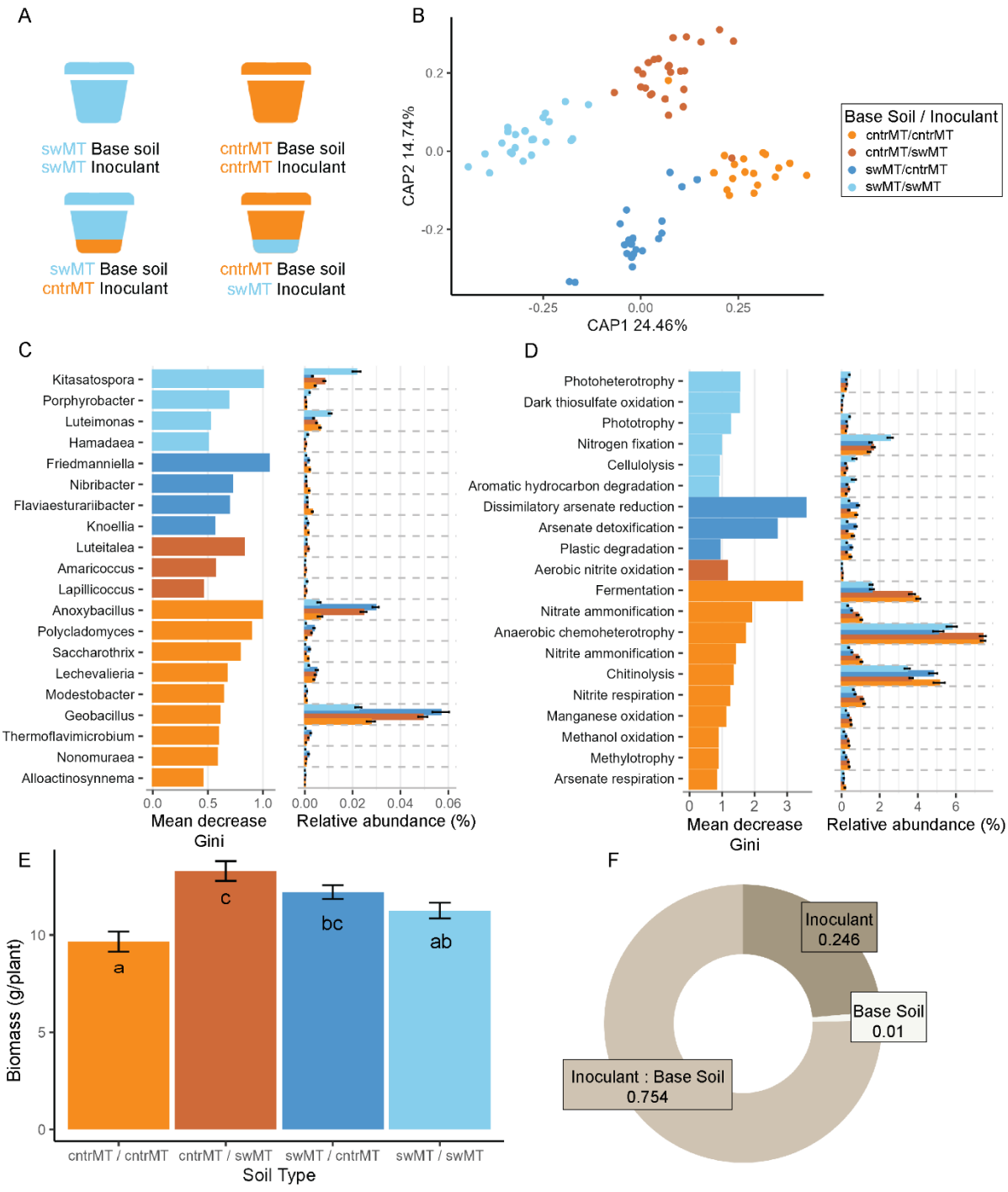

Figure 2.2. Impact of Soil Treatments on Rhizosphere Microbiome Composition and Barley Biomass (A) Soil treatments for greenhouse experiments are shown. (B) Constrained analysis of principal coordinates (CAP) of the weighted unifrac distances of the rhizosphere bacterial

communities based on the base soil and inoculant (PERMANOVA, $r^2 = 0.42$, $p < 0.001$) is displayed. Differentially abundant genera (C) and functions (D) predicted by a random forest model with a Mean Decrease Gini (MDA) threshold of 10. Functions were predicted from 16S sequences using the functional annotation of prokaryotic taxa (FAPROTAX) database. (E) Barley dry biomass at harvest across soil treatments. (F) Variance partitioning of the effects of base soil, inoculant, and their interaction on barley dry biomass. cntrMT: central Montana, swMT: southwest Montana.

Substantial overlap of genetic architecture contributing to microbial and agronomic traits

Returning to the field study, we investigated the contribution of barley genetic variation to interactions with the rhizosphere community. We considered the microbes sequenced from the barley rhizospheres as extended phenotypes[35] of each line for analysis in our Genome Wide Association Study (GWAS). We defined these extended phenotypes or 'microbial traits' as the normalized abundances of prevalent taxa (observed in at least 80% of lines) found in each location-year, calculated at each taxonomic rank (Fig. 2.2A). Most prevalent taxa met this requirement in most location-years, with Hawaii showing the least amount of overlap with other sites. A total of 351 microbial traits and 12 agronomic traits across the seven location-years were explored. The heritability of the 1228 total microbial trait by location-year combinations ranged from 0.000 to 0.974, where 30% had heritability of 0.3 or greater and 43% had heritability of 0 (Table A2.2). We detected a total of 637 microbial trait GWAS associations (Table A2.3).

The patterns of microbial trait QTL were consistent with pleiotropy or tight linkage and GxE underpinning their genetic architecture. We identified several hotspots where consecutive associations of microbial traits were not more than 1Mbp apart[36] (Fig. 2.3A). A 1.48Mbp hotspot on chromosome 3H exhibited 24 associations with microbial traits, 21 of which were from cntrMT 2022, and a 0.5Mbp hotspot spanning two markers on 6H exhibited 28 microbial trait

associations, all from swMT 2021. We also identified a supercluster of QTL on 5H that included 24 microbial trait associations across five QTL and 37.4Mbp (Fig. 2.3A, B). Each of the seven location-years was represented within this supercluster in a subset of the QTL; however, QTL varied between every location-year, consistent with GxE underlying microbial trait associations (Fig. 2.3B).

In total, we observed varying numbers of microbial trait QTL across our seven field trial data sets. No microbial hotspot was detected in every location-year (Fig. S2B), and 67 (51%) appeared in only one location-year, further supporting extensive GxE. For the adapted locations only, we screened the microbial trait QTL to identify whether the same microbial trait mapped to the same locus (within 1Mbp) in multiple location-years. We identified only four instances (Table A2.3). Altogether, the rhizosphere microbial traits in the S2MET population were sensitive to both genetic and environmental control.

Of particular interest were microbial trait loci that may also be associated with agronomic traits, which would be consistent with a role of the microbial taxon influencing plant traits facilitating adaptation[33,37]. In addition to scanning GWAS results for microbial and agronomic trait associations within 1Mbp of each other[36], we also used Wilcoxon's signed-rank tests to examine whether microbial trait QTL alleles were associated with agronomic traits. Together, these approaches uncovered 413 significant associations between microbial related loci or markers and agronomic traits across location-year combinations after multiple testing correction[38]. Within those associations, 30 loci were associated with at least one microbial trait and one agronomic trait coming from the same location-year (Fig. 2.3C). Like previous studies[39], we found abundance differences between bulk and rhizosphere samples for microbes associated

with these loci (Fig. A2.3, Table A2.4). Leveraging such connections between microbial traits and agronomic traits may advance genetic and agronomic gain within target environments[40].

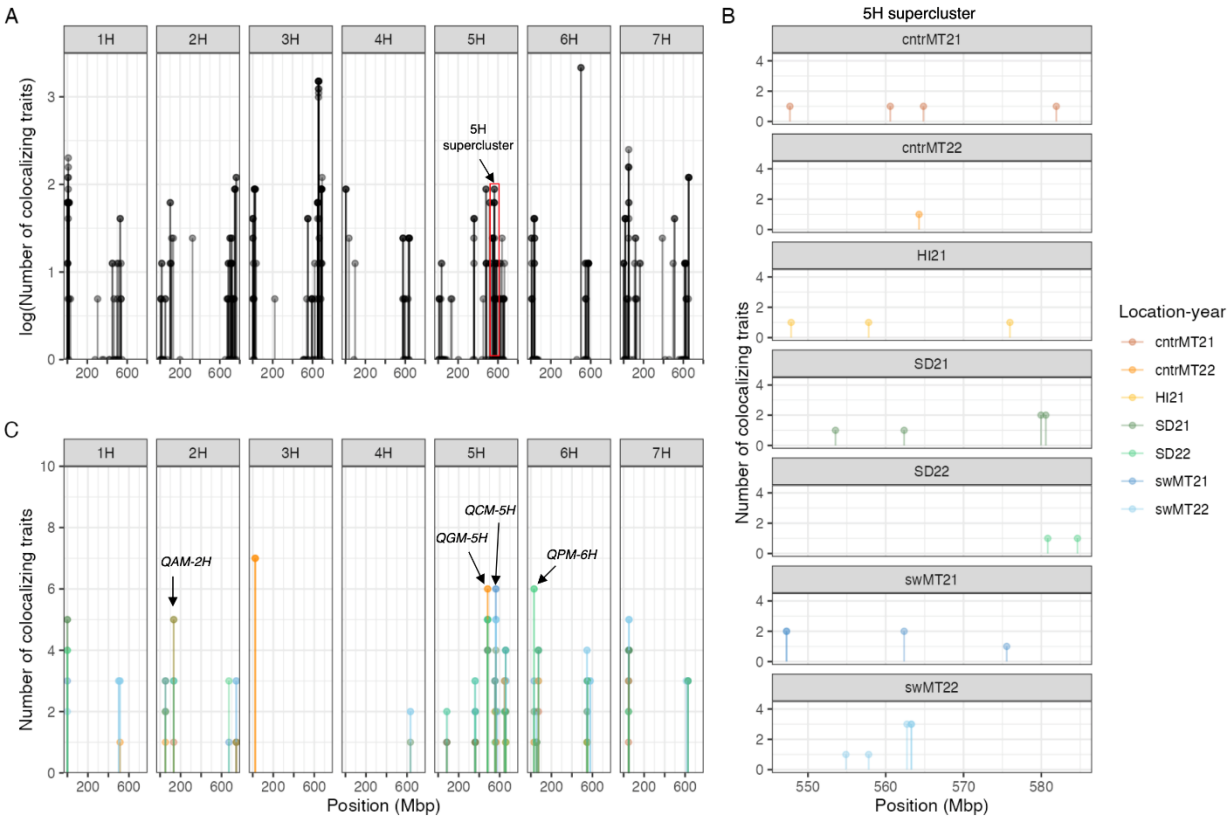

Figure 2.3. GWAS reveals genetic architecture of microbial and agronomic traits across field trials. (A) The genomic location and number of significant GWAS hits within 1Mbp across microbial traits for all locations are shown. (B) 5H supercluster GWAS QTL for microbial traits for each location year. (C) Colocalization within 1Mbp of microbial and agronomic trait associations from GWAS and Wilcoxon's tests are shown across genomic position, with the location-year of mapping indicated by color. QTL selected for in-depth consideration are indicated.

Evaluation of loci with colocalized agronomic and microbial traits

We examined the 30 loci for patterns of pleiotropy/tight linkage and environmental sensitivity for the microbial and agronomic traits (Table A2.5). Loci associated with a single microbial trait in one location-year in conjunction with multiple agronomic traits from multiple location-years comprised the most common pattern observed (at 11 loci), reflecting stability and pleiotropy/linkage at the locus for agronomic traits but environmental sensitivity and specificity for the microbial trait. The second most common pattern (at 9 loci) reflected pleiotropy/linkage and stability for agronomic traits and only pleiotropy/linkage for microbial traits. We observed three instances where a single microbial trait was associated with a single agronomic trait within a location-year.

We concentrated on loci with agronomic associations in multiple environments and associations with multiple microbes (Fig. 2.3C, Fig. 2.4). At *QAM-2H*, with "A" for "all and agronomic", we mapped agronomic traits at all locations. Four microbial traits were mapped in either cntrMT22 or SD21, and six agronomic traits were associated across all six locations-years outside Hawaii. The minor allele was associated with greater abundance of three microbial traits in cntrMT22, while grain fill duration and heading date did not colocalize at this locus for cntrMT but did for the other location-years. The presence/absence of plant genetic associations to these taxa in different locations are consistent with the associated microbes contributing to local adaptation. These effects are also consistent with conditional neutrality, where the effect of a QTL is dependent on the environment or genetic background. Conditional neutrality has been associated with local adaptation in a range of species, including barley[29,41,42].

We examined root gene expression of candidate genes at the QTL for variation in microbiome composition using previously published data[43]. For *QAM-2H* across the 18 genes located up to 1 Mbp up- and downstream, expression could be assessed for eight candidates. Of those expressed, one candidate of interest was identified based on function and expression level (Table A2.6). *HORVU.MOREX.r3.2HG0127420* was more highly expressed in roots than the other candidate genes. It encodes an anthocyanidin reductase-like protein that contributes to the biosynthesis of flavan-3-ols and proanthocyanidins, secondary metabolites that influence root-microbe interactions[44].

At the three other candidate QTL, we noted that most highly expressed candidate genes all have roles in plant cell death. *QGM-5H*, with "G" for "grain fill", associated with grain fill in five location-years and three other agronomic traits across multiple location-years alongside two microbial taxa in SD21. The most highly expressed gene at this locus *HORVU.MOREX.r3.5HG0480100* which encodes a papain-like cysteine protease which are associated with plant senescence[45] as well as plant-pathogen interactions[46]. *QPM-6H*, with "P" for prevalence, associated with four microbial taxa that were highly prevalent at the phyla or class level in SD22. This locus includes RPM1, the canonical pathogen resistance gene[47] and the most expressed gene encodes BAX INHIBITOR 1, a highly conserved regulator of cell death[48]. Finally, *QCM-5H*, with "C" for a cluster of associations, was within the 5H supercluster of mapped traits and corroborates a previously mapped barley rhizosphere QTL[38]. We found four microbial traits and six agronomic traits here, with expressed genes related to programmed cell death, immunity, and production of a microbial carbon resource, *N*-acetylglucosamine[49].

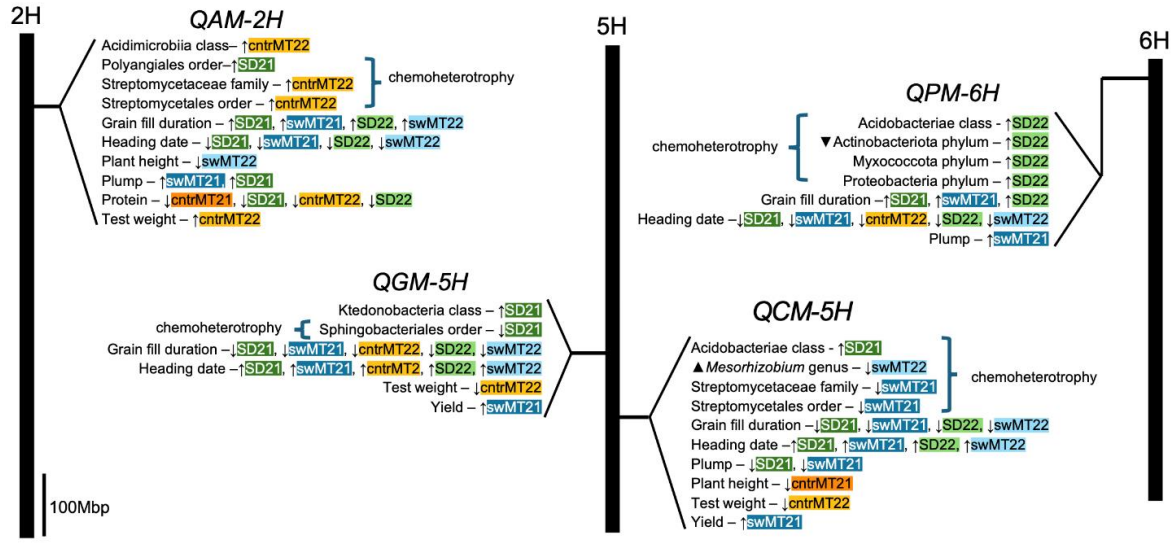

Fig. 2.4. Effects at highlighted QTL suggest candidate genes underlying plant-microbe interactions. The genomic location of four QTL with colocalizing microbial and agronomic traits. All trait by location-year combinations mapping to that locus are indicated. Curly braces indicate microbial function annotated with FAPROTAX. Arrows indicate the effect of the minor allele, positive (↑) or negative (↓). Arrow heads indicate enrichment (▲) or depletion (▼) in the rhizosphere versus bulk soil of microbial taxa as determined with DESeq2. For QHM-5H, the minor allele effect for Sphingobacteriales is shown specifically for SNP 5H_482526703 as the microbial trait mapped to multiple SNPs in this QTL and the direction of effect changed as the between major and minor allele throughout this QTL.

Discussion

We have expanded our understanding of plant genetic relationships with the rhizosphere microbiome, evaluated the association of those relationships with fitness traits targeted by breeding, and explored the role that environment plays in those interactions. Previous studies have demonstrated that plant recruitment of rhizosphere microorganisms varies with environmental factors[39,50]. We provide insight into the genetic variation that enables microbiome recruitment across and within environments. Consistent with local soil environmental effects[51,52], barley recruited distinct rhizosphere communities across and outside of its adapted range that nonetheless were locally consistent across years (Fig. 2.1B). This local rhizosphere variation

could be partitioned into components of abiotic soil properties and the background soil microbiome (Fig. 2.2B, C, D), which interacted to drive both rhizosphere variation and plant growth. Specifically, novel combinations of biotic and abiotic soil properties enhanced plant growth (Fig. 2.2E). Finally, rhizosphere compositions were mappable and colocalized with plant traits that suggest adaptation to local conditions. Together, these findings are consistent with the manipulation of microbial communities for specific environments to maximize plant productivity[53].

Since rhizosphere microbiomes assembled from the surrounding soil impact plants, and plants influence this assembly[21,22,37], cultivation of beneficial microbiomes through plant breeding is a logical next step. The sensitivity of the microbial community structure to environmental factors and interactions within the community makes genetic dissection challenging[22]. Nonetheless, we identified microbial associated genetic loci (Fig. 2.3A) in seven field environments (Table A2.1). Just over half of the loci were specific to a single field trial (Table A2.3), indicating GxE that could contribute to local adaptation[26,39,54,55]. We also found many loci associated with microbial traits across multiple field trials (Fig. A2.2B), though rarely with the same microbe, potentially reflecting high levels of functional redundancy among soil-born bacterial taxa[56]. Loci mapped repeatedly over multiple environments have potential for broad deployment in crop breeding to improve rhizosphere community composition[40,57]. The co-localizations of microbial traits between field trials as well as with QTL identified in previous barley rhizosphere microbiome mapping[38] lend confidence to the associations reported here.

Through extensive documentation of plant performance alongside the rhizosphere microbiome characterizations in multiple environments, we linked agronomic and microbial traits to the same genetic loci (Fig. 2.3C, Fig. 2.4) expanding on previous studies[17,26,38,40]. Patterns occurring at loci such as *QAM-2H* suggest that the impact of a genotype on plant fitness is changed upon encountering the right combination of environment and microbial taxa (Fig. 2.4). Greater relative abundance of a certain microbial taxon occurring during early host development might prime the plant for later success, or the genetic basis for a plant phenotype that impacts the relative abundance of certain microbial taxa might in turn improve plant fitness.

This pervasive co-localization of loci associated with microbial traits and with agronomic traits suggests a link between rhizospheric bacterial community composition and crop performance. Such co-localizations can arise from genetic linkage or pleiotropy. At several loci, we found clear connections to candidate genes with annotations which would facilitate rhizosphere interactions (Table S6), including pathogen response or perception and the production of root exudates. This aligns with candidate gene functions identified in similar QTL studies[22-24,39].

Disentangling the interconnected influences of plant genetics, microbiomes, and abiotic factors to identify cause and effect is a significant challenge[58], but when addressed will enable selection for microbial traits through breeding. Our results suggest that the general ability to conditionally recruit beneficial taxa under local soil and weather conditions is a viable pathway toward breeding for microbiomes beneficial to crop production. The loci we identified and the aboveground variation we observed together are consistent with conditional, adaptive recruitment by specific barley genotypes in response to local environments. Selecting plant

genotypes for conditional recruitment complements other strategies of engineering rhizospheres through inoculation[59] or selection for specific plant-microbe relationships[17], as it leverages the dynamic and variable microbial taxa that plant genotypes are expected to experience across their adaptive ranges. As knowledge of GxE controls on plant-microbe interactions develops, this strategy may prove more feasible at scale for developing productive and stress tolerant crop varieties.

Acknowledgements

The authors thank the Hawaii Agricultural Research and the Montana State Agricultural Experiment Stations. This work was supported by the United States Department of Agriculture (USDA) National Institute of Food and Agriculture (NIFA) Agriculture and Food Research Initiative (AFRI) award number 2020-67014-32138. Computational efforts were performed on the Tempest High Performance Computing System, operated and supported by University Information Technology Research Cyberinfrastructure at Montana State University. Mention of trade names or commercial products in this publication is solely for the purpose of providing specific information and does not imply recommendation or endorsement by the U.S. Department of Agriculture. The USDA is an equal opportunity provider and employer.

Materials and Methods

Plant materials and genotyping

We explored the S2MET Barley Mapping Population to understand the effect of the interaction between genotype and microbiome on performance. The S2MET panel includes lines from breeding programs at USDA-ARS Aberdeen in ID, University of Minnesota, Montana State

University, North Dakota State University, and Washington State University. It was previously genotyped by sequencing[28] and mapped to the MorexV1, IBSCv2 barley reference genome[43], and genotyping data is publicly available[60]. After matching the genotyping data to the subset of S2MET lines that were included in the current experiments, markers with a minor allele frequency (MAF) less than 5% were removed from the dataset. This left 4,787 single nucleotide polymorphism (SNP) markers that were used in the genome-wide association study (GWAS).

Field trial experimental design

Fields trials were performed in 2021 and 2022 at the Post Research Farm in Bozeman, MT (southwest Montana-swMT), the Central Agricultural Research Center in Moccasin, MT (central Montana-cntrMT), Brookings, South Dakota (SD), and in 2021 in Kunia, Hawaii (HI) (Table S1). An augmented randomized complete block design[61] was used for the field trials in which each of the 232 experimental lines appeared once in the trial at each location, and four barley check varieties (Odyssey, Hockett, Lavina, and Merit 57) appeared at random positions in each of twelve blocks. Standard agronomic practices for each region were used for fertility and pest management.

Field trial phenotyping

The barley population was assessed for various agronomic traits in the field trials. Heading and maturity dates (stages 59 and 89 on the Zadoks cereal growth scale[62]) were noted when seed heads were visible for half of the plants in a plot and when half of the seed heads had lost green color respectively. Duration of the grain fill period was calculated by subtracting heading date from maturity date. Plant height was measured after maturity from the base of the plant to the top of the seed head. After the plants had dried, three 6 in. sections were hand cut

from each plot and weighed for total biomass. Seed heads from these samples were counted to measure productive tiller number and were removed and threshed. The weight of this seed was divided by the total biomass to calculate harvest index. Full plots were harvested by combine after grain ripening, and seed was weighed for gross yield calculations. Test weight, percent plump grain, and percent grain protein were measured on cleaned grain samples from each plot. In Hawaii accessions remained vegetative, thus only total biomass was measured.

Field trial 16S sequencing

The rhizosphere was sampled at early stem elongation as previously described[63]. Briefly, 3-5 plants with intact roots were removed from each plot for a composite sample. Following collection, samples were transported on ice to the laboratory and stored at +4°C until rhizosphere isolation within 24 hours. For rhizosphere isolation, plant roots with attached soil were separated from shoots and placed on ice. 1% NaCl was added, samples were vortexed, and treated in a sonicating water bath for 1 min. Roots were removed and the remaining soil solution was centrifuged for 2 min at 2000 × g, decanted and the remaining soil pellet was resuspended in sterile DI or RO H_2O and stored at −80°C until DNA extractions were performed. Bulk soil (0-15 cm) samples were also collected at the time of rhizosphere sampling. DNA was purified from rhizosphere extracts and bulk soil using a QIAGEN DNeasy PowerSoil Pro DNA Isolation Kit (QIAGEN Inc., Germantown, MD, USA). Purified DNA was submitted to Integrated Microbiome Resource (Dalhousie University, Halifax, NS) for library preparation and amplicon sequencing of the bacterial 16S V6-V8 regions. Sequencing was performed on the Illumina MiSeq platform (Illumina, San Diego, CA, USA) using a 2x250 PE kit.

Bacterial community analysis

Quality filtering, trimming, chimera removal, and assembly of reads into error-corrected amplicon sequence variants (ASVs) was performed in R using the Dada2 package[64,65]. First, reads were trimmed to remove low quality sequences. Demultiplexed reads were trimmed by 5 bases from the beginning of each read, then each location-year was trimmed to retain reads with a quality score greater than 30. On average, forward and reverse reads were trimmed to 250 and 180 bases respectively. Only forward reads were used for downstream analysis due to low quality reverse reads. In all location-years except Hawaii 2021, filtering and trimming were performed with the default settings for the Dada2 pipeline. Reads from Hawaii were filtered with maximum expected error rate of 10, versus 2 at other location-years. Taxonomic assignment was performed using the SILVA v138.1 SSU database with a 99% identity- threshold[66]. Predictive functional profiling was performed by functional annotation of prokaryotic taxa (FAPROTAX)[67] as implemented in the microeco package[68].

Statistical analyses and data visualization were performed using phyloseq[69], microeco[68], and ggplot2[70] packages. Relative abundances of major taxa were visualized at the phylum level using a 1% average relative abundance threshold. To gain insight into differences between rhizosphere communities across different environments, we performed constrained analysis of principle coordinates (CAP) using the weighted unifrac distances, which accounts for phylogenetic distances between taxa within the community[71]. We constrained distances by site-year and tested this model using PERMANOVA. The model explained 13.4% of variation: 12.5% by location, 0.3% by year, and 0.6% by the interaction of location and year. A supervised random forest machine learning approach was used to identify indicator taxa associated with specific locations[72].

Greenhouse study

For the greenhouse study, barley lines were selected to compare those that were environmentally responsive versus unresponsive based on their relative yield performance in 2021 between the southwest and central Montana locations field studies [29]. Three lines each were selected for performing well at a single location (cntrMT or swMT), and four lines were selected for performing consistently across both locations.

The ten selected barley lines were grown under four soil conditions consisting of soil and inoculant from Post Farm in southwestern Montana or CARC in central Montana in a fully factorial design. Each pot contained 80% by volume of pasteurized field soil from either Bozeman, MT (swMT) or Moccasin, MT (cntrMT) to represent base soil. Ten percent by volume contained non-pasteurized soil from one field acting as the microbial inoculant. The final ten percent of each pot by volume contained pasteurized sand to increase water filtration and pore space for roots[73]. Each line and soil condition combination was replicated six times. All pots were watered every two days. Twice a week during watering, Peters Professional 20-20-20 fertilizer G99290 was added to the water at a concentration of 200 ppm nitrogen. Three replicates were removed at stem elongation to collect rhizosphere samples. Three replicates were grown to maturity.

Rhizosphere sampling and DNA purification was completed using the same protocols to the field samples. Purified DNA was submitted to Novogene (Sacramento, CA) for library preparation and amplicon sequencing of the bacterial 16S V4-V5 regions. Sequencing was performed on the paired-end Illumina platform. Library quality was evaluated using an Agilent Fragment Analyzer (Agilent, Santa Clara, CA) system, while effective library concentration was determined by qPCR. Microbial community analysis was performed as described above. To

compare soil environments in the greenhouse we performed a constrained analysis of principle coordinates (CAP) using the weighted unifrac distances similarly to the field microbiome data. We constrained distances by base soil and inoculant and tested this model using PERMANOVA. The model explained 42% of variation: 20.7% by base soil, 18.2% by inoculant, and only 2.8% by the interaction of base soil and inoculant.

Phenotypic Data Preparation for Genetic Analysis

Relative abundances of bacterial taxa in the rhizosphere samples were considered microbial traits of the plants and were prepared for analysis as follows. ASV read counts from each barley field plot were first agglomerated at each of the taxonomic ranks from phylum to genus. Following agglomeration at each rank and for ASVs themselves, only taxa with counts of at least one in at least 80% of rhizosphere samples within a location-year dataset were considered prevalent and retained for further processing and analysis. Centered log ratio (CLR) transformations[74] were performed on all taxa counts using the "compositions" R package[75], after first replacing counts of 0 with the small value of 0.000001. This transforms taxon counts into relative abundance representations that are comparable between samples[76].

Variance was partitioned using the R package, lmerTest[77] by fitting the following linear model for each taxon abundance:

$$Y_{ijk} = m + Checks_i + Block_j + Genotype_k + e_{ijk}$$

where $Checks_i$ was a fixed effect representing the replicated check varieties, $Block_j$ was a random effect, and $Genotype_k$ was a random effect representing the experimental barley lines from the S2MET population. The percentage of the total variance due genotype was calculated to determine heritability[78]. Microbial traits were not included in the GWAS if their heritability was

0. Then the percentage of total variance due to block was also determined and if this value was greater than 0, Best Linear Unbiased Predictions (BLUPs) were calculated for the trait to account for spatial variation within the fields by utilizing the augmented experimental design[79]. Coefficients of the $Genotype_k$ factor corresponding to each barley line were the BLUPs used as input for GWAS analysis. If the Block effect was 0, centered log ratio transformed values were used for genetic mapping of the trait without calculating BLUPs. The workflow for preparing microbial trait data for the GWAS is summarized in Fig. S4.

Genome Wide Association Studies

Genetic mapping was carried out in the program GAPIT using the FarmCPU model[80]. Two principal components were used to account for population structure in addition to adjustments using the kinship matrix produced by GAPIT, and these parameters appeared to provide appropriately fit models for traits when examining QQ plots. The significance threshold for trait marker associations was based on a value of $\alpha = 0.2$. For all microbial trait SNPs passing the GWAS significance threshold, Wilcoxon signed rank tests were performed to compare the effects of the major and minor alleles (homozygous) on each agronomic trait. Significance was determined with a Bonferroni correction ($P < 1.82909 \times 10^{-6}$).

Candidate gene annotation and expression

Four of the QTL for which both microbe and agronomic traits were detected were examined for candidate genes. The physical positions of these QTL were mapped with the barley IBSCv2 reference genome; therefore, gene names and associated unspliced gene DNA sequences +/- 1Mbp of the QTL regions were determined using BioMart from the Ensembl Plant release 37 (October 2017). BarleyMap[81] was used to align the DNA sequences with the barley MorexV3

genome[82] and extract gene names and annotations. Gene names were used to extract root expression data (FPKM)[43] using the BarleyExpDB[83].

Data Availability

The raw data for 16S rRNA sequencing are available in the NCBI Sequence Read Archive database under BioProject PRJNA909304.

Code availability

Code is available at https://github.com/erikthekillian/Uncovering-genetic-linkages-in-the-rhizosphere-contributing-to-adaptation.

References

1 Pii, Y. *et al.* Microbial interactions in the rhizosphere: beneficial influences of plant growth-promoting rhizobacteria on nutrient acquisition process. A review. *Biology and Fertility of Soils* **51**, 403-415 (2015).

2 Rosenblueth, M. *et al.* Nitrogen fixation in cereals. *Frontiers in Microbiology* **9**, 1794 (2018).

3 Babalola, O. O. *et al.* Rhizosphere microbiome cooperations: strategies for sustainable crop production. *Current Microbiology* **78**, 1069-1085 (2021).

4 Mendes, R. *et al.* Deciphering the rhizosphere microbiome for disease-suppressive bacteria. *Science* **332**, 1097-1100 (2011).

5 Castrillo, G. *et al.* Root microbiota drive direct integration of phosphate stress and immunity. *Nature* **543**, 513-518 (2017).

6 Mayak, S., Tirosh, T. & Glick, B. R. Plant growth-promoting bacteria that confer resistance to water stress in tomatoes and peppers. *Plant Science* **166**, 525-530 (2004).

7 Poudel, M. *et al.* The role of plant-associated bacteria, fungi, and viruses in drought stress mitigation. *Frontiers in Microbiology* **12**, 743512 (2021).

8 Zhang, J., Liu, W., Bu, J., Lin, Y. & Bai, Y. Host genetics regulate the plant microbiome. *Current Opinion in Microbiology* **72**, 102268 (2023).

9 Alori, E. T., Dare, M. O. & Babalola, O. O. Microbial inoculants for soil quality and plant health. *Sustainable Agriculture Reviews*, 281-307 (2017).

10 Kaminsky, L. M., Trexler, R. V., Malik, R. J., Hockett, K. L. & Bell, T. H. The inherent conflicts in developing soil microbial inoculants. *Trends in Biotechnology* **37**, 140-151 (2019).

11 Clouse, K. M. & Wagner, M. R. Plant genetics as a tool for manipulating crop microbiomes: Opportunities and challenges. *Frontiers in Bioengineering and Biotechnology* **9**, 567548 (2021).

12 Contreras-Liza, S. E. *Plant Breeding and Microbiome*. (IntechOpen, 2021).

13 Gopal, M. & Gupta, A. Microbiome selection could spur next-generation plant breeding strategies. *Frontiers in Microbiology* **7**, 1971 (2016).

14 Ahkami, A. H. *et al.* Emerging sensing, imaging, and computational technologies to scale nano-to macroscale rhizosphere dynamics–Review and research perspectives. *Soil Biology and Biochemistry*, 109253 (2023).

15 Chepsergon, J. & Moleleki, L. N. Rhizosphere bacterial interactions and impact on plant health. *Current Opinion in Microbiology* **73**, 102297 (2023).

16 Zolti, A., Green, S. J., Sela, N., Hadar, Y. & Minz, D. The microbiome as a biosensor: functional profiles elucidate hidden stress in hosts. *Microbiome* **8**, 71 (2020).

17 He, X. *et al.* Heritable microbiome variation is correlated with source environment in locally adapted maize varieties. *Nature Plants* **10**, 598-617 (2024).

18 Trivedi, P., Leach, J. E., Tringe, S. G., Sa, T. & Singh, B. K. Plant–microbiome interactions: from community assembly to plant health. *Nature Reviews Microbiology* **18**, 607-621 (2020).

19 Bulgarelli, D., Schlaeppi, K., Spaepen, S., Van Themaat, E. V. L. & Schulze-Lefert, P. Structure and functions of the bacterial microbiota of plants. *Annual Review of Plant Biology* **64**, 807-838 (2013).

20 Peiffer, J. A. *et al.* Diversity and heritability of the maize rhizosphere microbiome under field conditions. *Proceedings of the National Academy of Sciences* **110**, 6548-6553 (2013).

21 Walters, W. A. *et al.* Large-scale replicated field study of maize rhizosphere identifies heritable microbes. *Proceedings of the National Academy of Sciences* **115**, 7368-7373 (2018).

22 Bergelson, J., Mittelstrass, J. & Horton, M. W. Characterizing both bacteria and fungi improves understanding of the Arabidopsis root microbiome. *Scientific Reports* **9**, 24 (2019).

23 Sutherland, J., Bell, T., Trexler, R. V., Carlson, J. E. & Lasky, J. R. Host genomic influence on bacterial composition in the switchgrass rhizosphere. *Molecular Ecology* **31**, 3934-3950 (2022).

24 Oyserman, B. O. *et al.* Disentangling the genetic basis of rhizosphere microbiome assembly in tomato. *Nature Communications* **13**, 3228 (2022).

25 Bano, S., Wu, X. & Zhang, X. Towards sustainable agriculture: rhizosphere microbiome engineering. *Applied Microbiology and Biotechnology*, 1-20 (2021).

26 Meier, M. A. *et al.* Association analyses of host genetics, root-colonizing microbes, and plant phenotypes under different nitrogen conditions in maize. *Elife* **11**, e75790 (2022).

27 Robertson-Albertyn, S. *et al.* Root hair mutations displace the barley rhizosphere microbiota. *Frontiers in Plant Science* **8**, 1094 (2017).

28 Neyhart, J. L. *et al.* Registration of the S2MET barley mapping population for multi-environment genomewide selection. *Journal of Plant Registrations* **13**, 270-280 (2019).

29 Ewing, P. M. *et al.* Local adaptation and broad performance are synergistic to productivity in modern barley. *Crop Science* **64**, 192-199 (2024).
30 Eberly, J. O. *et al.* Compositional profiling of the rhizosphere microbiome of Canada thistle reveals consistent patterns across the United States northern Great Plains. *Scientific Reports* **14**, 18016 (2024).
31 Ling, N., Wang, T. & Kuzyakov, Y. Rhizosphere bacteriome structure and functions. *Nature Communications* **13**, 836 (2022).
32 Zhang, L. *et al.* Maize functional requirements drive the selection of rhizobacteria under long-term fertilization practices. *New Phytologist* **242**, 1275-1288 (2024).
33 Levy, A. *et al.* Genomic features of bacterial adaptation to plants. *Nature Genetics* **50**, 138-150 (2018).
34 Yue, H. *et al.* Plant domestication shapes rhizosphere microbiome assembly and metabolic functions. *Microbiome* **11**, 70 (2023).
35 Whitham, T. G. *et al.* Community and ecosystem genetics: a consequence of the extended phenotype. *Ecology* **84**, 559-573 (2003).
36 Karki, M. *et al.* The Hessian fly resistance gene HvRHF1 is localized in an NBS-LRR gene cluster in barley. *Theoretical and Applied Genetics* **137**, 71 (2024).
37 Deng, S. *et al.* Genome wide association study reveals plant loci controlling heritability of the rhizosphere microbiome. *The ISME journal* **15**, 3181-3194 (2021).
38 Escudero-Martinez, C. *et al.* Identifying plant genes shaping microbiota composition in the barley rhizosphere. *Nature Communications* **13**, 3443 (2022).
39 Edwards, J. A. *et al.* Genetic determinants of switchgrass-root-associated microbiota in field sites spanning its natural range. *Current Biology* **33**, 1926-1938. e1926 (2023).
40 Wang, Y. *et al.* GWAS, MWAS and mGWAS provide insights into precision agriculture based on genotype-dependent microbial effects in foxtail millet. *Nature Communications* **13**, 5913 (2022).
41 Anderson, J. T., Lee, C. R., Rushworth, C. A., Colautti, R. I. & Mitchell-Olds, T. Genetic trade-offs and conditional neutrality contribute to local adaptation. *Molecular Ecology* **22**, 699-708 (2013).
42 Tiffin, P. & Ross-Ibarra, J. Advances and limits of using population genetics to understand local adaptation. *Trends in Ecology & Evolution* **29**, 673-680 (2014).
43 Mascher, M. *et al.* A chromosome conformation capture ordered sequence of the barley genome. *Nature* **544**, 427-433 (2017).
44 Hassan, S. & Mathesius, U. The role of flavonoids in root–rhizosphere signalling: opportunities and challenges for improving plant–microbe interactions. *Journal of Experimental Botany* **63**, 3429-3444 (2012).
45 Liu, H., Hu, M., Wang, Q., Cheng, L. & Zhang, Z. Role of papain-like cysteine proteases in plant development. *Frontiers in Plant Science* **9**, 1717 (2018).
46 Shindo, T. & Van Der Hoorn, R. A. Papain-like cysteine proteases: key players at molecular battlefields employed by both plants and their invaders. *Molecular Plant Pathology* **9**, 119-125 (2008).
47 Grant, M. R. *et al.* Structure of the Arabidopsis RPM1 gene enabling dual specificity disease resistance. *Science* **269**, 843-846 (1995).

48 Tang, Z. *et al.* Alleviating protein-condensation-associated damage at the endoplasmic reticulum enhances plant disease tolerance. *Cell Host & Microbe* **32**, 1552-1565. e1558 (2024).
49 Ansari, S., Kumar, V., Bhatt, D. N., Irfan, M. & Datta, A. N-acetylglucosamine sensing and metabolic engineering for attenuating human and plant pathogens. *Bioengineering* **9**, 64 (2022).
50 Khasanova, A. *et al.* Quantitative genetic-by-soil microbiome interactions in a perennial grass affect functional traits. *Proceedings of the Royal Society B* **290**, 20221350 (2023).
51 Crowther, T. W. *et al.* The global soil community and its influence on biogeochemistry. *Science* **365** (2019).
52 Delgado-Baquerizo, M. *et al.* A global atlas of the dominant bacteria found in soil. *Science* **359**, 320-325 (2018).
53 Schnitzer, S. A. *et al.* Soil microbes drive the classic plant diversity–productivity pattern. *Ecology* **92**, 296-303 (2011).
54 Petipas, R. H., Geber, M. A. & Lau, J. A. Microbe-mediated adaptation in plants. *Ecology Letters* **24**, 1302-1317 (2021).
55 Revillini, D., Gehring, C. A. & Johnson, N. C. The role of locally adapted mycorrhizas and rhizobacteria in plant–soil feedback systems. *Functional Ecology* **30**, 1086-1098 (2016).
56 Louca, S. *et al.* Function and functional redundancy in microbial systems. *Nature Ecology & Evolution* **2**, 936-943 (2018).
57 Wallace, J. G., Rodgers-Melnick, E. & Buckler, E. S. On the road to breeding 4.0: unraveling the good, the bad, and the boring of crop quantitative genomics. *Annual Review of Genetics* **52**, 421-444 (2018).
58 Zancarini, A., Westerhuis, J. A., Smilde, A. K. & Bouwmeester, H. J. Integration of omics data to unravel root microbiome recruitment. *Current Opinion in Biotechnology* **70**, 255-261 (2021).
59 Mueller, U. G. & Linksvayer, T. A. Microbiome breeding: conceptual and practical issues. *Trends in Microbiology* **30**, 997-1011 (2022).
60 Neyhart, J. L. & Smith, K. P. SNP Genotyping Data for the Barley Population in" Registration of the S2MET Barley Mapping Population for Multi-Environment Genomewide Selection". (2019).
61 Federer, W. T. Augmented designs with one-way elimination of heterogeneity. *Biometrics* **17**, 447-473 (1961).
62 Zadoks, J. C., Chang, T. T. & Konzak, C. F. A decimal code for the growth stages of cereals. *Weed Research* **14**, 415-421 (1974).
63 Bulgarelli, D. *et al.* Structure and function of the bacterial root microbiota in wild and domesticated barley. *Cell Host & Microbe* **17**, 392-403 (2015).
64 Bolyen, E. *et al.* Reproducible, interactive, scalable and extensible microbiome data science using QIIME 2. *Nature Biotechnology* **37**, 852-857 (2019).
65 Callahan, B. J., McMurdie, P. J. & Holmes, S. P. Exact sequence variants should replace operational taxonomic units in marker-gene data analysis. *The ISME Journal* **11**, 2639-2643 (2017).

66 Quast, C. *et al.* The SILVA ribosomal RNA gene database project: improved data processing and web-based tools. *Nucleic Acids Research* **41**, D590-D596 (2012).
67 Louca, S., Parfrey, L. W. & Doebeli, M. Decoupling function and taxonomy in the global ocean microbiome. *Science* **353**, 1272-1277 (2016).
68 Liu, C., Cui, Y., Li, X. & Yao, M. microeco: an R package for data mining in microbial community ecology. *FEMS Microbiology Ecology* **97**, fiaa255 (2021).
69 McMurdie, P. J. & Holmes, S. phyloseq: an R package for reproducible interactive analysis and graphics of microbiome census data. *PloS One* **8**, e61217 (2013).
70 Wickham, H., Chang, W. & Wickham, M. H. Package 'ggplot2'. *Create elegant data visualisations using the grammar of graphics. Version* **2**, 1-189 (2016).
71 Lozupone, C. A., Hamady, M., Kelley, S. T. & Knight, R. Quantitative and qualitative β diversity measures lead to different insights into factors that structure microbial communities. *Applied and Environmental Microbiology* **73**, 1576-1585 (2007).
72 Paes da Costa, D. *et al.* Soil fertility impact on recruitment and diversity of the soil microbiome in sub-humid tropical pastures in northeastern Brazil. *Scientific Reports* **14**, 3919 (2024).
73 Nandede, B. M., Raheman, H. & Kumar, G. P. Standardization of potting mix and pot volume for the production of vegetable seedlings in paper pot. *Journal of Plant Nutrition* **37**, 1214-1226 (2014).
74 Aitchison, J. The statistical analysis of compositional data. *Journal of the Royal Statistical Society: Series B (Methodological)* **44**, 139-160 (1982).
75 Van den Boogaart, K. G. & Tolosana-Delgado, R. "Compositions": a unified R package to analyze compositional data. *Computers & Geosciences* **34**, 320-338 (2008).
76 Gloor, G. B., Macklaim, J. M., Pawlowsky-Glahn, V. & Egozcue, J. J. Microbiome datasets are compositional: and this is not optional. *Frontiers in Microbiology* **8**, 2224 (2017).
77 Kuznetsova, A., Brockhoff, P. B. & Christensen, R. H. B. lmerTest package: tests in linear mixed effects models. *Journal of Statistical Software* **82** (2017).
78 Holland, J. B., Nyquist, W. E., Cervantes-Martínez, C. T. & Janick, J. Estimating and interpreting heritability for plant breeding: an update. *Plant Breeding Reviews* **22** (2003).
79 Kehel, Z., Habash, D., Gezan, S., Welham, S. & Nachit, M. Estimation of spatial trend and automatic model selection in augmented designs. *Agronomy Journal* **102**, 1542-1552 (2010).
80 Wang, J. & Zhang, Z. GAPIT version 3: boosting power and accuracy for genomic association and prediction. *Genomics, Proteomics and Bioinformatics* **19**, 629-640 (2021).
81 Cantalapiedra, C. P., Boudiar, R., Casas, A. M., Igartua, E. & Contreras-Moreira, B. BARLEYMAP: physical and genetic mapping of nucleotide sequences and annotation of surrounding loci in barley. *Molecular Breeding* **35**, 1-11 (2015).
82 Mascher, M. *et al.* Long-read sequence assembly: a technical evaluation in barley. *The Plant Cell* **33**, 1888-1906 (2021).
83 Li, T. *et al.* BarleyExpDB: an integrative gene expression database for barley. *BMC Plant Biology* **23**, 170 (2023).

CHAPTER THREE

EXPLORING ENVIRONMENTAL INFLUENCE ON THE BARLEY RHIZOSPHERE MICROBIOME

Contribution of Authors and Co-Authors

Manuscript in Chapter 3

Author: Erik Z. Killian

Contributions: performing experiments, analysis, writing.

Co-Author: Jessica L. Williams

Contributions: performing experiments, analysis, writing.

Co-Author: Anna Halpin-McCormick

Contributions: performing experiments, analysis, writing.

Co-Author: Michael B. Kantar

Contributions: conceptualization, writing.

Co-Author: Patrick E. Ewing

Contributions: conceptualization, performing experiments, writing.

Co-Author: Jamie D. Sherman

Contributions: conceptualization, analysis, writing.

Co-Author: Jennifer Lachowiec

Contributions: conceptualization, analysis, writing.

Co-Author: Jed O. Eberly

Contributions: conceptualization, analysis, writing.

Manuscript Information

Status of Manuscript:
☒ Prepared for submission to a peer-reviewed journal
☐ Officially submitted to a peer-reviewed journal
☐ Accepted by a peer-reviewed journal
☐ Published in a peer-reviewed journal

Abstract

Soil microorganisms play a critical role in nutrient cycling, pathogen suppression, and plant performance. While plant-associated microbiomes are known to vary with environmental conditions, precise microbial community changes across geographic regions remains poorly understood in agricultural crops. This study investigates the rhizosphere microbiome of barley, using a population of elite cultivars across seven location-years, to examine the effects of environmental factors on bacterial and fungal community composition. Using 16S and ITS sequencing, we characterized bacterial and fungal microbiomes across multiple locations and years, employing variance partitioning and co-occurrence network analysis to assess the impact of soil chemistry, plant genotype, and environmental factors on microbial abundance and community structure. While bacterial diversity was largely consistent across barley-growing regions, fungal communities exhibited greater variability, with location-year and climatic factors shaping their composition. Co-occurrence network analysis identified candidate hub taxa that were location-year specific, suggesting dynamic plant-microbe interactions across environments. Genetic loci associated with microbial community variation were identified, highlighting genotype-by-environment interactions. These findings underscore the complex interplay between plant genotype, environment, and microbial community assembly, providing insights into how barley recruits distinct microbial communities in the rhizosphere and the potential for optimizing plant-microbe interactions to enhance agricultural sustainability.

Introduction

Soil microorganisms comprise an abundant and complex community involved in many plant-beneficial processes. These communities are critical factors for plant and human sustainability through their functions in nutrient cycling and pathogen suppression (Wall et al., 2015). Soil serves as a primary reserve for plant-associated microbes, where bacteria and fungi impact plant performance through direct and indirect interactions with plant roots (Chepsergon & Moleleki, 2023). Plant associated microbes can improve plant performance by improving nutrient availability (Zhao et al., 2021) and suppressing plant-pathogens (H. Liu et al., 2021). The soil microbial community is primarily composed of bacteria and fungi (Fierer, 2017). Large-scale surveys show that bacteria and fungi have different patterns of composition across the globe. Across many different environments, *Proteobacteria* and *Actinobacteria* are the predominant bacterial phyla, suggesting that bacterial communities generally consist of a few dominant groups and many rarer groups (Delgado-Baquerizo et al., 2018). A global survey measured over 14,000 samples from 365 locations to compare fungal community structure as a product of soil and climate conditions. They found that fungal communities were predominated by *Ascomycota and Basidiomycota*, however variance partitioning indicated that fungal species abundance was strongly predicted by climatic and soil chemical factors (Tedersoo et al., 2014).

Plants only associate with a subset of the total soil microbial population, creating a less diverse community in the rhizosphere – the environment directly surrounding plant roots (Santoyo, 2022). Plants influence the rhizosphere microbial community through the production of carbon-rich root exudates which are used by microbes (Walker et al., 2003). Multiple mechanisms exist for microbiome recruitment. Generally, the introduction of concentrated

nutrients via root exudates induces community-level changes to filter the rhizosphere microbiome (Bulgarelli et al., 2013). In addition, the recruitment of few highly influential hub taxa can facilitate larger microbial community changes (Agler et al., 2016; Banerjee et al., 2018; Berry & Widder, 2014).

Recent studies have measured specific plant genes impacting the rhizosphere microbiome through molecular signaling and regulating compounds involved in root morphology and root exudate profiles to explain plant-microbe recruitment mechanisms (Q. Liu et al., 2023). Studies in rice (Zhang et al., 2019) and maize (Yu et al., 2021) have identified genes responsible for root exudate production to recruit beneficial microbes.

In spite of these advances, little is known regarding the impact of plant genotype on individual soil taxa (Pacheco-Moreno, 2024). Recent work has shown cultivar-driven patterns of recruitment within the rhizosphere of barley which was driven by composition of the root exudates associated with gene loci that varied between a modern cultivar and a landrace (Pacheco-Moreno, 2024). While this work provides new insight into the plant genetic component of rhizosphere microbiome recruitment, it did not compare the relative influence of environmental variability. Furthermore, the ability of a plant to recruit microbes is limited by the available soil community from which specific rhizosphere taxa are recruited, and this soil community in turn, is shaped by the environment (Coller et al., 2019). There are many unknowns regarding how these factors and plant genetics shape the rhizosphere or how they rank in importance of impact on shaping the microbial community abundance and composition.

The objectives of this study were to i) explore the rhizosphere microbial community structure of a large barley population in and outside adapted environments; ii) assess the relative

contribution of plant genetics and environmental factors in shaping the rhizosphere microbiome; iii) identify the co-occurrence patterns of key taxa across environments. To address these objectives, we leveraged a population of elite barley cultivars grown across seven location-years. Through 16S and ITS amplicon sequencing of the barley rhizosphere, we compared the bacterial and fungal microbiome across locations and years. Through variance partitioning, we estimated the relative impact of plant genetics and environmental factors on the rhizosphere microbial community abundance and composition. We further explored microbe recruitment across environments using co-occurrence networks. These results provide new insight into the contribution of environmental and plant genetic factors shaping the rhizosphere community of barley.

Results

To examine barley rhizosphere microbial communities across environments, we performed 16S and ITS amplicon sequencing of rhizosphere and bulk soil from four locations and two years of field trials. Locations represented environments included in barley breeding programs in the northern Great Plains with the exception of Hawaii, which represented an unadapted region. After cleaning and filtering, a total of 2,005 bacterial and 1,432 fungal samples were retained with a median of 28,904 and 17,225 reads per sample, respectively (Table A3.1). Fungal sequencing from southwest Montana in 2021 returned extremely low reads per sample, so were removed from fungal analyses.

Bacterial rhizosphere community is consistent across location-years.

First, we compared the overall structure and diversity of the soil bacterial communities across locations and years. Alpha-diversity was significantly different across locations and years, but among Montana and South Dakota locations the average Shannon diversity was consistent, with values between five and six (Fig. 3.1A). Hawaii had significantly lower Shannon diversity compared to all other locations (Wilcox, $p < 0.001$, Table A3.2). To understand the composition of each location-year we compared bacteria at the phylum level. Actinobacteria was the most abundant phylum across all location-years; however, in Hawaii Actinobacteria represented 75% of bacteria in most rhizosphere samples, consistently more than any other location-year (Fig. 3.1B).

To further assess the differences between locations within barley growing regions we performed constrained principal coordinates analysis, incorporating potential environmental factors that contribute to microbial composition (Fig. 3.1C). The lack of explanatory power by location-year and soil factors demonstrates the similarity of bacterial communities examined. Potassium, organic matter, and nitrate concentrations explained the most variation (CAP 1, 1.45%); however, the first two principal coordinates only explain 2.19% of the variability in bacterial communities (Fig. 3.1C). Variability in South Dakota 2021 samples was due to variation in pH across trial blocks (Fig. A3.1).

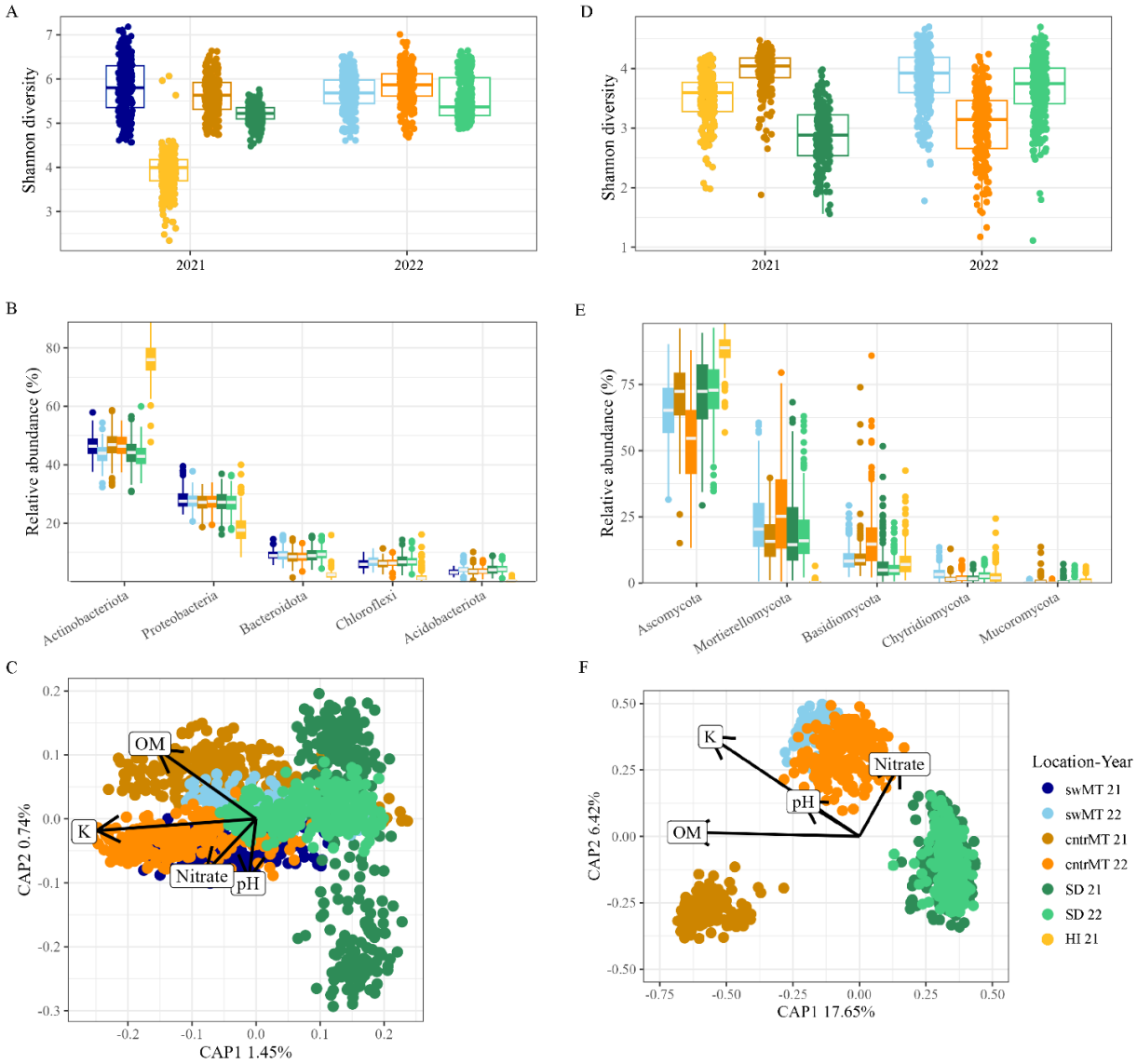

Figure 3.1: Summary of diversity in bacterial and fungal reads across location-years. (A) Shannon diversity of bacterial community structure. (B) Phylum relative abundance of bacteria across location-years. (C) Constrained ordination of bacterial communities by soil chemistry factors. Variation between location-years was significant and greater than variation within location-year (PERMANOVA, p = 0.0002, F = 10.32). (D) Shannon diversity of fungal community structure. (E) Phylum relative abundance of fungi across location-years. (F) Constrained ordination of fungal communities by soil chemistry factors. Variation between location-years was significant and greater than variation within location-years (PERMANOVA, p = 0.0002, F = 197.48).

Fungal communities are sensitive to environmental factors.

Fungal community diversity was variable across location-years, both within and between location-years (Fig. 3.1D, Table A3.3). Shannon diversity varied significantly more in fungi samples than bacteria within the same location-year across most Montana and South Dakota location-years (Table A3.4). Abundant phyla were also observed to vary within and between location-years in fungal samples (Fig. 3.1E). Constrained principal coordinate analysis showed that the first two principal coordinates explained over 24.07% of variation in fungal communities (Fig. 3.1F).

Due to the overall similarity of the barley microbiome across growing locations, we estimated the sources of variability underlying the abundance of each genus across samples. We used variance partitioning to calculate the proportion of total variance (termed "variance scores") attributed to potential explanatory factors for rhizosphere ASVs as previously described (Meier et al., 2021; Tedersoo et al., 2014). ASVs were filtered with a relative abundance threshold of 0.005% and prevalence threshold of 10%, resulting in a total of 667 ASVs from 72 genera in bacteria and 452 ASVs from 181 genera in fungi. Variance partitioning factors included location-year and soil chemistry (pH, OM, NO_3^-, K_2O). To estimate the relative importance of location-year and each soil factor in shaping the rhizosphere microbiome composition, ASVs were ranked by variance score, and only ASVs above a five percent variance explained threshold were retained (Meier et al., 2021).

Partitioning by ASV revealed soil
and location-year effects in bacteria.

In bacteria, location-year explained over five percent variance in 37% or 250 of ASVs, with maximum variance explained of 41% (Fig. 3.2A). Soil chemistry factors also explained

variance at the ASV level, up to 21%. Potassium concentration explained over 5% abundance variability in 13% or 88 of prevalent ASVs. Likewise, pH and organic matter explained over 5% abundance variability in 40 and 48 ASVs respectively. Together, soil chemistry factors explained 146 unique ASVs, with most taxa only significantly explained by one chemistry factor (Table A3.5).

We also examined the sources of variance affecting fungal community abundance using variance partitioning on fungal ASVs. Fungal ASV abundance was most determined by location-year. Similar to bacteria, most fungal ASVs abundance variances were not associated with soil chemistry factors (Fig. 3.2B, Table A3.6). This suggests that while some fungi are responsive to soil chemistry, the abundance of most fungal community members are determined by environment.

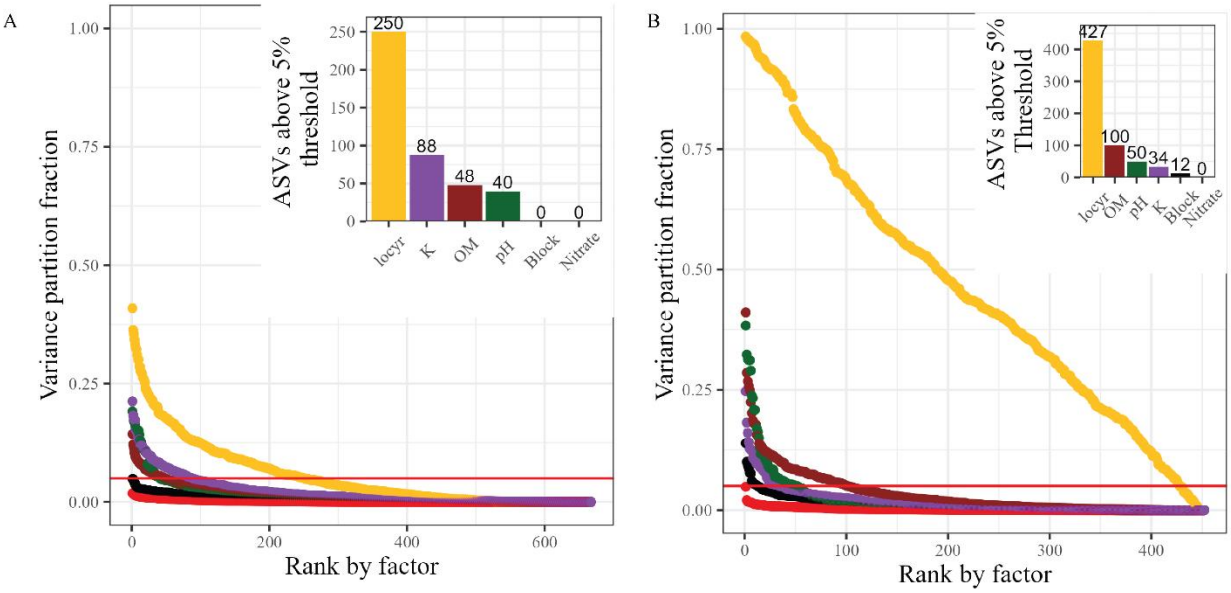

Figure 3.2: Variance partitioning for microbial ASV abundances. A linear model was calculated per genus as fixed qualitative and random categorical variables (~ pH + OM + K + Nitrate + (1|locyr) + (1|Block)). (A) Bacterial ASV abundance variance is more explained by environment and plant genotype than when averaged to genus. (B) Variance partitioning by fungal ASVs were

significantly explained by location-year, echoing the location-year variability found with constrained principal coordinate analysis.

Bacteria network ASV are conserved, however hub taxa are rarely consistent across location or year.

Finding specific ASVs variable by environmental factors, we next examined whether the microbiome network structure varied across location-years. Co-occurrence networks were built within each location-year using the same subset of 667 prevalent ASVs used for variance partitioning (Fig. A3.2). In bacteria, we found that co-occurrence networks were built from a consistent group of ASVs (Fig. 3.3A). Most were present in-network across a majority of location-years.

We classified hub taxa that could be responsible for creating defining networks of microbes. Hub taxa were defined using hub score, originally defined for hyperlink networks and commonly used in rhizosphere network analysis (Kleinberg, 1999; Layeghifard et al., 2017). Scores represent relative interconnectivity of nodes in a network, where hub taxa have many connections to other highly connected taxa. Between 6-40 hubs were identified across location-years. Interestingly, we found that hub taxa were unique to each network and rarely identified as a hub in more than one network (Fig. 3.3B).

Though hubs varied, network structure was consistent across location-years and showed similar patterns to other soil rhizosphere microbiome studies in that most nodes were only directly correlated with a few other nodes, while a small subset of nodes was correlated with many nodes, measured by network degree (Agler et al., 2016; Edwards et al., 2015)(Fig. A3.2).

This pattern of a relative minority of nodes that are highly connected to the broader network was consistent across network parameters (Fig. 3.3C).

Fungal network parameters were similar to bacterial co-occurrence networks, showing few highly connected nodes (Fig. 3.4C). Specifically, degree and betweenness centrality were commonly low in networks with high interconnectivity being rarer among nodes. We found that the majority of ASVs in fungal co-occurrence networks were unique to a single location-year network (Fig. 3.4A). Further, hub taxa were also unique to fungal networks (Fig. 3.4B).

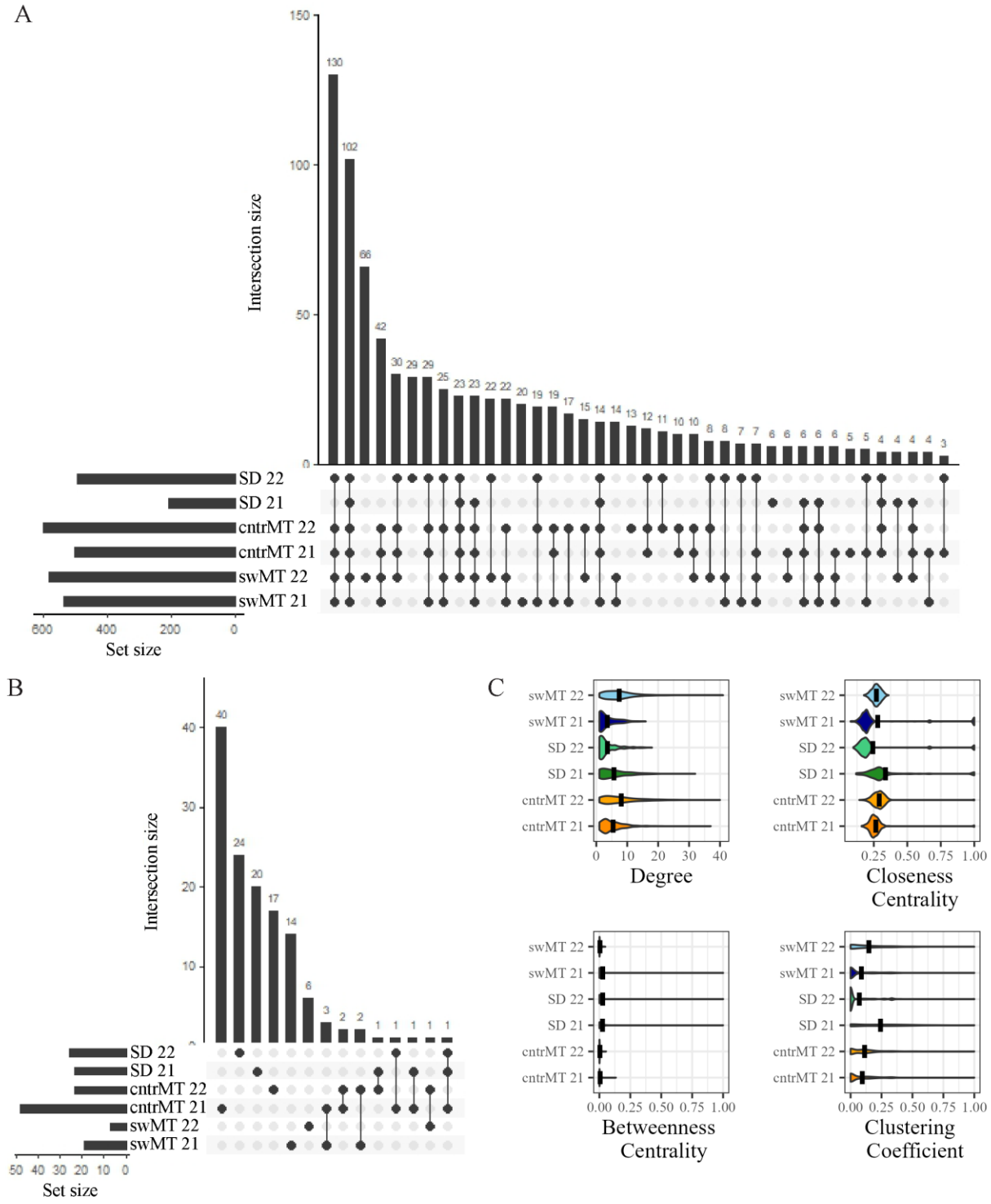

Figure 3.3: Bacterial co-occurrence network comparison showing conserved ASV nodes and ASV hubs. (A) Similarity of ASVs present in networks. Set size measures how many unique ASVs were in each location-year network. Intersection size measures how many ASVs were seen

at a certain number of networks, shown by the connected dots. Most ASVs were present in more than one network. (B) Number of shared and unique ASVs identified as hub taxa in networks. Across every network most hub taxa were unique to each location-year. (C) Co-occurrence network parameters across location-years.

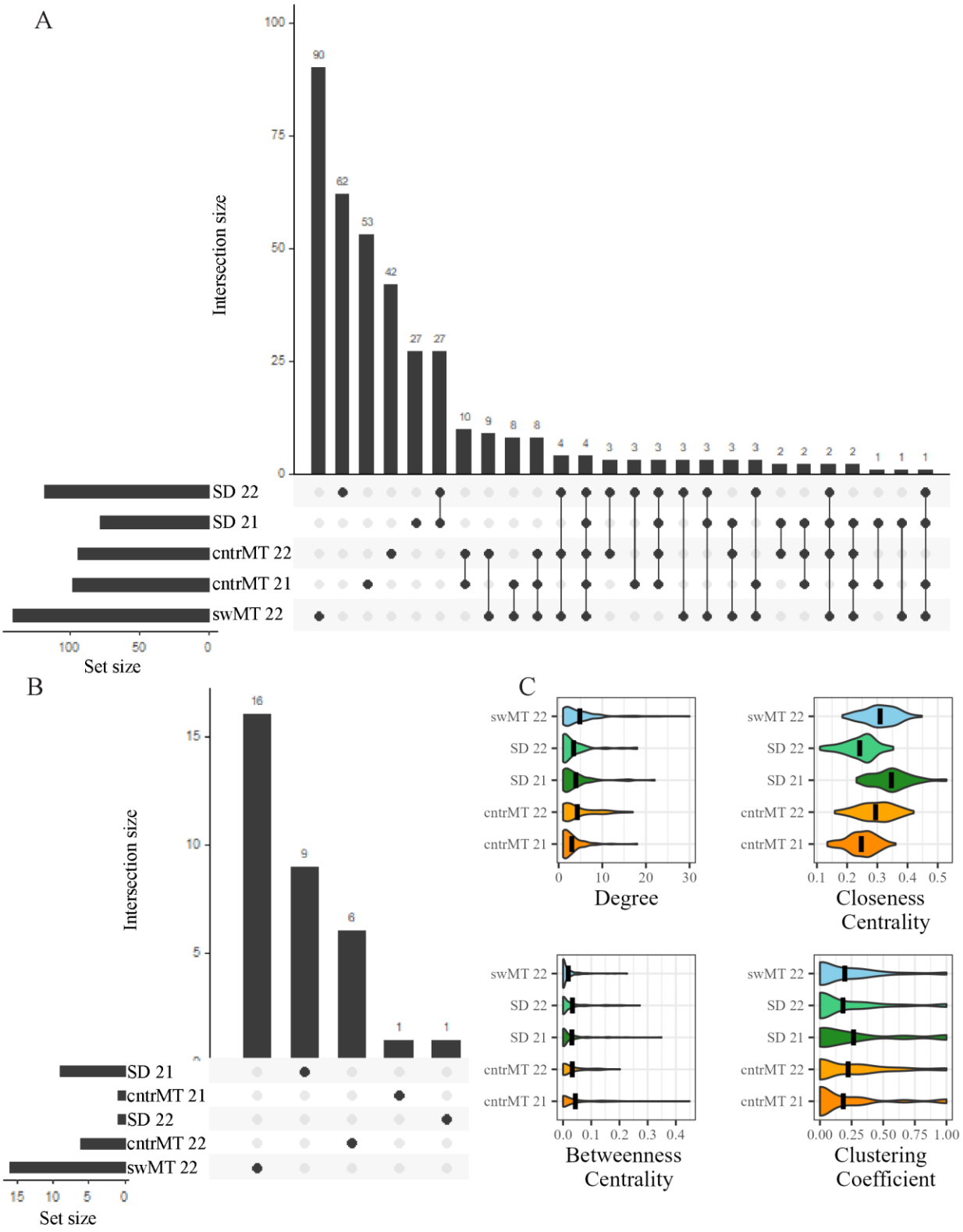
A
Intersection size
100
75
50
25
0
90
62
53
42
27
27
10
9
8
8
4
4
3
3
3
3
3
3
3
2
2
2
2
1
1
1
SD 22
SD 21
cntrMT 22
cntrMT 21
swMT 22
100
50
0
Set size
B
Intersection size
16
15
10
9
6
5
1
1
SD 21
cntrMT 21
SD 22
cntrMT 22
swMT 22
15
10
5
0
Set size
C
swMT 22
SD 22
SD 21
cntrMT 22
cntrMT 21
0
10
20
30
Degree
0.1
0.2
0.3
0.4
0.5
Closeness Centrality
0.0
0.1
0.2
0.3
0.4
Betweenness Centrality
0.00
0.25
0.50
0.75
1.00
Clustering Coefficient

Figure 3.4: Fungal co-occurrence network comparison showing conserved ASV nodes and ASV hubs. (A) ASVs are most commonly unique to specific location-years. (B) Hub fungal ASVs were not consistent across locations or years. (C) Network structure is consistent.

Previous GWAS analyses across the same barley population suggested multiple quantitative trait loci (QTL) were associated with specific bacterial taxa (Williams et al., 2025). Given the potential interactions of these QTL with specific bacterial taxa, we tested genetic loci as factors in our variance partitioning models. Variance partitioning highlighted 92 ASVs from 39 genera that were significantly variable by allele. Single nucleotide polymorphisms (SNPs) from three previously identified QTL (Williams et. al., 2025) were included in the variance partition model to rank the relative importance of each on ASV abundance (Fig. A3.3). Interestingly, QTL explained the variance of many ASVs but only when nested by location-year, suggesting a genotype by environment interaction, as previously found in the rhizosphere microbiome (Peiffer et al., 2013; Schlatter et al., 2020). This is also consistent with our previous GWAS study, where QTL only colocalized with bacterial taxa at specific location-years and not in others. Variance partitioning, however, found novel microbes affected by QTL compared to previous GWAS results (Tables A3.7-A3.10).

Discussion

Rhizosphere microorganisms play a fundamental role in plant survival and productivity by mediating nutrient acquisition and providing pathogen and abiotic stress protection (Wall et al., 2015). Our findings provide new insight into the role of plant genetics and environmental

factors and interactions between these factors in shaping this community in a genetically similar elite barley population.

The bacterial rhizosphere community composition was consistent across locations within barley growing regions of the US Northern Great Plains. In contrast, a distinct rhizosphere community was recruited in a contrasting environment in Oahu, Hawaii demonstrating the limits of plant recruitment of soil microorganisms. Through variance partitioning we identified and ranked the effect of environmental components on bacterial and fungal communities. Overall, little bacterial community variation was attributed to individual soil factors. Location-year explained the most variability in ASVs, suggesting differences in weather from year-to-year contributed to difference in the rhizosphere community. Soil microbial communities are sensitive to changes in temperature and moisture and these factors also alter host plant physiology (Meier et al., 2021). Climate factors could not be included in variance partition models because conditions such as precipitation and temperature were aggregated at the location-year level.

While other studies have identified microbial taxa that are responsive to differences in plant genotypes (Oyserman et al., 2022; Pacheco-Moreno et al., 2024) or are associated with specific plant gene loci (Escudero-Martinez et al., 2022), much of this work has been performed with a small number of genotypes or under limited environmental variation. Our results demonstrate the importance of evaluating rhizosphere recruitment in the context of both plant genetics and environment. While location and yearly variation due to changes in temperature and precipitation explained most of the variance, select plant gene loci also explained variance within some taxa (Fig. A3.3) demonstrating the potential of breeding plants for specific microbial interactions.

The subgenus variability in ASVs abundance within some genera suggests subgenus functional differences exist within taxa that would not be detected by higher level β-diversity or differential abundance analysis (Fig. A3.4). Similar findings have been reported in other crops such as maize and soybean (Meier et al., 2021). At the phylum level, bacterial communities were consistent with previous bacterial soil surveys, predominantly comprised of *Actinobacteriota* and *Proteobacteria* (Maestre et al., 2015). Interestingly in Hawaii, the location outside barley's adapted growing range, *Actinobacteriota* relative abundance averaged 75.7% across the barley population, whereas across the mainland locations the maximum abundance of *Actinobacteria* was 60%. Actinobacteriota is prevalent across many ecological regions, making it among the most abundant bacterial taxa (Maestre et al., 2015). Members of the Actinobacteriota phylum have shown to proliferate under copiotrophic (nutrient rich) and oligotrophic (nutrient limited) environments, suggesting its ability to thrive under a wide array of environmental conditions (Ho et al., 2017). In a novel growing environment for barley such as in Oahu Hawaii, barley could be unable to respond to the novel microbial community, thereby allowing for opportunistic bacteria such as Actinobacteria to colonize.

Bacterial co-occurrence networks built within each location-year had consistent interconnected ASVs, further exhibiting similarity across growing conditions. Interestingly however, networks were unique when considering the most highly interconnected ASVs. Network nodes were considered hubs with greater than 0.1 hub score, a metric used to define the number and importance of connections stemming from each node (Osborne et al., 2024). While hub ASVs were consistently present across multiple networks they were rarely ever considered a hub ASV in more than one network. This differs from previous research on global microbe (Ma

et al., 2020) and phyllosphere microbiome co-occurrence networks (Agler et al., 2016) which suggested that hub microbes persist through environmental variation. However rhizosphere microbes seem to be more variable, as found in a previous study in dryland wheat (Schlatter et al., 2020). Similar to our study, Schlatter et al. (2020) found a significant location effect on plant-associated microbes. These results suggest a broader, less constrained and interconnected network structure, without reliance on one taxon to establish the community (Agler et al., 2016; Coller et al., 2019). Instead, local environmental factors such as moisture content and ground temperatures seem to play a primary role in shaping the plant-associated microbial community (Islam et al., 2020).

Fungal community differences predominantly varied due to location-year, followed by soil chemistry factors. Soil factors were less ubiquitous across prevalent taxa but explained as much as 41% of variability in ASVs. Due to the low overlap in ASVs detected by location-year, ASV were also unique to co-occurrence network. While ASV variability was relatively high in fungal communities across location-years, results were similar in that overall fungal communities were consistently characterized by the phylum Ascomycota, as previously found in a global survey of soil samples (Egidi et al., 2019). These findings support the idea that fungal taxa are more deterministic, driven by climatic factors for dissemination rather than local soil conditions (Egidi et al., 2019).

Previous studies in other plants related microbial abundance to host genetics (Clouse & Wagner, 2021; Zhang et al., 2019). Plant-microbe interactions are influenced by specific host genes, as determined by genome-wide association studies (GWAS) (Deng et al., 2021; Horton et al., 2014). Previous work with this dataset revealed barley QTL associated with microbes,

dependent on location-year (Williams et al., 2025). These QTL were used for variance partitioning and the results found many microbe co-localizations were consistent with previous GWAS results while additional low abundance taxa were also identified. These findings support our previous GWAS results and other barley studies and suggest that barley genetics play a role in soil bacterial community structure (Chang et al., 2014; Pacheco-Moreno et al., 2024).

Our findings suggest plants have less influence in shaping the rhizosphere fungal community. For plant breeding, this highlights a gap in the extended phenotype where the relationship between barley and associated below ground fungi can be improved. As seen in many crop plants, fungal species are capable of significantly improving plant performance (Adedayo & Babalola, 2023). To start, a better understanding of barley interactions with fungi is needed. Based on these findings, we plan to perform GWAS similar to the bacterial taxa to target further potential QTL responsible for fungal abundance in the rhizosphere. Due to the large environmental effects, we expect to see a large environmental dependance on plant-fungi interactions in both the GWAS and following variance partition models including QTL factors. To further utilize the barley rhizosphere for plant performance, more specific interaction effects between plants, environment, and microbes must be measured. Our study found location-year effected ASVs differently within the same genus, suggesting that microbe by environment interactions are more specific than commonly measured surveys which group taxa at the genus level and above (Mishra et al., 2023). Further, we were unable to partition between important environmental factors including precipitation and temperature throughout the growing season – significant factors that drive microbe community structure (Islam et al., 2020).

Conclusions

Across barley growing regions of Montana and South Dakota, we found that the bacterial rhizosphere microbiome was consistent, evidence that plants were capable of creating a similar habitat for microbes in the rhizosphere. While the bacterial microbiome was consistent in overall structure, there was a notable lack of consistent hub bacteria across location-years. This suggests that the barley population associated consistently with bacterial community at broad levels, but plants were not able to consistently recruit specific microbes under variable environmental conditions. This was further discovered in the rhizosphere fungal community, where the abundance of fungal taxa was significantly impacted by environmental conditions.

For future applications, this work highlights the large environmental effect influencing the associated barley microbiome. Breeding for beneficial barley rhizosphere communities will need to account for this environmental effect to maintain benefits under variable locations and growing seasons.

Methods and Materials

The S2MET barley population was grown across four locations over two years in 2021 and 2022: Post Research Farm in Bozeman, MT; Central Agricultural Research Station in Moccasin, MT; Brookings, SD, and for one year in 2021 grown at the University of Hawaii Research Farm in Oahu, HI. At each field site 232 of the elite barley lines from the S2MET population (Neyhart et al., 2019) were randomly assigned into 12 blocks in an augmented block design. Four common Montana barley varieties, Hockett, Odyssey, Merit-57, and Lavina were replicated once per block. Locations in MT and SD represent barley growing regions of the Northern Great Plains and are representative of environments included in barley breeding programs in this region. Hawaii was selected as a contrasting environment far outside the

adapted environments represented in the barley breeding programs contributing to the S2MET population. At each field site, common management practices for the location were followed. At the Post Farm, plots were planted as three-row, twelve-foot plots. Crop rotations here were standard in both years following fallow-oats-barley. At CARC plots were planted in 5 rows, six feet long. Field history at CARC varied by growing year, where the 2021 field had mustard-oats-barley and the 2022 field had oats-mustard-barley. Brookings SD planted larger 5-row, 15-foot-long plots.

At each location developmental metrics were measured including heading and maturity date, plot length, and plant height. Heading and maturity dates were measured every other day per plot. Plot length was collected via measuring tape to the average ends of each plot across the 3 or 5 rows depending on location. Finally, plant height was collected by measuring three representative plants in each plot via measuring stick after plants were considered mature. After plant height was measured, plots were harvested independently into bags for threshing and yield metrics.

Rhizosphere soil sampling followed a standardized protocol across all location-years. Sampling was timed to occur when plots were on average at stem elongation stage. We decided to collect all rhizosphere samples at once to standardize the length of time they were exposed to plants. In each plot, three plants were dug up with a trowel with the aim of maintaining as much of the roots as possible. After lightly shaking off any large peds, the plants were stored in ZipLock bags and put in iced containers. In the second year of sampling to simplify downstream processing we separated plant shoots from the roots at this step and put plant shoots into brown

paper bags to weigh. In the first year the plant shoots were separated from roots in the lab and weighed for aboveground biomass.

Once the sampling was complete, root samples were deposited into a freezer at -80C for longer term storage. In batches of 8, root samples were removed from the freezer and put through a sonication bath for one minute with a 0.7% NaCl solution to remove the rhizosphere soil. The solution was sieved and centrifuged, then the precipitate soil was stored at -80C in a 2-mL tube. Samples at this point consisted of just rhizosphere soil.

DNA extractions were conducted using the Qiagen DNeasy PowerSoil Pro DNA Isolation Kit (Qiagen Inc., Germantown, MD, USA) in batches of 24 samples. Samples were then analyzed on a NanoDrop Spectrophotometer (Thermo Fisher Scientific (Waltham, MA USA) for assessing concentration and quality.Purified DNA was submitted to Integrated Microbiome Resource (Dalhousie University, Halifax, NS) for amplicon sequencing of the bacterial 16S V6-V8 region and fungal ITS2 region on the Illumina MiSeq platform (Illumina, San Diego, CA, USA) using a 2 × 300 PE kit.

Quality filtering, sequence variant assignment, and alpha and beta diversity analysis were performed using the Workflow for Microbiome Data Analysis in R (Callahan et al., 2017). First, reads were trimmed to remove low quality sequences. The first 5 bases were removed from the 5' end of each read then reads were trimmed to keep the quality score greater than 30. On average forward and reverse reads were trimmed to 250 and 180 bases respectively. Only forward reads were used for downstream analysis due to the low quality of the reverse reads. Reads from Hawaii were filtered with maximum expected error rate of 10, versus 2 at other location-years due to lower read quality. Dereplication, chimera removal, and taxonomy assignment were

performed using Dada2. After filtering, all location-years were combined into a single phyloseq object before constructing a phylogenetic tree.

Fungal ITS filtering followed the same workflow at bacterial 16S filtering with the following changes. Due to the widely variable read lengths, we used the R package ShortRead in conjunction with dada2 and Biostrings to recognize and remove primers from forward and reverse reads instead of trimming by a set length. Converse to 16S reads, forward and reverse reads overlapped sufficiently to merge reads.

Statistical Analysis

Variance partitioning was performed on ASVs with center-log-transformed relative abundances to estimate the contribution of environmental, soil physical and chemical parameters, and management factors to changes in microbiome composition in rhizosphere. Following previous reports, we used a 5% variance partition threshold to filter more meaningful factors (Meier et al., 2021). Mixed effects models were used to assess fixed quantitative effects such as soil chemistry and random categorical effects including location-year and block. Using linear model notation this looked like; (~ pH + Nitrate + OM + K + (1|locyr) + (1|Block)). When running variance partitioning with QTL, these were included as random factors (pH + Nitrate + OM + K + (1|locyr) + (1|Block) + (1|S5_480129120) + (1|S5_480129120:locyr)). QTL were nested by location-year to account for any interaction effects seen across growing locations.
To explore the effects of environment and other location-specific factors on microbial co-occurrence patterns, networks were constructed using the SPIEC-EASI (Sparse Inverse Covariance Estimation for Ecological Association Inference) method implemented in the SpiecEasi (v1.1.3) (Kurtz et al.2015) and microeco (Liu et al. 2021) R packages. For network

inference, only ASVs with a relative abundance greater than 0.005% and prevalence over 10% across all samples were used. Networks were visualized in Cytoscape (Shannon et al., 2003) and graphical model inference was performed by the Meinshausen and Buehlmann neighborhood selection method (Kurtz et al. 2015). The resulting node tables were imported into R to compare network parameters between locations.

References

Adedayo, A. A., & Babalola, O. O. (2023). Fungi That Promote Plant Growth in the Rhizosphere Boost Crop Growth. Journal of Fungi, 9(2), 239. https://doi.org/10.3390/jof9020239

Agler, M. T., Ruhe, J., Kroll, S., Morhenn, C., Kim, S.-T., Weigel, D., & Kemen, E. M. (2016). Microbial Hub Taxa Link Host and Abiotic Factors to Plant Microbiome Variation. *PLOS Biology*, *14*(1), e1002352. https://doi.org/10.1371/journal.pbio.1002352

Banerjee, S., Schlaeppi, K., & Van Der Heijden, M. G. A. (2018). Keystone taxa as drivers of microbiome structure and functioning. *Nature Reviews Microbiology*, *16*(9), 567–576. https://doi.org/10.1038/s41579-018-0024-1

Berry, D., & Widder, S. (2014). Deciphering microbial interactions and detecting keystone species with co-occurrence networks. *Frontiers in Microbiology*, *5*. https://doi.org/10.3389/fmicb.2014.00219

Breitkreuz, C., Herzig, L., Buscot, F., Reitz, T., & Tarkka, M. (2021). Interactions between soil properties, agricultural management and cultivar type drive structural and functional adaptations of the wheat rhizosphere microbiome to drought. *Environmental Microbiology*, *23*(10), 5866–5882. https://doi.org/10.1111/1462-2920.15607

Bulgarelli, D., Schlaeppi, K., Spaepen, S., Van Themaat, E. V. L., & Schulze-Lefert, P. (2013). Structure and Functions of the Bacterial Microbiota of Plants. *Annual Review of Plant Biology*, *64*(1), 807–838. https://doi.org/10.1146/annurev-arplant-050312-120106

Chang, P., Gerhardt, K. E., Huang, X.-D., Yu, X.-M., Glick, B. R., Gerwing, P. D., & Greenberg, B. M. (2014). Plant Growth-Promoting Bacteria Facilitate the Growth of Barley and Oats in Salt-Impacted Soil: Implications for Phytoremediation of Saline Soils. *International Journal of Phytoremediation*, *16*(11), 1133–1147. https://doi.org/10.1080/15226514.2013.821447

Chepsergon, J., & Moleleki, L. N. (2023). Rhizosphere bacterial interactions and impact on plant health. *Current Opinion in Microbiology*, *73*, 102297. https://doi.org/10.1016/j.mib.2023.102297

Clouse, K. M., & Wagner, M. R. (2021). Plant Genetics as a Tool for Manipulating Crop Microbiomes: Opportunities and Challenges. *Frontiers in Bioengineering and Biotechnology*, *9*, 567548. https://doi.org/10.3389/fbioe.2021.567548

Coller, E., Cestaro, A., Zanzotti, R., Bertoldi, D., Pindo, M., Larger, S., Albanese, D., Mescalchin, E., & Donati, C. (2019). Microbiome of vineyard soils is shaped by geography and management. *Microbiome*, *7*(1), 140. https://doi.org/10.1186/s40168-019-0758-7

Delgado-Baquerizo, M., Oliverio, A. M., Brewer, T. E., Benavent-González, A., Eldridge, D. J., Bardgett, R. D., Maestre, F. T., Singh, B. K., & Fierer, N. (2018). A global atlas of the dominant bacteria found in soil. *Science*, *359*(6373), 320–325. https://doi.org/10.1126/science.aap9516

Deng, S., Caddell, D. F., Xu, G., Dahlen, L., Washington, L., Yang, J., & Coleman-Derr, D. (2021). Genome wide association study reveals plant loci controlling heritability of the rhizosphere microbiome. *The ISME Journal*, *15*(11), 3181–3194. https://doi.org/10.1038/s41396-021-00993-z

Edwards, J., Johnson, C., Santos-Medellín, C., Lurie, E., Podishetty, N. K., Bhatnagar, S., Eisen, J. A., & Sundaresan, V. (2015). Structure, variation, and assembly of the root-associated microbiomes of rice. *Proceedings of the National Academy of Sciences*, *112*(8). https://doi.org/10.1073/pnas.1414592112

Egidi, E., Delgado-Baquerizo, M., Plett, J. M., Wang, J., Eldridge, D. J., Bardgett, R. D., Maestre, F. T., & Singh, B. K. (2019). A few Ascomycota taxa dominate soil fungal communities worldwide. *Nature Communications*, *10*(1), 2369. https://doi.org/10.1038/s41467-019-10373-z

Escudero-Martinez, C., Coulter, M., Alegria Terrazas, R., Foito, A., Kapadia, R., Pietrangelo, L., Maver, M., Sharma, R., Aprile, A., Morris, J., Hedley, P. E., Maurer, A., Pillen, K., Naclerio, G., Mimmo, T., Barton, G. J., Waugh, R., Abbott, J., & Bulgarelli, D. (2022). Identifying plant genes shaping microbiota composition in the barley rhizosphere. *Nature Communications*, *13*(1), 3443. https://doi.org/10.1038/s41467-022-31022-y

Fierer, N. (2017). Embracing the unknown: Disentangling the complexities of the soil microbiome. *Nature Reviews Microbiology*, *15*(10), 579–590. https://doi.org/10.1038/nrmicro.2017.87

Ho, A., Lonardo, D. P. D., & Bodelier, P. L. E. (2017). Revisiting life strategy concepts in environmental microbial ecology. *FEMS Microbiology Ecology*, fix006. https://doi.org/10.1093/femsec/fix006

Horton, M. W., Bodenhausen, N., Beilsmith, K., Meng, D., Muegge, B. D., Subramanian, S., Vetter, M. M., Vilhjálmsson, B. J., Nordborg, M., Gordon, J. I., & Bergelson, J. (2014). Genome-wide association study of Arabidopsis thaliana leaf microbial community. *Nature Communications*, *5*(1), 5320. https://doi.org/10.1038/ncomms6320

Islam, W., Noman, A., Naveed, H., Huang, Z., & Chen, H. Y. H. (2020). Role of environmental factors in shaping the soil microbiome. *Environmental Science and Pollution Research*, *27*(33), 41225–41247. https://doi.org/10.1007/s11356-020-10471-2

Kleinberg, J. M. (1999). Authoritative sources in a hyperlinked environment. *Journal of the ACM*, *46*(5), 604–632. https://doi.org/10.1145/324133.324140

Kurtz, Z. D., Müller, C. L., Miraldi, E. R., Littman, D. R., Blaser, M. J., & Bonneau, R. A. (2015). Sparse and Compositionally Robust Inference of Microbial Ecological Networks. *PLOS Computational Biology*, *11*(5), e1004226. https://doi.org/10.1371/journal.pcbi.1004226

Layeghifard, M., Hwang, D. M., & Guttman, D. S. (2017). Disentangling Interactions in the Microbiome: A Network Perspective. *Trends in Microbiology*, *25*(3), 217–228. https://doi.org/10.1016/j.tim.2016.11.008

Liu, C., Cui, Y., Li, X., & Yao, M. (2021). microeco: An R package for data mining in microbial community ecology. *FEMS Microbiology Ecology*, *97*(2), fiaa255. https://doi.org/10.1093/femsec/fiaa255

Liu, H., Li, J., Carvalhais, L. C., Percy, C. D., Prakash Verma, J., Schenk, P. M., & Singh, B. K. (2021). Evidence for the plant recruitment of beneficial microbes to suppress soil-borne pathogens. *New Phytologist*, *229*(5), 2873–2885. https://doi.org/10.1111/nph.17057

Liu, Q., Cheng, L., Nian, H., Jin, J., & Lian, T. (2023). Linking plant functional genes to rhizosphere microbes: A review. *Plant Biotechnology Journal*, *21*(5), 902–917. https://doi.org/10.1111/pbi.13950

Ma, B., Wang, Y., Ye, S., Liu, S., Stirling, E., Gilbert, J. A., Faust, K., Knight, R., Jansson, J. K., Cardona, C., Röttjers, L., & Xu, J. (2020). Earth microbial co-occurrence network reveals interconnection pattern across microbiomes. *Microbiome*, *8*(1), 82. https://doi.org/10.1186/s40168-020-00857-2

Maestre, F. T., Delgado-Baquerizo, M., Jeffries, T. C., Eldridge, D. J., Ochoa, V., Gozalo, B., Quero, J. L., García-Gómez, M., Gallardo, A., Ulrich, W., Bowker, M. A., Arredondo, T., Barraza-Zepeda, C., Bran, D., Florentino, A., Gaitán, J., Gutiérrez, J. R., Huber-Sannwald, E., Jankju, M., … Singh, B. K. (2015). Increasing aridity reduces soil microbial diversity and abundance in global drylands. *Proceedings of the National Academy of Sciences*, *112*(51), 15684–15689. https://doi.org/10.1073/pnas.1516684112

Meier, M. A., Lopez-Guerrero, M. G., Guo, M., Schmer, M. R., Herr, J. R., Schnable, J. C., Alfano, J. R., & Yang, J. (2021). Rhizosphere Microbiomes in a Historical Maize-Soybean Rotation System Respond to Host Species and Nitrogen Fertilization at the Genus and Subgenus Levels. *Applied and Environmental Microbiology*, *87*(12), e03132-20. https://doi.org/10.1128/AEM.03132-20

Mishra, A., Singh, L., & Singh, D. (2023). Unboxing the black box—one step forward to understand the soil microbiome: A systematic review. *Microbial Ecology*, *85*(2), 669–683. https://doi.org/10.1007/s00248-022-01962-5

Neyhart, J. L., Sweeney, D., Sorrells, M., Kapp, C., Kephart, K. D., Sherman, J., Stockinger, E. J., Fisk, S., Hayes, P., Daba, S., Mohammadi, M., Hughes, N., Lukens, L., Barrios, P. G., Gutiérrez, L., & Smith, K. P. (n.d.). Registration of the S2MET Barley Mapping Population for Multi-Environment Genomewide Selection. *Journal of Plant Registrations*.

Ning, D., Yuan, M., Wu, L., Zhang, Y., Guo, X., Zhou, X., Yang, Y., Arkin, A. P., Firestone, M. K., & Zhou, J. (2020). A quantitative framework reveals ecological drivers of grassland microbial community assembly in response to warming. *Nature Communications*, *11*(1), 4717. https://doi.org/10.1038/s41467-020-18560-z

Osborne, M. G., Simons, A. L., Molano, G., Tolentino, B., Singh, A., Arismendi, G. J. M., Alberto, F., & Nuzhdin, S. V. (2024). Investigating the relationship between microbial network features of giant kelp "seedbank" cultures and subsequent farm performance. *PLOS ONE*, *19*(3), e0295740. https://doi.org/10.1371/journal.pone.0295740

Oyserman, B. O., Flores, S. S., Griffioen, T., Pan, X., Van Der Wijk, E., Pronk, L., Lokhorst, W., Nurfikari, A., Paulson, J. N., Movassagh, M., Stopnisek, N., Kupczok, A., Cordovez, V., Carrión, V. J., Ligterink, W., Snoek, B. L., Medema, M. H., & Raaijmakers, J. M. (2022). Disentangling the genetic basis of rhizosphere microbiome assembly in tomato. *Nature Communications*, *13*(1), 3228. https://doi.org/10.1038/s41467-022-30849-9

Pacheco-Moreno, A., Bollmann-Giolai, A., Chandra, G., Brett, P., Davies, J., Thornton, O., Poole, P., Ramachandran, V., Brown, J. K. M., Nicholson, P., Ridout, C., DeVos, S., & Malone, J. G. (2024). The genotype of barley cultivars influences multiple aspects of their associated microbiota via differential root exudate secretion. *PLOS Biology*, *22*(4), e3002232. https://doi.org/10.1371/journal.pbio.3002232

Peiffer, J. A., Spor, A., Koren, O., Jin, Z., Tringe, S. G., Dangl, J. L., Buckler, E. S., & Ley, R. E. (2013). Diversity and heritability of the maize rhizosphere microbiome under field

conditions. *Proceedings of the National Academy of Sciences*, *110*(16), 6548–6553. https://doi.org/10.1073/pnas.1302837110

Santoyo, G. (2022). How plants recruit their microbiome? New insights into beneficial interactions. *Journal of Advanced Research*, *40*, 45–58. https://doi.org/10.1016/j.jare.2021.11.020

Schlatter, D. C., Yin, C., Hulbert, S., & Paulitz, T. C. (2020). Core Rhizosphere Microbiomes of Dryland Wheat Are Influenced by Location and Land Use History. *Applied and Environmental Microbiology*, *86*(5), e02135-19. https://doi.org/10.1128/AEM.02135-19

Shannon, P., Markiel, A., Ozier, O., Baliga, N. S., Wang, J. T., Ramage, D., Amin, N., Schwikowski, B., & Ideker, T. (2003). Cytoscape: A Software Environment for Integrated Models of Biomolecular Interaction Networks. *Genome Research*, *13*(11), 2498–2504. https://doi.org/10.1101/gr.1239303

Tedersoo, L., Bahram, M., Põlme, S., Kõljalg, U., Yorou, N. S., Wijesundera, R., Ruiz, L. V., Vasco-Palacios, A. M., Thu, P. Q., Suija, A., Smith, M. E., Sharp, C., Saluveer, E., Saitta, A., Rosas, M., Riit, T., Ratkowsky, D., Pritsch, K., Põldmaa, K., … Abarenkov, K. (2014). Global diversity and geography of soil fungi. *Science*, *346*(6213), 1256688. https://doi.org/10.1126/science.1256688

Walker, T. S., Bais, H. P., Grotewold, E., & Vivanco, J. M. (2003). Root Exudation and Rhizosphere Biology. *Plant Physiology*, *132*(1), 44–51. https://doi.org/10.1104/pp.102.019661

Wall, D. H., Nielsen, U. N., & Six, J. (2015). Soil biodiversity and human health. *Nature*, *528*(7580), 69–76. https://doi.org/10.1038/nature15744

Yu, P., He, X., Baer, M., Beirinckx, S., Tian, T., Moya, Y. A. T., Zhang, X., Deichmann, M., Frey, F. P., Bresgen, V., Li, C., Razavi, B. S., Schaaf, G., Von Wirén, N., Su, Z., Bucher, M., Tsuda, K., Goormachtig, S., Chen, X., & Hochholdinger, F. (2021). Plant flavones enrich rhizosphere Oxalobacteraceae to improve maize performance under nitrogen deprivation. *Nature Plants*, *7*(4), 481–499. https://doi.org/10.1038/s41477-021-00897-y

Zhang, J., Liu, Y.-X., Zhang, N., Hu, B., Jin, T., Xu, H., Qin, Y., Yan, P., Zhang, X., Guo, X., Hui, J., Cao, S., Wang, X., Wang, C., Wang, H., Qu, B., Fan, G., Yuan, L., Garrido-Oter, R., … Bai, Y. (2019). NRT1.1B is associated with root microbiota composition and nitrogen use in field-grown rice. *Nature Biotechnology*, *37*(6), 676–684. https://doi.org/10.1038/s41587-019-0104-4

Zhao, M., Zhao, J., Yuan, J., Hale, L., Wen, T., Huang, Q., Vivanco, J. M., Zhou, J., Kowalchuk, G. A., & Shen, Q. (2021). Root exudates drive soil-microbe-nutrient feedbacks in response to plant growth. *Plant, Cell & Environment*, *44*(2), 613–628. https://doi.org/10.1111/pce.13928

CHAPTER FOUR

UTILIZING QGIS FOR OPEN-SOURCE UAS IMAGERY

PLANT CLASSIFICATION AND PLOT SEGMENTATION

Contribution of Authors and Co-Authors

Manuscript in Chapter 4

Co-Author: Erik Z. Killian

Contributions: conceptualization, data curation, formal analysis, investigation, methodology, validation, visualization, writing - original draft, writing - review & editing

Co-Author: Jed O. Eberly

Contributions: funding acquisition, project administration, resources, supervision

Co-Author: Jennifer Lachowiec

Contributions: conceptualization, funding acquisition, project administration, resources, software, supervision, writing - review & editing

Manuscript Information

Status of Manuscript:
☐ Prepared for submission to a peer-reviewed journal
☒ Officially submitted to a peer-reviewed journal
☐ Accepted by a peer-reviewed journal
☐ Published in a peer-reviewed journal

Submitted: March 28, 2025, to The Plant Phenome Journal

Abstract

The analysis of unoccupied aerial system (UAS) imagery remains a bottleneck to obtaining actionable data due to its complexity and required specialized skill set. We introduce a workflow designed to balance usability and flexibility in processing UAS imagery using QGIS, an open-source geographic information system (GIS) software. The workflow consists of four sequential steps: semi-automated plant classification, user-corrected plot delineation, spectral index calculation, and data extraction. We tested this workflow on barley UAS image data, collected over 12 flights throughout the growing season. As a proof-of-concept, multiple RGB indices were calculated to test for relationships to ground-sampled data and exemplify applications of spectral analysis. Our results indicate a strong correlation between the Visible Atmospheric Resistant Index (VARI) and ground truth data, particularly when integrated over multiple flights. This open-source workflow provides a lower barrier-to-entry solution for researchers and producers, facilitating the broader adoption of UAS technology in agriculture. By automating routine tasks while allowing user intervention for critical adjustments, this approach enhances the efficiency of agricultural data analysis.

Introduction

Unoccupied aerial systems (UAS) are gaining popularity for their ability to collect high resolution imagery on demand in agricultural settings, enabling real-time decision making (Candiago et al., 2015). This technology has been used to measure plant health (Sahoo et al., 2024), stand counts (Zortea et al., 2018), and identify invasive weeds (Rasmussen et al., 2019). Collecting information on crop performance using (UAS) is efficient and inexpensive, but analyzing imagery remains time-consuming and complicated and thus is one of the main barriers to utilizing UAS in agricultural research (Lachowiec et al., 2024). Accessible and inexpensive analysis workflows are valuable to process the growing number of datasets utilizing UAS (Istiak et al., 2023) into useful information for producers and researchers.

Ideally, image processing pipelines are both easy to use and flexible (Adler et al., 1999a). A usable workflow has a low learning curve, little entry cost, and minimal required computer processing power. A flexible program gives users the tools to revise steps in the process to fit their goals. However, there is a tradeoff between usability and flexibility (Adler et al., 1999a), as users are given more tools, flexibility improves at the cost of reduced simplicity. The challenge when creating an imagery analysis workflow is to balance usability and flexibility to align with the types of datasets the workflow is intended to process.

Previous work in maize (Liu et al., 2022), faba beans (Ji et al., 2023), and wheat (Lu et al., 2019) demonstrate the utility of UAV-collected red-green-blue (RGB) imagery as proxies for ground-collected plant metrics. In this process, crops of interest need to be isolated from the rest of the image and each plot must be correctly identified and delineated. Flexible approaches that

can be applied to a diversity of crops which vary in shape, size, and color are desirable. The classification of pixels representing a crop in an image is sensitive to the plant of interest and the surrounding growing environment (Wu et al., 2014; Zhang et al., 2014). One semi-automated approach utilizes the calculation of an index based on RGB pixel values wherein pixels are classified as representing plants based on a manually selected threshold value of the index. As healthy plants reflect large amounts of green light and low amounts of red, multiple color-based indices are capable of performing plant classification (Upendar et al., 2021). The selection of a threshold value for the index lends the approach flexibility to identify diverse crops as well as avoiding misclassification of pixels from soil, shadows, and other objects as plants (Rasmussen et al., 2019).

For use in small-plot research, UAS data processing pipelines should also be flexible to varied plot layouts. Common plot segmentation methods use the dimensions of plots, plot spacing, and total field extent to populate a grid upon an image, assuming no variability in plot shape (Bhandari et al., 2021; Haghighattalab et al., 2016; Matias et al., 2020). However, the size and shape of plots can be specific to each research program or planting location, including irregularities like variable plot sizes or misaligned plots. In instances where plots are tightly spaced or misaligned, a simple grid will not accurately segment plots. Plot segmentation protocols available can handle challenging field layouts, such as staggered rows, but lack functions for adjusting single plot shapes or are closed-source software (Ha et al., 2022; Anderson et al. 2020).

Here, we introduce a workflow combining manual and automated actions to maximize usability and flexibility in UAS imagery analysis. We leverage the functionality of the free and

open-source geographic information system software QGIS for extracting data from imagery. This workflow functions sequentially in four stages: first, the input image is semi-automatically classified to discern plant pixels from any other background pixels. Second, the user semi-automatically defines an accurate plot map to distinguish between plots. Third, one or more spectral indices can be calculated per plot. Finally, any statistical summary of each spectral index can be calculated and extracted into a spreadsheet format. We demonstrate the workflow's use in a small plot trial by testing spectral indices as proxies of heading and maturity dates in barley. Barley, an annual crop, is planted in the spring. After emergence, barley tillers before the main stem begins elongation. Heading date is defined when barley heads emerge from the elongated stem. Finally, barley is harvested once grain has senesced. We observe strong correlations between ground truth data and the spectral imagery data that was collected across barley growth stages. Currently the ability to analyze and extract useful information from aerial imagery represents one of the largest barriers to entry for many growers and researchers (Istiak et al., 2023; Lachowiec et al., 2024). By offering an additional open-source workflow to the quickly developing suite of options, we introduce a simpler, lower barrier-to-entry process for those who are not familiar with remote sensing and imagery analysis.

Materials and Methods

Study Site and Data Collection

We conducted flights at the Montana State University Post Research Farm in Bozeman, Montana using a Mavic 2 Pro quadcopter with an integrated Hasselblad sensor. Flown at 30-meter altitude, this sensor captured Red, Green, and Blue (RGB) wavelength imagery with an approximate resolution less than one cm per pixel (Supp Table A4.1). This flight plan was repeated 12 times throughout the growing season with higher frequency of flights during heading and maturity (Table 4.1). Flights were scheduled twice a week during the early season and every two days during heading and maturity, given suitable weather conditions. Raw imagery, calibration details, and stitched orthomosaics of these flights are available (Killian et al., 2023). Heading and maturity dates were determined through visual assessment of barley plots on the ground. Starting when plants reached Zadoks stage 5 (Zadoks et al., 1974), we assessed the field every two days until all plots were defined as headed or matured respectively. Each plot was scored as headed when at least 50% of heads were exposed from the boot. Maturity was similarly scored when at least 50% of plant heads had senesced. Plant height was measured by walking through each plot with a meter stick and recording the height of four randomly selected plants. Grain yield was measured after harvesting plots and extrapolated to kg/hectare based on plot size.

Table 4.1. Schedule of UAS flights and plant measurements throughout growing season.

Date	Days After Planting	Flight Number	Measurement Stage
April 26	0		Planting
June 16	51	1	
June 21	56	2	
June 24	59	3	
June 25	60		Heading began
July 01	66	4	
July 11	76		Heading finished
July 12	77	5	
July 15	80	6	
July 19	84	7	
July 21	86	8	
July 25	90	9	Maturity began
July 27	92	10	
August 5	101	11	
August 8	104	12	
August 10	106		Maturity finished
August 11	107		Plant height measured

Orthomosaic Creation

After collecting remote sensing imagery, raw images were stitched to create an orthomosaic image using the open-source, commercial-grade software OpenDroneMap (Toffanin et al., 2023). OpenDroneMap performed consistently well to commercial opens including Pix4Dmapper and Agisoft in agricultural imagery (Pell et al., 2022). To retain spatial resolution and maximize efficiency, OpenDroneMap default stitching parameters were altered as detailed in the previously published dataset (Killian et al., 2023). In brief, 4000 tie points were used to stitch images, potential moving objects were processed with gaussian dampening, and no cropping or compression were performed.

QGIS: Tools and Models

QGIS is an open-source geographic information software capable of processing imagery as specific light bands. We developed a series of workflows for processing imagery, using a combination of built-in QGIS functions, referred to as "*Tools"*, and combined these tools to automate tasks, referred to as "*Models*". While models combine and automate tasks, they can still be run as separate tools to debug and alter any aspect of the workflow. Stitched orthomosaics from OpenDroneMap were loaded into QGIS for all further analysis. All models are available with instructions at https://github.com/erikkillian/multiPLOT. The workflow uses Models and Tools to perform threshold-based classification on input images. In parallel users create a semi-automated grid to accurately designate plots in the field. Finally, mean band values are extracted for analysis (Figure 4.1).

Figure 4.1: A flowchart describing the workflow from input images to tabular data. Raw images are classified into plant pixels for accurate data extraction. Plots are delineated semi-autonomously then used to extract plot-level data.

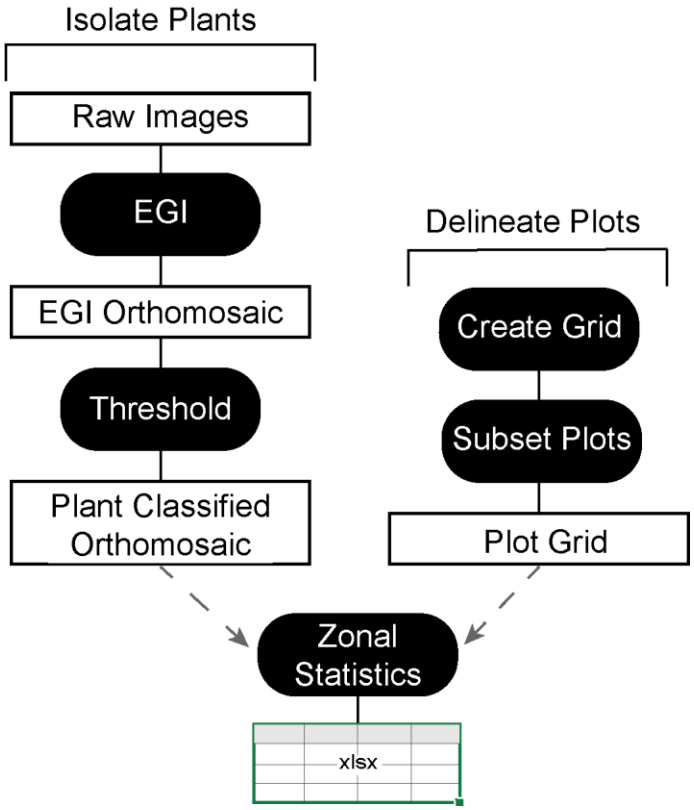

Plant Classification

We created a QGIS Model to automate soil masking and identify pixels representing plants. This model uses the 1) original orthomosaic and 2) a user-defined Excess Greenness Threshold number as inputs—this produces a single orthomosaic containing the masked bands as an output. The Excess Greenness Threshold is defined from the Excess Greenness Index (EGI), (Rodene et al., 2022):

$$EGI = (2 * Green) - (Red + Blue)$$

where Green refers to a pixel's green value, Red refers to a pixel's red value, and Blue refers to a pixel's blue value. EGI can accurately classify plants within an image due to the relatively high greenness of plants compared to their background (Hennessy et al., 2020; Rasmussen et al., 2007; Upendar et al., 2021). First, EGI was calculated for each pixel, resulting in an orthomosaic containing EGI values; using the layer properties in QGIS, EGI values are displayed as a histogram (Figure 4.2). For agricultural field imagery the EGI distribution is typically bimodal since pixels most often contain either plant or soil. Plants reflect green wavelengths of light more than red or blue, while soil reflects relatively more red and blue wavelengths of light (Meyer & Neto, 2008).

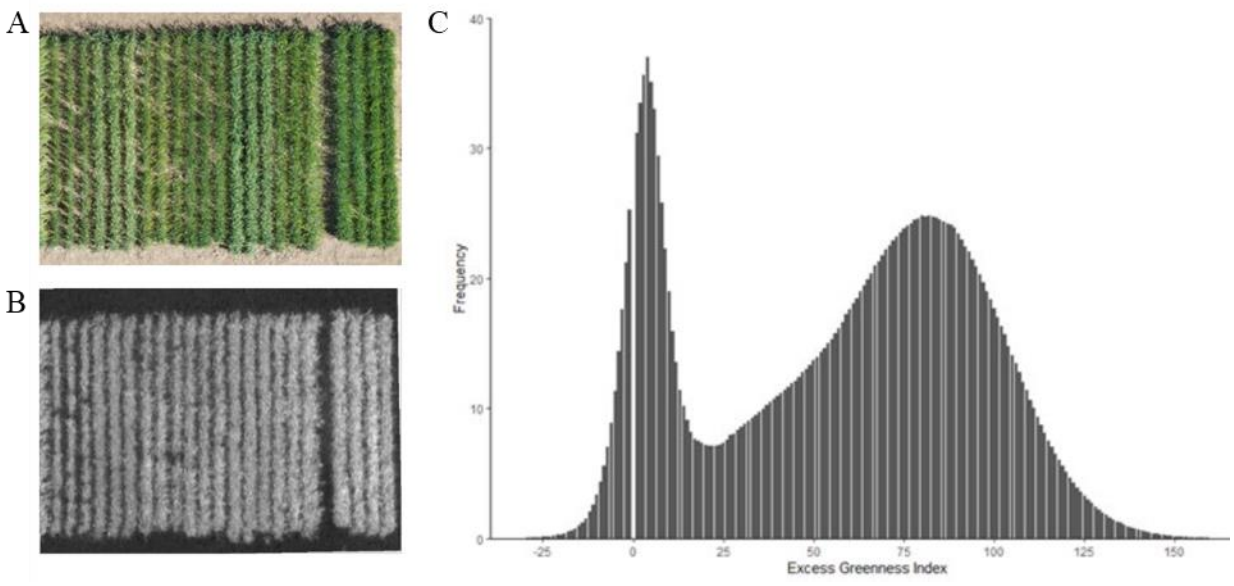

Figure 4.2. Classifying plants versus soil. (A) Segment of the true-color input image. (B) Mapped excess greenness index values of the same image. Lighter colors represent higher EGI. This shows how EGI can distinguish both soil and shadows from plants in the image (C) Histogram of EGI values across entire image.

Based on this distribution, user-defined thresholds of 40-60 were used to classify plants versus non-plant pixels in this study. First, the inflection point between the two distribution peaks was used as a reference threshold of 25 to separate the image into two distinct groups (Otsu, 1979). Through visual inspection this threshold was ill-suited to our dataset as it failed to mask out many shadows. Through testing more conservative thresholds, we found the range of 40-60 successfully masked out soil and shadow pixels while maintaining the maximum amount of plant pixels. These threshold values were then tested on each flight date. Appropriate thresholds in other studies may vary from these values based on the EGI histogram. The defined threshold was used to create a binary mask layer from the EGI layer, where plant pixels equaled one and non-plant pixels equaled zero. Once created, the value of each band of the original image was multiplied by the binary mask layer to retain plant pixels and remove non-plant pixels. Finally, the bands were recombined into a single orthomosaic image that contains only plant pixels. We combined these steps into a classification model that is run by simply inputting the orthomosaic image and a threshold value. Importantly, this soil mask model can be bypassed if users want to implement an alternative classification method. The alternative classified image can be imported to QGIS as a TIFF file for all downstream analysis.

Plot Segmentation

In small plot studies, plots may be very tightly spaced. For this reason, defining plots through canopy cover (Machefer et al., 2020; Zheng et al., 2022) or simple grids lead to misalignment in defining plot boundaries. Misaligned plots will create data errors by assigning plants into the wrong plots. We found that previous automated methods (Haghighattalab et al., 2016; Matais et al., 2020) do not have tools to account for the irregular planting in our field, so

we developed the workflow for semi-automated plot delineation to accurately delineate tightly planted and non-uniformly sized plots. First, a simple line grid was created based on the size and number of plots in the image using the *Create Grid* tool. Similar to other automated gridding tools, a grid was automatically populated based on user-provided plot height and width information plus the field extent (Matias et al., 2020). Importantly, for any errors in the grid, user-mediated changes can be made at the field scale and from plot to plot. Field-level changes were made by selecting and moving any single line or vertex; with simple plot layouts and large plot margins this provides an accurate plot map.

Further refinement of any smaller errors is done by redefining plots as polygons. First, the line grid was transformed into a polygon grid using the *Polygons* tool which then allows the sides and vertices of each plot to be manipulated independently for complete control over each plot extent (Figure 4.3). This was capable of accounting for uneven plot sizes or planting errors by individually altering or removing inaccurate plots and those not used in the study. Once accurately defined, a single grid can be used across any number of georeferenced images.

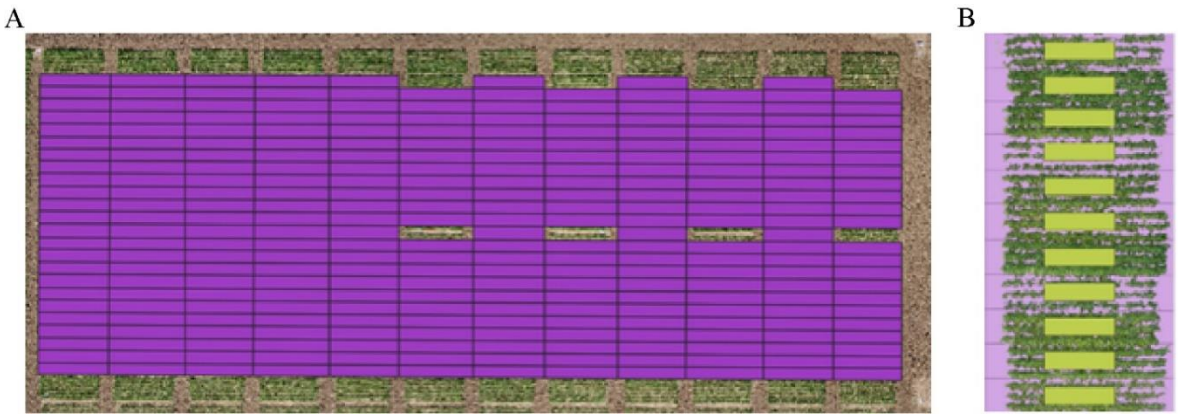

Figure 4.3. Plot identification and subsetting. (A) Polygon grid with unused plots removed to ease downstream analysis. (B) EGI-masked orthomosaic of a subset of barley plots. Subset polygons (yellow) provide a boundary between plots to account for any plot overlapping or grid inaccuracies.

Subset Polygons

An optional step during plot segmentation is subsetting, which was a simple two-step process. Subsetting plots will create a smaller plot section at the center of each plot to help minimize plot edge effects. This step is most useful when plot borders are extremely close together or in cases where plant canopies overhang into neighboring plots (Figure 4.3B). First, the *Centroids* tool was used in conjunction with the polygon grid to create a point at the center of each plot. Second, the *rectangles, Ovals, Diamonds* tool created a user-defined polygon of any size centered around each centroid point previously created. This plot subset can account for plot boundary issues or irregularities.

Data Extraction

Data extraction converts the identified plant pixel data into numerical tabular data. Using the *Zonal Statistics* tool, values were extracted per plot based on a predefined polygonal grid as previously described. The average pixel value of each band within each plot was independently extracted to create a final table of reflectance values by plot. In addition to mean, other statistics such as minimum, maximum, and standard deviation can be run in parallel to be output together. The mean band values were then used to create vegetation indices. Outputting spectral data in a table simplifies calculating and comparing indices as information is independent of the large spatial files and can be instead run in programs such as Excel or R. Alternatively indices can be calculated within QGIS using the *Raster Calculator* tool where vegetation indices are stored per-pixel.

Data Analysis

Following data extraction using the above pipeline, we extracted the mean pixel values for red, green, and blue wavelengths across each plot. By geolocating the stitched images from each date, we applied the same plot map across all 12 flights. The extracted color bands were used to calculate indices (Table 4.2), including Visible Atmospherically Resistant Index (VARI), Green Leaf Index (GLI), and Red-Green-Blue Vegetation Index (RGBVI) using mean band values per plot (Lussem et al., 2018). The relationship between each index and plant traits including yield, biomass, and development stages heading date and maturity date were calculated by Pearson's correlation (SuppTable A4.2). For data analysis we used Hmisc (Harrell, 2024) in R version 4.4.1.

Table 4.2. Vegetation Indices

Vegetation Index	**Equation**
VARI	(G – R) / (G + R – B)
GLI	(2*G – R – B) / (2*G + R + B)
EGI	2*G – R – B
RGBVI	(G*G) – (R*B) / (G*G) + (R*B)

Results

To illustrate the workflow presented in the Methods, we used high resolution RGB imagery collected with an unoccupied aerial system throughout the growing season of a barley experiment consisting of over 200 barley varieties (Killian et al., 2023). In total we collected imagery during 12 flights launched between seedling emergence and plant maturity. Killian 2023 provides additional background on image stitching and calibration.

First, we classified image pixels to isolate plants from the surrounding soil. This required defining a manual EGI threshold value based on the original image's EGI histogram. By visually examining the bimodal EGI distribution, we selected multiple thresholds for classification. We found it best to select a higher, more stringent threshold than the intermodal minimum, as some shadows and other background pixels were included. To compare and test the robustness of the user-defined EGI plant classification threshold value, we classified plants using five EGI thresholds. We determined the impact of the manual selection of threshold by processing each image at each EGI threshold through the whole workflow. The effective RGB index Variable Atmospheric Resistance Index (VARI) (Gitelson, Stark, et al., 2002; Adak et al., 2024) was used to compare the effect of varying thresholds. VARI correlation to each of the four plant metrics was highly consistent across thresholds during the growing season (Figure 4.4). The correlation to plant traits is robust to the user-defined threshold value.

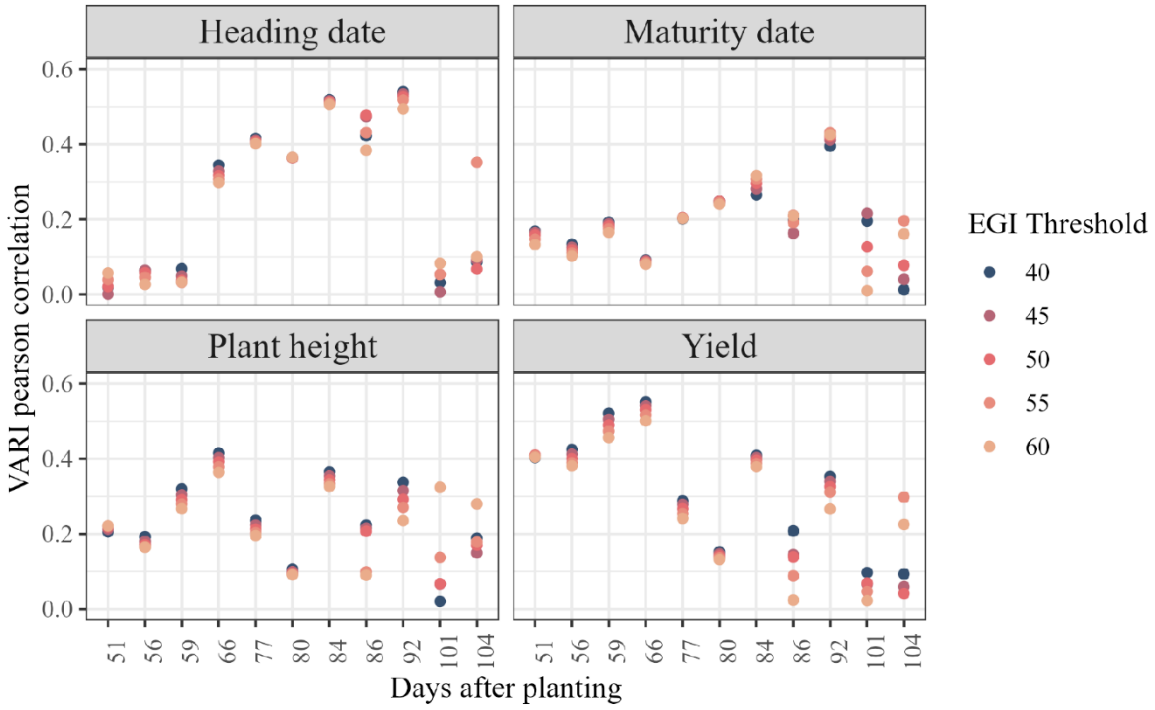

Figure 4.4. Testing the effect of Excess Greenness Index (EGI) threshold on correlation between VARI and plant traits at each flight date. Correlations were robust to changing thresholds, showing that threshold choice did not significantly alter the data results.

From the plant classified image we extracted plot-specific data from each flight testing several approaches. Using canopy cover to segment plots overestimated plot numbers when plants were separated by soil, and the lack of plot spacing led to plots aggregating together (Supp Fig A4.2). We next tested multiple automated plot boundary gridding approaches (Haghighattalab et al., 2016; Matais et al., 2020), but we found that the borderless and inconsistent plot spacing in the field required a more supervised approach to correctly define plots versus a purely automated workflow.

We then compared the performance of a user-corrected grid to an automated plot grid on the orthomosaic image from 90 DAP to delineate plots of mature plants. The automated grid

followed common automated plot delineation protocols by defining the field extent and plot dimensions (1m x 5.5m) while the semi-automated plot grid was created as described above. We then scored each grid on plot accuracy (Table 4.3). Each of the 280 plots was designated as having a large, small, minute, or no error based on how many plants in a plot exceeded the plot boundary. A minute error was defined as having only a few plant pixels crossing a plot boundary. Small errors occurred when multiple tillers of one to a few plants crossed a plot boundary. A large error occurred when most plants in a row crossed or were completely defined under the wrong plot. With these quality scores, precision (the ratio between true positive and false positives) and F-1 (a definition of accuracy including both precision and recall ranging from zero to one with values being better closer to one (Robb et al., 2020)) was compared across the approaches. Both the automated and user-corrected approaches contained the correct number of plots so there were no false plots identified. The automated plot grid generated the largest number of minute, small, and large errors. Subsetting plots within the automated grid greatly reduced the large error number, improving the precision and F-1. However, the user corrected plot grid had no large errors and further subsetting of user corrected plots resulted in precision and F-1 scores of 1 (Table 4.3).

Table 4.3. Comparing plot segmentation accuracy between user-corrected and autogenerated grid. Errors report how many of the 280 plots were considered to have minute, small, or large errors.

Plot Method	**Errors**			**Precision**	**F-1**
	Minute	**Small**	**Large**		
Automated	17	38	187	0.16	0.27
Automated - Subset	22	21	69	0.61	0.75
User Corrected	54	24	0	0.73	0.84
User Corrected – Subset	0	0	0	1	1

After correctly delineating plots, we calculated average per-plot vegetation indices across all flight dates. Several RGB indices were used including Excess Greenness Index (EGI) (Woebbecke et al., 1995), Normalized Excess Greenness Index (NEGI), Variable Atmospheric Resistance Index (VARI) (Gitelson, Kaufman, et al., 2002), Red Green Blue Vegetation Index (RGBVI) (Bendig et al., 2015), and Green Leaf Index (GLI) (Louhaichi et al., 2001). The correlation to plant metrics varied across these spectral indices, but VARI regularly correlated best with yield and heading date (Supp. Table A4.2). For this reason, VARI was selected for further examination.

In barley, grain fill timing and duration affect plant yields in semi-arid conditions (Christopher et al., 2016; Williams et al., 2022). We examined how the spectral index VARI could be used to predict traits related to grain fill. The correlation of VARI and heading date increased over time, peaking at 0.61 at 86 DAP and then proceeded to quickly and steadily decrease thereafter (Figure 5). This peak correlation came ten days after all plots were called as headed by ground sampling. The correlation between VARI and maturity date also increased during later dates with a decrease just after heading completed and a peak correlation of 0.55 during senescence. The VARI – Yield correlation over time was highest earlier in the year with a maximum at 0.53, sixty-six days after planting. This peak decreased after heading to between 0.2 and 0.4 until harvest (Supp Table 4.2).

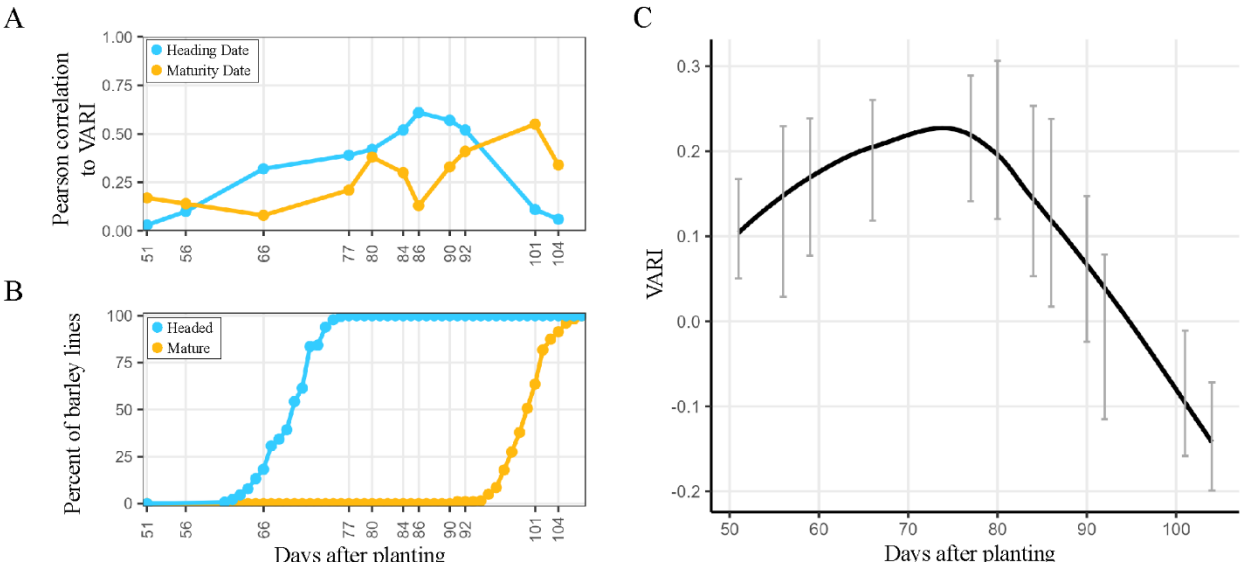

Figure 4.5. Examining the relationship between agronomic traits and the VARI index. (A) Visualizing the correlation between VARI and the plant traits heading date and maturity date at each flight date to compare to (B) the percentage of barley plants defined as headed or mature by ground-sampling. (C) VARI by flight date. Bars represent the range of values within each flight.

To utilize the temporal resolution of our dataset, we focused next on the changes in VARI throughout plant development. VARI increased from emergence through vegetative growth before decreasing as plants matured (Figure 4.5C). To summarize the time-series we calculated the integral of VARI across all flight dates (Matias et al., 2022). In yield and heading date, the integral provided similar correlation strength to the best performing single-date flights (Table 4.4). To target grain-fill period we also integrated VARI across flights conducted during grain-fill (77-104 DAP). Correlations with heading and maturity date increased versus overall integral, while yield and plant height decreased (Table 4.4). While the ability to estimate plant traits was inconsistent across flights, summarizing the data through the integral improved estimation power to compete with the best performing single flights, and the magnitude of the correlation likely

reflects whether the growth stages that most influence the traits of interest were included (Carneiro et al., 2019; Kaur et al., 2015).

Table 4.4. Pearson correlation between VARI and plant traits at each flight days after planting (DAP).

Date	Yield	Plant Height	Heading Date	Maturity Date
	Pearson correlation coefficient			
Integral[a]	0.523	0.371	0.486	0.244
Grain fill integral[b]	0.325	0.226	0.531	0.454
DAP 51	0.398	0.213	0.028	-0.173
DAP 56	0.366	0.238	0.136	-0.117
DAP 66	0.526	0.403	0.316	-0.078
DAP 77	0.255	0.208	0.386	0.209
DAP 80	0.188	0.026	0.423	0.379
DAP 84	0.400	0.348	0.516	0.302
DAP 86	0.273	0.355	0.606	0.127
DAP 90	0.377	0.349	0.567	0.332
DAP 92	0.393	0.341	0.517	0.413
DAP 101	0.227	-0.029	0.113	0.550
DAP 104	0.200	0.058	0.064	0.341

[a] Integral is calculated using VARI across flights 51-104 days after planting.

[b] Grain fill integral is calculated using VARI across flights 77-104 days after planting.

Discussion

While collecting and storing UAS data has become more efficient and financially viable (Bendig et al., 2012; Candiago et al., 2015), processing and analysis remains expensive and inaccessible without robust, open-source methods (Lachowiec et al., 2024). Here we outline and demonstrate an open-source workflow employing flexible steps merged into semi-automated models to maximize usability. Using this workflow, we isolated plants and extracted plot-level data from a highly accurate plot map on a densely planted field of barley.

Plant classification from UAS imagery is a complex task due to variability in plant phenotypic variability and background color. There are both manual and automated solutions that have their own benefits and drawbacks (Peña et al., 2014). EGI thresholding provides an accurate, semi-automated approach to plant classification that does not require large training datasets and processing power. However, it is not capable of automatically accounting for alterations across imagery sets. For this reason, one limitation is the scalability for large datasets. Threshold classification requires user supervision. Conversely, the threshold approach is advantageous for processing consistent sets of imagery quickly. For researchers and growers implementing UAS as only one part of their study, this approach provides a streamlined workflow for extracting plant spectral data. Further, implementation in QGIS is modular, allowing users to import their own classified images to use on downstream plot delineation and data extraction steps.

After plant classification, accurate plot segmentation is necessary to compare plants within and between images. Plot segmentation is often automated but can introduce significant errors if not user corrected or implemented properly (Robb et al., 2020). We identified two

sources of large errors that could be introduced when using an automated grid approach. First, we observed frameshifts in plot identification where the grid drifted away from the correct boundaries and the extracted plots would contain a portion of two plots at once (Supp Figure A4.1). In such cases plots need to be refined by manually moving plot boundaries to remove errors. The second issue we found in automated plots occurred during later dates when tall plants overlap with neighboring plots. Unlike grid drift, this issue could not be solved by moving plot boundaries. To extract consistent plot data, we subset plots to ignore edges where overlaps occurred.

Ground truth data and UAS-collected data may not capture the same aspects of plants and are both influenced by technical errors in data collection. For example, data collection of maize heights is more accurate/precise when collected via UAS versus traditional collection using measuring sticks (Tirado et al., 2020). Similarly, we observed time delays in when UAS-collected data was best correlated with ground truth data. Heading date was determined through ground sampling when half the plants in a plot have headed. However, the UAS imagery considers all identified plants. This explains why the correlation between VARI index and heading date is highest in the days after ground sampling defined all plots as headed.

An alternative approach to measuring plants over a season is integrating the values of an index across flights over time into a single value. While specific single flights correlated accurately with ground-truth data, there was significant variation in correlation across flight dates. We found that integrating over the whole time series correlated more accurately to plant metrics than the average single-flight correlation (Kuenzer et al., 2015; Leinenkugel et al., 2013). Further we isolated the integral to grain-filling time to target heading and maturity date.

Interestingly this did improve the correlation between VARI and both heading and maturity dates but decreased correlation to yield and plant height. Timing the optimal flight dates during the growing season is challenging, so integrating across the time series could be a more robust way to extract accurate information about plants (Matias et al., 2022). This workflow demonstrates how UAS imagery can be classified and delineated in QGIS to extract spectral information. Using QGIS's open-source and versatile toolset allows for further applications across imagery and study systems. Currently the workflow only is capable of classifying RGB imagery. Expansion to multispectral wavelengths would enable calculation of additional, proven spectral indices (Radocaj et al., 2023). Importantly, plant classification and plot segmentation approaches introduced are agnostic to the number of bands in QGIS, allowing users to use these steps with any data in TIFF format. Our pipeline operates as an open framework allowing users to load and unload layers as needed, allowing for integration between these steps and other processing pipelines. For growers who do not work with remote sensing data often, we aimed to create an approach that is fast with a minimal learning curve. At the same time, the workflow is modular to allow experts in remote sensing analysis to use and edit the workflow to fit their needs at any step of the process.

While extremely powerful, the costs and capacity to collect and analyze UAS datasets remain a large barrier for researchers and growers. A survey of agricultural researchers reported that the most common barrier to entry was the "high cost of instruments/devices or software" and the "lack of knowledge or trained personnel to analyze data" (Lachowiec et al., 2024). Here we present an open-source workflow with an annotated guide for users with limited or no experience

to process UAS imagery. In contrast to currently available workflows, we aim to provide a method that is free to use and broadly adaptable to various datasets.

Data Availability

An instruction manual for the QGIS workflow is available at https://github.com/erikthekillian/multiPLOT.

Acknowledgements

We thank Greg Lutgen, Dr. Jessica Williams, and Dr. Jamie Sherman for their contributions to the barley field experiment. We also thank Chloe Hinson, Jared Lile, and Connor Nelle for comments on this manuscript.

Supplemental Material

Supplemental materials contain data used to justify the workflow and the spectral index VARI used in image analysis. Figure A4.1 exemplifies the issue of plot drift that we experienced when trying to create an automatic plot grid based on plot size and spacing. Figure A4.2 exemplifies the issues we experienced when trying to automate plot segmentation using canopy cover. Table A4.1 provides a brief summary of sensor information for reference. Table A4.2 shows the Pearson correlation coefficient between each calculated index and the corresponding plant metric across all flight dates. This is included to provide justification for analyzing VARI in the manuscript as opposed to other measured indices.

References

Adak, A., DeSalvio, A. J., Arik, M. A., & Murray, S. C. (2024). Field-based high-throughput phenotyping enhances phenomic and genomic predictions for grain yield and plant height across years in maize. *G3: Genes, Genomes, Genetics*, *14*(7), jkae092. https://doi.org/10.1093/g3journal/jkae092

Adler, P. S., Goldoftas, B., & Levine, D. I. (1999). Flexibility versus efficiency? A case study of model changeovers in the toyota production system. *Organization Science*, *10*(1), 43–68. https://doi.org/10.1287/orsc.10.1.43

Anderson, S. L., & Murray, S. C. (2020). R/UAStools::plotshpcreate: Create Multi-Polygon Shapefiles for Extraction of Research Plot Scale Agriculture Remote Sensing Data. *Frontiers in Plant Science*, *11*, 511768. https://doi.org/10.3389/fpls.2020.511768

Bendig, J., Bolten, A., & Bareth, G. (2012). Introducing a low-cost mini-UAV for thermal- and multispectral-imaging. *The International Archives of the Photogrammetry, Remote Sensing and Spatial Information Sciences*, *39-B1*, 345–349. https://doi.org/10.5194/isprsarchives-XXXIX-B1-345-2012

Bendig, J., Bolten, A., Bennertz, S., Broscheit, J., Eichfuss, S., & Bareth, G. (2014). Estimating biomass of barley using crop surface models (CSMs) derived from UAV-based RGB imaging. *Remote Sensing*, *6*(11), 10395–10412. https://doi.org/10.3390/rs61110395

Bendig, J., Yu, K., Aasen, H., Bolten, A., Bennertz, S., Broscheit, J., Gnyp, M. L., & Bareth, G. (2015). Combining UAV-based plant height from crop surface models, visible, and near infrared vegetation indices for biomass monitoring in barley. *International Journal of Applied Earth Observation and Geoinformation*, *39*, 79–87. https://doi.org/10.1016/j.jag.2015.02.012

Bhandari, M., Baker, S., Rudd, J. C., Ibrahim, A. M. H., Chang, A., Xue, Q., Jung, J., Landivar, J., & Auvermann, B. (2021). Assessing the effect of drought on winter wheat growth using unmanned aerial system (UAS)-based phenotyping. *Remote Sensing*, *13*(6), 1144. https://doi.org/10.3390/rs13061144

Bian, C., Shi, H., Wu, S., Zhang, K., Wei, M., Zhao, Y., Sun, Y., Zhuang, H., Zhang, X., & Chen, S. (2022). Prediction of field-scale wheat yield using machine learning method and multi-spectral UAV data. *Remote Sensing*, *14*(6). https://doi.org/10.3390/rs14061474

Candiago, S., Remondino, F., De Giglio, M., Dubbini, M., & Gattelli, M. (2015). Evaluating multispectral images and vegetation indices for precision farming applications from UAV images. *Remote Sensing*, *7*(4), 4026–4047. https://doi.org/10.3390/rs70404026

Carneiro, F. M., Furlani, C. E. A., Zerbato, C., Menezes, P. C. D., & Gírio, L. A. D. S. (2019). Correlations among vegetation indices and peanut traits during different crop development stages. *Engenharia Agrícola*, *39*(spe), 33–40. https://doi.org/10.1590/1809-4430-eng.agric.v39nep33-40/2019

Christopher, J. T., Christopher, M. J., Borrell, A. K., Fletcher, S., & Chenu, K. (2016). Stay-green traits to improve wheat adaptation in well-watered and water-limited environments. *Journal of Experimental Botany*, *67*(17), 5159–5172. https://doi.org/10.1093/jxb/erw276

D. M. Woebbecke, G. E. Meyer, K. Von Bargen, & D. A. Mortensen. (1995). Color indices for weed identification under various soil, residue, and lighting conditions. *Transactions of the ASAE*, *38*(1), 259–269. https://doi.org/10.13031/2013.27838

Elhariri, E., El-Bendary, N., & Hassanien, A. E. (2014). Plant classification system based on leaf features. *2014 9th International Conference on Computer Engineering & Systems (ICCES)*, 271–276. https://doi.org/10.1109/ICCES.2014.7030971

Gitelson, A. A., Kaufman, Y. J., Stark, R., & Rundquist, D. (2002). Novel algorithms for remote estimation of vegetation fraction. *Remote Sensing of Environment*, *80*(1), 76–87. https://doi.org/10.1016/S0034-4257(01)00289-9

Gitelson, A. A., Stark, R., Grits, U., Rundquist, D., Kaufman, Y., & Derry, D. (2002). Vegetation and soil lines in visible spectral space: a concept and technique for remote estimation of vegetation fraction. *International Journal of Remote Sensing*, *23*(13), 2537–2562. https://doi.org/10.1080/01431160110107806

Ha, T., Duddu, H., Vandenberg, A., & Shirtliffe, S. (2022). A semi-automatic workflow for plot boundary extraction of irregularly sized and spaced field plots from UAV imagery. *The Plant Phenome Journal*, *5*(1), e20039. https://doi.org/10.1002/ppj2.20039

Haghighattalab, A., González Pérez, L., Mondal, S., Singh, D., Schinstock, D., Rutkoski, J., Ortiz-Monasterio, I., Singh, R. P., Goodin, D., & Poland, J. (2016). Application of unmanned aerial systems for high throughput phenotyping of large wheat breeding nurseries. *Plant Methods*, *12*(1), 35. https://doi.org/10.1186/s13007-016-0134-6

Harrell Jr F (2024). _Hmisc: Harrell Miscellaneous_. R package version 5.2-1, <https://CRAN.R-project.org/package=Hmisc>.

Hennessy, A., Clarke, K., & Lewis, M. (2020). Hyperspectral classification of plants: a review of waveband selection generalisability. *Remote Sensing*, *12*(1), 113. https://doi.org/10.3390/rs12010113

Istiak, Md. A., Syeed, M. M. M., Hossain, M. S., Uddin, M. F., Hasan, M., Khan, R. H., & Azad, N. S. (2023). Adoption of unmanned aerial vehicle (UAV) imagery in agricultural management: a systematic literature review. *Ecological Informatics*, *78*, 102305. https://doi.org/10.1016/j.ecoinf.2023.102305

Ji, Y., Liu, R., Xiao, Y., Cui, Y., Chen, Z., Zong, X., & Yang, T. (2023 Faba bean above-ground biomass and bean yield estimation based on consumer-grade unmanned aerial vehicle RGB images and ensemble learning. *Precision Agriculture*, *24*(4), 1439–1460. https://doi.org/10.1007/s11119-023-09997-5

Jing, Y., Zhang, Y., Hu, M., Chu, Q., & Ma, R. (2019). MODIS-satellite-based analysis of long-term temporal-spatial dynamics and drivers of algal blooms in a plateau lake Dianchi, China. *Remote Sensing*, *11*(21), 2582. https://doi.org/10.3390/rs11212582

Kaur, R., Singh, B., Singh, M., & Thind, S. K. (2015). Hyperspectral indices, correlation and regression models for estimating growth parameters of wheat genotypes. *Journal of the Indian Society of Remote Sensing*, *43*(3), 551–558. https://doi.org/10.1007/s12524-014-0425-1

Killian, E., Lachowiec, J., Sherman, J., Lutgen, G., & Eberly, J. (2023). *High resolution aerial imagery of barley over a growing season* [Dataset]. Dryad. https://doi.org/10.5061/dryad.bk3j9kdhp

Kuenzer, C., Dech, S., & Wagner, W. (2015). Remote sensing time series revealing land surface dynamics: status quo and the pathway ahead. In C. Kuenzer, S. Dech, & W. Wagner (Eds.), *Remote Sensing Time Series* (Vol. 22, pp. 1–24). Springer International Publishing. https://doi.org/10.1007/978-3-319-15967-6_1

Lachowiec, J., Feldman, M. J., Matias, F. I., LeBauer, D., & Gregory, A. (2024). Adoption of unoccupied aerial systems in agricultural research. *The Plant Phenome Journal*, *7*(1), e20098. https://doi.org/10.1002/ppj2.20098

Leinenkugel, P., Kuenzer, C., Oppelt, N., & Dech, S. (2013). Characterisation of land surface phenology and land cover based on moderate resolution satellite data in cloud prone areas—a novel product for the Mekong Basin. *Remote Sensing of Environment*, *136*, 180–198. https://doi.org/10.1016/j.rse.2013.05.004

Liu, S., Yin, D., Feng, H., Li, Z., Xu, X., Shi, L., & Jin, X. (2022 Estimating maize seedling number with UAV RGB images and advanced image processing methods. *Precision Agriculture*, *23*(5), 1604–1632. https://doi.org/10.1007/s11119-022-09899-y

Louhaichi, M., Borman, M. M., & Johnson, D. E. (2001). Spatially located platform and aerial photography for documentation of grazing impacts on wheat. *Geocarto International*, *16*(1), 65–70. https://doi.org/10.1080/10106040108542184

Lu, N., Zhou, J., Han, Z., Li, D., Cao, Q., Yao, X., Tian, Y., Zhu, Y., Cao, W., & Cheng, T. (2019). Improved estimation of aboveground biomass in wheat from RGB imagery and point cloud data acquired with a low-cost unmanned aerial vehicle system. *Plant Methods*, *15*(1), 17. https://doi.org/10.1186/s13007-019-0402-3

Lussem, U., Bolten, A., Gnyp, M. L., Jasper, J., & Bareth, G. (2018). Evaluation of RGB-based vegetation indices from UAV imagery to estimate forage yield in grassland. *The International Archives of the Photogrammetry, Remote Sensing and Spatial Information Sciences*, *42–3*, 1215–1219. https://doi.org/10.5194/isprs-archives-XLII-3-1215-2018

Matias, F. I., Caraza-Harter, M. V., & Endelman, J. B. (2020). FIELDimageR: An R package to analyze orthomosaic images from agricultural field trials. *The Plant Phenome Journal*, *3*(1), e20005. https://doi.org/10.1002/ppj2.20005

Matias, F. I., Green, A., Lachowiec, J. A., LeBauer, D., & Feldman, M. (2022). Bison-Fly: an open-source UAV pipeline for plant breeding data collection. *The Plant Phenome Journal*, *5*(1), e20048. https://doi.org/10.1002/ppj2.20048

Meyer, G. E., & Neto, J. C. (2008). Verification of color vegetation indices for automated crop imaging applications. *Computers and Electronics in Agriculture*, *63*(2), 282–293. https://doi.org/10.1016/j.compag.2008.03.009

Otsu, N. (1979). A Threshold Selection Method from Gray-Level Histograms. *IEEE Transactions on Systems, Man, and Cybernetics,* 9(1), 62-66. https://doi.org/10.1109/TSMC.1979.4310076

Pell, T., Li, J. Y. Q., & Joyce, K. E. (2022). Demystifying the Differences between Structure-from-MotionSoftware Packages for Pre-Processing Drone Data. *Drones*, *6*(1), 24. https://doi.org/10.3390/drones6010024

Peña, J., Gutiérrez, P., Hervás-Martínez, C., Six, J., Plant, R., & López-Granados, F. (2014). Object-based image classification of summer crops with machine learning methods. *Remote Sensing*, *6*(6), 5019–5041. https://doi.org/10.3390/rs6065019

Radočaj, D., Šiljeg, A., Marinović, R., & Jurišić, M. (2023). State of Major Vegetation Indices in Precision Agriculture Studies Indexed in Web of Science: A Review. Agriculture, 13(3), 707. https://doi.org/10.3390/agriculture13030707

Rasmussen, J., Nielsen, J., Streibig, J. C., Jensen, J. E., Pedersen, K. S., & Olsen, S. I. (2019). Pre-harvest weed mapping of Cirsium arvense in wheat and barley with off-the-shelf

UAVs. *Precision Agriculture*, *20*(5), 983–999. https://doi.org/10.1007/s11119-018-09625-7

Rasmussen, J., Nørremark, M., & Bibby, B. (2007). Assessment of leaf cover and crop soil cover in weed harrowing research using digital images. *Weed Research*, *47*(4), 299–310. https://doi.org/10.1111/j.1365-3180.2007.00565.x

Robb, C., Hardy, A., Doonan, J. H., & Brook, J. (2020). Semi-automated field plot segmentation from UAS imagery for experimental agriculture. *Frontiers in Plant Science*, *11*, 591886. https://doi.org/10.3389/fpls.2020.591886

Rodene, E., Xu, G., Palali Delen, S., Zhao, X., Smith, C., Ge, Y., Schnable, J., & Yang, J. (2022). A UAV-based high-throughput phenotyping approach to assess time-series nitrogen responses and identify trait-associated genetic components in maize. *The Plant Phenome Journal*, *5*(1), e20030. https://doi.org/10.1002/ppj2.20030

Sahoo, R. N., Rejith, R. G., Gakhar, S., Ranjan, R., Meena, M. C., Dey, A., Mukherjee, J., Dhakar, R., Meena, A., Daas, A., Babu, S., Upadhyay, P. K., Sekhawat, K., Kumar, S., Kumar, M., Chinnusamy, V., & Khanna, M. (2024). Drone remote sensing of wheat N using hyperspectral sensor and machine learning. *Precision Agriculture*, *25*(2), 704–728. https://doi.org/10.1007/s11119-023-10089-7

Tirado, S. B., Hirsch, C. N., & Springer, N. M. (2020). UAV-based imaging platform for monitoring maize growth throughout development. *Plant Direct*, *4*(6), e00230. https://doi.org/10.1002/pld3.230

WebODM (2023). *OpenDroneMap/WebODM* (Version v2.0.0) [Software]. OpenDroneMap

Trujillano, F., Flores, A., Saito, C., Balcazar, M., & Racoceanu, D. (2018). Corn classification using deep learning with UAV imagery. An operational proof of concept. *2018 IEEE 1st Colombian Conference on Applications in Computational Intelligence (ColCACI)*, 1–4. https://doi.org/10.1109/ColCACI.2018.8484845

Upendar, K., Agrawal, K. N., Chandel, N. S., & Singh, K. (2021). Greenness identification using visible spectral colour indices for site specific weed management. *Plant Physiology Reports*, *26*(1), 179–187. https://doi.org/10.1007/s40502-020-00562-0

Wei, Z., Gu, X., Sun, Q., Hu, X., & Gao, Y. (2021). Analysis of the spatial and temporal pattern of changes in abandoned farmland based on long time series of remote sensing data. *Remote Sensing*, *13*(13), 2549. https://doi.org/10.3390/rs13132549

Williams, J. L., Sherman, J. D., Lamb, P., Cook, J., Lachowiec, J. A., & Bourgault, M. (2022). Relationships between roots, the stay-green phenotype, and agronomic performance in barley and wheat grown in semi-arid conditions. *The Plant Phenome Journal*, *5*(1), e220050. https://doi.org/10.1002/ppj2.20050

Wu, B., Meng, J., Li, Q., Yan, N., Du, X., & Zhang, M. (2014). Remote sensing-based global crop monitoring: experiences with China's CropWatch system. *International Journal of Digital Earth*, *7*(2), 113–137. https://doi.org/10.1080/17538947.2013.821185

Zadoks, J. C., Chang, T. T., & Konzak, C. F. (1974). A decimal code for the growth stages of cereals. *Weed Research*, *14*(6), 415–421. https://doi.org/10.1111/j.1365-3180.1974.tb01084.x

Zhang, M., Wu, B., Yu, M., Zou, W., & Zheng, Y. (2014). Crop condition assessment with adjusted NDVI using the uncropped arable land ratio. *Remote Sensing*, *6*(6), 5774–5794. https://doi.org/10.3390/rs6065774

Zortea, M., Nery, M., Ruga, B., Carvalho, L. B., & Bastos, A. C. (2018). Oil-palm tree detection in aerial images combining deep learning classifiers. *IGARSS 2018 - 2018 IEEE International Geoscience and Remote Sensing Symposium*, 657–660. https://doi.org/10.1109/IGARSS.2018.8519239

CHAPTER FIVE

CONCLUSIONS AND FUTURE RESEARCH

In this dissertation, I present a collection of approaches extending our definition of the plant phenotype. Through large-scale field experiments across multiple growing environments, I investigated the rhizosphere microbiome and how barley roots interact with this community. The objectives of this work were to enhance our understanding of how barley and associated soil microbes interact in an agricultural environment. I also measured barley spectral reflectance using high resolution imagery collected by unoccupied aerial system (UAS) to assess plant development. These perspectives collectively aim to provide a more comprehensive understanding of plant phenotype as I expand from directly measuring agricultural traits like yield and biomass.

Barley soil microbiome phenotype

Chapters 2 and 3 I examined the microbial community structure in the barley rhizosphere by amplicon sequencing across an elite panel of barley lines in four distinct locations and over two years. In chapter 2, a genome-wide association study (GWAS) was performed to establish a connection between specific barley alleles and abundance of specific bacterial taxa. Results showed that these relationships were dependent on location, suggesting that there is a gene by environment interaction affecting barley rhizosphere recruitment. A greenhouse study was conducted to support these findings, demonstrating that under a controlled environment, resident soil microbes and soil chemistry had significant and distinct effects on rhizosphere microbial

community structure, suggesting environmental conditions help define the resulting plant-associated microbiome.

Chapter 3, further examined the plant and environmental effects shaping the rhizosphere microbiome. Across locations and years, the bacterial community was remarkably consistent, supporting the important role of plants in shaping the rhizosphere bacterial community composition within adapted barley growing regions. Similar findings have been reported in rice (Xiong et al., 2021) and wheat (Schlatter et al., 2020). Through variance partitioning, I found that bacterial genera abundance rarely changed as a result of soil factors or location. Strikingly however, there was significant sub-genus variability that was hidden when measured at the genus level. The relative abundance of amplicon sequent variants (ASV) indicated that many taxa were influenced by location, soil, and plant factors. This suggests that the bacterial rhizosphere community structure is built on specific interactions between bacterial species and strains, highlighting the need for sub-genus taxonomic classifications to accurately assess environmental effects on community structure.

In addition to environmental factors, I found specific bacterial ASVs that varied in abundance in response to plant genotype. I included four plant QTLs in the variance partition approach in chapter 3 based on significant QTL found to be associated with microbe abundance in chapter 2. Of these, QTL QGM-5H explained abundance variation in over 30 ASVs, including the *Sphingobacteriales* order which was also identified by GWAS. Importantly, this genetic association was dependent on the environment, similar to other studies that have measured genetic control on the rhizosphere microbiome (Ji et al., 2023; Yue et al., 2024).

In contrast to the bacterial microbiome, the fungal microbiome exhibited significantly greater variability within and across locations and years. This variability was primarily attributed to location-year interactions, suggesting that the fungal rhizosphere community in barley is primarily determined by environmental factors rather than plant recruitment. Geographically determined fungal rhizosphere communities have also been found in Italian vineyard soils (Coller et al., 2019) and a broad survey of Chinese farmlands (Yang et al., 2021).

These findings provide new insight into the complex relationship between barley and its immediate soil environment. I found that the bacterial rhizosphere was largely consistent across locations at a phylum level. This was attributed to overall similar growing conditions similar to previous crop studies (Peiffer et al., 2013; Schlatter et al., 2020). Hawaii exemplified how strong environmental differences can shape barley phenotype irrespective of plant genetics, including both rhizosphere structure and plant performance. The consistency in Montana and South Dakota was telling for barley-microbe breeding, as there was a similar resident community to recruit from, and the genetically distinct population of elite barley varieties recruited a similar bacterial rhizosphere population. Conversely, fungal species in the rhizosphere and bulk soil were defined by the environment, indicating that barley has relatively little control over fungal taxa to recruit from. For improving barley varieties, the patterns measured here in bacteria and fungi inform differing approaches.

The consistency of bacterial community structure at a phylum level in Montana and South Dakota soil suggests that barley is exposed to similar bacteria from which to recruit a beneficial microbiome. For barley breeding, this represents a consistent environment where beneficial microbiome recruitment could be a broadly adapted trait in environments across

Montana to South Dakota. However, I found that environment had a significant effect on bacteria and fungi when measured by specific ASV. This suggests that while the broad taxonomic groups are similar, there are very specific interactions between plant host, environment, and microbe species. To maximize the plant-microbe interactions for plant benefit, these relationships must be further understood at a functional level.

Another important gap for breeding effective rhizosphere recruiting barley is targeting loci based on their effects on plant phenotype and microbiome (Clouse & Wagner, 2021). I identified candidate loci within the S2MET barley population and measured effects on the microbiome, but further study on mechanisms of recruitment is required.

To elucidate gene-microbe mechanisms in barley, a combined sequencing and exudate approach is warranted to measure the relationship between barley genes and root exudate patterns. In a recent study, two barley cultivars were compared using RNA sequencing, chromatography-mass spectrometry, and 16S sequencing to measure gene expression, root exudate profiles, and bacterial rhizosphere community respectively (Pacheco-Moreno et al., 2024). They found three candidate genes responsible for *Pseudomonas fluorescens* recruitment through hexose sugar concentration in root exudates. While specific microbial relationships such as this have been studied, there remains a gap in understanding how root exudates control the broader rhizosphere community in barley. Based on our findings, hub taxa were not responsible for rhizosphere community structure in barley, suggesting that in addition to searching for specific bacterial relationships, a community-based approach is required. A broader survey from a diverse population of barley cultivars can capture root exudation based on genotype, similar to previous studies in other plant species including maize (Da Silva Lima et al., 2014) and the

model grass crop *Brachypodium distachyon* (Mavrodi et al., 2021). Microbial rhizosphere community structure changes can then be compared with exudate profiles and plant genotype to elucidate gene-exudate-microbiome interactions. Better understanding of plant gene-microbe mechanisms in barley is the next step for selection of traits effecting the soil microbiome for plant benefits, offering novel genetic diversity for breeding programs to select for.

The plant spectral phenotype

Plant spectral characteristics offer another novel phenotype to measure plant improvement (Gano et al., 2024). In chapter 4 I developed a novel remote sensing image analysis workflow utilizing open-source software. Remote sensing using unoccupied aerial systems (UAS) can measure plant traits that would otherwise be time or cost inhibitive by collecting low-altitude, high-resolution imagery over agricultural fields. Collecting imagery with UAS has become more accessible as platforms and sensors become less expensive, yet synthesizing images into actionable data remains a challenge for growers and researchers. Proprietary analysis software is often expensive and does not provide image stitching and calibration details, making it impossible to accurately report how the data was analyzed (Pell et al., 2022). Meanwhile, less expensive workflows exist in open-source formats but lack the adaptability to handle non-normal filed layouts (Haghighattalab et al., 2016; Matias et al., 2020).

To address these challenges, I developed a workflow in the open-source software to classify plants and segment images into plots of interest. Results showed plant classification from background soil was possible throughout the barley growing season, independent of development stage. To extract plot-specific spectral data, it was also necessary to develop a supervised plot segmentation process where an automated plot map was overlayed and adjusted

by the user to accommodate uneven plot boundaries caused by differences in plot spacing and uneven rows. This approach allows almost any field to be accurately segmented, since plot size and shape can be edited on a field scale and for specific plots.

The workflow can be further developed to process a wider variety of datasets. Currently plant classification is limited to a threshold approach based on the Excess Greenness Index. By allowing users to create their own index threshold, threshold approaches can be applied based on the requirements for the dataset of interest. The other limitation for users is that only three bands are currently supported for automated plant classification. Optimized for RGB imagery, the workflow cannot currently address multispectral bands. To address this, automated plant classification needs to be expanded to be agnostic to the number of bands. With this step being automated, users could use this pipeline across any sensor available that collects tiff data, including popular multispectral sensors that measure near-infrared and red-edge wavelengths in addition to red, green, and blue. With these added features, the workflow will be more widely compatible with current data collection methods (Aslan et al., 2022). Additionally, because the process is completely open source using general public license (GPL) software, I hope to see users modify and add to the pipeline based on their own project design and dataset. Streamlined workflows for rapid imagery analysis facilitate better integration of this data into current breeding and research methods.

Extended phenotyping for sustainable agriculture

Since the beginning of plant domestication, plant phenotype variability has been used to select for the best performing cultivars. Initially this targeted variability in plant height, yield, and pest resistance. As traits are selected for, genetic variability decreases, leading to a

diminishing rate of return until the trait can become fixed (Yan, 2021). To maintain plant improvement, it is necessary to either introduce novel genetic material or address novel traits. Breeding has expanded the definition of plant phenotype in the past, including less visible traits such as protein content (Loskutov & Khlestkina, 2021; Maqbool et al., 2021) and nitrogen use efficiency (Ali et al., 2022; Fiaz et al., 2021) for significant improvements in plant performance. More recently remote sensing has further extended the plant phenotype, showing that spectral reflectance can accurately predict plant performance (Gano et al., 2024). This work adds to research across many agriculturally significant crops to support the introduction of plant associated microbes as an extended phenotype to target in plant breeding.

This dissertation builds on previous genetic and ecological studies that expand the definition of plant phenotype by examining its interactions with the immediate environment. Novel phenotype metrics allow for additional selections to be made in breeding material and expands our understanding of how the environment affects crop performance. Together this means more precise cultivars bred to perform well under a more defined range of environmental conditions.

References

Ali, M. A., Ghazy, A. I., Alotaibi, K. D., Ibrahim, O. M., & Al-Doss, A. A. (2022). Nitrogen efficiency indexes association with nitrogen recovery, utilization, and use efficiency in spring barley at various nitrogen application rates. *Agronomy Journal*, *114*(4), 2290–2309. https://doi.org/10.1002/agj2.21128

Aslan, M. F., Durdu, A., Sabanci, K., Ropelewska, E., & Gültekin, S. S. (2022). A Comprehensive Survey of the Recent Studies with UAV for Precision Agriculture in Open Fields and Greenhouses. *Applied Sciences*, *12*(3), 1047. https://doi.org/10.3390/app12031047

Clouse, K. M., & Wagner, M. R. (2021). Plant Genetics as a Tool for Manipulating Crop Microbiomes: Opportunities and Challenges. *Frontiers in Bioengineering and Biotechnology*, *9*, 567548. https://doi.org/10.3389/fbioe.2021.567548

Coller, E., Cestaro, A., Zanzotti, R., Bertoldi, D., Pindo, M., Larger, S., Albanese, D., Mescalchin, E., & Donati, C. (2019). Microbiome of vineyard soils is shaped by geography and management. *Microbiome*, *7*(1), 140. https://doi.org/10.1186/s40168-019-0758-7

Da Silva Lima, L., Olivares, F. L., Rodrigues De Oliveira, R., Vega, M. R. G., Aguiar, N. O., & Canellas, L. P. (2014). Root exudate profiling of maize seedlings inoculated with Herbaspirillum seropedicaeand humic acids. *Chemical and Biological Technologies in Agriculture*, *1*(1), 23. https://doi.org/10.1186/s40538-014-0023-z

Fiaz, S., Wang, X., Khan, S. A., Ahmar, S., Noor, M. A., Riaz, A., Ali, K., Abbas, F., Mora-Poblete, F., Figueroa, C. R., & Alharthi, B. (2021). Novel plant breeding techniques to advance nitrogen use efficiency in rice: A review. *GM Crops & Food*, *12*(2), 627–646. https://doi.org/10.1080/21645698.2021.1921545

Gano, B., Bhadra, S., Vilbig, J. M., Ahmed, N., Sagan, V., & Shakoor, N. (2024). Drone-based imaging sensors, techniques, and applications in plant phenotyping for crop breeding: A comprehensive review. *The Plant Phenome Journal*, *7*(1), e20100. https://doi.org/10.1002/ppj2.20100

Haghighattalab, A., González Pérez, L., Mondal, S., Singh, D., Schinstock, D., Rutkoski, J., Ortiz-Monasterio, I., Singh, R. P., Goodin, D., & Poland, J. (2016). Application of unmanned aerial systems for high throughput phenotyping of large wheat breeding nurseries. *Plant Methods*, *12*(1), 35. https://doi.org/10.1186/s13007-016-0134-6

Ji, N., Liang, D., Clark, L. V., Sacks, E. J., & Kent, A. D. (2023). Host genetic variation drives the differentiation in the ecological role of the native Miscanthus root-associated microbiome. *Microbiome*, *11*(1), 216. https://doi.org/10.1186/s40168-023-01646-3

Loskutov, I. G., & Khlestkina, E. K. (2021). Wheat, Barley, and Oat Breeding for Health Benefit Components in Grain. *Plants*, *10*(1), 86. https://doi.org/10.3390/plants10010086

Maqbool, M. A., Beshir Issa, A., & Khokhar, E. S. (2021). Quality protein maize (QPM): Importance, genetics, timeline of different events, breeding strategies and varietal adoption. *Plant Breeding*, *140*(3), 375–399. https://doi.org/10.1111/pbr.12923

Matias, F. I., Caraza-Harter, M. V., & Endelman, J. B. (2020). FIELDimageR: An R package to analyze orthomosaic images from agricultural field trials. *The Plant Phenome Journal*, *3*(1), e20005. https://doi.org/10.1002/ppj2.20005

Mavrodi, O. V., McWilliams, J. R., Peter, J. O., Berim, A., Hassan, K. A., Elbourne, L. D. H., LeTourneau, M. K., Gang, D. R., Paulsen, I. T., Weller, D. M., Thomashow, L. S., Flynt, A. S., & Mavrodi, D. V. (2021). Root Exudates Alter the Expression of Diverse Metabolic, Transport, Regulatory, and Stress Response Genes in Rhizosphere Pseudomonas. *Frontiers in Microbiology*, *12*, 651282. https://doi.org/10.3389/fmicb.2021.651282

Pacheco-Moreno, A., Bollmann-Giolai, A., Chandra, G., Brett, P., Davies, J., Thornton, O., Poole, P., Ramachandran, V., Brown, J. K. M., Nicholson, P., Ridout, C., DeVos, S., & Malone, J. G. (2024). The genotype of barley cultivars influences multiple aspects of their associated microbiota via differential root exudate secretion. *PLOS Biology*, *22*(4), e3002232. https://doi.org/10.1371/journal.pbio.3002232

Peiffer, J. A., Spor, A., Koren, O., Jin, Z., Tringe, S. G., Dangl, J. L., Buckler, E. S., & Ley, R. E. (2013). Diversity and heritability of the maize rhizosphere microbiome under field conditions. *Proceedings of the National Academy of Sciences*, *110*(16), 6548–6553. https://doi.org/10.1073/pnas.1302837110

Pell, T., Li, J. Y. Q., & Joyce, K. E. (2022). Demystifying the Differences between Structure-from-MotionSoftware Packages for Pre-Processing Drone Data. *Drones*, *6*(1), 24. https://doi.org/10.3390/drones6010024

Schlatter, D. C., Yin, C., Hulbert, S., & Paulitz, T. C. (2020). Core Rhizosphere Microbiomes of Dryland Wheat Are Influenced by Location and Land Use History. *Applied and Environmental Microbiology*, *86*(5), e02135-19. https://doi.org/10.1128/AEM.02135-19

Xiong, J., Lu, J., Li, X., Qiu, Q., Chen, J., & Yan, C. (2021). Effect of rice (Oryza sativa L.) genotype on yield: Evidence from recruiting spatially consistent rhizosphere microbiome. *Soil Biology and Biochemistry*, *161*, 108395. https://doi.org/10.1016/j.soilbio.2021.108395

Yan, W. (2021). A Systematic Narration of Some Key Concepts and Procedures in Plant Breeding. *Frontiers in Plant Science*, *12*, 724517. https://doi.org/10.3389/fpls.2021.724517

Yang, W., Li, S., Wang, X., Liu, F., Li, X., & Zhu, X. (2021). Soil properties and geography shape arbuscular mycorrhizal fungal communities in black land of China. *Applied Soil Ecology*, *167*, 104109. https://doi.org/10.1016/j.apsoil.2021.104109

Yue, H., Sun, X., Wang, T., Zhang, A., Han, D., Wei, G., Song, W., & Shu, D. (2024). Host genotype-specific rhizosphere fungus enhances drought resistance in wheat. *Microbiome*, *12*(1), 44. https://doi.org/10.1186/s40168-024-01770-8

CUMULATIVE REFERENCES CITED

Adak, A., DeSalvio, A. J., Arik, M. A., & Murray, S. C. (2024). Field-based high-throughput phenotyping enhances phenomic and genomic predictions for grain yield and plant height across years in maize. G3: Genes, Genomes, Genetics, 14(7), jkae092. https://doi.org/10.1093/g3journal/jkae092

Adler, P. S., Goldoftas, B., & Levine, D. I. (1999). Flexibility versus efficiency? A case study of model changeovers in the toyota production system. Organization Science, 10(1), 43–68. https://doi.org/10.1287/orsc.10.1.43

Agler, M. T., Ruhe, J., Kroll, S., Morhenn, C., Kim, S.-T., Weigel, D., & Kemen, E. M. (2016). Microbial Hub Taxa Link Host and Abiotic Factors to Plant Microbiome Variation. PLOS Biology, 14(1), e1002352. https://doi.org/10.1371/journal.pbio.1002352

Ahkami, A. H. et al. (2023). Emerging sensing, imaging, and computational technologies to scale nano- to macroscale rhizosphere dynamics–Review and research perspectives. Soil Biology and Biochemistry, 109253.

Ahkami, A. H., Qafoku, O., Roose, T., Mou, Q., Lu, Y., Cardon, Z. G., Wu, Y., Chou, C., Fisher, J. B., Varga, T., Handakumbura, P., Aufrecht, J. A., Bhattacharjee, A., & Moran, J. J. (2024). Emerging sensing, imaging, and computational technologies to scale nano-to macroscale rhizosphere dynamics – Review and research perspectives. Soil Biology and Biochemistry, 189, 109253. https://doi.org/10.1016/j.soilbio.2023.109253

Aitchison, J. (1982). The statistical analysis of compositional data. Journal of the Royal Statistical Society: Series B (Methodological) 44, 139-160.

Alabouvette, C. (1999). Fusarium wilt suppressive soils: An example of disease-suppressive soils. Australasian Plant Pathology, 28(1), 57. https://doi.org/10.1071/AP99008

Alori, E. T., Dare, M. O. & Babalola, O. O. (2017). Microbial inoculants for soil quality and plant health. Sustainable Agriculture Reviews, 281-307.

Anderson, D. W. (1988). The effect of parent material and soil development on nutrient cycling in temperate ecosystems. Biogeochemistry, 5(1), 71–97. https://doi.org/10.1007/BF02180318

Anderson, J. T., Lee, C. R., Rushworth, C. A., Colautti, R. I. & Mitchell-Olds, T. (2013). Genetic trade-offs and conditional neutrality contribute to local adaptation. Molecular Ecology 22, 699-708.

Anderson, S. L., & Murray, S. C. (2020). R/UAStools::plotshpcreate: Create Multi-Polygon Shapefiles for Extraction of Research Plot Scale Agriculture Remote Sensing Data. Frontiers in Plant Science, 11, 511768. https://doi.org/10.3389/fpls.2020.511768

Ansari, S., Kumar, V., Bhatt, D. N., Irfan, M. & Datta, A. (2022). N-acetylglucosamine sensing and metabolic engineering for attenuating human and plant pathogens. Bioengineering 9, 64.

Arshad, M., Shaharoona, B., & Mahmood, T. (2008). Inoculation with Pseudomonas spp. Containing ACC-Deaminase Partially Eliminates the Effects of Drought Stress on Growth, Yield, and Ripening of Pea (Pisum sativum L.). Pedosphere, 18(5), 611–620. https://doi.org/10.1016/S1002-0160(08)60055-7

Babalola, O. O., Emmanuel, O. C., Adeleke, B. S., Odelade, K. A., Nwachukwu, B. C., Ayiti, O. E., Adegboyega, T. T., & Igiehon, N. O. (2021). Rhizosphere Microbiome Cooperations: Strategies for Sustainable Crop Production. Current Microbiology, 78(4), 1069–1085. https://doi.org/10.1007/s00284-021-02375-2

Banerjee, S., Schlaeppi, K., & Van Der Heijden, M. G. A. (2018). Keystone taxa as drivers of microbiome structure and functioning. Nature Reviews Microbiology, 16(9), 567–576. https://doi.org/10.1038/s41579-018-0024-1

Bano, S., Wu, X. & Zhang, X. (2021). Towards sustainable agriculture: rhizosphere microbiome engineering. Applied Microbiology and Biotechnology, 1-20.

Bendig, J., Bolten, A., & Bareth, G. (2012). Introducing a low-cost mini-UAV for thermal- and multispectral-imaging. The International Archives of the Photogrammetry, Remote Sensing and Spatial Information Sciences, 39-B1, 345–349. https://doi.org/10.5194/isprsarchives-XXXIX-B1-345-2012

Bendig, J., Bolten, A., Bennertz, S., Broscheit, J., Eichfuss, S., & Bareth, G. (2014). Estimating biomass of barley using crop surface models (CSMs) derived from UAV-based RGB imaging. Remote Sensing, 6(11), 10395–10412. https://doi.org/10.3390/rs61110395

Bendig, J., Yu, K., Aasen, H., Bolten, A., Bennertz, S., Broscheit, J., Gnyp, M. L., & Bareth, G. (2015). Combining UAV-based plant height from crop surface models, visible, and near infrared vegetation indices for biomass monitoring in barley. International Journal of Applied Earth Observation and Geoinformation, 39, 79–87. https://doi.org/10.1016/j.jag.2015.02.012

Bergelson, J., Mittelstrass, J., & Horton, M. W. (2019). Characterizing both bacteria and fungi improves understanding of the Arabidopsis root microbiome. Scientific Reports, 9(1), 24. https://doi.org/10.1038/s41598-018-37208-z

Berry, D., & Widder, S. (2014). Deciphering microbial interactions and detecting keystone species with co-occurrence networks. Frontiers in Microbiology, 5. https://doi.org/10.3389/fmicb.2014.00219

Bhandari, M., Baker, S., Rudd, J. C., Ibrahim, A. M. H., Chang, A., Xue, Q., Jung, J., Landivar, J., & Auvermann, B. (2021). Assessing the effect of drought on winter wheat growth using unmanned aerial system (UAS)-based phenotyping. Remote Sensing, 13(6), 1144. https://doi.org/10.3390/rs13061144

Bian, C., Shi, H., Wu, S., Zhang, K., Wei, M., Zhao, Y., Sun, Y., Zhuang, H., Zhang, X., & Chen, S. (2022). Prediction of field-scale wheat yield using machine learning method and multi-spectral UAV data. Remote Sensing, 14(6). https://doi.org/10.3390/rs14061474

Bigeard, J., Colcombet, J., & Hirt, H. (2015). Signaling Mechanisms in Pattern-Triggered Immunity (PTI). Molecular Plant, 8(4), 521–539. https://doi.org/10.1016/j.molp.2014.12.022

Boitt, G., Simpson, Z. P., Tian, J., Black, A., Wakelin, S. A., & Condron, L. M. (2018). Plant biomass management impacts on short-term soil phosphorus dynamics in a temperate grassland. Biology and Fertility of Soils, 54(3), 397–409. https://doi.org/10.1007/s00374-018-1269-6

Bolyen, E. et al. (2019). Reproducible, Interactive, Scalable and Extensible Microbiome Data Science Using QIIME 2. Nature Biotechnology 37, 852-857.

Braum, S. M., & Helmke, P. A. (1995). White lupin utilizes soil phosphorus that is unavailable to soybean. Plant and Soil, 176(1), 95–100. https://doi.org/10.1007/BF00017679

Breitkreuz, C., Herzig, L., Buscot, F., Reitz, T., & Tarkka, M. (2021). Interactions between soil properties, agricultural management and cultivar type drive structural and functional adaptations of the wheat rhizosphere microbiome to drought. Environmental Microbiology, 23(10), 5866–5882. https://doi.org/10.1111/1462-2920.15607

Brisco, B., Brown, R. J., Hirose, T., McNairn, H., & Staenz, K. (1998). Precision Agriculture and the Role of Remote Sensing: A Review. Canadian Journal of Remote Sensing, 24(3), 315–327. https://doi.org/10.1080/07038992.1998.10855254

Brown, S. P., Grillo, M. A., Podowski, J. C., & Heath, K. D. (2020). Soil Origin and Plant Genotype Structure Distinct Microbiome Compartments In the Model Legume Medicago Truncatula. Microbiome, 8(1), 139. https://doi.org/10.1186/s40168-020-00915-9

Brundrett, M. C., & Tedersoo, L. (2018). Evolutionary History of Mycorrhizal Symbioses and Global Host Plant Diversity. New Phytologist, 220(4), 1108–1115. https://doi.org/10.1111/nph.14976

Bulgarelli, D. et al. (2015). Structure and Function of the Bacterial Root Microbiota in Wild and Domesticated Barley. Cell Host & Microbe 17, 392-403.

Bulgarelli, D., Schlaeppi, K., Spaepen, S., Van Themaat, E. V. L., & Schulze-Lefert, P. (2013). Structure and Functions of the Bacterial Microbiota of Plants. Annual Review of Plant Biology, 64(1), 807–838. https://doi.org/10.1146/annurev-arplant-050312-120106

Butterly, C. R., Bünemann, E. K., McNeill, A. M., Baldock, J. A., & Marschner, P. (2009). Carbon pulses but not phosphorus pulses are related to decreases in microbial biomass during repeated drying and rewetting of soils. Soil Biology and Biochemistry, 41(7), 1406–1416. https://doi.org/10.1016/j.soilbio.2009.03.018

Callahan, B. J., McMurdie, P. J. & Holmes, S. P. (2017). Exact sequence variants should replace operational taxonomic units in marker-gene data analysis. The ISME Journal 11, 2639-2643.

Candiago, S., Remondino, F., De Giglio, M., Dubbini, M., & Gattelli, M. (2015). Evaluating multispectral images and vegetation indices for precision farming applications from UAV images. Remote Sensing, 7(4), 4026–4047. https://doi.org/10.3390/rs70404026

Cantalapiedra, C. P., Boudiar, R., Casas, A. M., Igartua, E. & Contreras-Moreira, B. (2015). BARLEYMAP: physical and genetic mapping of nucleotide sequences and annotation of surrounding loci in barley. Molecular Breeding 35, 1-11.

Carneiro, F. M., Furlani, C. E. A., Zerbato, C., Menezes, P. C. D., & Gírio, L. A. D. S. (2019). Correlations among vegetation indices and peanut traits during different crop development stages. Engenharia Agrícola, 39(spe), 33–40. https://doi.org/10.1590/1809-4430-eng.agric.v39nep33-40/2019

Cassman, K. G., & Grassini, P. (2020). A global perspective on sustainable intensification research. Nature Sustainability, 3(4), 262–268. https://doi.org/10.1038/s41893-020-0507-8

Castrillo, G., Teixeira, P. J. P. L., Paredes, S. H., Law, T. F., De Lorenzo, L., Feltcher, M. E., Finkel, O. M., Breakfield, N. W., Mieczkowski, P., Jones, C. D., Paz-Ares, J., & Dangl, J. L. (2017). Root microbiota drive direct integration of phosphate stress and immunity. Nature, 543(7646), 513–518. https://doi.org/10.1038/nature21417

Chang, P., Gerhardt, K. E., Huang, X.-D., Yu, X.-M., Glick, B. R., Gerwing, P. D., & Greenberg, B. M. (2014). Plant Growth-Promoting Bacteria Facilitate the Growth of Barley and Oats in Salt-Impacted Soil: Implications for Phytoremediation of Saline Soils. International Journal of Phytoremediation, 16(11), 1133–1147. https://doi.org/10.1080/15226514.2013.821447

Chapman, S. C., Chakraborty, S., Dreccer, M. F., & Howden, S. M. (2012). Plant adaptation to climate change—Opportunities and priorities in breeding. Crop and Pasture Science, 63(3), 251. https://doi.org/10.1071/CP11303

Che, J., Wu, Y., Yang, H., Wu, W., Lyu, L., Wang, X., & Li, W. (2024). Beneficial ecological networks dominate the dynamic root endosphere microbiome during long-term symbiosis with host plants. Plant and Soil, 501(1–2), 289–305. https://doi.org/10.1007/s11104-024-06519-8

Chen, S., Waghmode, T. R., Sun, R., Kuramae, E. E., Hu, C., & Liu, B. (2019). Root-associated microbiomes of wheat under the combined effect of plant development and nitrogen fertilization. Microbiome, 7(1), 136. https://doi.org/10.1186/s40168-019-0750-2

Chepsergon, J., & Moleleki, L. N. (2023). Rhizosphere bacterial interactions and impact on plant health. Current Opinion in Microbiology, 73, 102297. https://doi.org/10.1016/j.mib.2023.102297

Christopher, J. T., Christopher, M. J., Borrell, A. K., Fletcher, S., & Chenu, K. (2016). Stay-green traits to improve wheat adaptation in well-watered and water-limited environments. Journal of Experimental Botany, 67(17), 5159–5172. https://doi.org/10.1093/jxb/erw276

Clouse, K. M., & Wagner, M. R. (2021). Plant Genetics as a Tool for Manipulating Crop Microbiomes: Opportunities and Challenges. Frontiers in Bioengineering and Biotechnology, 9, 567548. https://doi.org/10.3389/fbioe.2021.567548

Coller, E., Cestaro, A., Zanzotti, R., Bertoldi, D., Pindo, M., Larger, S., Albanese, D., Mescalchin, E., & Donati, C. (2019). Microbiome of vineyard soils is shaped by geography and management. Microbiome, 7(1), 140. https://doi.org/10.1186/s40168-019-0758-7

Contreras-Liza, S. E. Plant Breeding and Microbiome. (IntechOpen, 2021).

Corti, G., Agnelli, A., Cuniglio, R., Sanjurjo, M. F., & Cocco, S. (2005). Characteristics of rhizosphere soil from natural and agricultural environments. In Biogeochemistry of Trace Elements in the Rhizosphere (pp. 57–128). Elsevier. https://doi.org/10.1016/B978-044451997-9/50005-2

Crowther, T. W. et al. The global soil community and its influence on biogeochemistry. Science 365 (2019).

D. M. Woebbecke, G. E. Meyer, K. Von Bargen, & D. A. Mortensen. (1995). Color indices for weed identification under various soil, residue, and lighting conditions. Transactions of the ASAE, 38(1), 259–269. https://doi.org/10.13031/2013.27838

Delgado-Baquerizo, M. et al. A global atlas of the dominant bacteria found in soil. Science 359, 320-325 (2018).

Delgado-Baquerizo, M., Oliverio, A. M., Brewer, T. E., Benavent-González, A., Eldridge, D. J., Bardgett, R. D., Maestre, F. T., Singh, B. K., & Fierer, N. (2018). A global atlas of the dominant bacteria found in soil. Science, 359(6373), 320–325. https://doi.org/10.1126/science.aap9516

Deng, S. et al. (2021). Genome wide association study reveals plant loci controlling heritability of the rhizosphere microbiome. The ISME journal 15, 3181-3194.

Dong, W., & Song, Y. (2020). The Significance of Flavonoids in the Process of Biological Nitrogen Fixation. International Journal of Molecular Sciences, 21(16), 5926. https://doi.org/10.3390/ijms21165926

Eberly, J. O. et al. (2024). Compositional profiling of the rhizosphere microbiome of Canada thistle reveals consistent patterns across the United States northern Great Plains. Scientific Reports 14, 18016.

Eduardo Contreras-Liza, S. (2021). Plant Breeding and Microbiome. In I. Y. Abdurakhmonov (Ed.), Plant Breeding—Current and Future Views. IntechOpen. https://doi.org/10.5772/intechopen.94948

Edwards, J. A. et al. (2023). Genetic determinants of switchgrass-root-associated microbiota in field sites spanning its natural range. Current Biology 33, 1926-1938. e1926.

Edwards, J., Johnson, C., Santos-Medellín, C., Lurie, E., Podishetty, N. K., Bhatnagar, S., Eisen, J. A., & Sundaresan, V. (2015). Structure, variation, and assembly of the root-associated microbiomes of rice. Proceedings of the National Academy of Sciences, 112(8). https://doi.org/10.1073/pnas.1414592112

Egidi, E., Delgado-Baquerizo, M., Plett, J. M., Wang, J., Eldridge, D. J., Bardgett, R. D., Maestre, F. T., & Singh, B. K. (2019). A few Ascomycota taxa dominate soil fungal communities worldwide. Nature Communications, 10(1), 2369. https://doi.org/10.1038/s41467-019-10373-z

Elhariri, E., El-Bendary, N., & Hassanien, A. E. (2014). Plant classification system based on leaf features. 2014 9th International Conference on Computer Engineering & Systems (ICCES), 271–276. https://doi.org/10.1109/ICCES.2014.7030971

Escudero-Martinez, C. et al. (2022). Identifying plant genes shaping microbiota composition in the barley rhizosphere. Nature Communications 13, 3443.

Ewing, P. M. et al. (2024). Local adaptation and broad performance are synergistic to productivity in modern barley. Crop Science 64, 192-199.

Federer, W. T. (1961). Augmented designs with one-way elimination of heterogeneity. Biometrics 17, 447-473.

Fierer, N. (2017). Embracing the unknown: Disentangling the complexities of the soil microbiome. Nature Reviews Microbiology, 15(10), 579–590. https://doi.org/10.1038/nrmicro.2017.87

Fischer, R. A. (2015). Definitions and determination of crop yield, yield gaps, and of rates of change. Field Crops Research, 182, 9–18. https://doi.org/10.1016/j.fcr.2014.12.006

French, E., Tran, T., & Iyer-Pascuzzi, A. S. (2020). Tomato Genotype Modulates Selection and Responses to Root Microbiota. Phytobiomes Journal, 4(4), 314–326. https://doi.org/10.1094/PBIOMES-02-20-0020-R

Gaind, S. (2016). Phosphate dissolving fungi: Mechanism and application in alleviation of salt stress in wheat. Microbiological Research, 193, 94–102. https://doi.org/10.1016/j.micres.2016.09.005

Garg, N. & Geetanjali. (2009). Symbiotic Nitrogen Fixation in Legume Nodules: Process and Signaling: A Review. In E. Lichtfouse, M. Navarrete, P. Debaeke, S. Véronique, & C. Alberola (Eds.),

Sustainable Agriculture (pp. 519–531). Springer Netherlands. https://doi.org/10.1007/978-90-481-2666-8_32

Gitelson, A. A., Kaufman, Y. J., Stark, R., & Rundquist, D. (2002). Novel algorithms for remote estimation of vegetation fraction. Remote Sensing of Environment, 80(1), 76–87. https://doi.org/10.1016/S0034-4257(01)00289-9

Gitelson, A. A., Stark, R., Grits, U., Rundquist, D., Kaufman, Y., & Derry, D. (2002). Vegetation and soil lines in visible spectral space: a concept and technique for remote estimation of vegetation fraction. International Journal of Remote Sensing, 23(13), 2537–2562. https://doi.org/10.1080/01431160110107806

Gloor, G. B., Macklaim, J. M., Pawlowsky-Glahn, V. & Egozcue, J. J. (2017). Microbiome datasets are compositional: and this is not optional. Frontiers in Microbiology 8, 2224.

Gontia-Mishra, I., Sapre, S., Deshmukh, R., Sikdar, S., & Tiwari, S. (2020). Microbe-Mediated Drought Tolerance in Plants: Current Developments and Future Challenges. In A. N. Yadav, J. Singh, A. A. Rastegari, & N. Yadav (Eds.), Plant Microbiomes for Sustainable Agriculture (Vol. 25, pp. 351–379). Springer International Publishing. https://doi.org/10.1007/978-3-030-38453-1_12

Gopal, M., & Gupta, A. (2016). Microbiome Selection Could Spur Next-Generation Plant Breeding Strategies. Frontiers in Microbiology, 7. https://doi.org/10.3389/fmicb.2016.01971

Grant, M. R. et al. (1995). Structure of the Arabidopsis RPM1 gene enabling dual specificity disease resistance. Science 269, 843-846.

Gupta, A., Rico-Medina, A., & Caño-Delgado, A. I. (2020). The physiology of plant responses to drought. Science, 368(6488), 266–269. https://doi.org/10.1126/science.aaz7614

Gutjahr, C., & Paszkowski, U. (2013). Multiple control levels of root system remodeling in arbuscular mycorrhizal symbiosis. Frontiers in Plant Science, 4. https://doi.org/10.3389/fpls.2013.00204

Ha, T., Duddu, H., Vandenberg, A., & Shirtliffe, S. (2022). A semi-automatic workflow for plot boundary extraction of irregularly sized and spaced field plots from UAV imagery. The Plant Phenome Journal, 5(1), e20039. https://doi.org/10.1002/ppj2.20039

Haghighattalab, A., González Pérez, L., Mondal, S., Singh, D., Schinstock, D., Rutkoski, J., Ortiz-Monasterio, I., Singh, R. P., Goodin, D., & Poland, J. (2016). Application of unmanned aerial systems for high throughput phenotyping of large wheat breeding nurseries. Plant Methods, 12(1), 35. https://doi.org/10.1186/s13007-016-0134-6

Hajishengallis, G., Darveau, R. P., & Curtis, M. A. (2012). The keystone-pathogen hypothesis. Nature Reviews Microbiology, 10(10), 717–725. https://doi.org/10.1038/nrmicro2873

Harrell Jr F (2024). _Hmisc: Harrell Miscellaneous_. R package

Hassan, S. & Mathesius, U. (2012). The role of flavonoids in root–rhizosphere signalling: opportunities and challenges for improving plant–microbe interactions. Journal of Experimental Botany 63, 3429-3444.

He, X., Wang, D., Jiang, Y., Li, M., Delgado-Baquerizo, M., McLaughlin, C., Marcon, C., Guo, L., Baer, M., Moya, Y. A. T., Von Wirén, N., Deichmann, M., Schaaf, G., Piepho, H.-P., Yang, Z., Yang, J., Yim, B., Smalla, K., Goormachtig, S., … Yu, P. (2024). Heritable microbiome variation is correlated with source environment in locally adapted maize varieties. Nature Plants. https://doi.org/10.1038/s41477-024-01654-7

Hedley, M., & McLaughlin, M. (2015). Reactions of Phosphate Fertilizers and By-Products in Soils. In J. Thomas Sims & A. N. Sharpley (Eds.), Agronomy Monographs (pp. 181–252). American Society of Agronomy, Crop Science Society of America, and Soil Science Society of America. https://doi.org/10.2134/agronmonogr46.c7

Hennessy, A., Clarke, K., & Lewis, M. (2020). Hyperspectral classification of plants: a review of waveband selection generalisability. Remote Sensing, 12(1), 113. https://doi.org/10.3390/rs12010113

Herms, C. H., Hennessy, R. C., Bak, F., Dresbøll, D. B., & Nicolaisen, M. H. (2022). Back to our roots: Exploring the role of root morphology as a mediator of beneficial plant–microbe interactions. Environmental Microbiology, 24(8), 3264–3272. https://doi.org/10.1111/1462-2920.15926

Ho, A., Lonardo, D. P. D., & Bodelier, P. L. E. (2017). Revisiting life strategy concepts in environmental microbial ecology. FEMS Microbiology Ecology, fix006. https://doi.org/10.1093/femsec/fix006

Holland, J. B., Nyquist, W. E., Cervantes-Martínez, C. T. & Janick, J. Estimating and interpreting heritability for plant breeding: an update. Plant Breeding Reviews 22 (2003).

Hunter, P. (2016). Plant microbiomes and sustainable agriculture: Deciphering the plant microbiome and its role in nutrient supply and plant immunity has great potential to reduce the use of fertilizers and biocides in agriculture. EMBO Reports, 17(12), 1696–1699. https://doi.org/10.15252/embr.201643476

Iannetta, P. P. M., Young, M., Bachinger, J., Bergkvist, G., Doltra, J., Lopez-Bellido, R. J., Monti, M., Pappa, V. A., Reckling, M., Topp, C. F. E., Walker, R. L., Rees, R. M., Watson, C. A., James, E. K., Squire, G. R., & Begg, G. S. (2016). A Comparative Nitrogen Balance and Productivity Analysis of Legume and Non-legume Supported Cropping Systems: The Potential Role of Biological Nitrogen Fixation. Frontiers in Plant Science, 7. https://doi.org/10.3389/fpls.2016.01700

Ilyas, N., Mumtaz, K., Akhtar, N., Yasmin, H., Sayyed, R. Z., Khan, W., Enshasy, H. A. E., Dailin, D. J., Elsayed, E. A., & Ali, Z. (2020). Exopolysaccharides Producing Bacteria for the Amelioration of Drought Stress in Wheat. Sustainability, 12(21), 8876. https://doi.org/10.3390/su12218876

Istiak, Md. A., Syeed, M. M. M., Hossain, M. S., Uddin, M. F., Hasan, M., Khan, R. H., & Azad, N. S. (2023). Adoption of Unmanned Aerial Vehicle (UAV) imagery in agricultural management: A systematic literature review. Ecological Informatics, 78, 102305. https://doi.org/10.1016/j.ecoinf.2023.102305

Istiak, Md. A., Syeed, M. M. M., Hossain, M. S., Uddin, M. F., Hasan, M., Khan, R. H., & Azad, N. S. (2023). Adoption of unmanned aerial vehicle (UAV) imagery in agricultural management: a systematic literature review. Ecological Informatics, 78, 102305. https://doi.org/10.1016/j.ecoinf.2023.102305

Janiak, A., Kwaśniewski, M., & Szarejko, I. (2016). Gene expression regulation in roots under drought. Journal of Experimental Botany, 67(4), 1003–1014. https://doi.org/10.1093/jxb/erv512

Ji, Y., Liu, R., Xiao, Y., Cui, Y., Chen, Z., Zong, X., & Yang, T. (2023). Faba bean above-ground biomass and bean yield estimation based on consumer-grade unmanned aerial vehicle RGB images and ensemble learning. Precision Agriculture, 24(4), 1439–1460. https://doi.org/10.1007/s11119-023-09997-5

Jing, Y., Zhang, Y., Hu, M., Chu, Q., & Ma, R. (2019). MODIS-satellite-based analysis of long-term temporal-spatial dynamics and drivers of algal blooms in a plateau lake Dianchi, China. Remote Sensing, 11(21), 2582. https://doi.org/10.3390/rs11212582

Kaminsky, L. M., Trexler, R. V., Malik, R. J., Hockett, K. L. & Bell, T. H. (2019). The inherent conflicts in developing soil microbial inoculants. Trends in Biotechnology 37, 140-151.

Karki, M. et al. (2024). The Hessian fly resistance gene HvRHF1 is localized in an NBS-LRR gene cluster in barley. Theoretical and Applied Genetics 137, 71.

Kaur, R., Singh, B., Singh, M., & Thind, S. K. (2015). Hyperspectral indices, correlation and regression models for estimating growth parameters of wheat genotypes. Journal of the Indian Society of Remote Sensing, 43(3), 551–558. https://doi.org/10.1007/s12524-014-0425-1

Kehel, Z., Habash, D., Gezan, S., Welham, S. & Nachit, M. Estimation of spatial trend and automatic model selection in augmented designs. Agronomy Journal 102, 1542-1552 (2010).

Khanal, S., Kc, K., Fulton, J. P., Shearer, S., & Ozkan, E. (2020). Remote Sensing in Agriculture—Accomplishments, Limitations, and Opportunities. Remote Sensing, 12(22), 3783. https://doi.org/10.3390/rs12223783

Khasanova, A. et al. (2023). Quantitative genetic-by-soil microbiome interactions in a perennial grass affect functional traits. Proceedings of the Royal Society B 290, 20221350.

Killian, E., Lachowiec, J., Sherman, J., Lutgen, G., & Eberly, J. (2023). High resolution aerial imagery of barley over a growing season [Dataset]. Dryad. https://doi.org/10.5061/dryad.bk3j9kdhp

Kishore, N., Pindi, P. K., & Ram Reddy, S. (2015). Phosphate-Solubilizing Microorganisms: A Critical Review. In B. Bahadur, M. Venkat Rajam, L. Sahijram, & K. V. Krishnamurthy (Eds.), Plant Biology and Biotechnology (pp. 307–333). Springer India. https://doi.org/10.1007/978-81-322-2286-6_12

Kleinberg, J. M. (1999). Authoritative sources in a hyperlinked environment. Journal of the ACM, 46(5), 604–632. https://doi.org/10.1145/324133.324140

Kuenzer, C., Dech, S., & Wagner, W. (2015). Remote sensing time series revealing land surface dynamics: status quo and the pathway ahead. In C. Kuenzer, S. Dech, & W. Wagner (Eds.), Remote Sensing Time Series (Vol. 22, pp. 1–24). Springer International Publishing. https://doi.org/10.1007/978-3-319-15967-6_1

Kun Yuan, Zhang, H., Yu, C., Luo, N., Yan, J., Zheng, S., Hu, Q., Zhang, D., Kou, L., Meng, X., Jing, Y., Chen, M., Ban, X., Yan, Z., Lu, Z., Wu, J., Zhao, Y., Liang, Y., Wang, Y., … Wang, B. (2023). Low phosphorus promotes NSP1–NSP2 heterodimerization to enhance strigolactone biosynthesis and regulate shoot and root architecture in rice. Molecular Plant, 16(11), 1811–1831. https://doi.org/10.1016/j.molp.2023.09.022

Kurtz, Z. D., Müller, C. L., Miraldi, E. R., Littman, D. R., Blaser, M. J., & Bonneau, R. A. (2015). Sparse and Compositionally Robust Inference of Microbial Ecological Networks. PLOS Computational Biology, 11(5), e1004226. https://doi.org/10.1371/journal.pcbi.1004226

Kuznetsova, A., Brockhoff, P. B. & Christensen, R. H. B. (2017). lmerTest package: tests in linear mixed effects models. Journal of Statistical Software 82.

Lachowiec, J., Feldman, M. J., Matias, F. I., LeBauer, D., & Gregory, A. (2024). Adoption of unoccupied aerial systems in agricultural research. The Plant Phenome Journal, 7(1), e20098. https://doi.org/10.1002/ppj2.20098

Layeghifard, M., Hwang, D. M., & Guttman, D. S. (2017). Disentangling Interactions in the Microbiome: A Network Perspective. Trends in Microbiology, 25(3), 217–228. https://doi.org/10.1016/j.tim.2016.11.008

Leinenkugel, P., Kuenzer, C., Oppelt, N., & Dech, S. (2013). Characterisation of land surface phenology and land cover based on moderate resolution satellite data in cloud prone areas—a novel product for the Mekong Basin. Remote Sensing of Environment, 136, 180–198. https://doi.org/10.1016/j.rse.2013.05.004

Levy, A. et al. (2018). Genomic features of bacterial adaptation to plants. Nature Genetics 50, 138-150.

Li, T. et al. (2023). BarleyExpDB: an integrative gene expression database for barley. BMC Plant Biology 23, 170.

Liang, L., Liu, B., Huang, D., Kuang, Q., An, T., Liu, S., Liu, R., Xu, B., Zhang, S., Deng, X., Macrae, A., & Chen, Y. (2022). Arbuscular Mycorrhizal Fungi Alleviate Low Phosphorus Stress in Maize Genotypes with Contrasting Root Systems. Plants, 11(22), 3105. https://doi.org/10.3390/plants11223105

Ling, N., Wang, T. & Kuzyakov, Y. (2022). Rhizosphere bacteriome structure and functions. Nature Communications 13, 836.

Liu, C., Cui, Y., Li, X., & Yao, M. (2021). microeco: An R package for data mining in microbial community ecology. FEMS Microbiology Ecology, 97(2), fiaa255. https://doi.org/10.1093/femsec/fiaa255

Liu, F., Hewezi, T., Lebeis, S. L., Pantalone, V., Grewal, P. S., & Staton, M. E. (2019). Soil indigenous microbiome and plant genotypes cooperatively modify soybean rhizosphere microbiome assembly. BMC Microbiology, 19(1), 201. https://doi.org/10.1186/s12866-019-1572-x

Liu, H., Hu, M., Wang, Q., Cheng, L. & Zhang, Z. (2018). Role of papain-like cysteine proteases in plant development. Frontiers in Plant Science 9, 1717.

Liu, H., Li, J., Carvalhais, L. C., Percy, C. D., Prakash Verma, J., Schenk, P. M., & Singh, B. K. (2021). Evidence for the plant recruitment of beneficial microbes to suppress soil-borne pathogens. New Phytologist, 229(5), 2873–2885. https://doi.org/10.1111/nph.17057

Liu, Q., Cheng, L., Nian, H., Jin, J., & Lian, T. (2023). Linking plant functional genes to rhizosphere microbes: A review. Plant Biotechnology Journal, 21(5), 902–917. https://doi.org/10.1111/pbi.13950

Liu, S., Yin, D., Feng, H., Li, Z., Xu, X., Shi, L., & Jin, X. (2022). Estimating maize seedling number with UAV RGB images and advanced image processing methods. Precision Agriculture, 23(5), 1604–1632. https://doi.org/10.1007/s11119-022-09899-y

Louca, S. et al. (2018). Function and functional redundancy in microbial systems. Nature Ecology & Evolution 2, 936-943.

Louca, S., Parfrey, L. W. & Doebeli, M. (2016). Decoupling function and taxonomy in the global ocean microbiome. Science 353, 1272-1277.

Louhaichi, M., Borman, M. M., & Johnson, D. E. (2001). Spatially located platform and aerial photography for documentation of grazing impacts on wheat. Geocarto International, 16(1), 65–70. https://doi.org/10.1080/10106040108542184

Lozupone, C. A., Hamady, M., Kelley, S. T. & Knight, R. (2007). Quantitative and qualitative β diversity measures lead to different insights into factors that structure microbial communities. Applied and Environmental Microbiology 73, 1576-1585.

Lu, N., Zhou, J., Han, Z., Li, D., Cao, Q., Yao, X., Tian, Y., Zhu, Y., Cao, W., & Cheng, T. (2019). Improved estimation of aboveground biomass in wheat from RGB imagery and point cloud data acquired with a low-cost unmanned aerial vehicle system. Plant Methods, 15(1), 17. https://doi.org/10.1186/s13007-019-0402-3

Lu, X., Liu, S.-F., Yue, L., Zhao, X., Zhang, Y.-B., Xie, Z.-K., & Wang, R.-Y. (2018). Epsc Involved in the Encoding of Exopolysaccharides Produced by Bacillus amyloliquefaciens FZB42 Act to Boost the Drought Tolerance of Arabidopsis thaliana. International Journal of Molecular Sciences, 19(12), 3795. https://doi.org/10.3390/ijms19123795

Lundberg, D. S., Lebeis, S. L., Paredes, S. H., Yourstone, S., Gehring, J., Malfatti, S., Tremblay, J., Engelbrektson, A., Kunin, V., Rio, T. G. D., Edgar, R. C., Eickhorst, T., Ley, R. E., Hugenholtz, P., Tringe, S. G., & Dangl, J. L. (2012). Defining the core Arabidopsis thaliana root microbiome. Nature, 488(7409), 86–90. https://doi.org/10.1038/nature11237

Lussem, U., Bolten, A., Gnyp, M. L., Jasper, J., & Bareth, G. (2018). Evaluation of RGB-based vegetation indices from UAV imagery to estimate forage yield in grassland. The International Archives of the Photogrammetry, Remote Sensing and Spatial Information Sciences, 42–3, 1215–1219. https://doi.org/10.5194/isprs-archives-XLII-3-1215-2018

López-Bucio, J., Cruz-Ramírez, A., & Herrera-Estrella, L. (2003). The role of nutrient availability in regulating root architecture. Current Opinion in Plant Biology, 6(3), 280–287. https://doi.org/10.1016/S1369-5266(03)00035-9

Maestre, F. T., Delgado-Baquerizo, M., Jeffries, T. C., Eldridge, D. J., Ochoa, V., Gozalo, B., Quero, J. L., García-Gómez, M., Gallardo, A., Ulrich, W., Bowker, M. A., Arredondo, T., Barraza-Zepeda, C., Bran, D., Florentino, A., Gaitán, J., Gutiérrez, J. R., Huber-Sannwald, E., Jankju, M., … Singh, B. K. (2015). Increasing aridity reduces soil microbial diversity and abundance in global drylands. Proceedings of the National Academy of Sciences, 112(51), 15684–15689. https://doi.org/10.1073/pnas.1516684112

Mascher, M. et al. (2017). A chromosome conformation capture ordered sequence of the barley genome. Nature 544, 427-433.

Mascher, M. et al. (2021). Long-read sequence assembly: a technical evaluation in barley. The Plant Cell 33, 1888-1906.

Masson-Boivin, C., & Sachs, J. L. (2018). Symbiotic nitrogen fixation by rhizobia—The roots of a success story. Current Opinion in Plant Biology, 44, 7–15. https://doi.org/10.1016/j.pbi.2017.12.001

Matias, F. I., Caraza-Harter, M. V., & Endelman, J. B. (2020). FIELDimageR: An R package to analyze orthomosaic images from agricultural field trials. The Plant Phenome Journal, 3(1), e20005. https://doi.org/10.1002/ppj2.20005

Matias, F. I., Green, A., Lachowiec, J. A., LeBauer, D., & Feldman, M. (2022). Bison-Fly: an open-source UAV pipeline for plant breeding data collection. The Plant Phenome Journal, 5(1), e20048. https://doi.org/10.1002/ppj2.20048

Mayak, S., Tirosh, T., & Glick, B. R. (2004). Plant growth-promoting bacteria that confer resistance to water stress in tomatoes and peppers. Plant Science, 166(2), 525–530. https://doi.org/10.1016/j.plantsci.2003.10.025

McMurdie, P. J. & Holmes, S. phyloseq: an R package for reproducible interactive analysis and graphics of microbiome census data. PloS One 8, e61217 (2013).

Meier, M. A. et al. (2022). Association analyses of host genetics, root-colonizing microbes, and plant phenotypes under different nitrogen conditions in maize. Elife 11, e75790.

Meier, M. A., Lopez-Guerrero, M. G., Guo, M., Schmer, M. R., Herr, J. R., Schnable, J. C., Alfano, J. R., & Yang, J. (2021). Rhizosphere Microbiomes in a Historical Maize-Soybean Rotation System Respond to Host Species and Nitrogen Fertilization at the Genus and Subgenus Levels. Applied and Environmental Microbiology, 87(12), e03132-20. https://doi.org/10.1128/AEM.03132-20

Mendes, R., Kruijt, M., De Bruijn, I., Dekkers, E., Van Der Voort, M., Schneider, J. H. M., Piceno, Y. M., DeSantis, T. Z., Andersen, G. L., Bakker, P. A. H. M., & Raaijmakers, J. M. (2011). Deciphering the Rhizosphere Microbiome for Disease-Suppressive Bacteria. Science, 332(6033), 1097–1100. https://doi.org/10.1126/science.1203980

Meyer, G. E., & Neto, J. C. (2008). Verification of color vegetation indices for automated crop imaging applications. Computers and Electronics in Agriculture, 63(2), 282–293. https://doi.org/10.1016/j.compag.2008.03.009

Miransari, M. (2013). Soil microbes and the availability of soil nutrients. Acta Physiologiae Plantarum, 35(11), 3075–3084. https://doi.org/10.1007/s11738-013-1338-2

Mueller, U. G. & Linksvayer, T. A. (2022). Microbiome breeding: conceptual and practical issues. Trends in Microbiology 30, 997-1011.

Murphy, D. J. (2007). People, Plants and Genes: The Story of Crops and Humanity (1st ed.). Oxford University PressOxford. https://doi.org/10.1093/acprof:oso/9780199207145.001.0001

Nandede, B. M., Raheman, H. & Kumar, G. P. (2014). Standardization of potting mix and pot volume for the production of vegetable seedlings in paper pot. Journal of Plant Nutrition 37, 1214-1226.

Naseem, H., & Bano, A. (2014). Role of plant growth-promoting rhizobacteria and their exopolysaccharide in drought tolerance of maize. Journal of Plant Interactions, 9(1), 689–701. https://doi.org/10.1080/17429145.2014.902125

Naylor, D., & Coleman-Derr, D. (2018). Drought Stress and Root-Associated Bacterial Communities. Frontiers in Plant Science, 8, 2223. https://doi.org/10.3389/fpls.2017.02223

Neyhart, J. L. & Smith, K. P. (2019). SNP Genotyping Data for the Barley Population in" Registration of the S2MET Barley Mapping Population for Multi-Environment Genomewide Selection".

Neyhart, J. L. et al. (2019). Registration of the S2MET barley mapping population for multi-environment genomewide selection. Journal of Plant Registrations 13, 270-280.

Ning, D., Yuan, M., Wu, L., Zhang, Y., Guo, X., Zhou, X., Yang, Y., Arkin, A. P., Firestone, M. K., & Zhou, J. (2020). A quantitative framework reveals ecological drivers of grassland microbial community assembly in response to warming. Nature Communications, 11(1), 4717. https://doi.org/10.1038/s41467-020-18560-z

Okamoto, M., Peterson, F. C., Defries, A., Park, S.-Y., Endo, A., Nambara, E., Volkman, B. F., & Cutler, S. R. (2013). Activation of dimeric ABA receptors elicits guard cell closure, ABA-regulated gene expression, and drought tolerance. Proceedings of the National Academy of Sciences, 110(29), 12132–12137. https://doi.org/10.1073/pnas.1305919110

Olson, D., & Anderson, J. (2021). Review on unmanned aerial vehicles, remote sensors, imagery processing, and their applications in agriculture. Agronomy Journal, 113(2), 971–992. https://doi.org/10.1002/agj2.20595

Otsu, N. (1979). A Threshold Selection Method from Gray-Level Histograms. IEEE Transactions on Systems, Man, and Cybernetics, 9(1), 62-66. https://doi.org/10.1109/TSMC.1979.4310076

Oyserman, B. O. et al. (2022). Disentangling the genetic basis of rhizosphere microbiome assembly in tomato. Nature Communications 13, 3228.

Oyserman, B. O., Flores, S. S., Griffioen, T., Pan, X., Van Der Wijk, E., Pronk, L., Lokhorst, W., Nurfikari, A., Paulson, J. N., Movassagh, M., Stopnisek, N., Kupczok, A., Cordovez, V., Carrión, V. J., Ligterink, W., Snoek, B. L., Medema, M. H., & Raaijmakers, J. M. (2022). Disentangling the genetic basis of rhizosphere microbiome assembly in tomato. Nature Communications, 13(1), 3228. https://doi.org/10.1038/s41467-022-30849-9

Pacheco-Moreno, A., Bollmann-Giolai, A., Chandra, G., Brett, P., Davies, J., Thornton, O., Poole, P., Ramachandran, V., Brown, J. K. M., Nicholson, P., Ridout, C., DeVos, S., & Malone, J. G. (2024). The genotype of barley cultivars influences multiple aspects of their associated microbiota via differential root exudate secretion. PLOS Biology, 22(4), e3002232. https://doi.org/10.1371/journal.pbio.3002232

Paes da Costa, D. et al. Soil fertility impact on recruitment and diversity of the soil microbiome in sub-humid tropical pastures in northeastern Brazil. Scientific Reports 14, 3919 (2024).

Pandey, N. (2018). Role of Plant Nutrients in Plant Growth and Physiology. In M. Hasanuzzaman, M. Fujita, H. Oku, K. Nahar, & B. Hawrylak-Nowak (Eds.), Plant Nutrients and Abiotic Stress Tolerance (pp. 51–93). Springer Singapore. https://doi.org/10.1007/978-981-10-9044-8_2

Pearson, G., Robinson, F., Beers Gibson, T., Xu, B., Karandikar, M., Berman, K., & Cobb, M. H. (2001). Mitogen-Activated Protein (MAP) Kinase Pathways: Regulation and Physiological Functions*. Endocrine Reviews, 22(2), 153–183. https://doi.org/10.1210/edrv.22.2.0428

Peiffer, J. A., Spor, A., Koren, O., Jin, Z., Tringe, S. G., Dangl, J. L., Buckler, E. S., & Ley, R. E. (2013). Diversity and heritability of the maize rhizosphere microbiome under field conditions. Proceedings of the National Academy of Sciences, 110(16), 6548–6553. https://doi.org/10.1073/pnas.1302837110

Pell, T., Li, J. Y. Q., & Joyce, K. E. (2022). Demystifying the Differences between Structure-from-MotionSoftware Packages for Pre-Processing Drone Data. Drones, 6(1), 24. https://doi.org/10.3390/drones6010024

Pervaiz, Z. H., Contreras, J., Hupp, B. M., Lindenberger, J. H., Chen, D., Zhang, Q., Wang, C., Twigg, P., & Saleem, M. (2020). Root microbiome changes with root branching order and root chemistry in peach rhizosphere soil. Rhizosphere, 16, 100249. https://doi.org/10.1016/j.rhisph.2020.100249

Petipas, R. H., Geber, M. A. & Lau, J. A. (2021). Microbe-mediated adaptation in plants. Ecology Letters 24, 1302-1317.

Peña, J., Gutiérrez, P., Hervás-Martínez, C., Six, J., Plant, R., & López-Granados, F. (2014). Object-based image classification of summer crops with machine learning methods. Remote Sensing, 6(6), 5019–5041. https://doi.org/10.3390/rs6065019

Pii, Y., Mimmo, T., Tomasi, N., Terzano, R., Cesco, S., & Crecchio, C. (2015). Microbial interactions in the rhizosphere: Beneficial influences of plant growth-promoting rhizobacteria on nutrient acquisition process. A review. Biology and Fertility of Soils, 51(4), 403–415. https://doi.org/10.1007/s00374-015-0996-1

Poudel, M., Mendes, R., Costa, L. A. S., Bueno, C. G., Meng, Y., Folimonova, S. Y., Garrett, K. A., & Martins, S. J. (2021). The Role of Plant-Associated Bacteria, Fungi, and Viruses in Drought Stress Mitigation. Frontiers in Microbiology, 12, 743512. https://doi.org/10.3389/fmicb.2021.743512

Pérez-Torres, C.-A., López-Bucio, J., Cruz-Ramírez, A., Ibarra-Laclette, E., Dharmasiri, S., Estelle, M., & Herrera-Estrella, L. (2009). Phosphate Availability Alters Lateral Root Development in Arabidopsis by Modulating Auxin Sensitivity via a Mechanism Involving the TIR1 Auxin Receptor. The Plant Cell, 20(12), 3258–3272. https://doi.org/10.1105/tpc.108.058719

Qiao, Q., Wang, F., Zhang, J., Chen, Y., Zhang, C., Liu, G., Zhang, H., Ma, C., & Zhang, J. (2017). The Variation in the Rhizosphere Microbiome of Cotton with Soil Type, Genotype and Developmental Stage. Scientific Reports, 7(1), 3940. https://doi.org/10.1038/s41598-017-04213-7

Quast, C. et al. (2012). The SILVA ribosomal RNA gene database project: improved data processing and web-based tools. Nucleic Acids Research 41, D590-D596.

Radočaj, D., Šiljeg, A., Marinović, R., & Jurišić, M. (2023). State of Major Vegetation Indices in Precision Agriculture Studies Indexed in Web of Science: A Review. Agriculture, 13(3), 707.

Rajamanickam, V., Vinod, K. K., Vengavasi, K., Kumar, T., Chinnusamy, V., & Pandey, R. (2024). Root Architectural Adaptations to Phosphorus Deficiency: Unraveling Genotypic Variability in Wheat Seedlings. Agriculture, 14(3), 447. https://doi.org/10.3390/agriculture14030447

Rasmussen, J., Nielsen, J., Streibig, J. C., Jensen, J. E., Pedersen, K. S., & Olsen, S. I. (2019). Pre-harvest weed mapping of Cirsium arvense in wheat and barley with off-the-shelf UAVs. Precision Agriculture, 20(5), 983–999. https://doi.org/10.1007/s11119-018-09625-7

Rasmussen, J., Nørremark, M., & Bibby, B. (2007). Assessment of leaf cover and crop soil cover in weed harrowing research using digital images. Weed Research, 47(4), 299–310. https://doi.org/10.1111/j.1365-3180.2007.00565.x

Rawat, P., Das, S., Shankhdhar, D., & Shankhdhar, S. C. (2021). Phosphate-Solubilizing Microorganisms: Mechanism and Their Role in Phosphate Solubilization and Uptake. Journal of Soil Science and Plant Nutrition, 21(1), 49–68. https://doi.org/10.1007/s42729-020-00342-7

Ray, D. K., Mueller, N. D., West, P. C., & Foley, J. A. (2013). Yield Trends Are Insufficient to Double Global Crop Production by 2050. PLoS ONE, 8(6), e66428. https://doi.org/10.1371/journal.pone.0066428

Revillini, D., Gehring, C. A. & Johnson, N. C. (2016). The role of locally adapted mycorrhizas and rhizobacteria in plant–soil feedback systems. Functional Ecology 30, 1086-1098.

Robb, C., Hardy, A., Doonan, J. H., & Brook, J. (2020). Semi-automated field plot segmentation from UAS imagery for experimental agriculture. Frontiers in Plant Science, 11, 591886. https://doi.org/10.3389/fpls.2020.591886

Robertson-Albertyn, S. et al. (2017). Root hair mutations displace the barley rhizosphere microbiota. Frontiers in Plant Science 8, 1094.

Rodene, E., Xu, G., Palali Delen, S., Zhao, X., Smith, C., Ge, Y., Schnable, J., & Yang, J. (2022). A UAV-based high-throughput phenotyping approach to assess time-series nitrogen responses and identify trait-associated genetic components in maize. The Plant Phenome Journal, 5(1), e20030. https://doi.org/10.1002/ppj2.20030

Rogan, J., & Chen, D. (2004). Remote sensing technology for mapping and monitoring land-cover and land-use change. Progress in Planning, 61(4), 301–325. https://doi.org/10.1016/S0305-9006(03)00066-7

Rolli, E., Marasco, R., Vigani, G., Ettoumi, B., Mapelli, F., Deangelis, M. L., Gandolfi, C., Casati, E., Previtali, F., Gerbino, R., Pierotti Cei, F., Borin, S., Sorlini, C., Zocchi, G., & Daffonchio, D. (2015). Improved plant resistance to drought is promoted by the root-associated microbiome as a water stress-dependent trait. Environmental Microbiology, 17(2), 316–331. https://doi.org/10.1111/1462-2920.12439

Rosenblueth, M., Ormeño-Orrillo, E., López-López, A., Rogel, M. A., Reyes-Hernández, B. J., Martínez-Romero, J. C., Reddy, P. M., & Martínez-Romero, E. (2018). Nitrogen Fixation in Cereals. Frontiers in Microbiology, 9, 1794. https://doi.org/10.3389/fmicb.2018.01794

Sahoo, R. N., Rejith, R. G., Gakhar, S., Ranjan, R., Meena, M. C., Dey, A., Mukherjee, J., Dhakar, R., Meena, A., Daas, A., Babu, S., Upadhyay, P. K., Sekhawat, K., Kumar, S., Kumar, M., Chinnusamy, V., & Khanna, M. (2024). Drone remote sensing of wheat N using hyperspectral sensor and machine learning. Precision Agriculture, 25(2), 704–728. https://doi.org/10.1007/s11119-023-10089-7

Santoyo, G. (2022). How plants recruit their microbiome? New insights into beneficial interactions. Journal of Advanced Research, 40, 45–58. https://doi.org/10.1016/j.jare.2021.11.020

Schlatter, D. C., Yin, C., Hulbert, S., & Paulitz, T. C. (2020). Core Rhizosphere Microbiomes of Dryland Wheat Are Influenced by Location and Land Use History. Applied and Environmental Microbiology, 86(5), e02135-19. https://doi.org/10.1128/AEM.02135-19

Schlatter, D., Kinkel, L., Thomashow, L., Weller, D., & Paulitz, T. (2017). Disease Suppressive Soils: New Insights from the Soil Microbiome. Phytopathology®, 107(11), 1284–1297. https://doi.org/10.1094/PHYTO-03-17-0111-RVW

Schnitzer, S. A. et al. (2011). Soil microbes drive the classic plant diversity–productivity pattern. Ecology 92, 296-303.

Shannon, P., Markiel, A., Ozier, O., Baliga, N. S., Wang, J. T., Ramage, D., Amin, N., Schwikowski, B., & Ideker, T. (2003). Cytoscape: A Software Environment for Integrated Models of Biomolecular Interaction Networks. Genome Research, 13(11), 2498–2504. https://doi.org/10.1101/gr.1239303

Shi, Q., Liu, Y., Shi, A., Cai, Z., Nian, H., Hartmann, M., & Lian, T. (2020). Rhizosphere Soil Fungal Communities of Aluminum-Tolerant and -Sensitive Soybean Genotypes Respond Differently to Aluminum Stress in an Acid Soil. Frontiers in Microbiology, 11, 1177. https://doi.org/10.3389/fmicb.2020.01177

Shindo, T. & Van Der Hoorn, R. A. (2008). Papain-like cysteine proteases: key players at molecular battlefields employed by both plants and their invaders. Molecular Plant Pathology 9, 119-125.

Smith, S. E., Smith, F. A., & Jakobsen, I. (2003). Mycorrhizal Fungi Can Dominate Phosphate Supply to Plants Irrespective of Growth Responses. Plant Physiology, 133(1), 16–20. https://doi.org/10.1104/pp.103.024380

Snowdon, R. J., Wittkop, B., Chen, T.-W., & Stahl, A. (2021). Crop adaptation to climate change as a consequence of long-term breeding. Theoretical and Applied Genetics, 134(6), 1613–1623. https://doi.org/10.1007/s00122-020-03729-3

Sutherland, J., Bell, T., Trexler, R. V., Carlson, J. E. & Lasky, J. R. (2022). Host genomic influence on bacterial composition in the switchgrass rhizosphere. Molecular Ecology 31, 3934-3950.

Sánchez-Calderón, L., López-Bucio, J., Chacón-López, A., Cruz-Ramírez, A., Nieto-Jacobo, F., Dubrovsky, J. G., & Herrera-Estrella, L. (2005). Phosphate Starvation Induces a Determinate Developmental Program in the Roots of Arabidopsis thaliana. Plant and Cell Physiology, 46(1), 174–184. https://doi.org/10.1093/pcp/pci011

Tang, Z. et al. (2024). Alleviating protein-condensation-associated damage at the endoplasmic reticulum enhances plant disease tolerance. Cell Host & Microbe 32, 1552-1565. e1558.

Tedersoo, L., Bahram, M., Põlme, S., Kõljalg, U., Yorou, N. S., Wijesundera, R., Ruiz, L. V., Vasco-Palacios, A. M., Thu, P. Q., Suija, A., Smith, M. E., Sharp, C., Saluveer, E., Saitta, A., Rosas, M., Riit, T., Ratkowsky, D., Pritsch, K., Põldmaa, K., … Abarenkov, K. (2014). Global diversity and geography of soil fungi. Science, 346(6213), 1256688. https://doi.org/10.1126/science.1256688

Tiffin, P. & Ross-Ibarra, J. (2014). Advances and limits of using population genetics to understand local adaptation. Trends in Ecology & Evolution 29, 673-680.

Tirado, S. B., Hirsch, C. N., & Springer, N. M. (2020). UAV-based imaging platform for monitoring maize growth throughout development. Plant Direct, 4(6), e00230. https://doi.org/10.1002/pld3.230

Todorović, I., Moënne-Loccoz, Y., Raičević, V., Jovičić-Petrović, J., & Muller, D. (2023). Microbial diversity in soils suppressive to Fusarium diseases. Frontiers in Plant Science, 14, 1228749. https://doi.org/10.3389/fpls.2023.1228749

Tong, Y., Zheng, X., Hu, Y., Wu, J., Liu, H., Deng, Y., Lv, W., Yao, H., Chen, J., & Ge, T. (2024). Root exudate-mediated plant–microbiome interactions determine plant health during disease infection. Agriculture, Ecosystems & Environment, 370, 109056. https://doi.org/10.1016/j.agee.2024.109056

Trivedi, P., Leach, J. E., Tringe, S. G., Sa, T. & Singh, B. K. (2020). Plant–microbiome interactions: from community assembly to plant health. Nature Reviews Microbiology 18, 607-621.

Trujillano, F., Flores, A., Saito, C., Balcazar, M., & Racoceanu, D. (2018). Corn classification using deep learning with UAV imagery. An operational proof of concept. 2018 IEEE 1st Colombian Conference on Applications in Computational Intelligence (ColCACI), 1–4. https://doi.org/10.1109/ColCACI.2018.8484845

Turner, B. L., Driessen, J. P., Haygarth, P. M., & Mckelvie, I. D. (2003). Potential contribution of lysed bacterial cells to phosphorus solubilisation in two rewetted Australian pasture soils. Soil Biology and Biochemistry, 35(1), 187–189. https://doi.org/10.1016/S0038-0717(02)00244-4

Upendar, K., Agrawal, K. N., Chandel, N. S., & Singh, K. (2021). Greenness identification using visible spectral colour indices for site specific weed management. Plant Physiology Reports, 26(1), 179–187. https://doi.org/10.1007/s40502-020-00562-0

Van Elsas, J. D., Chiurazzi, M., Mallon, C. A., Elhottovā, D., Krištůfek, V., & Salles, J. F. (2012). Microbial diversity determines the invasion of soil by a bacterial pathogen. Proceedings of the National Academy of Sciences, 109(4), 1159–1164. https://doi.org/10.1073/pnas.1109326109

Van den Boogaart, K. G. & Tolosana-Delgado, R. (2008). “Compositions”: a unified R package to analyze compositional data. Computers & Geosciences 34, 320-338.

Walder, F., Niemann, H., Natarajan, M., Lehmann, M. F., Boller, T., & Wiemken, A. (2012). Mycorrhizal Networks: Common Goods of Plants Shared under Unequal Terms of Trade. Plant Physiology, 159(2), 789–797. https://doi.org/10.1104/pp.112.195727

Walker, T. S., Bais, H. P., Grotewold, E., & Vivanco, J. M. (2003). Root Exudation and Rhizosphere Biology. Plant Physiology, 132(1), 44–51. https://doi.org/10.1104/pp.102.019661

Wall, D. H., Nielsen, U. N., & Six, J. (2015). Soil biodiversity and human health. Nature, 528(7580), 69–76. https://doi.org/10.1038/nature15744

Wallace, J. G., Rodgers-Melnick, E. & Buckler, E. S. (2018). On the road to breeding 4.0: unraveling the good, the bad, and the boring of crop quantitative genomics. Annual Review of Genetics 52, 421-444.

Walters, W. A. et al. (2018). Large-scale replicated field study of maize rhizosphere identifies heritable microbes. Proceedings of the National Academy of Sciences 115, 7368-7373.

Wang, B., & Qiu, Y.-L. (2006). Phylogenetic distribution and evolution of mycorrhizas in land plants. Mycorrhiza, 16(5), 299–363. https://doi.org/10.1007/s00572-005-0033-6

Wang, J. & Zhang, Z. (2021). GAPIT version 3: boosting power and accuracy for genomic association and prediction. Genomics, Proteomics and Bioinformatics 19, 629-640.

Wang, R., Zhang, H., Sun, L., Qi, G., Chen, S., & Zhao, X. (2017). Microbial community composition is related to soil biological and chemical properties and bacterial wilt outbreak. Scientific Reports, 7(1), 343. https://doi.org/10.1038/s41598-017-00472-6

Wang, Y. et al. (2022). GWAS, MWAS and mGWAS provide insights into precision agriculture based on genotype-dependent microbial effects in foxtail millet. Nature Communications 13, 5913.

WebODM (2023). OpenDroneMap/WebODM (Version v2.0.0) [Software]. OpenDroneMap

Wei, Z., Gu, X., Sun, Q., Hu, X., & Gao, Y. (2021). Analysis of the spatial and temporal pattern of changes in abandoned farmland based on long time series of remote sensing data. Remote Sensing, 13(13), 2549. https://doi.org/10.3390/rs13132549

Weller, D. M., Raaijmakers, J. M., Gardener, B. B. M., & Thomashow, L. S. (2002). MICROBIAL POPULATIONS RESPONSIBLE FOR SPECIFIC SOIL SUPPRESSIVENESS TO PLANT PATHOGENS. Annual Review of Phytopathology, 40(1), 309–348. https://doi.org/10.1146/annurev.phyto.40.030402.110010

Whitham, T. G. et al. (2003). Community and ecosystem genetics: a consequence of the extended phenotype. Ecology 84, 559-573.

Wickham, H., Chang, W. & Wickham, M. H. (2016). Package ‘ggplot2’. Create elegant data visualisations using the grammar of graphics. Version 2, 1-189.

Williams, J. L., Sherman, J. D., Lamb, P., Cook, J., Lachowiec, J. A., & Bourgault, M. (2022). Relationships between roots, the stay-green phenotype, and agronomic performance in barley and wheat grown in semi-arid conditions. The Plant Phenome Journal, 5(1), e220050. https://doi.org/10.1002/ppj2.20050

Williamson, L. C., Ribrioux, S. P. C. P., Fitter, A. H., & Leyser, H. M. O. (2001). Phosphate Availability Regulates Root System Architecture in Arabidopsis. Plant Physiology, 126(2), 875–882. https://doi.org/10.1104/pp.126.2.875

Woll, K., Borsuk, L. A., Stransky, H., Nettleton, D., Schnable, P. S., & Hochholdinger, F. (2005). Isolation, Characterization, and Pericycle-Specific Transcriptome Analyses of the Novel Maize Lateral and Seminal Root Initiation Mutant rum1. Plant Physiology, 139(3), 1255–1267. https://doi.org/10.1104/pp.105.067330

Woodcroft, B. J., Singleton, C. M., Boyd, J. A., Evans, P. N., Emerson, J. B., Zayed, A. A. F., Hoelzle, R. D., Lamberton, T. O., McCalley, C. K., Hodgkins, S. B., Wilson, R. M., Purvine, S. O., Nicora, C. D., Li, C., Frolking, S., Chanton, J. P., Crill, P. M., Saleska, S. R., Rich, V. I., & Tyson, G. W. (2018). Genome-centric view of carbon processing in thawing permafrost. Nature, 560(7716), 49–54. https://doi.org/10.1038/s41586-018-0338-1

Wu, B., Meng, J., Li, Q., Yan, N., Du, X., & Zhang, M. (2014). Remote sensing-based global crop monitoring: Experiences with China's CropWatch system. International Journal of Digital Earth, 7(2), 113–137. https://doi.org/10.1080/17538947.2013.821185

Xu, Y., Li, J., Qiao, C., Yang, J., Li, J., Zheng, X., Wang, C., Cao, P., Li, Y., & Chen, Q. (2024). Rhizosphere bacterial community is mainly determined by soil environmental factors, but the active bacterial diversity is mainly shaped by plant selection. BMC Microbiology, 24(1), 450. https://doi.org/10.1186/s12866-024-03611-y

Yadav, D. S., Jaiswal, B., Gautam, M., & Agrawal, M. (2020). Soil Acidification and its Impact on Plants. In P. Singh, S. K. Singh, & S. M. Prasad (Eds.), Plant Responses to Soil Pollution (pp. 1–26). Springer Singapore. https://doi.org/10.1007/978-981-15-4964-9_1

Yang, J., Lan, L., Jin, Y., Yu, N., Wang, D., & Wang, E. (2022). Mechanisms underlying legume–rhizobium symbioses. Journal of Integrative Plant Biology, 64(2), 244–267. https://doi.org/10.1111/jipb.13207

Yu, P., He, X., Baer, M., Beirinckx, S., Tian, T., Moya, Y. A. T., Zhang, X., Deichmann, M., Frey, F. P., Bresgen, V., Li, C., Razavi, B. S., Schaaf, G., Von Wirén, N., Su, Z., Bucher, M., Tsuda, K.,

Goormachtig, S., Chen, X., & Hochholdinger, F. (2021). Plant flavones enrich rhizosphere Oxalobacteraceae to improve maize performance under nitrogen deprivation. Nature Plants, 7(4), 481–499. https://doi.org/10.1038/s41477-021-00897-y

Yu, Y., Gui, Y., Li, Z., Jiang, C., Guo, J., & Niu, D. (2022). Induced Systemic Resistance for Improving Plant Immunity by Beneficial Microbes. Plants, 11(3), 386. https://doi.org/10.3390/plants11030386

Yue, H. et al. (2023). Plant domestication shapes rhizosphere microbiome assembly and metabolic functions. Microbiome 11, 70.

Yue, H., Sun, X., Wang, T., Zhang, A., Han, D., Wei, G., Song, W., & Shu, D. (2024). Host genotype-specific rhizosphere fungus enhances drought resistance in wheat. Microbiome, 12(1), 44. https://doi.org/10.1186/s40168-024-01770-8

Zadoks, J. C., Chang, T. T., & Konzak, C. F. (1974). A decimal code for the growth stages of cereals. Weed Research, 14(6), 415–421. https://doi.org/10.1111/j.1365-3180.1974.tb01084.x

Zancarini, A., Westerhuis, J. A., Smilde, A. K. & Bouwmeester, H. J. (2021). Integration of omics data to unravel root microbiome recruitment. Current Opinion in Biotechnology 70, 255-261.

Zhang, H., Huang, Y., Ye, X., & Xu, F. (2011). Genotypic variation in phosphorus acquisition from sparingly soluble P sources is related to root morphology and root exudates in Brassica napus. Science China Life Sciences, 54(12), 1134–1142. https://doi.org/10.1007/s11427-011-4254-y

Zhang, J., Liu, W., Bu, J., Lin, Y., & Bai, Y. (2023). Host genetics regulate the plant microbiome. Current Opinion in Microbiology, 72, 102268. https://doi.org/10.1016/j.mib.2023.102268

Zhang, J., Liu, Y.-X., Zhang, N., Hu, B., Jin, T., Xu, H., Qin, Y., Yan, P., Zhang, X., Guo, X., Hui, J., Cao, S., Wang, X., Wang, C., Wang, H., Qu, B., Fan, G., Yuan, L., Garrido-Oter, R., … Bai, Y. (2019). NRT1.1B is associated with root microbiota composition and nitrogen use in field-grown rice. Nature Biotechnology, 37(6), 676–684. https://doi.org/10.1038/s41587-019-0104-4

Zhang, L. et al. (2024). Maize functional requirements drive the selection of rhizobacteria under long-term fertilization practices. New Phytologist 242, 1275-1288.

Zhang, M., Wu, B., Yu, M., Zou, W., & Zheng, Y. (2014). Crop Condition Assessment with Adjusted NDVI Using the Uncropped Arable Land Ratio. Remote Sensing, 6(6), 5774–5794. https://doi.org/10.3390/rs6065774

Zhao, M., Zhao, J., Yuan, J., Hale, L., Wen, T., Huang, Q., Vivanco, J. M., Zhou, J., Kowalchuk, G. A., & Shen, Q. (2021). Root exudates drive soil-microbe-nutrient feedbacks in response to plant growth. Plant, Cell & Environment, 44(2), 613–628. https://doi.org/10.1111/pce.13928

Zolti, A., Green, S. J., Sela, N., Hadar, Y., & Minz, D. (2020). The microbiome as a biosensor: Functional profiles elucidate hidden stress in hosts. Microbiome, 8(1), 71. https://doi.org/10.1186/s40168-020-00850-9

Zortea, M., Nery, M., Ruga, B., Carvalho, L. B., & Bastos, A. C. (2018). Oil-palm tree detection in aerial images combining deep learning classifiers. IGARSS 2018 - 2018 IEEE International Geoscience and Remote Sensing Symposium, 657–660. https://doi.org/10.1109/IGARSS.2018.8519239

APPENDICES

APPENDIX A

ADDITIONAL TABLES FOR CHAPTER TWO

Table A2.1: Soil and climate data from the four growing locations. Soil data was averaged across the two years in locations where applicable.

Table S1.				
	Location			
	Bozeman, MT	**Moccasin, MT**	**Brookings, SD**	**Kunia, HI**
Coordinates	45.673484, -111.155487	47.06242, -109.94765	44.350227, -96.806430	21.384253, -158.038122
Mean annual rainfall (mm)	411.2	388.6	640	813.1
Mean growing season temperature (°C)	13.8	13.3	15.4	22
Frost free days	110	112	145	365
Cummulative precipitation May 1-August 31 2021	172.0	171	204	296.7
Cummulative precipitation May 1-August 31 2022	198.0	115	360	NA
Soil classification	Amsterdam silt loam	Danvers-Judith clay loam	Barnes Lay Loam	Molokai silty clay loam
Taxonomic Class	Fine-silty, mixed, superactive, frigid Typic Haplustolls	Fine-loamy, carbonatic, frigid Typic Calciustolls	Fine-loamy, mixed, superactive, frigid Calcic Hapludolls	Very-fine, kaolinitic, isohyperthermic Typic Eutrotorrox
Soil depth (cm)	40-121	30-60	>200	38-127
pH (in water)	6.1	7.9	6.7	6.8
OM (%)	3.45	4.6	3.5	NA
Nitrate-N (ppm)	6.2	7	4.7	2.1
P_2O_5 (ppm, Mehlich)	50.7	35.1	8.4	6
K_2O (ppm)	277.9	826.8	127	380
Sulfate-S (ppm)	5.6	12.6	7	21
Ca (ppm)	2111.5	4469	2463	1066
Mg (ppm)	460.6	193.2	377	329
Mn (ppm)	19.8	48.8	13	149

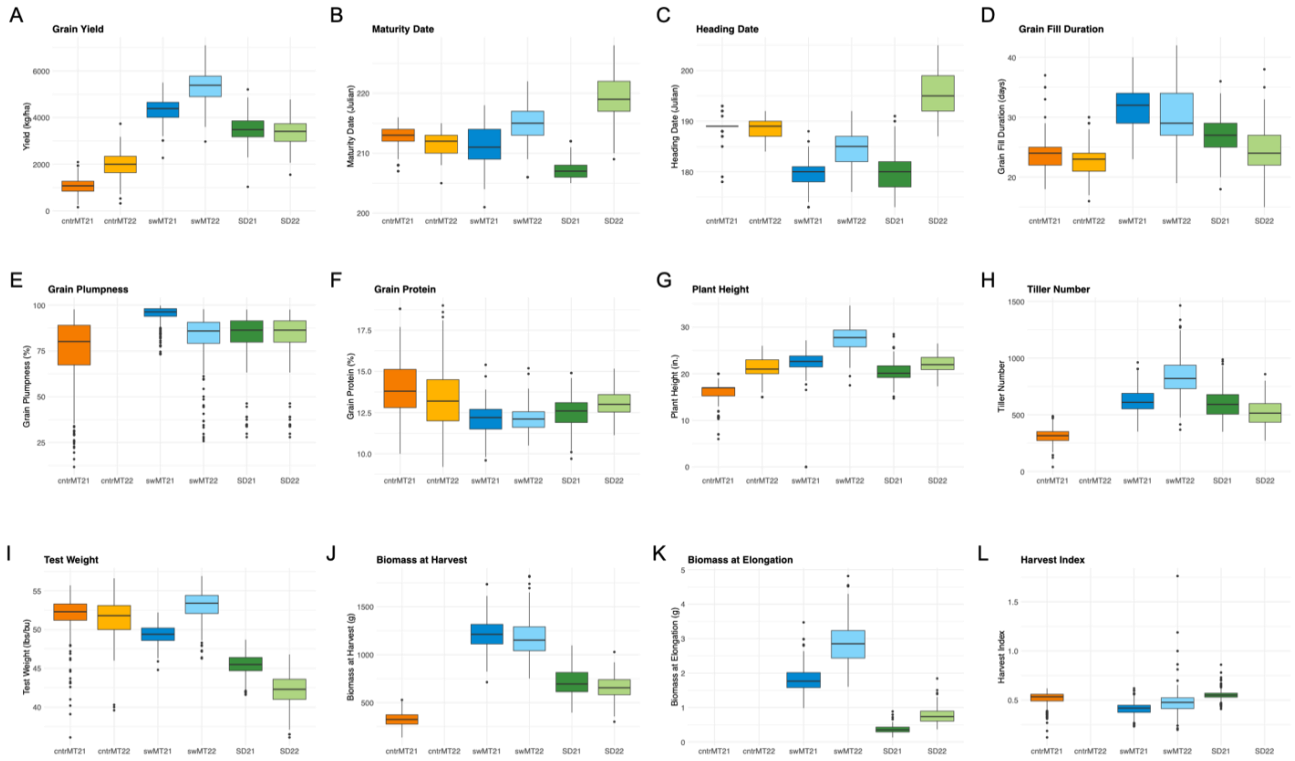

Figure A2.1. Distributions of agronomic traits for the barley lines across field trials.

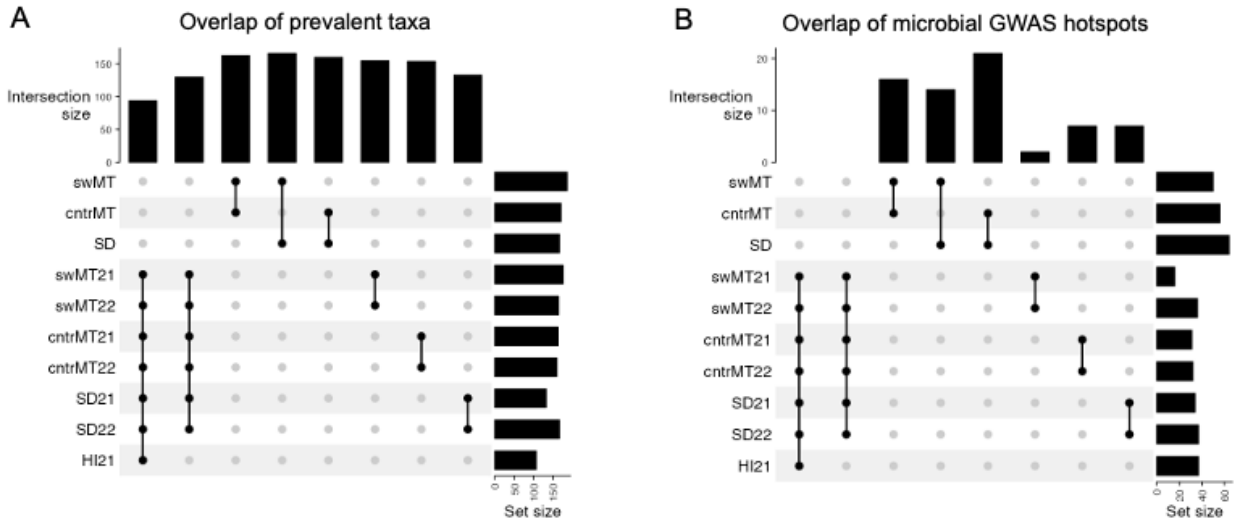

Figure A2.2. Similarities of microbe prevalence and genetic associations across field trials. (A) The number of taxa detected in the rhizospheres of at least 80% of barley lines per field trial or combination of field trials is shown. (B) The number of microbial trait hotspots appearing in each field trial or combination of field trials is shown.

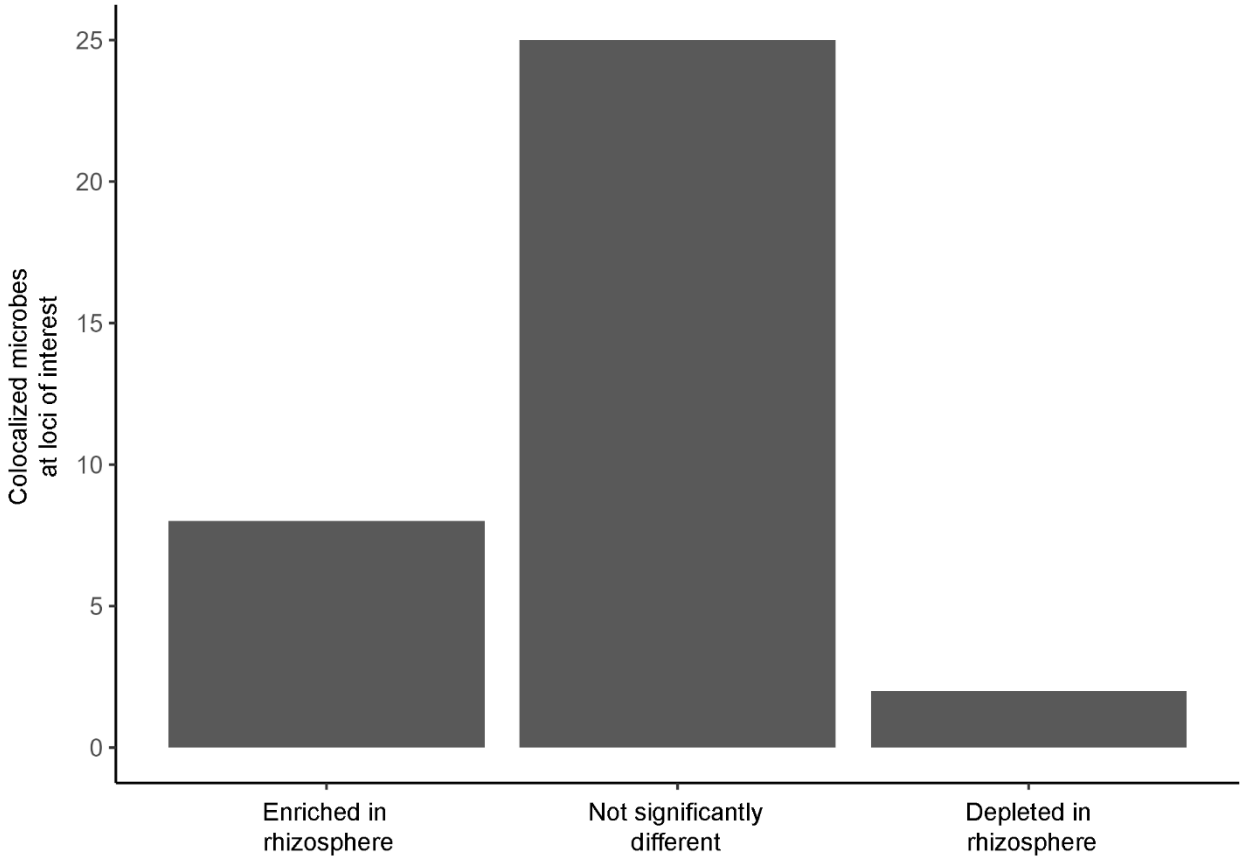

Figure A2.3. Differential abundance between rhizosphere microbial taxa and bulk microbial taxa. Differential abundance was calculated using DESeq2 (Love 2014) for taxa that colocalized with agronomic traits. Wald's test was used to calculate the significance of difference between rhizosphere and bulk soil abundance per taxa. Bonferroni correction was performed for adjusted p-values. Taxa with a greater than 0-fold change and an adjusted *p* value less than 0.05 were considered enriched. Depleted taxa had a fold change less than 0 and an adjusted *p* value less than 0.05.

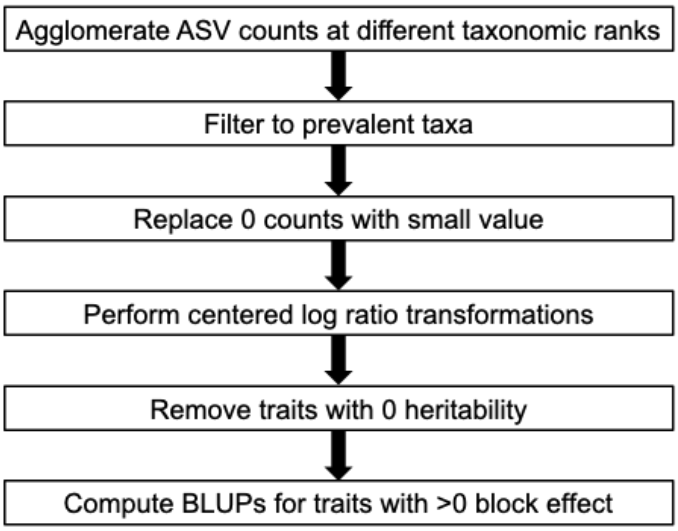

Figure A2.4. Workflow for preparing microbial trait data for the GWAS from ASV read counts. For agronomic traits, the same linear model was used as for microbial traits to calculate heritability and BLUPs. The inputs for this were raw collected values from a single location-year. As with the microbial traits, agronomic traits with 0 heritability were omitted from the GWAS, and raw values were used in cases where variance due to block was 0, otherwise BLUPs were used to account for spatial variation.

APPENDIX B

ADDITIONAL FIGURES FOR CHAPTER THREE

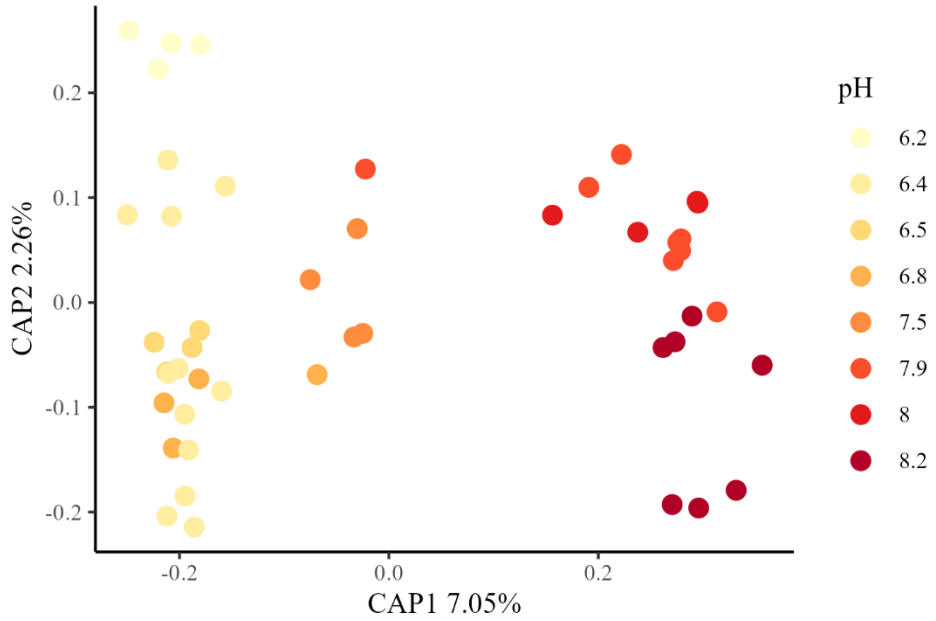

Figure A3.1: Constrained ordination of samples from South Dakota 2021.

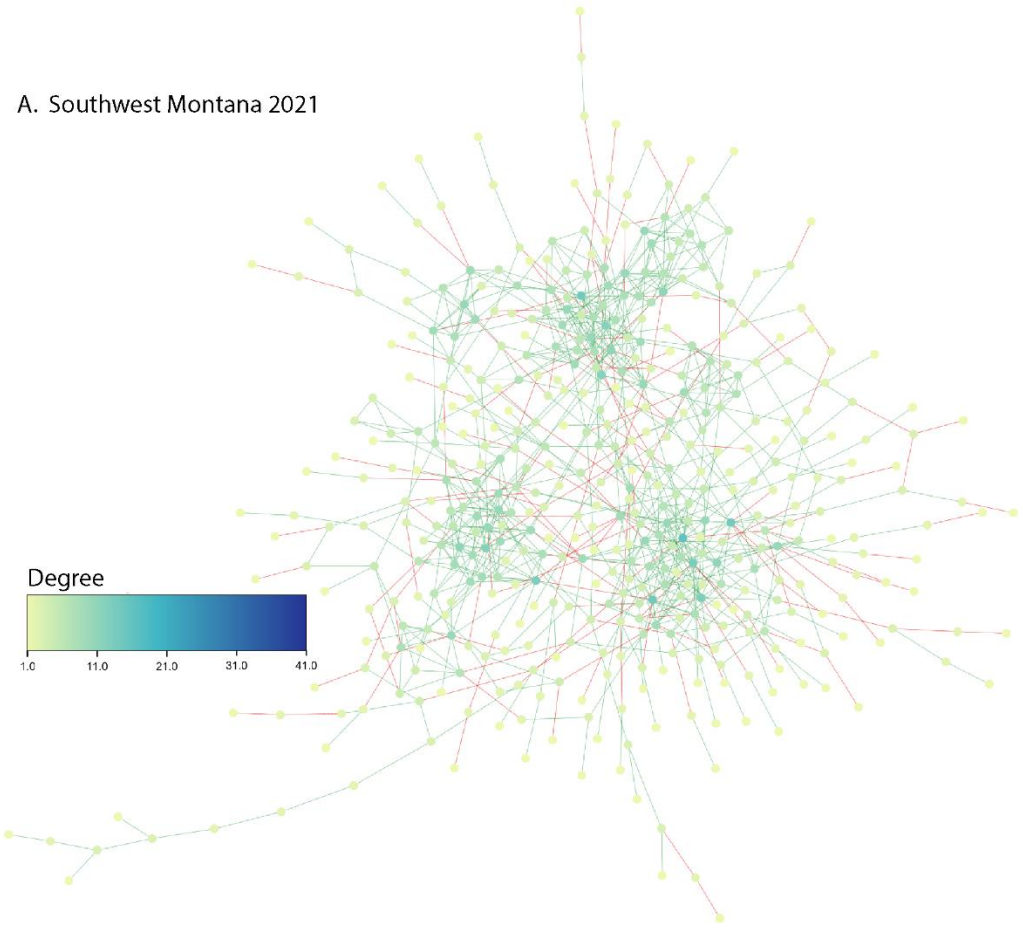
A. Southwest Montana 2021
Degree
1.0
11.0
21.0
31.0
41.0

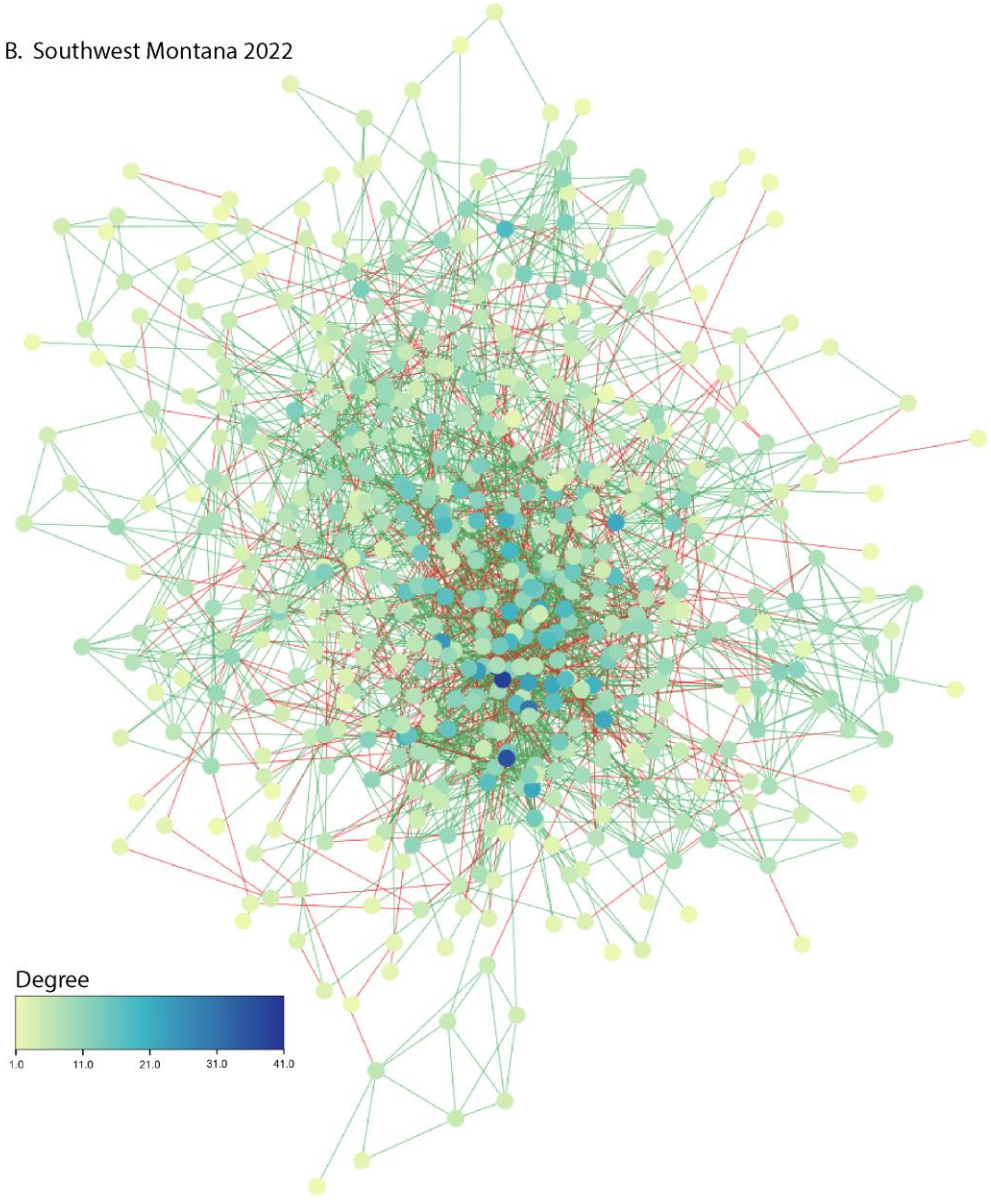
B. Southwest Montana 2022
Degree
1.0
11.0
21.0
31.0
41.0

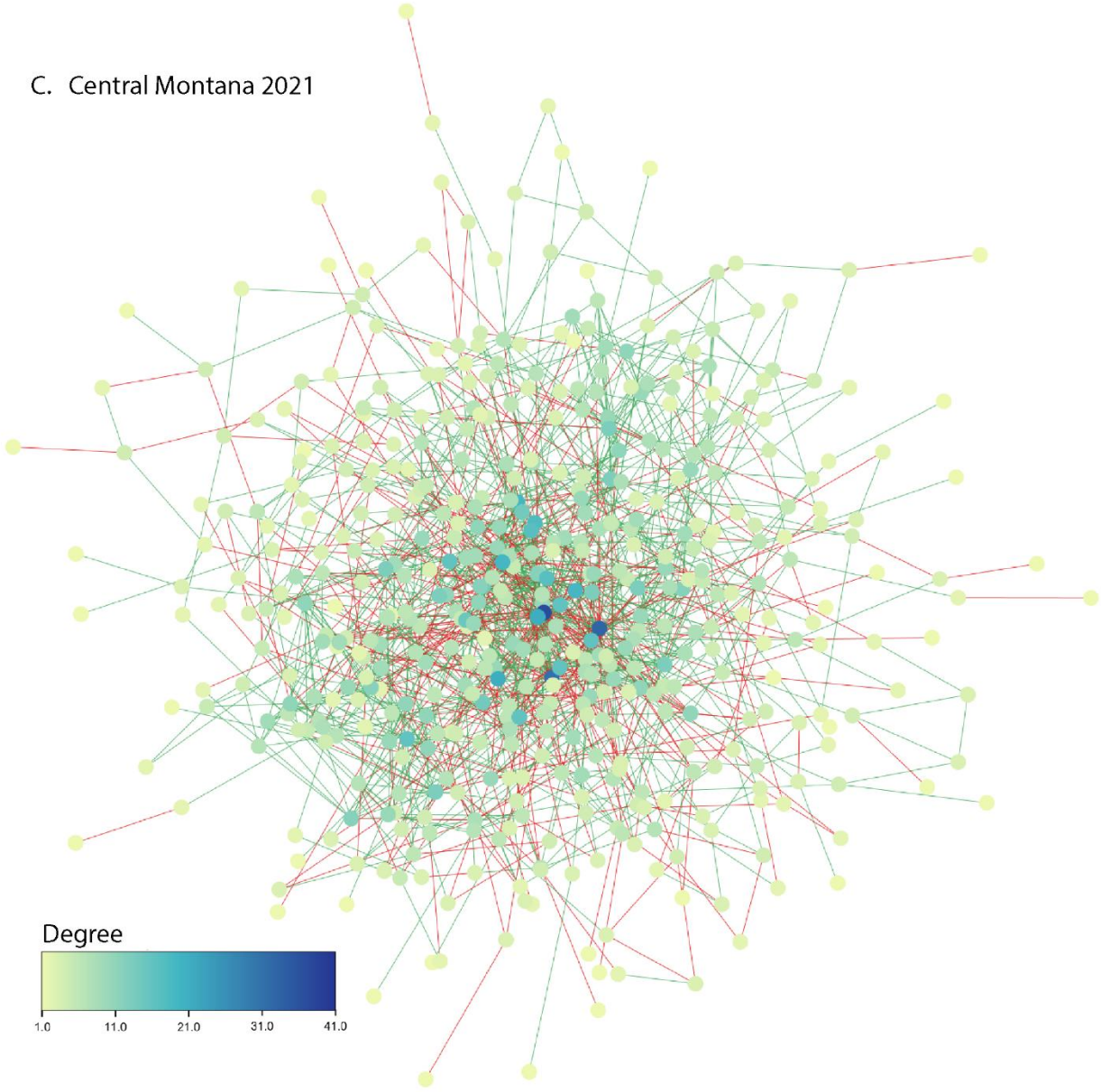
C. Central Montana 2021
Degree
1.0
11.0
21.0
31.0
41.0

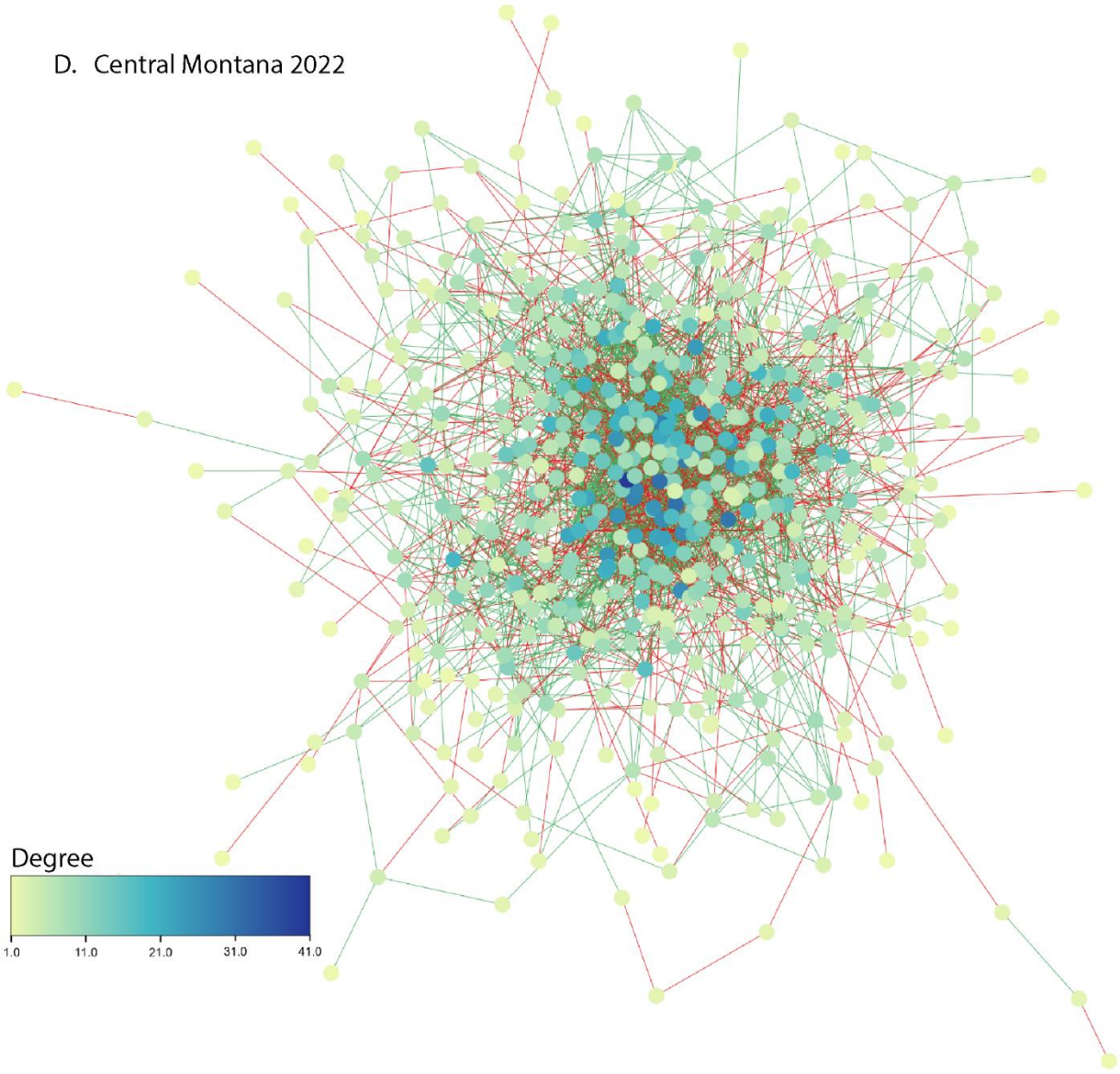
D. Central Montana 2022
Degree
1.0
11.0
21.0
31.0
41.0

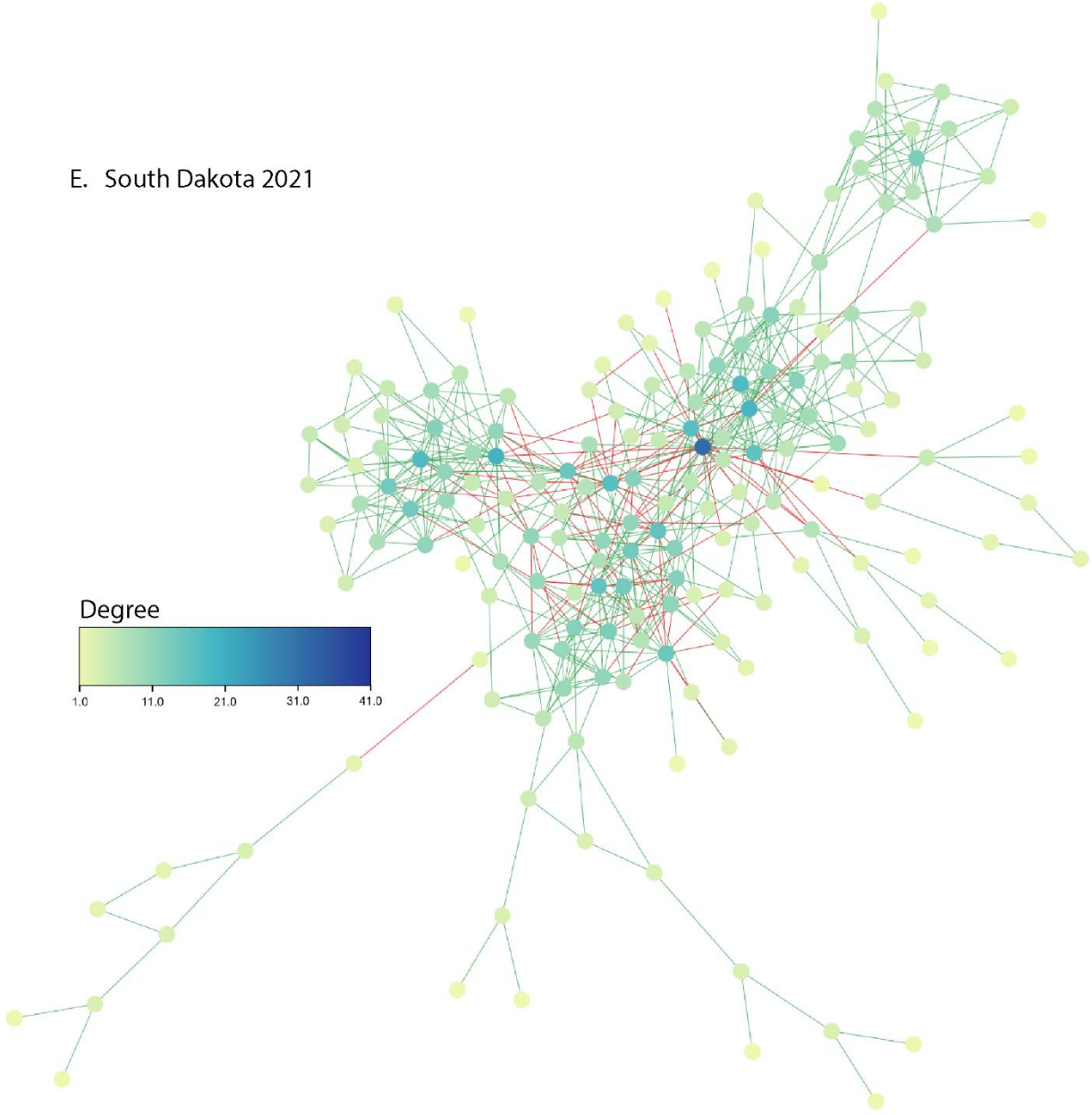
E. South Dakota 2021
Degree
1.0
11.0
21.0
31.0
41.0

F. South Dakota 2022

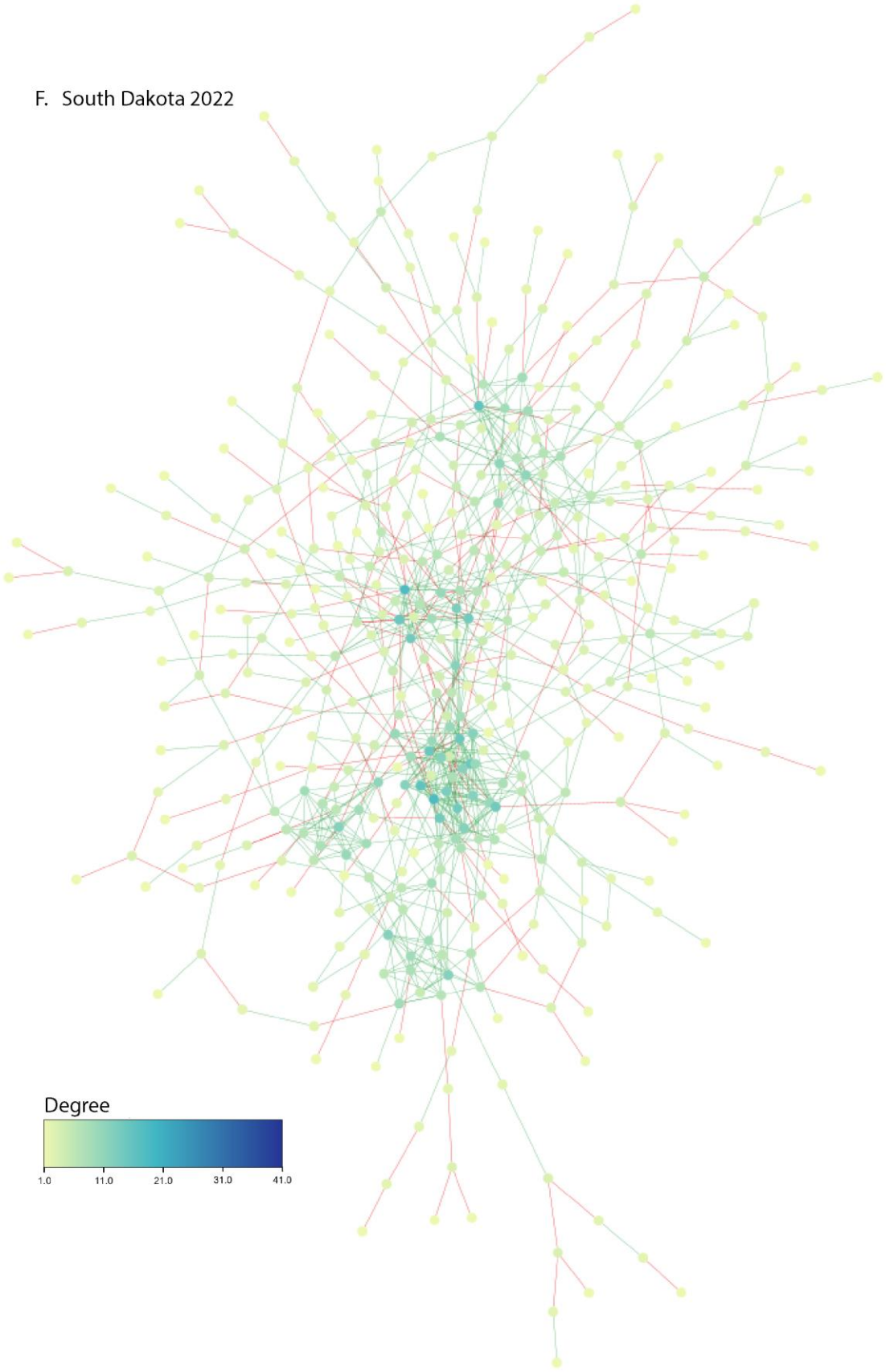

Figure A3.2: Co-occurrence networks by location year. Nodes are colored by degree, and edges are colored by a positive relationship in green, negative relationship in red.

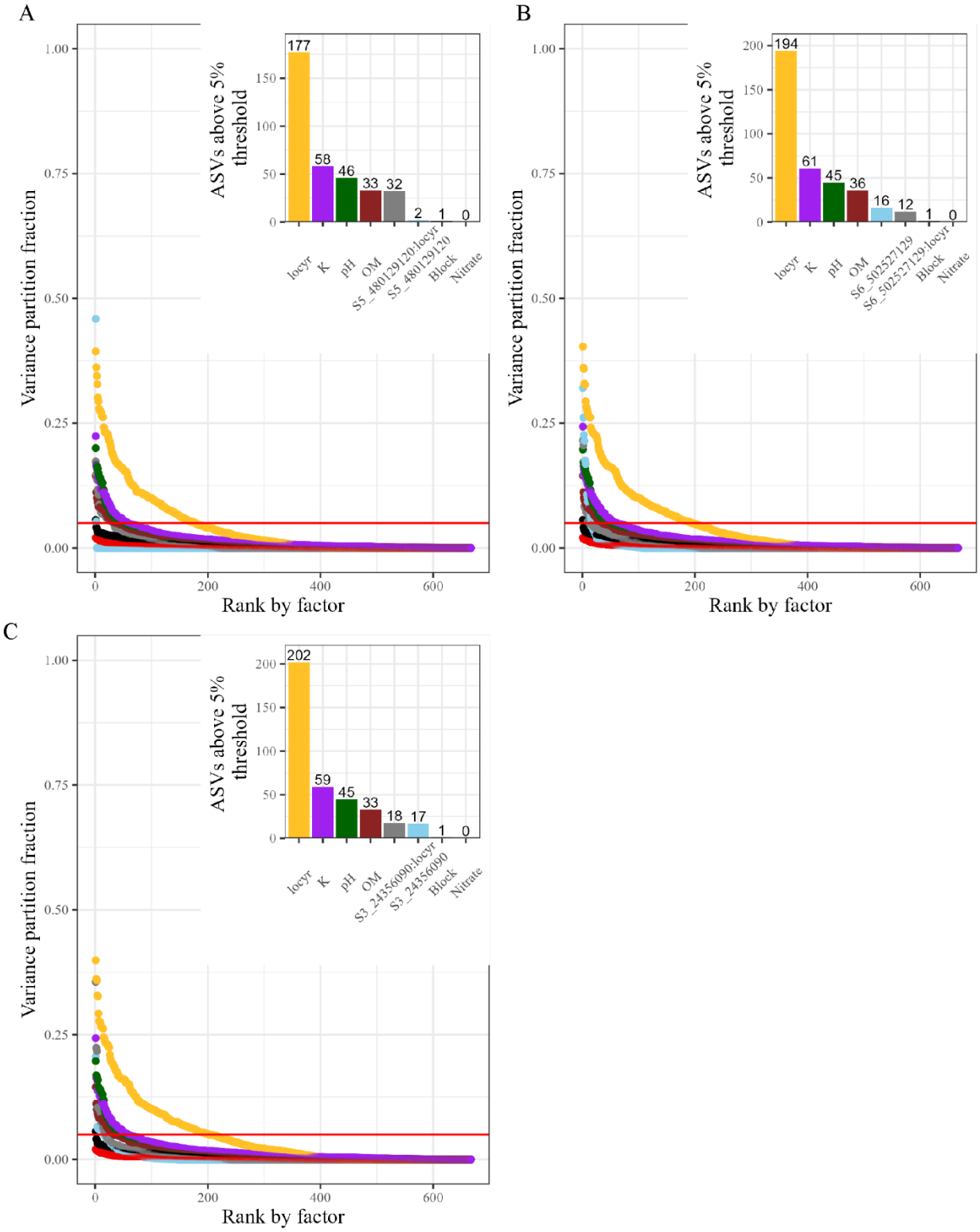

Figure A3.3: QTL variance partitions.

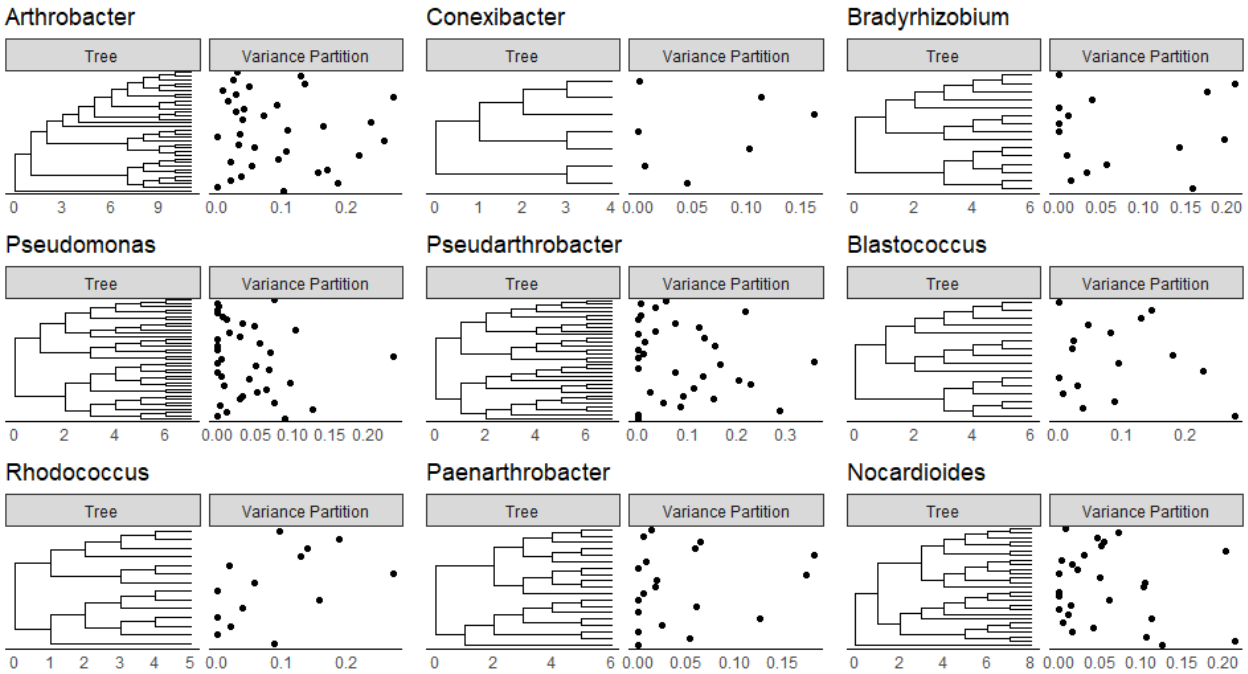

Figure A3.4: Example of subgenus variability from bacterial variance partitioning. Each plot shows the variance partitioned to Location-year across all ASVs of a genus. While some ASVs show significant variance partitioned to Location-year, ASVs of the same genus show no variance partitioned.

Table A3.1: Sample depth across location-years.

Bacteria samples and sample depth across location-years

	BZ21	BZ22	MO21	MO22	SD21	SD22	HI 21
Samples	242	262	233	246	284	286	269
Mean depth	43492.66	37876	35716	45781	20478	32874	35434
Median Depth	35453	35149	33148	42748	20089	23819	29484
Bulk samples	37	45	0	7	47	47	0
Mean depth	48240	38987	0	46352	16337	23120	0
Median Depth	42853	39740	0	46456	16322	17840	0

Fungal samples and sample depth across location-years

	BZ21	BZ22	MO21	MO22	SD21	SD22	HI21
Samples	2	266	205	210	203	245	218
Mean depth	10687	24584	27479	16327	13467	15596	22472
Median Depth	10687	24066	25400	15417	12875	14707	18828
Bulk samples	25	44	0	8	0	6	0
Mean depth	17212	22635	0	16722	0	14945	0
Median Depth	16795	22496	0	15287	0	14240	0

Table A3.2: Bacterial Shannon Diversity Wilcox test.

Comparison	Measure	Method	Group	P.unadj	P.adj	Significance
BZ_2021 - MO_2021	Shannon	Wilcoxon Rank Sum Test	BZ_2021	0.00012408	0.000153275	***
BZ_2021 - HI_2021	Shannon	Wilcoxon Rank Sum Test	BZ_2021	5.21E-89	2.73E-88	***
BZ_2021 - SD_2021	Shannon	Wilcoxon Rank Sum Test	BZ_2021	1.95E-38	4.56E-38	***
BZ_2021 - BZ_2022	Shannon	Wilcoxon Rank Sum Test	BZ_2021	0.010235588	0.01194152	*
BZ_2021 - MO_2022	Shannon	Wilcoxon Rank Sum Test	MO_2022	0.415424267	0.415424267	ns
BZ_2021 - SD_2022	Shannon	Wilcoxon Rank Sum Test	BZ_2021	1.15E-07	1.72E-07	***
MO_2021 - HI_2021	Shannon	Wilcoxon Rank Sum Test	MO_2021	9.30E-81	3.26E-80	***
MO_2021 - SD_2021	Shannon	Wilcoxon Rank Sum Test	MO_2021	2.20E-31	4.61E-31	***
MO_2021 - BZ_2022	Shannon	Wilcoxon Rank Sum Test	BZ_2022	0.02991672	0.033065848	*
MO_2021 - MO_2022	Shannon	Wilcoxon Rank Sum Test	MO_2022	2.11E-09	3.40E-09	***
MO_2021 - SD_2022	Shannon	Wilcoxon Rank Sum Test	MO_2021	0.055004919	0.057755165	ns
HI_2021 - SD_2021	Shannon	Wilcoxon Rank Sum Test	SD_2021	2.40E-94	2.52E-93	***
HI_2021 - BZ_2022	Shannon	Wilcoxon Rank Sum Test	BZ_2022	1.09E-92	7.62E-92	***
HI_2021 - MO_2022	Shannon	Wilcoxon Rank Sum Test	MO_2022	6.01E-85	2.52E-84	***
HI_2021 - SD_2022	Shannon	Wilcoxon Rank Sum Test	SD_2022	5.90E-96	1.24E-94	***
SD_2021 - BZ_2022	Shannon	Wilcoxon Rank Sum Test	BZ_2022	1.15E-54	3.03E-54	***
SD_2021 - MO_2022	Shannon	Wilcoxon Rank Sum Test	MO_2022	2.73E-65	8.18E-65	***
SD_2021 - SD_2022	Shannon	Wilcoxon Rank Sum Test	SD_2022	1.33E-16	2.54E-16	***
BZ_2022 - MO_2022	Shannon	Wilcoxon Rank Sum Test	MO_2022	2.94E-06	4.11E-06	***
BZ_2022 - SD_2022	Shannon	Wilcoxon Rank Sum Test	BZ_2022	2.38E-05	3.12E-05	***
MO_2022 - SD_2022	Shannon	Wilcoxon Rank Sum Test	MO_2022	2.02E-12	3.53E-12	***

Table A3.3: Fungal Shannon Diversity Wilcox test.

Comparison	Measure	Method	Group	P.unadj	P.adj	Significance
MO_2021 - SD_2021	Shannon	Wilcoxon Rank Sum Test	MO_2021	1.23E-57	9.24E-57	***
MO_2021 - HI_2021	Shannon	Wilcoxon Rank Sum Test	MO_2021	1.87E-29	4.02E-29	***
MO_2021 - BZ_2022	Shannon	Wilcoxon Rank Sum Test	MO_2021	0.033622538	0.033622538	*
MO_2021 - MO_2022	Shannon	Wilcoxon Rank Sum Test	MO_2021	8.15E-49	4.07E-48	***
MO_2021 - SD_2022	Shannon	Wilcoxon Rank Sum Test	MO_2021	2.60E-12	3.55E-12	***
SD_2021 - HI_2021	Shannon	Wilcoxon Rank Sum Test	HI_2021	1.31E-34	3.27E-34	***
SD_2021 - BZ_2022	Shannon	Wilcoxon Rank Sum Test	BZ_2022	2.94E-60	4.41E-59	***
SD_2021 - MO_2022	Shannon	Wilcoxon Rank Sum Test	MO_2022	4.70E-05	5.03E-05	***
SD_2021 - SD_2022	Shannon	Wilcoxon Rank Sum Test	SD_2022	1.88E-43	5.64E-43	***
HI_2021 - BZ_2022	Shannon	Wilcoxon Rank Sum Test	BZ_2022	1.11E-18	1.84E-18	***
HI_2021 - MO_2022	Shannon	Wilcoxon Rank Sum Test	HI_2021	1.44E-17	2.16E-17	***
HI_2021 - SD_2022	Shannon	Wilcoxon Rank Sum Test	SD_2022	2.39E-05	2.76E-05	***
BZ_2022 - MO_2022	Shannon	Wilcoxon Rank Sum Test	BZ_2022	8.47E-46	3.18E-45	***
BZ_2022 - SD_2022	Shannon	Wilcoxon Rank Sum Test	BZ_2022	3.45E-06	4.32E-06	***
MO_2022 - SD_2022	Shannon	Wilcoxon Rank Sum Test	SD_2022	1.10E-27	2.05E-27	***

Table A3.4: Levene test to compare Shannon diversity between bacteria and fungi.

Levene Test results comparing the variability in bacterial versus fungal Shannon Diversity within location-year.

Location-year	F value	P	
swMT 21	/	/	
swMT_22	4.0865	0.04366	*
cntrMT_21	17.342	3.76E-05	***
cntrMT_22	23.622	1.60E-06	***
SD_21	187.48	2.20E-16	***
SD_22	0.6434	0.4228	
HI_21	0.0198	0.8883	

Bacteria Shannon diversity summary by location-year

Location-year	Measure	N	Mean	SD	SE
swMT 21	Shannon	279	5.817767	0.6114164	0.036605
swMT_22	Shannon	307	5.692747	0.4022675	0.022959
cntrMT_21	Shannon	233	5.619741	0.4299275	0.028165
cntrMT_22	Shannon	253	5.853511	0.4135016	0.025997
SD_21	Shannon	331	5.214829	0.2004695	0.011019
SD_22	Shannon	333	5.569714	0.487691	0.026725
HI_21	Shannon	269	3.930877	0.4540159	0.027682

Fungal Shannon diversity summary by location-year

Location-year	Measure	N	Mean	SD	SE
swMT 21	Shannon	27	4.165743	0.2588402	0.049814
swMT_22	Shannon	309	3.852792	0.4636731	0.026377
cntrMT_21	Shannon	205	3.943513	0.3680745	0.025707
cntrMT_22	Shannon	217	3.054972	0.5872307	0.039864
SD_21	Shannon	203	2.858925	0.4854634	0.034073
SD_22	Shannon	250	3.662589	0.516505	0.032667
HI_21	Shannon	217	3.50542	0.4267298	0.028968

Table A3.5: Bacterial Variance Partitioning Results

	Block	locyr	pH	Nitrate	OM	K	Residuals
ASV310	0.007379	0.169239	0.053372	6.98E-05	0.053574	0.027915	0.688452
ASV60	0.020706	0.102617	0.018827	0.004469	0.001875	0.001602	0.849903
ASV712	0.00694	0.154134	0.022502	0.000922	0.000381	0.002177	0.812944
ASV295	0.000692	0.025808	0.002621	8.60E-05	0.008272	0.000886	0.961635
ASV448	0.00653	0.071296	0.006711	0.006603	0.016445	0.00121	0.891204
ASV53	2.39E-12	0.101207	0.151838	3.88E-06	0.001789	0.000148	0.745014
ASV275	0.009767	0.126933	0.000134	0.002788	0.021072	0.075194	0.764112
ASV203	1.96E-08	0.041374	0.070131	6.13E-05	0.007659	7.57E-07	0.880774
ASV490	0.006868	0.023716	0.009638	0.006611	7.72E-07	0.001403	0.951763
ASV512	1.30E-12	0.023313	0.001331	0.00013	0.005233	0.002777	0.967216
ASV518	0.003507	0.011153	0.005618	0.000715	0.003692	0.015388	0.959927
ASV173	0.010937	0.034498	0.022048	0.001503	0.00429	0.016438	0.910286
ASV132	0.007978	0.050782	0.008251	9.48E-06	0.029736	0.001964	0.90128
ASV536	0.025042	0	0.013308	0.001015	0.02156	0.004717	0.934358
ASV282	0.008064	0.11449	0.010265	0.000185	0.01274	0.00527	0.848987
ASV27	0.015703	0.2144	9.85E-05	1.64E-05	0.052186	0.045378	0.672218
ASV228	0.022223	0.106315	0.030932	0.000314	0.058186	0.007159	0.774872
ASV738	0.009182	0.061153	0.001818	0.002932	0.002953	0.018817	0.903145
ASV356	0.021129	9.96E-17	0.005515	0.004484	4.57E-05	0.000175	0.968651
ASV337	0.00844	1.26E-15	0.00249	0.002216	1.24E-05	0.003445	0.983396
ASV634	1.30E-19	0.004377	0.00436	0.002241	4.26E-06	0.022938	0.96608
ASV341	0	0	0.00155	2.11E-05	0.002756	0.005922	0.989751
ASV462	0.005161	0	0.009735	0.000383	0.001507	0.011874	0.971339
ASV612	1.69E-09	0.003022	0.003292	0.00103	0.003719	0.000115	0.988822
ASV279	0.000305	3.26E-10	0.000239	2.27E-07	0.006893	0.006478	0.986085
ASV472	0.002555	0.025386	0.039999	0.000264	0.050045	0.003516	0.878234
ASV5	0.006027	0.342661	0.142072	0.000942	0.011176	0.029286	0.467837
ASV170	0.013764	4.59E-11	0.038118	0.000151	0.075664	0.033606	0.838697
ASV369	0.004379	0.112725	0.001915	0.001707	0.076905	0.079586	0.722784
ASV455	0.011426	0.021096	0.001327	0.000506	1.75E-05	0.00507	0.960557
ASV154	0.012073	0.018583	0.000715	0.000554	0.000136	0.029649	0.93829
ASV100	0.001589	0.161854	0.016074	2.20E-05	0.028469	0.029224	0.762768
ASV54	0.003965	0.234374	0.022522	0.000699	0.038907	0.003192	0.696339
ASV268	0.005202	0.00786	0.001859	0.000504	0.000584	0.002476	0.981515
ASV247	0.012031	0.124807	0.070349	8.60E-05	0.000205	0.005	0.787523
ASV290	9.87E-11	0.166354	0.009366	0.001567	0.012601	0.091054	0.719057
ASV136	0.001681	0.076694	0.000166	0.000657	0.000383	0.002686	0.917734
ASV539	0.001664	0.072609	0.037737	0.007632	0.000397	0.008861	0.8711
ASV17	0.011424	0.187091	3.84E-06	0.001212	0.001819	0.029077	0.769373

ASV412	0.003984	0.018006	0.015279	1.73E-05	0.006614	0.007548	0.948551
ASV20	0.009631	0.285987	0.03262	2.32E-05	0.114142	0.004122	0.553475
ASV250	0.006365	0.063181	0.023591	0.000157	0.025638	0.008468	0.872601
ASV265	0.004666	0	0.008173	0.005384	0.026255	0.026398	0.929124
ASV307	0.004217	0.028347	0.005149	0.000394	0.003424	0.001893	0.956574
ASV404	0.003785	0.029777	0.008602	0.002974	0.02838	0.000503	0.925979
ASV511	1.86E-10	0.043133	0.001474	1.39E-05	0.000725	1.23E-05	0.954641
ASV388	4.45E-16	0.005366	0.021575	0.006874	0.001584	0.02808	0.936521
ASV127	0.005227	0.136452	0.003585	4.89E-05	0.03718	0.073456	0.744051
ASV9	0.015131	0.016877	0.019089	0.000252	0.079565	0.010485	0.858601
ASV206	0.006327	0.069607	0.004565	5.11E-05	3.11E-05	0.006354	0.913065
ASV645	0.003101	0.07922	0.016344	0.012219	0.003694	0.011592	0.87383
ASV831	0.005217	0	0.000119	0.003552	9.09E-05	0.013282	0.977738
ASV618	0	0	0.001863	9.80E-06	0.003968	0.000194	0.993965
ASV24	0.007219	0.020001	0.102964	0.000148	0.00481	0.051197	0.813661
ASV585	3.75E-10	0.043796	0.006478	0.003858	1.24E-05	0.012254	0.933601
ASV488	0.00068	0.048025	0.001185	0.001932	0.00635	0.01996	0.921868
ASV200	0.001286	0.005971	0.021926	0.000575	0.063637	0.002211	0.904395
ASV79	0.001133	0.310731	0.047114	0.000375	0.064024	0.077976	0.498647
ASV106	0.007747	0.252416	0.00042	0.004277	0.017775	0.054062	0.663303
ASV451	0.001086	0.036065	0.002151	6.31E-05	0.013561	0.000957	0.946117
ASV476	0	0	0.012578	2.56E-05	0.010666	0.003041	0.97369
ASV726	0.008959	0	0.023159	0.000162	0.003235	0.004395	0.96009
ASV19	4.34E-12	0.089957	1.28E-06	1.50E-05	0.001083	0.008225	0.900719
ASV522	0.012672	0	0.003438	0.000604	0.000139	9.72E-07	0.983145
ASV546	0.00281	0.020453	4.68E-05	5.15E-05	0.01511	0.02158	0.93995
ASV340	0.001283	0.000477	0.0101	2.95E-05	0.003432	0.003019	0.981659
ASV360	9.11E-17	0.080415	3.41E-06	0.000107	0.022576	0.065746	0.831154
ASV373	0.013393	0	0.042758	0.000593	0.01315	0.000291	0.929815
ASV43	0.004399	0.087718	0.001485	0.0014	0.038174	0.039957	0.826868
ASV270	0.002145	3.67E-14	0.001034	0.003949	0.006695	0.011997	0.97418
ASV540	0.00621	0.030645	0.010329	0.000116	0.001027	0.006805	0.944868
ASV529	0.002737	0.132665	0.014821	0.000128	0.021459	0.014248	0.813941
ASV180	0.006653	0.055689	0.011567	5.95E-05	0.011676	0.032498	0.881857
ASV689	0.014349	0.025655	0.008896	0.001299	0.008217	0.003592	0.937992
ASV199	0.010684	0.285301	0.016689	0.015946	0.010739	0.146782	0.513859
ASV690	0.010957	0	0.011864	0.009103	0.001157	4.10E-08	0.966919
ASV639	0.00625	0.053711	0.01355	0.006445	6.64E-05	0.004878	0.9151
ASV870	0.004917	0.005317	0.010431	0.004859	0.003245	0.031702	0.939528
ASV74	0.006157	0.01462	0.008016	1.60E-05	0.00013	0.028493	0.942569
ASV264	0.003128	0.085559	0.017531	0.003644	0.007268	0.016256	0.866614

ASV47	0.007094	0.01922	0.000604	0.000319	0.029082	0.045827	0.897855
ASV191	0.010066	0.11262	0.002258	0.001471	0.092426	0.074448	0.70671
ASV126	0.00934	0.158183	0.005979	0.000406	0.025712	0.065527	0.734853
ASV400	0.006723	0	0.004302	8.62E-06	0.007584	0.017288	0.964094
ASV561	0.002759	0.058107	0.014415	0.007054	0.001385	0.031097	0.885183
ASV77	0.04089	0.150838	0.028843	1.39E-05	0.007863	0.007805	0.763748
ASV121	0.002063	0.04412	0.036759	0.003	0.008395	0.019292	0.88637
ASV102	0	0.180361	0.014816	0.007007	0.000976	0.098427	0.698413
ASV84	0.006672	0.011426	0.005059	1.27E-05	0.018191	4.83E-05	0.958591
ASV286	0.004906	0.091795	0.003732	0.007879	0.008048	0.011872	0.871768
ASV201	0.009641	0.176063	0.049816	0.000217	0.058362	0.132511	0.573389
ASV61	0.004072	0.00531	0.022126	0.000461	0.098141	0.088914	0.780977
ASV475	0.010241	2.31E-18	0.002347	0.003581	0.005192	0.005467	0.973172
ASV231	0.004296	0.001189	0.001275	0.000172	0.013295	0.006327	0.973445
ASV311	2.14E-08	0.033156	0.023682	0.000929	0.003679	0.000202	0.938352
ASV441	1.13E-10	0.009909	7.77E-05	2.19E-08	0.001195	0.001107	0.987711
ASV7	0.025069	0.04997	0.012181	0.005374	0.010285	0.090933	0.806188
ASV665	0.003821	0	0.000338	0.002513	0.011132	0.00834	0.973855
ASV553	0.011459	0.010746	0.001828	0.002002	0.018723	0.040303	0.914938
ASV347	0.003867	0	0.002326	0.007055	0.008375	0.003135	0.975243
ASV420	0.011828	0.005647	0.009051	0.011662	3.50E-05	0.01489	0.946887
ASV715	0.025862	5.11E-17	0.000717	9.21E-06	3.96E-05	0.007492	0.965881
ASV424	0.023391	0.13818	0.005507	0.002451	0.033878	0.087432	0.709162
ASV222	0.018811	0.108368	0.001885	0.004582	0.013776	0.063491	0.789087
ASV210	0.02042	0.014526	0.026655	0.000707	0.032992	0.022982	0.881717
ASV368	0	0	0.019228	0.007999	0.009546	0.001292	0.961935
ASV468	0.020457	0	0.017607	0.000285	0.000127	0.007007	0.954518
ASV470	0.006339	0	0.00476	0.008961	0.001438	0.000474	0.978027
ASV364	0.000842	0.056055	0.001097	1.66E-05	0.004979	0.001299	0.935711
ASV80	0.008297	0	0.005911	0.001203	0.026026	0.001404	0.95716
ASV723	0.002182	0.089586	0.036339	0.007337	0.011746	0.072961	0.779849
ASV293	0.0051	0.001619	0.002355	0.000203	0.002875	0.014718	0.973131
ASV122	0.002553	0.054086	0.010784	0.003695	0.028673	0.121158	0.779051
ASV494	0.012864	0.0109	0.003459	0.000332	0.004021	0.005982	0.962442
ASV515	8.10E-11	0.048835	0.002329	0.00173	0.002652	0.015645	0.928809
ASV109	1.66E-13	0.178106	0.003313	0.006197	0.043432	0.083754	0.685197
ASV491	0.005637	0	0.000724	0.000836	0.011849	0.000102	0.980852
ASV981	0.001109	0.010842	0.00246	0.004949	0.005121	0.014595	0.960923
ASV563	0.001346	0	0.004699	0.002205	0.00966	0.000771	0.981319
ASV30	0.006521	0.102557	0.053118	0.00248	0.072454	0.042295	0.720575
ASV447	0	0.019431	0.004477	0.00317	0.000308	0.001172	0.971442

ASV182	0.009665	0.111502	0.015001	0.00054	0.001118	0.059577	0.802598
ASV568	6.56E-12	0.004535	0.000202	0.002103	0.001681	0.003611	0.987866
ASV413	0.000166	0	0.000606	0.002484	0.000794	0.000815	0.995136
ASV314	0.002453	1.47E-16	0.00738	0.000835	0.000211	0.002048	0.987075
ASV701	0.002038	0.001266	8.28E-05	0.002291	0.008007	0.007005	0.97931
ASV579	0.00314	0.033196	0.012596	0.001296	0.005329	0.00213	0.942313
ASV519	0.004796	0.006564	0.003459	0.003125	0.007642	0.012732	0.961681
ASV520	3.94E-19	0.057741	0.011816	0.000951	0.00376	0.000545	0.925187
ASV40	0.000589	0.226707	0.000269	1.47E-06	0.064769	0.044124	0.663539
ASV92	0.024881	0.057397	0.000959	5.14E-05	0.02475	0.057413	0.834547
ASV269	0.010286	0.003853	0.001937	0.000637	0.002428	5.71E-05	0.980802
ASV287	0.011517	0.051972	0.052237	0.018293	0.004578	0.013491	0.847912
ASV345	0.027647	0.113676	0.034173	1.14E-07	0.039822	0.042446	0.742236
ASV162	0.004378	0.00239	0.004083	0.001766	0.00013	0.000437	0.986816
ASV1046	0.011106	0.066327	0.006025	0.001377	0.046948	0.102188	0.766028
ASV48	0.009596	0.203018	0.002571	0.00208	0.143244	0.182885	0.456605
ASV363	0.004171	0.102764	0.014959	0.007079	0.009596	0.043762	0.81767
ASV320	0.004047	0.006319	0.012392	0.000679	0.023856	0.00435	0.948356
ASV130	0.001044	0.127415	0.000419	0.00063	0.05016	0.045514	0.774819
ASV615	0.003822	0.00733	0.003322	3.78E-05	0.015821	0.018675	0.950991
ASV489	0.00692	0.021886	8.33E-05	0.000317	0.01336	0.022422	0.935011
ASV198	3.82E-16	0	0.003066	0.000532	0.005952	0.001086	0.989364
ASV346	0.00603	0.011342	0.013369	0.0054	0.007715	0.008207	0.947938
ASV233	0	0.006571	0.001317	5.88E-05	0.005066	0.004186	0.982801
ASV212	1.28E-18	0.01987	0.021249	0.002377	3.65E-05	0.006727	0.94974
ASV164	0.001281	0.03624	0.022246	6.57E-05	0.000512	0.004347	0.935308
ASV37	0.012143	0.409085	0.003252	2.09E-05	0.000121	0.172593	0.402786
ASV302	0.004616	0.003135	0.000397	0.006562	0.002685	0.00049	0.982115
ASV113	0.001696	0.102313	0.000375	6.69E-05	0.000279	0.000189	0.895081
ASV297	0.000516	0.013235	0.007174	4.11E-05	0.000278	0.008527	0.970228
ASV641	0.013129	6.98E-17	0.000804	0.002603	0.001396	0.010812	0.971256
ASV29	0.003396	0.300955	0.013222	0.000678	0.030168	0.010976	0.640604
ASV478	0.005809	0.089466	8.06E-05	1.41E-05	0.00654	0.013373	0.884718
ASV595	0	0	0.002866	9.17E-07	0.002745	0.003986	0.990403
ASV224	0.010022	0.044746	0.003481	0.001142	0.014206	0.016638	0.909764
ASV55	0.020081	0.165855	0.150564	0.002561	0.053156	0.001315	0.606468
ASV172	0.004647	0.085525	0.02522	0.002639	0.034641	0.040904	0.806424
ASV249	1.74E-13	0.005754	0.001731	0.004244	0.00905	4.73E-07	0.979219
ASV153	8.84E-13	0.065324	0.000752	0.006962	0.087714	0.00256	0.836688
ASV190	0.004034	0.046367	0.007813	3.16E-05	0.05567	0.052088	0.833997
ASV367	0.001274	0	0.014846	0.00018	0.014297	0.006987	0.962416

ASV28	0.006954	0.031085	0.126749	0.000403	0.012232	0.006624	0.815953
ASV243	0.008633	0.024179	0.047146	6.42E-05	0.002066	0.000792	0.917121
ASV93	0.005345	0.051774	0.071903	0.000202	0.009145	0.00268	0.85895
ASV251	0.022395	0.121985	0.058282	0.000171	0.031355	0.083228	0.682583
ASV386	0.00394	0	0.011818	0.000176	0.000257	0.009268	0.97454
ASV544	0	0	9.75E-05	1.37E-05	0.00161	0.002675	0.995604
ASV538	0.009383	0.015293	0.003849	0.00044	0.001585	0.023395	0.946056
ASV686	0.005892	0	0.000875	0.003631	0.001112	0.007902	0.980588
ASV339	0.002762	0.0306	0.000698	0.000491	0.005806	0.002005	0.957638
ASV97	0.010171	0.10289	0.02891	0.000414	0.006799	0.000432	0.850384
ASV592	0.001223	0.082503	0.019185	0.00114	0.001236	0.018505	0.876208
ASV105	0.009259	0.322558	0.125088	0.000421	0.068315	0.062152	0.412207
ASV181	0.007026	0.183906	0.010517	0.000776	0.030869	0.030171	0.736735
ASV235	0.000842	0.090599	0.045345	4.98E-07	0.003637	0.025825	0.833752
ASV1151	0.019424	0.000903	0.021731	0.001073	0.027118	0.001148	0.928602
ASV728	0.048345	0	0.000559	0.010083	0.0089	8.24E-05	0.932031
ASV477	4.51E-12	0.010041	0.026383	1.24E-06	7.12E-05	0.000821	0.962682
ASV221	0.012293	0.142447	0.002689	0.001236	0.005288	0.034879	0.801168
ASV482	0.006802	0.009308	0.00524	0.000847	0.001433	0.002434	0.973935
ASV108	0.014852	0.178694	0.068981	0.001666	0.011675	0.001949	0.722182
ASV644	0.006416	0.093433	0.035259	0.005839	0.01854	0.021376	0.819137
ASV445	0.009977	0.036005	0.001174	0.000186	0.002923	0.001309	0.948426
ASV444	0.01947	0.008804	0.029372	0.0043	0.000113	0.071033	0.866907
ASV342	0.005618	0.024402	0.001297	0.001701	0.007156	0.04557	0.914256
ASV391	0.006238	0.016545	0.00725	0.000864	0.000251	0.001656	0.967195
ASV343	0.009331	0.004748	0.002331	6.21E-05	0.00695	0.007103	0.969475
ASV276	0.026325	0	0.001061	3.25E-07	0.00941	0.003601	0.959603
ASV457	0.00403	0	0.000779	6.65E-06	0.002071	0.01097	0.982143
ASV765	0.012696	0.075195	0.002118	0.001391	0.000297	0.015131	0.893171
ASV554	0.005261	0	1.69E-09	2.82E-06	0.012918	1.27E-05	0.981806
ASV308	0.005279	0.042032	0.041049	0.002992	0.000331	0.013563	0.894754
ASV78	0.00234	0.075768	1.82E-05	7.92E-07	2.60E-05	0.000938	0.920908
ASV125	5.44E-15	0.029418	0.010765	0.00078	0.054506	0.005567	0.898965
ASV408	0.011353	0.00991	0.000702	0.001851	0.002847	0.000246	0.973091
ASV525	0.010956	0.098117	0.000692	0.007303	0.022888	0.042177	0.817868
ASV149	0.005054	1.51E-17	9.55E-05	0.000555	0.055709	0.036294	0.902292
ASV425	0.007195	0.094011	0.020914	2.60E-05	0.001425	0.000733	0.875696
ASV439	8.30E-14	0	0.005617	0.001631	0.001449	0.004623	0.98668
ASV397	0.004074	0.001639	1.38E-06	6.48E-05	0.002015	7.04E-05	0.992135
ASV317	0.005909	0.101762	0.000181	0.00013	0.014511	0.012335	0.865172
ASV596	0.011505	0.083234	0.028467	0.008828	0.003618	0.035279	0.829069

ASV711	0	0	0.002324	0.001067	0.000442	0.017001	0.979166
ASV421	0.004202	0.032609	0.000603	0.002026	0.001253	0.000408	0.958899
ASV492	0.012411	0.130285	0.001138	0.000495	0.02106	0.014833	0.819777
ASV556	0.001591	1.79E-11	0.001012	0.002246	0.015636	0.007375	0.97214
ASV460	1.39E-12	0.006907	0.00022	0.000549	0.001156	0.010051	0.981118
ASV56	0.008206	0.363178	0.039493	0.00067	0.068797	0.118447	0.401209
ASV299	0	0.070703	0.006125	1.12E-06	0.020867	0.017898	0.884406
ASV318	0.006955	0.04651	0.045683	0.0006	0.025222	5.37E-05	0.874975
ASV187	0.007346	0	0.001543	0.001941	0.006541	0.009781	0.972849
ASV90	0.005775	0.031071	0.002061	2.32E-05	0.034176	0.008324	0.918569
ASV219	0	0	4.06E-06	8.14E-05	0.005325	0.005076	0.989513
ASV248	0.010864	0.15724	0.011195	0.000832	0.018194	0.006334	0.795341
ASV237	0	0	0.002252	6.22E-06	4.11E-05	2.99E-05	0.997671
ASV124	0.000912	0.036919	0.000187	0.000201	0.026048	0.043075	0.892657
ASV305	0.001496	0.074111	0.112457	0.000214	0.030836	0.0011	0.779787
ASV751	0.001517	0.062694	0.003698	0.000272	0.001561	0.004252	0.926005
ASV678	0.011642	0	0.006035	0.002051	0.011574	0.035437	0.933261
ASV469	0.005865	0	0.000471	0.00256	0.004699	0.000715	0.98569
ASV258	0.002236	0	0.000697	0.002706	0.003097	0.001861	0.989403
ASV608	0.000468	0.015069	0.009536	0.003658	0.001227	0.017184	0.952857
ASV461	0.000706	0.007793	0.005966	0.000189	0.000805	2.34E-06	0.984539
ASV548	0.002016	0.018757	0.000518	0.000138	2.04E-05	4.99E-08	0.978551
ASV336	0.00072	0.024336	0.000532	0.005037	0.041614	0.008375	0.919386
ASV410	0.013115	0.185159	0.048193	0.005715	0.08368	0.038776	0.625362
ASV414	0.00208	4.82E-16	0.007508	0.00057	0.001708	0.009992	0.978142
ASV16	0.006823	0.080813	0.047546	0.001081	0.029127	0.006079	0.828531
ASV485	5.98E-15	0.004369	0.000176	0.000553	0.010324	0.001772	0.982806
ASV406	0.000264	0.012239	0.001733	0.002267	0.004432	0.003004	0.976061
ASV403	0.009182	0.026049	0.008218	0.000142	0.000796	0.001878	0.953734
ASV312	7.62E-06	0.020062	0.002822	3.32E-06	8.77E-06	0.002791	0.974306
ASV534	0.012629	0.004966	0.001304	0.008133	0.016715	0.002451	0.953801
ASV591	0.004853	0.05399	0.018829	0.000216	0.00105	0.018219	0.902844
ASV91	6.84E-11	0.115947	0.00047	0.002174	0.031331	0.035751	0.814328
ASV497	0.004518	0	0.007489	0.002456	0.000917	0.001513	0.983107
ASV304	0.00443	0.006258	0.007401	0.001519	0.006152	0.001371	0.972868
ASV679	2.63E-12	0.176925	0.029137	0.000824	0.00749	0.000663	0.784961
ASV479	0.004391	0	0.000268	0.005542	0.004358	0.00703	0.978411
ASV505	0.015165	1.69E-13	0.004579	1.05E-06	0.01042	0.009702	0.960133
ASV523	0	0.056377	0.016257	0.000822	0.009199	0.001208	0.916138
ASV214	0.002466	0.129638	0.039677	0.000375	0.019096	0.043094	0.765653
ASV357	0.003968	0.002455	0.020099	8.28E-05	0.01701	4.03E-05	0.956344

ASV274	0.001017	0.038817	0.009594	0.005295	0.001813	0.0011	0.942364
ASV178	0	0.077438	2.19E-05	0.002396	0.007993	0.034979	0.877171
ASV440	0.017826	1.11E-18	0.009247	0.000174	0.003289	0.005474	0.96399
ASV402	0.007072	0.144587	0.004045	0.000358	0.103862	0.0663	0.673775
ASV71	0.012449	0.112846	0.003158	7.62E-06	0.017296	0.111021	0.743222
ASV349	0.004874	0.018823	0.026991	0.002514	0.016537	0.000108	0.930154
ASV502	0.00676	0.048871	5.90E-05	0.002165	0.005011	0.009908	0.927227
ASV211	3.91E-08	0.060575	0.016347	0.000758	0.001577	0.016679	0.904063
ASV389	0.00172	0.018181	0.019094	2.09E-05	0.015906	0.012902	0.932177
ASV365	0.008493	0	0.013493	0.006889	0.007093	0.009375	0.954657
ASV437	0.014806	0.010553	0.006913	0.000984	0.000412	0.030297	0.936035
ASV87	0.005187	0	0.00078	0.000663	0.007565	0.006294	0.979512
ASV607	0	0.010171	0.007518	0.000112	0.004625	0.008671	0.968903
ASV166	0.001423	0	0.000371	4.78E-06	0.065517	0.011194	0.92149
ASV21	0.01841	0.06056	0.037442	0.000527	0.035833	0.027219	0.82001
ASV873	0.006967	0.26277	0.005833	2.34E-05	0.082448	0.032762	0.609196
ASV821	0.006013	0.146364	0.042257	3.83E-05	0.000299	0.014517	0.790513
ASV614	0.00228	0.119253	0.013944	8.39E-08	0.007254	0.108024	0.749245
ASV338	0.021051	0	0.00726	0.00436	0.000524	0.011932	0.954873
ASV352	0.018272	0	3.49E-05	0.002294	4.41E-05	0.021808	0.957546
ASV245	0.004146	0.014148	0.000865	0.000901	0.000489	0.017492	0.96196
ASV14	0.002793	0.300937	0.00662	0.002351	0.000623	0.038868	0.647808
ASV900	2.79E-18	0.044141	0.000401	0.001622	0.000362	0.003184	0.95029
ASV517	5.71E-17	0	0.006865	0.000943	0.004073	0.00077	0.98735
ASV481	0.004774	0.032621	0.015986	0.001052	0.000645	0.000584	0.944337
ASV632	0.010618	0.033084	0.011927	0.000147	0.039566	4.18E-05	0.904617
ASV487	0.011927	0	0.004131	0.007224	0.004349	0.001838	0.97053
ASV319	0.013683	0.068871	1.43E-06	0.005082	0.000469	0.022243	0.889651
ASV227	0.014284	0.037425	0.009888	0.001747	0.001771	0.003987	0.930898
ASV390	0	0.001293	0.000181	3.07E-05	0.000742	0.002647	0.995106
ASV687	0.009855	0.046449	5.03E-05	0.000263	0.007966	0.02073	0.914687
ASV255	0.011376	0.059617	0.00164	0.00104	0.015452	0.006975	0.903901
ASV246	1.96E-17	0.016781	0.002246	0.000215	0.035509	9.29E-06	0.94524
ASV3	0.010071	0.155091	0.105824	5.40E-05	0.001164	0.000807	0.726989
ASV184	0.005485	0.185611	0.019942	0.000315	0.044429	0.112003	0.632215
ASV467	0.001449	0.015862	0.005461	5.85E-05	0.010715	0.001095	0.96536
ASV438	0.016497	0.122936	0.048938	1.22E-06	0.020045	0.002052	0.789531
ASV589	0.002052	0.015857	0.01321	0.002847	0.012851	0.000144	0.953038
ASV261	0.011982	0.067929	0.000271	0.001353	0.024587	0.073639	0.820239
ASV484	0.009599	0.025062	0.023008	0.000149	0.006704	0.013375	0.922102
ASV1	0.003151	0.170417	0.011267	0.000126	0.014903	2.71E-08	0.800136

ASV230	0	0.100871	0.000137	0.0002	0.009181	0.000627	0.888984
ASV284	5.55E-15	0.04525	0.007763	0.00057	0.023515	0.002223	0.92068
ASV401	0.006014	0	0.004314	0.008194	5.82E-05	0.002267	0.979153
ASV189	1.77E-16	0.071083	0.000383	2.52E-05	0.012029	0.021995	0.894486
ASV119	0.013962	0.216596	0.008299	0.004479	0.061223	0.05721	0.638231
ASV277	0.003381	0.103603	0.066974	0.003809	0.032188	0.007166	0.782878
ASV704	4.96E-12	0.064662	0.002561	0.002018	0.017975	0.000552	0.912232
ASV748	0	0.084856	0.026757	0.002387	0.027724	0.000183	0.858092
ASV204	0	0	0.003277	0.000129	0.006667	0.004781	0.985146
ASV509	0.023071	0.03199	0.002558	0.000777	0.007441	0.005962	0.928202
ASV333	0.003294	0	0.006422	0.002127	0.010879	0.019358	0.957921
ASV380	0.001406	0	0.003661	9.64E-07	0.006003	0.000103	0.988827
ASV507	0.009019	0	0.004396	4.71E-05	0.012159	0.02166	0.952719
ASV309	0.005445	0	0.000705	3.32E-05	0.007223	0.001239	0.985355
ASV110	0.01369	0.126976	0.038733	0.001905	0.03219	0.126671	0.659835
ASV82	1.04E-08	0.2258	0.08096	0.004838	0.012558	0.003061	0.672783
ASV680	0.002447	0.008468	0.002589	0.000158	0.003516	0.002288	0.980533
ASV325	1.11E-15	0.027316	0.001637	1.47E-07	0.002854	0.00732	0.960873
ASV332	3.93E-05	0.102411	0.032564	0.004894	0.013424	0.078399	0.768268
ASV500	0.037577	0.061769	0.011339	0.001124	0.03114	0.024378	0.832672
ASV236	3.66E-17	0.034174	0.004392	0.001357	0.030908	0.005581	0.923587
ASV36	0.002025	0	0.045231	0.009353	0.047924	0.029407	0.86606
ASV675	0.008328	0.006317	0.000286	0.000381	0.006346	0.018049	0.960291
ASV330	0.002339	0.045879	0.002723	0.003157	0.013218	0.013442	0.919242
ASV973	5.45E-05	0	0.008247	0.00411	9.09E-05	0.002256	0.985241
ASV175	0.007981	0.008074	0.042713	0.000154	0.00721	0.001997	0.93187
ASV426	0.031959	0	0.000367	0.000565	0.018717	0.000227	0.948167
ASV466	0.000259	0.032865	0.002988	0.000172	0.002002	0.001466	0.960249
ASV433	0.015111	0	0.002664	0.003648	0.007126	3.16E-05	0.97142
ASV123	0.005806	0.033581	0.004596	9.47E-05	0.003558	0.006132	0.946232
ASV140	0	0.058099	0.00186	0.001016	0.020869	0.03211	0.886046
ASV464	0	0.077377	0.003979	0.004524	0.002284	0.046928	0.864909
ASV685	0.004789	0.004071	0.000376	5.60E-06	0.001556	0.004019	0.985183
ASV453	0.006257	0	0.000776	0.005898	0.002406	0.003531	0.981131
ASV208	1.98E-12	0.028404	0.00151	0.002229	0.001099	0.01713	0.949629
ASV733	0.014078	0.044175	0.003975	0.000681	0.000225	0.006721	0.930146
ASV273	3.31E-15	0.009321	0.000538	1.55E-06	0.000664	0.0018	0.987675
ASV371	0.013048	0.012303	0.006877	0.005354	0.000142	0.021404	0.940871
ASV377	0	0.008316	0.010729	0.000214	0.000929	0.000479	0.979333
ASV117	0.004497	1.12E-17	0.002755	0.001352	0.019796	0.012971	0.958629
ASV582	0.008619	0.029261	0.001393	0.000173	0.007394	0.007543	0.945618

ASV278	0.005316	0.005347	0.004681	0.000959	0.013447	0.001263	0.968986
ASV418	0.026729	0.036497	3.26E-07	6.33E-05	5.35E-06	0.014211	0.922494
ASV521	0.004056	0.038918	0.003696	0.007297	0.003136	0.006099	0.936798
ASV138	0.0128	0.276579	0.024246	0.002322	0.044274	0.174293	0.465487
ASV560	2.96E-12	0.119721	0.003761	0.003331	0.010975	0.07277	0.789443
ASV769	0.009914	0.058218	0.021533	2.55E-07	0.001934	0.013017	0.895384
ASV604	0.008456	0.023779	0.001459	0.000766	0.005721	0.010336	0.949482
ASV649	0	0	0.006785	0.010734	0.001835	0.010546	0.970101
ASV653	0.026679	0.037966	0.013532	0.003677	0.017858	0.025378	0.87491
ASV430	0.007894	0.025414	0.017904	1.61E-06	0.022841	0.000107	0.925839
ASV840	2.17E-11	0.004842	0.005364	0.001649	0.000438	0.010673	0.977034
ASV442	0	0.106066	0.003292	0.000328	0.007074	0.010908	0.872333
ASV252	0.001173	0.045547	0.002975	0.002784	0.007957	0.012505	0.927059
ASV103	0.006381	0.048576	0.00056	0.002532	0.001555	0.080796	0.8596
ASV776	2.84E-11	0.012397	0.000121	0.000341	0.005048	0.010577	0.971516
ASV527	0.000428	0.037558	0.045232	0.001123	0.039605	0.001426	0.874628
ASV83	0.009022	0.005333	0.012186	0.00074	0.012495	0.008517	0.951707
ASV385	4.89E-11	0.024777	0.002319	0.002526	0.009509	0.000627	0.960242
ASV73	0.019606	0.089828	0.009884	0.000613	0.053719	0.040982	0.785369
ASV629	0.003443	0.010057	0.002116	0.000955	0.035064	0.004026	0.944339
ASV52	0.029239	0.182696	0.001805	0.000801	0.045383	0.036628	0.703446
ASV296	0.002622	0	0.01672	0.001455	0.010382	2.01E-05	0.968801
ASV322	0.005331	0.003636	0.001095	3.08E-05	0.017687	0.01923	0.95299
ASV280	0.011001	0.037097	0.000852	1.59E-05	0.055391	0.049117	0.846525
ASV324	0	0.129815	0.005582	0.000344	0.01515	0.063537	0.785572
ASV2	0.010916	0.219664	0.004666	9.49E-06	0.013823	0.004985	0.745936
ASV395	0.005895	0	0.000246	0.000852	5.65E-05	0.001576	0.991374
ASV549	2.56E-19	0.056292	0.000546	0.006258	0.005011	0.010066	0.921827
ASV10	0.022314	0.105787	0.077627	0.000131	0.000554	0.085932	0.707655
ASV542	0.010523	0.067432	3.66E-05	0.000287	0.05472	0.066059	0.800941
ASV384	0.009996	0.050898	0.028793	0.000275	0.00742	0.002786	0.899832
ASV382	0.009807	0.038798	0.016724	0.002455	0.015228	0.021346	0.895642
ASV259	0.004956	0.059859	0.000127	0.000193	0.019566	0.040026	0.875273
ASV242	0.003855	0.044143	0.030111	0.000723	0.036355	0.002866	0.881947
ASV116	0.02353	0.051398	0.002444	0.000613	0.007055	0.006866	0.908094
ASV32	0.000496	0.140166	0.040386	2.06E-06	0.011168	0.059416	0.748366
ASV285	0.004929	3.39E-16	0.001298	0.001639	0.00287	0.010912	0.978353
ASV129	0.002176	0	0.014401	0.002329	0.016045	0.06102	0.904029
ASV65	0.002787	0.057461	0.014945	0.000162	6.27E-05	0.067061	0.857521
ASV432	2.10E-09	0.074492	0.029646	0.000195	0.010802	0.000921	0.883944
ASV417	0.010694	0	0.001043	4.09E-05	0.026142	0.003458	0.958622

ASV767	0.018335	0.005937	0.004236	0.000221	5.05E-05	0.006544	0.964676
ASV88	0.009568	0	0.000813	0.000603	0.002678	0.014196	0.972142
ASV234	0.000761	0.021843	0.000903	0.005226	0.000657	0.001731	0.968879
ASV292	0.031111	0.013702	0.029008	9.45E-05	0.016601	0.018687	0.890797
ASV393	0.01076	0.055383	0.00562	0.013718	0.005893	0.015291	0.893334
ASV597	0	0	0.0059	1.55E-05	3.18E-05	0.006413	0.98764
ASV144	0.000595	0.124466	0.005157	0.001244	0.025853	0.111565	0.73112
ASV213	0.006864	0.011189	0.003327	0.008233	0.055337	0.000593	0.914457
ASV57	0.015305	0.078874	0.034664	0.000284	0.055505	0.043079	0.77229
ASV471	0.003679	0.017987	0.036008	0.000789	0.015308	0.009107	0.917122
ASV574	0.016869	0.028651	0.056797	1.64E-06	0.036199	0.00031	0.861173
ASV506	0.008425	0.02365	0.001154	0.002502	6.93E-05	0.001335	0.962864
ASV291	0.00704	0.016116	0.005072	0.002202	0.00291	0.004918	0.961741
ASV209	0.009447	2.38E-10	9.46E-05	0.010351	9.00E-06	0.000325	0.979773
ASV257	0.010964	0.133027	0.013136	0.003983	0.004081	0.000444	0.834365
ASV289	4.63E-16	0.11702	6.01E-06	0.018203	0.010631	0.032197	0.821943
ASV315	0.01247	0.011681	3.60E-06	0.000286	0.000574	0.002309	0.972678
ASV316	0	0	0.003267	0.001093	0.000936	3.81E-05	0.994666
ASV26	0.00086	0.20793	0.002478	0.002619	0.004876	0.057206	0.724032
ASV630	0.025877	0.032136	0.001454	0.00326	0.006807	0.008414	0.922052
ASV266	0.016662	0.20161	0.036905	0.005045	0.026373	0.137697	0.575708
ASV34	0.004335	0.023337	0.002345	0.000361	0.009165	0.002176	0.958281
ASV648	5.84E-09	0.045535	0.004146	0.00041	9.23E-09	0.011512	0.938396
ASV157	0.007156	0.002067	0.006769	0.000358	0.00616	0.002126	0.975363
ASV566	0	0.017155	0.012929	0.000794	9.60E-05	0.029322	0.939703
ASV409	0.001003	0.092971	0.038872	0.00052	0.026295	0.003375	0.836964
ASV232	0.014858	0.028151	0.026352	0.003173	0.01491	0.027555	0.885
ASV625	0.015285	0.088547	0.005157	0.000873	0.012219	0.037293	0.840626
ASV165	0.008307	0.091319	0.010897	0.00379	0.007025	0.119624	0.759038
ASV45	0.016837	0.157075	0.007967	0.004353	0.002235	0.085343	0.72619
ASV183	0.011714	0	0.000298	4.55E-05	0.00102	0.00069	0.986232
ASV111	0.0136	0.324797	0.152257	0.000401	0.001718	0.000553	0.506674
ASV220	0.00219	0.002815	0.001667	0.001122	0.006442	0.010106	0.975658
ASV372	1.44E-10	0.022707	0.007266	2.11E-05	0.001669	0.008257	0.96008
ASV458	0.006459	0	0.001823	0.006646	0.021769	0.007527	0.955776
ASV415	0.003366	0.002943	7.46E-05	1.26E-06	3.78E-05	0.007168	0.98641
ASV197	0	0	0.033321	0.001295	0.000437	0.001855	0.963092
ASV151	0.006495	0.153425	0.006898	0.001983	0.017317	0.029963	0.783918
ASV459	0.004616	0.058689	0.004732	6.75E-05	0.010494	0.013337	0.908064
ASV196	0.009865	0.158438	8.80E-06	0.000127	0.055486	0.050285	0.725789
ASV216	0.005188	0.087271	0.006693	3.29E-05	0.008996	0.020838	0.870981

ASV192	0.001578	0.031204	0.000956	0.000264	0.012384	0.011046	0.942568
ASV327	0.000155	0.004284	0.020676	0.001721	0.012218	0.00024	0.960705
ASV501	5.40E-11	0.006384	0.001422	7.75E-05	0.010812	0.00256	0.978745
ASV267	0.008304	0.008379	1.86E-05	0.001068	0.005094	0.005906	0.971231
ASV35	0.003559	0.176158	0.010953	0.001634	0.016959	0.019773	0.770962
ASV298	0.001709	0.012856	0.007702	0.0012	0.003249	0.003822	0.969463
ASV370	0.006432	0.135384	0.000215	0.007091	0.03444	0.151087	0.665351
ASV387	0.009772	0.076464	0.000192	0.00047	1.22E-05	0.006289	0.9068
ASV69	0.01915	0.221604	0.018408	0.001281	0.0697	0.212412	0.457445
ASV288	0.004537	0	0.002853	0.002732	0.008105	0.003318	0.978455
ASV431	0.004173	0.125813	0.00014	0.012211	0.037101	0.062596	0.757965
ASV383	0.0029	0.024143	3.57E-06	0.000363	0.014539	0.007104	0.950948
ASV510	0.004667	0.034063	0.001048	0.003317	0.004576	0.00179	0.95054
ASV8	0.013127	0.108228	0.05971	0.000113	0.004743	0.001356	0.812723
ASV473	0.01759	0.083399	0.004192	0.001075	0.040505	0.044256	0.808982
ASV524	0.004312	0.005144	0.013005	0.000947	0.003739	0.000276	0.972577
ASV176	0.000475	0.000878	0.000849	0.000375	2.45E-05	0.002198	0.995199
ASV361	0.003008	0.001994	0.005976	0.002161	0.006621	0.003924	0.976316
ASV150	0.006634	0.037439	0.00898	0.000931	0.035589	0.011695	0.898732
ASV709	0.002461	0	0.000624	0.000145	0.000336	0.017151	0.979283
ASV262	0.013364	0.172229	0.000848	0.00406	0.082999	0.150032	0.576469
ASV283	0.007421	0.074394	0.001188	0.000124	0.026355	0.054991	0.835526
ASV6	0.008614	0.354487	9.35E-05	5.69E-05	0.021884	0.019682	0.595183
ASV804	0.001423	0	0.00759	5.30E-05	0.027586	0.005133	0.958216
ASV146	0.021386	0.08362	0.008131	3.85E-05	0.035921	0.022038	0.828865
ASV486	0.003635	0.000718	0.000439	0.000342	4.10E-05	0.012979	0.981847
ASV253	0.003712	0.258135	0.015062	0.014096	0.000269	0.086785	0.621941
ASV33	0.029376	0.004303	1.29E-05	0.000986	5.58E-05	0.047507	0.91776
ASV96	0.019361	0.028578	0.000355	0.001988	0.001374	0.008088	0.940255
ASV64	0.004831	0.032772	0.023558	0.000359	0.001662	0.002828	0.93399
ASV120	0.004432	0.271004	0.013962	1.51E-05	0.005947	0.075361	0.62928
ASV435	0.020912	0.025655	7.00E-06	5.90E-05	0.009048	0.006711	0.937609
ASV480	0	0	0.00172	2.09E-05	0.004543	0.006151	0.987565
ASV671	0.004295	0	0.013046	0.01356	0.000797	0.005369	0.962933
ASV207	0.009965	0.012933	0.018771	8.85E-05	0.008134	0.014345	0.935764
ASV1519	0.048315	0.103928	0.000467	0.000188	0.025196	0.028323	0.793583
ASV193	9.64E-17	0.106578	0.010334	0.006811	0.018231	0.036094	0.821952
ASV557	0.001711	0.023825	0.003939	0.001306	0.030997	0.000462	0.93776
ASV50	0.02733	0.182466	0.011702	0.000793	0.000421	0.029896	0.747391
ASV89	0.007953	0.332926	0.191255	1.56E-05	0.001119	0.018666	0.448065
ASV11	0.003891	0.01747	0.011031	0.00109	0.044375	0.09834	0.823803

ASV359	0.017585	0.085973	0.018127	9.38E-05	0.00024	0.00871	0.869272
ASV513	0.007735	0	4.51E-05	0.000475	0.000769	0.000656	0.99032
ASV908	0.003182	1.46E-13	0.002345	0.000243	0.003364	0.037773	0.953093
ASV58	0.00228	0.089264	0.012523	0.004172	0.020347	0.011827	0.859587
ASV195	0.008429	0.065177	0.020234	0.000104	1.50E-05	0.004272	0.901769
ASV537	4.66E-16	0.094481	0.00075	2.46E-05	0.008927	0.023067	0.87275
ASV223	0.008771	0.168172	0.025638	1.77E-05	0.046638	0.100611	0.650152
ASV586	0.014991	0	0.000216	0.001156	0.003459	0.000267	0.979912
ASV63	0.01987	0.022666	0.001064	2.18E-05	0.002626	5.20E-05	0.9537
ASV717	0.001459	0.005623	0.00821	0.000123	0.021105	0.01608	0.9474
ASV392	0.016003	0.030877	0.027787	8.34E-05	0.033184	0.006388	0.885677
ASV300	0.01465	0.006116	0.002198	0.001483	0.000935	0.000508	0.974111
ASV328	0.006795	1.53E-12	5.38E-05	0.002848	0.009161	0.002423	0.978719
ASV115	0	0.260853	0.109083	0.000173	0.008669	0.013324	0.607899
ASV171	9.24E-11	0.104805	0.020803	0.001816	5.42E-06	0.00132	0.87125
ASV454	0.003186	0.203548	5.58E-06	0.003051	0.121459	0.06759	0.60116
ASV46	0.005656	0.16416	0.011894	0.000115	0.009499	0.009752	0.798924
ASV735	6.60E-16	0.145719	0.010476	8.33E-05	0.064185	0.103961	0.675576
ASV326	0.000233	0	0.004717	0.003975	0.0009	0.001431	0.988743
ASV39	0	0.053129	0.047261	0.007646	0.009245	0.015383	0.867335
ASV148	0.007385	0.01276	0.002226	4.58E-05	0.002405	0.000289	0.974889
ASV621	0.002657	0.047073	0.000781	0.00347	0.001281	0.000249	0.94449
ASV85	3.13E-12	0.127244	0.018485	2.18E-05	0.006641	0.003582	0.844026
ASV353	0.008026	0.196546	0.155272	0.001068	0.016288	0.025351	0.597451
ASV620	4.47E-14	0.004699	0.000555	0.000257	0.005601	0.000313	0.988575
ASV86	0.005729	0.202606	0.111034	0.000262	0.004588	0.013451	0.662329
ASV186	0.003543	0.098251	0.026508	0.002163	0.017367	0.063479	0.788688
ASV112	0.020311	0.187651	0.162958	0.001548	0.026321	0.00209	0.59912
ASV416	1.48E-08	0.051994	0.002653	0.004771	0.005107	1.12E-05	0.935464
ASV12	0.006674	0.094171	0.032766	0.009998	0.009239	0.070501	0.776651
ASV133	0.00968	0.065317	0.036891	5.19E-05	0.087502	0.025017	0.775542
ASV710	3.50E-14	0.024268	0.004032	8.19E-06	0.008179	0.0005	0.963013
ASV344	0.003565	0	0.00635	8.83E-07	0.000318	0.000723	0.989043
ASV137	0.001188	0.003008	0.023628	0.00018	0.000499	0.000589	0.970907
ASV147	0.005065	0.039868	0.023705	3.64E-06	2.46E-06	0.003081	0.928275
ASV13	0.012011	0.236633	0.105158	0.000148	0.000236	0.031046	0.614768
ASV168	1.84E-13	0.128721	0.010359	0.001155	0.012658	0.00522	0.841886
ASV303	0.002926	4.85E-14	0.003791	0.000173	0.005784	0.002301	0.985025
ASV541	0.004116	0	3.81E-05	2.80E-06	0.002583	0.004734	0.988526
ASV42	1.89E-06	0.056104	0.008559	0.000365	0.008243	0.012721	0.914005
ASV31	0.011253	0.094502	0.16887	0.000187	0.000223	2.01E-05	0.724945

ASV743	0.026504	0	0.001657	0.000159	0.000628	0.001124	0.969929
ASV693	0.003752	0.048893	0.014884	0.001686	0.004518	0.000308	0.925958
ASV49	0.013913	0.134132	0.001555	1.53E-05	0.012066	0.00026	0.838059
ASV375	0.015787	0.017005	0.000897	1.41E-05	0.037573	0.031867	0.896857
ASV281	0	0.011512	0.00954	0.003327	0.001927	0.003344	0.97035
ASV508	0.00097	0.018296	0.015559	0.001313	0.023257	0.000952	0.939653
ASV605	3.49E-14	0.10353	0.01462	0.0127	0.000817	0.006691	0.861642
ASV526	8.71E-09	0.107294	0.045178	0.003436	0.00695	0.042321	0.794821
ASV378	0.005633	0.007119	0.010973	0.000212	0.003106	0.001315	0.971641
ASV68	0.020497	0.203388	0.019062	0.002412	0.078233	0.132119	0.544289
ASV744	0.007468	0.059067	0.000434	8.25E-05	0.002878	0.002105	0.927965
ASV434	0.01664	0.00772	0.000895	1.29E-06	0.004728	0.015185	0.954831
ASV131	0.020644	0.128472	0.000184	0.010332	0.048149	0.08328	0.708938
ASV547	0.002859	0	0.007782	0.001152	0.000269	0.000887	0.987052
ASV535	0	0.016599	0.000976	5.37E-05	0.004556	0.023517	0.954299
ASV159	0.0078	0.029459	0.01245	8.93E-05	0.029607	0.024698	0.895897
ASV742	0.0048	1.08E-16	0.000574	0.004062	0.002243	2.67E-08	0.988321
ASV202	0.001216	0.125268	0.048907	0.002857	0.035435	0.001484	0.784833
ASV747	1.43E-17	0.009866	0.014242	0.001494	0.003568	0.023611	0.947218
ASV188	0.016579	0.02218	0.01297	3.86E-05	0.026556	0.014391	0.907286
ASV396	0.000906	0.03971	0.052471	2.73E-05	0.058736	0.003773	0.844376
ASV114	1.44E-19	0.052423	0.017891	0.000792	0.015697	1.09E-08	0.913197
ASV225	0.009566	0.004001	0.008306	0.001041	0.010796	0.022347	0.943944
ASV428	1.37E-11	0.008363	0.00432	0.001921	0.000917	0.002419	0.982059
ASV134	0.007612	0.023084	0.000349	0.000758	0.011284	0.005356	0.951557
ASV576	0.007034	0.007981	0.012896	0.00179	0.037143	0.001778	0.931377
ASV59	0.016059	0.133285	0.010898	0.001196	0.093187	0.018897	0.726477
ASV301	0.011139	0.075518	4.34E-06	0.001229	0.017012	0.029974	0.865123
ASV66	0.016567	0.034835	0.018233	0.000747	0.032684	0.089044	0.807891
ASV374	0	0.095656	0.013427	0.000312	4.42E-05	0.023829	0.866732
ASV449	2.89E-18	0	6.05E-06	0.001122	0.012036	0.0017	0.985135
ASV329	0	0.057216	0.05912	1.32E-05	0.004722	0.021095	0.857834
ASV660	0	0	0.000131	0.003888	0.005485	0.001598	0.988898
ASV465	0.008168	2.73E-12	6.81E-05	0.000381	0.002031	0.010416	0.978936
ASV504	0.01605	4.35E-15	0.004787	0.003056	4.84E-05	0.010966	0.965093
ASV76	0.005607	0.103029	0.007715	0.003506	0.010491	0.057607	0.812045
ASV323	0.003287	0.104208	0.016098	7.46E-06	0.049731	0.050139	0.77653
ASV167	9.44E-10	0.001502	0.004236	0.004762	0.001102	0.005591	0.982807
ASV158	0.009348	0.048555	0.019341	0.001497	0.018954	0.025676	0.876629
ASV271	0.003695	0.007432	0.028459	0.003417	0.003843	0.002125	0.951028
ASV350	0.008118	8.51E-17	0.000112	0.000849	0.010451	0.014089	0.966381

ASV229	0.006356	0.074441	0.000345	0.001886	0.02217	0.071226	0.823575
ASV724	0.000669	0.01732	0.001679	0.000479	0.002944	0.02027	0.956637
ASV145	8.13E-12	0.00591	0.004196	0.001968	0.035596	0.017801	0.934529
ASV731	0.010051	0.130985	0.002476	0.000296	0.000197	0.020491	0.835504
ASV635	0.002669	0	0.000728	0.000218	1.47E-05	0.003646	0.992724
ASV185	1.94E-11	0.005482	0.00126	4.85E-09	0.009746	0.004692	0.97882
ASV44	0.044532	0.005729	0.013348	3.01E-05	0.020558	0.028172	0.88763
ASV107	0.013125	0.055744	0.018919	0.000802	0.002555	0.054565	0.854291
ASV637	0.001742	0	3.37E-05	3.34E-05	0.000819	0.005712	0.99166
ASV254	0.01053	0.030655	0.000808	2.72E-05	0.031359	0.002637	0.923984
ASV67	0.006013	0.056523	0.01467	0.000133	0.001678	0.016273	0.904709
ASV496	0.004374	0	0.000293	0.000101	0.000557	0.000212	0.994461
ASV844	0.011213	0.008464	0.002418	0.008243	0.000256	0.013843	0.955563
ASV755	0.022837	0.02184	0.001343	0.000215	0.028862	0.049185	0.875719
ASV135	0.012926	0.094008	0.17086	0.00633	0.001357	0.077948	0.636571
ASV4	5.39E-14	0.216786	0.012864	0.00174	0.00588	0.009702	0.753028
ASV94	0.003297	0.117304	0.002882	0.00049	2.25E-05	0.009789	0.866215
ASV362	0.008908	0	0.000831	0.000403	0.004974	0.01839	0.966495
ASV161	0.007217	0.230501	0.064187	0.000869	0.000332	0.055487	0.641407
ASV570	0.004987	0	0.007525	0.001898	0.006569	0.002251	0.97677
ASV18	0.020632	0.27297	0.005428	0.001671	0.068096	0.034767	0.596435
ASV155	2.08E-11	0.085452	0.043198	0.001955	0.007184	0.016493	0.845718
ASV141	0.016131	0.055762	4.91E-05	0.000166	0.004558	0.004013	0.91932
ASV779	0.003867	0.027508	0.00698	0.009527	0.015044	0.00203	0.935045
ASV376	0.007067	0.025918	6.28E-05	6.89E-06	0.035317	0.042396	0.889233
ASV306	0.001421	0.020529	0.004836	0.003533	0.001916	0.00256	0.965205
ASV169	1.46E-15	0.091349	0.002478	1.03E-05	0.003893	0.016294	0.885975
ASV664	0.007533	0.046768	0.000383	0.000587	0.032221	0.050655	0.861852
ASV75	0.008822	0.029569	0.04672	0.002226	0.075268	0.036459	0.800936
ASV239	0.008155	0	0.001996	0.001527	0.006154	0.003221	0.978946
ASV238	3.18E-12	0.017987	0.001538	1.07E-05	0.002268	0.026558	0.951637
ASV272	0.003596	0.071389	1.74E-05	0.010326	0.010714	0.061014	0.842942
ASV351	0.034115	0.056799	0.000282	0.000154	0.041525	0.069366	0.797758
ASV174	0.011138	0.091387	0.00893	0.008905	2.05E-05	0.098505	0.781116
ASV379	0.019292	0.024481	0.016135	0.00057	0.004745	0.012843	0.921933
ASV555	0.009714	0.022997	0.00955	0.001486	0.018532	0.002163	0.935559
ASV493	0.006535	0	0.008414	0.000161	0.000674	9.84E-05	0.984118
ASV871	0.003295	0.013412	0.001325	0.002558	0.000736	0.024485	0.954189
ASV531	1.11E-12	0.041346	0.004882	0.010119	0.001869	0.001757	0.940027
ASV331	0.001808	0.038016	0.00188	0.000406	0.007565	0.007365	0.94296
ASV194	0.015084	0.006949	0.001442	0.000171	0.014664	0.02294	0.93875

ASV707	0.002289	0.018766	0.001076	0.001008	0.001655	0.020587	0.954619
ASV156	0.01183	0.167454	0.00335	0.011996	0.016734	0.035608	0.753027
ASV143	0.004612	0.036447	0.000525	3.45E-06	0.000207	0.004776	0.953429
ASV226	0.001042	0.016017	0.030184	0.00344	0.011159	0.001584	0.936575
ASV474	0.001262	0.026984	0.027703	2.90E-06	0.00161	0.008595	0.933844
ASV737	0.006346	0.032177	0.028256	0.000825	0.00548	0.003943	0.922973
ASV718	1.85E-10	0.015382	0.00051	0.001225	3.19E-05	7.17E-05	0.98278
ASV865	0.002575	0.001516	3.81E-06	0.004154	0.005772	0.03567	0.950309
ASV443	1.73E-11	0.005961	1.80E-05	2.24E-06	0.001922	0.014042	0.978054
ASV218	8.29E-10	0.087968	0.043965	0.001655	0.033021	0.028204	0.805186
ASV577	0.001514	0.005989	0.001239	5.81E-06	0.011312	0.019903	0.960036
ASV820	0.000609	4.22E-05	0.002883	0.000626	0.011929	0.005719	0.978192
ASV530	0.006384	0.004921	0.000785	0.000327	0.014785	0.011033	0.961765
ASV411	0.009813	0.019221	0.009031	0.001685	0.000117	0.000165	0.959967
ASV358	0.02542	1.31E-17	4.71E-07	0.001866	0.013849	0.001949	0.956915
ASV463	0.000701	0	0.001566	0.000295	0.000401	0.004502	0.992534
ASV483	0.007376	0	0.019503	0.002828	9.47E-05	0.02467	0.945528
ASV15	0.019599	0.137151	0.016702	3.46E-05	0.000654	0.007589	0.818271
ASV260	0.001366	1.54E-13	0.014467	0.000245	0.006736	0.007757	0.969429
ASV313	0.012981	0.083861	0.000511	0.004393	0.006722	0.096259	0.795275
ASV663	0.016685	0.018827	0.004799	0.002678	0.014712	0.001351	0.940949
ASV669	0.004949	0	0.001931	0.001185	0.016438	0.015999	0.959498
ASV516	0	0	9.19E-05	0.000154	0.003652	0.04179	0.954312
ASV588	0.009808	0.001672	0.003183	0.000629	6.73E-06	0.011072	0.973629
ASV25	0.000521	0.04065	0.002654	0.00157	0.063273	0.060739	0.830593
ASV725	0.001421	0	0.00019	0.003256	0.011721	0.016787	0.966626
ASV398	0.000789	0.120792	0.000787	7.83E-05	0.045285	0.025353	0.806915
ASV682	0.008415	0.019252	7.89E-05	0.000884	0.023298	0.01213	0.935943
ASV499	0.00428	0.015217	0.0035	0.001122	0.004276	0.020984	0.950621
ASV72	0.01194	0.073258	0.025875	0.001384	0.01197	0.003428	0.872145
ASV427	0.006772	0	0.000693	0.014914	0.037415	0.050788	0.889419
ASV565	0.010225	0.023872	0.064747	0.002652	0.025002	0.002936	0.870564
ASV602	0	0	9.00E-05	0.002379	0.003028	0.006589	0.987914
ASV244	0.003824	0.009448	0.00277	0.001083	0.001346	0.017169	0.96436
ASV354	0.005637	0.047153	0.130118	4.08E-06	0.035023	0.010263	0.771801
ASV849	0	0.03614	0.029922	0.000482	0.000899	0.051553	0.881005
ASV1025	0.015106	0	0.002319	6.96E-05	0.002436	0.011718	0.968352
ASV399	6.69E-11	0.005519	0.00402	0.008009	0.003636	0.015456	0.96336
ASV70	0.00835	0.003072	0.003393	0.000248	0.00094	0.000147	0.983851
ASV81	0.009008	0.174047	0.002447	9.30E-05	0.039815	0.000483	0.774107
ASV95	0.008392	0.068107	5.37E-06	0.003894	0.016693	0.1017	0.801209

ASV394	0.009457	0.091665	1.06E-05	0.008156	0.005393	0.010585	0.874733
ASV613	9.09E-22	0.002498	0.016911	0.001537	0.000148	0.00707	0.971837
ASV217	0.011983	0.071328	0.008174	1.02E-05	0.00965	0.022506	0.876348
ASV436	0.003577	9.08E-18	0.008827	0.000985	0.008098	0.015822	0.962691
ASV101	0.004259	0	0.017476	0.00011	0.002134	0.02228	0.953741
ASV241	0.001964	0.001883	0.012887	8.73E-06	0.005956	0.001205	0.976096
ASV450	4.00E-19	0.003991	0.004042	0.006468	0.000262	0.001039	0.984199
ASV163	0.003645	0.182332	0.114385	8.55E-05	0.023688	0.000597	0.675267
ASV564	9.18E-20	0.015662	0.010461	0.000201	0.005871	0.000505	0.9673
ASV616	4.50E-11	0.041199	0.000361	7.00E-06	0.001356	0.000245	0.956832
ASV603	0.009283	0.017176	0.002055	0.000194	0.008345	0.046615	0.916332
ASV263	0.015059	0.083815	0.000892	0.004295	0.015013	0.036466	0.84446
ASV446	0.002783	0.011359	0.033533	0.005496	2.05E-05	0.004945	0.941863
ASV691	0.017668	6.00E-18	0.000249	3.17E-06	0.00174	0.004553	0.975786
ASV23	0.023213	0.123419	0.107307	0.001379	0.004383	0.04177	0.69853
ASV139	0.000882	0.035296	0.039191	1.28E-05	0.019371	0.000692	0.904554
ASV381	0.015455	0.003459	0.001339	0.000712	0.044163	0.020281	0.914591
ASV62	0.009691	0.074288	0.00302	1.57E-05	0.007819	0.002913	0.902253
ASV456	0	0.02047	2.04E-06	0.000526	0.002723	0.009307	0.966973
ASV533	0.007133	0.077238	0.006854	0.000727	0.014216	0.000802	0.89303
ASV41	0.028404	0.23983	0.184013	0.000141	1.91E-05	0.000616	0.546977
ASV334	0.025605	0.000592	0.03858	9.58E-05	0.003153	0.009447	0.922528
ASV99	0.010874	0.027301	7.97E-05	0.001223	0.008764	0.006794	0.944964
ASV152	0.005004	0.119173	0.01981	0.003523	0.000797	0.116238	0.735455
ASV118	9.91E-12	0.058246	0.001991	0.009735	0.004092	0.035773	0.890162
ASV160	0.027156	0.208215	0.001069	0.001637	0.058082	0.172291	0.53155
ASV177	0.00329	0.046494	0.002331	0.000346	7.71E-05	2.97E-05	0.947432
ASV528	0	0	0.004698	0.00011	0.001045	0.001139	0.993008
ASV594	0.002546	0.000659	0.003262	0.000985	0.001681	0.008261	0.982606
ASV38	0.006579	0.006866	0.001848	0.00199	0.019633	0.005952	0.957132
ASV256	0.000966	0.089912	0.02854	0.005707	0.003067	9.83E-05	0.87171
ASV142	0.004877	0.050428	0.010742	8.30E-05	0.00867	0.04495	0.88025
ASV205	0.005073	0.017732	0.015798	0.000139	0.022032	0.013295	0.925931
ASV713	2.00E-12	0.018986	0.000272	0.001774	0.008856	0.004146	0.965966
ASV128	0.010004	0.130183	0.151484	0.000321	0.001921	0.027922	0.678166
ASV240	0.007544	0	0.000196	0.000567	0.004632	0.001062	0.985999
ASV626	0.019641	0.038421	0.004771	0.002183	0.052003	0.00272	0.880262
ASV98	0.001971	0.012707	0.045527	0.005555	0.005203	3.17E-06	0.929033
ASV321	0.002865	0.015825	0.004451	0.008446	0.019308	0.001654	0.94745
ASV335	0.009246	0.17019	0.001611	0.004912	0.009899	0.034819	0.769323
ASV567	0.000889	0	0.013112	0.005657	0.000813	5.08E-05	0.979478

ASV423	0.023753	1.23E-21	0.000307	0.000899	0.002169	0.00167	0.971202
ASV294	0.00204	0.14284	0.023243	0.004325	0.010199	0.083845	0.733509
ASV51	0.01116	0.022001	3.40E-05	3.31E-06	0.000195	0.063237	0.903369
ASV215	0.007486	0.072982	0.012036	9.12E-06	0.035727	0.028988	0.842771
ASV452	0.005868	0.001997	0.021278	0.000168	0.021509	0.000466	0.948713
ASV348	0.001984	0	0.006371	0.004405	0.006664	0.000114	0.980462
ASV610	0.009811	8.28E-13	0.001766	2.37E-05	0.001567	3.97E-05	0.986792
ASV22	0.017449	0.007693	0.068547	0.001078	0.044148	0.018171	0.842915
ASV601	0	0	9.00E-05	0.000904	0.002549	0.014557	0.981901
ASV429	0.007161	2.93E-11	0.0027	0.005109	0.002696	0.001595	0.980739
ASV104	0.003023	0.033896	0.029345	0.004768	0.001183	0.004491	0.923294
ASV179	0.004799	0	0.001209	0.004931	0.002592	0.000602	0.985867
ASV532	0.003261	0	0.000321	0.00042	0.000161	0.000529	0.995307

Table A3.6: Fungal variance partitioning results.

	Block	locyr	pH	Nitrate	OM	K	Residuals
ASV34	0.003056	0.378369	0.000558	0.008144	0.000207	0.108334	0.501332
ASV97	4.60E-11	0.243999	0.000519	0.048535	0.004778	0.054545	0.647625
ASV188	0.00687	0.555964	0.003677	4.46E-05	0.001814	0.00725	0.42438
ASV190	6.57E-15	0.692481	0.05529	0.000147	0.010311	0.001235	0.240537
ASV306	0.049215	0.112315	0.005519	1.36E-07	0.02879	0.000513	0.803647
ASV334	0.001036	0.918552	0.00015	0.000195	0.002213	2.46E-05	0.077829
ASV352	0.028923	0.413152	0.053478	0.000744	0.138363	0.03544	0.329902
ASV388	0.016113	0.282485	0.001766	0.000538	0.006578	0.031302	0.661218
ASV424	0.014267	0.514262	0.001056	0.000184	0.108755	0.092893	0.268583
ASV442	0.03799	0.348396	0.003993	0.006944	0.086271	0.000775	0.515631
ASV454	0.004072	0.770912	0.006722	0.001379	0.024609	0.004688	0.187618
ASV463	0.003367	0.022293	0.004508	0.003507	0.01755	0.066946	0.881828
ASV494	0.00167	0.07254	0.000196	0.003787	0.00717	0.002473	0.912163
ASV512	0.014952	0.04835	0.001403	0.000519	0.004741	0.04416	0.885875
ASV515	0.007258	0.664384	0.007421	0.000241	0.041561	0.034277	0.244857
ASV522	1.14E-13	0.291923	0.00037	0.000344	0.005019	0.031935	0.670409
ASV527	0	0.195988	0.053605	0.00192	0.037218	0.024536	0.686734
ASV535	0.001362	0.768064	0.000495	0.000104	0.003894	5.24E-05	0.226029
ASV560	0.007754	0.178992	0.000109	0.000538	0.029275	0.016326	0.767005
ASV564	0.004465	0.866372	0.005856	2.33E-06	0.000701	0.002195	0.120407
ASV582	0.007579	0.389612	0.008335	0.008815	0.041852	0.018166	0.525641
ASV617	0.025026	0.499466	0.006911	3.79E-05	0.056783	0.003029	0.408746
ASV620	0.00285	0.784761	3.65E-06	0.003836	0.004772	0.001449	0.202329
ASV633	0.002122	0.866282	0.018402	0.000301	0.006964	0.005408	0.100521
ASV653	0.000243	0.865966	0.02251	1.14E-05	0.008461	0.009717	0.093091
ASV661	8.11E-17	0.177855	0.001132	0.001939	0.075961	0.001168	0.741945
ASV696	0.015539	0.577136	0.067803	0.004466	0.002555	0.001711	0.330791
ASV707	0.009262	0.55369	0.000875	0.000621	0.004538	0.012449	0.418564
ASV762	0.002326	0.897147	0.003469	0.000117	0.00046	0.001432	0.095049
ASV766	6.32E-11	0.017391	0.014648	0.001568	0.117414	0.001647	0.847332
ASV817	0.001988	0.000964	0.000867	0.00153	0.073951	0.016036	0.904664
ASV819	0	0.317645	0.003094	0.000191	0.027712	0.000834	0.650524
ASV841	0.033614	0.331267	0.015007	0.000324	0.153436	0.008165	0.458187
ASV843	4.13E-11	0.535683	0.000253	0.005837	0.017003	0.005459	0.435766
ASV856	0.100172	0.01913	0.065957	0.012886	0.084495	0.024783	0.692577
ASV876	0.001422	0.607461	0.004248	0.000401	0.054645	1.26E-07	0.331823
ASV904	0.000271	0.940265	0.000504	0.000114	0.00665	0.000918	0.051279
ASV998	0.015189	0.404409	7.43E-05	0.00162	0.03792	0.051373	0.489414
ASV1003	0.009113	0.401853	0.323057	0.004413	0.026808	0.049821	0.184935

ASV1014	0.005434	0.174031	0.024759	0.003187	0.061167	0.005449	0.725974
ASV1023	0.00355	0.691915	0.000147	0.001363	0.002645	0.000365	0.300015
ASV1083	0.028409	0.393155	0.00139	4.52E-05	0.084942	0.003564	0.488495
ASV1113	0	0.065634	0.008907	0.000111	0.055234	0.006293	0.86382
ASV1115	0.014492	0.205267	0.049899	7.28E-05	0.120236	1.16E-05	0.610022
ASV1122	0.008344	0.261646	0.009971	0.004326	0.004999	0.023156	0.687558
ASV1128	6.53E-11	0.048535	0.000859	0.00827	0.000505	0.005249	0.936582
ASV1214	0.000581	0.205162	0.000377	0.000792	0.000624	0.02092	0.771544
ASV1262	0.005218	0.490375	0.004846	0.01117	0.028124	0.01664	0.443627
ASV1305	0.002214	0.750233	0.00028	0.001298	0.001744	0.006718	0.237514
ASV1332	0.011234	0.254936	0.009101	0.001164	0.02437	0.1255	0.573696
ASV1333	0.04563	0.341087	0.208088	0.000367	0.087803	0.000282	0.316743
ASV1364	0.002016	0.645484	0.022635	0.000247	0.003107	0.000691	0.32582
ASV1369	0.02452	0.866556	0.005987	0.006025	0.000236	0.000304	0.096372
ASV1370	0.012926	0.328601	0.001652	0.010932	0.020818	0.033883	0.591187
ASV1421	0.005098	0.609938	0.025649	0.001426	0.026914	0.003538	0.327437
ASV1423	0.00899	0.217643	0.008688	2.91E-05	0.005957	0.022371	0.736321
ASV1443	4.11E-14	0.150076	0.00015	0.000883	0.057132	0.007782	0.783977
ASV1455	0	0.212997	0.003736	0.007886	0.01399	0.002111	0.75928
ASV1456	0.041758	0.300914	0.045604	0.003141	0.02805	0.006797	0.573736
ASV1470	0.012746	0.140634	0.017602	0.002093	0.410714	0.001082	0.415128
ASV1531	0.028023	0.217257	0.209446	0.001447	0.100695	0.00115	0.441981
ASV1538	0.010906	0.245923	0.003228	0.004779	8.04E-05	0.022612	0.712471
ASV1581	0.008357	0.205289	0.018008	0.001602	0.002644	0.022912	0.741187
ASV1582	0.007594	0.699	0.031545	4.69E-05	0.007942	8.93E-05	0.253783
ASV1623	0.005823	0.59632	0.000281	0.001695	2.75E-06	0.015661	0.380218
ASV1677	0.015718	0.550107	0.000899	0.001313	0.00748	6.99E-06	0.424475
ASV1697	1.85E-10	0.045427	0.000592	0.017687	7.58E-06	0.040533	0.895754
ASV1718	0.00719	0.88508	0.023569	0.000178	1.21E-07	0.001534	0.082449
ASV1738	0.005411	0.229016	0.003483	9.14E-07	0.125652	0.000155	0.636281
ASV1764	0.027385	0.474285	0.16262	0.001947	0.060702	0.086237	0.186824
ASV1781	2.82E-16	0.575356	0.000605	0.000988	0.000994	0.030071	0.391986
ASV1785	0.000591	0.969066	1.05E-06	7.39E-08	0.002054	0.003778	0.02451
ASV1811	0.002729	0.588247	0.002772	0.002548	0.015428	0.002673	0.385604
ASV1861	0	0.652258	0.061751	0.001672	0.052739	0.00094	0.230639
ASV1884	0.007315	0.477945	0.003311	0.000506	0.089486	0.000478	0.420959
ASV1911	0.019986	0.323581	0.001232	0.000661	0.014862	0.009423	0.630256
ASV1947	0.021509	0.408485	0.016334	0.001302	0.00094	0.001232	0.550197
ASV1961	0.005114	0.686678	0.003873	0.001335	0.000761	0.001739	0.3005
ASV2002	0.04153	0.225357	0.112825	0.000368	0.002409	0.004329	0.613181
ASV2009	0.01046	0.233205	0.007072	0.000706	0.039961	0.014407	0.694189

ASV2010	0.052323	0.54842	0.046094	0.000105	0.066116	0.010981	0.275962
ASV2017	0.001112	0.79168	0.000207	0.000761	0.000497	5.14E-05	0.205691
ASV2036	0.003352	0.573548	0.232613	0.001764	0.003955	0.034659	0.150109
ASV2154	0.022832	0.293883	0.058137	0.002961	0.084954	0.050565	0.486667
ASV2173	0.009212	0.549654	0.033719	0.000133	0.021342	6.55E-05	0.385875
ASV2225	0.002094	0.778543	0.00383	3.71E-07	0.04785	0.001979	0.165705
ASV2237	0.013321	0.330251	0.000783	0.006376	0.057156	0.047942	0.544171
ASV2253	6.17E-09	0.371113	0.003416	0.000346	0.037742	2.28E-05	0.58736
ASV2262	0.009358	0.074396	0.003014	0.000376	0.002377	0.050521	0.859959
ASV2264	0.002337	0.318832	0.015677	0.001657	0.098382	0.007772	0.555342
ASV2267	0.000825	0.957688	0.000251	0.000276	0.001106	1.14E-05	0.039842
ASV2303	0.005275	0.1887	0.063359	0.000138	0.063992	0.039359	0.639178
ASV2307	0.038972	0.461194	0.099613	0.000993	0.085136	0.008226	0.305865
ASV2308	0.006636	0.343404	0.000576	0.000189	0.026445	0.009592	0.61316
ASV2310	0.007413	0.594381	0.004233	0.004504	0.000684	0.008281	0.380505
ASV2345	0.028707	0.066466	0.017699	0.001145	0.050756	0.027019	0.808209
ASV2346	0.006131	0.188144	0.004182	0.002428	0.000139	0.035543	0.763432
ASV2359	0.022626	0.480404	0.31131	4.16E-05	0.070509	0.003214	0.111896
ASV2385	0.002735	0.681759	0.002251	0.000188	0.001495	9.13E-05	0.31148
ASV2403	0.004556	0.617343	0.005602	0.001329	0.074167	0.003975	0.293029
ASV2420	0	0.695593	0.001731	0.003364	0.001726	0.003678	0.293907
ASV2437	0.006293	0.908088	0.000578	0.000193	0.005029	0.003118	0.0767
ASV2467	0.001897	0.209283	0.001615	0.000298	0.017069	0.006926	0.762912
ASV2493	0.054964	0.509478	0.032232	0.001487	0.068554	0.00183	0.331455
ASV2522	0.004432	0.652402	0.000516	7.24E-05	0.001917	6.64E-08	0.34066
ASV2546	0.018949	0.460312	0.000906	0.002788	0.000102	0.001925	0.51502
ASV2552	0.000127	0.212195	0.000731	2.02E-05	0.002873	0.033894	0.75016
ASV2554	0.007961	0.398876	0.006182	0.004654	0.03751	0.080006	0.464811
ASV2555	0	0.023623	0.015864	0.000738	0.086085	0.010853	0.862838
ASV2564	8.46E-11	0.325037	0.003407	2.26E-05	0.080071	8.50E-05	0.591377
ASV2566	0.000916	0.941211	0.006634	0.000103	0.001009	0.000283	0.049844
ASV2625	0.009276	0.75092	0.000531	4.31E-06	0.0024	0.001071	0.235798
ASV2629	0	0.937285	0.00015	0.000176	0.001728	7.83E-06	0.060653
ASV2630	0.015116	0.036207	0.015216	0.000553	0.002497	0.028828	0.901582
ASV2642	0.005917	0.110348	0.015158	0.008747	0.201813	0.00171	0.656307
ASV2644	0.004575	0.529106	0.002216	0.003434	0.032806	0.000403	0.42746
ASV2777	0.00822	0.433083	0.033051	0.00121	0.000782	0.002966	0.520687
ASV2793	0.007652	0.265803	0.005409	0.00124	0.018952	0.026772	0.674173
ASV2817	0.010894	0.745449	0.027157	0.00043	0.001979	0.003248	0.210843
ASV2827	8.04E-13	0.318621	0.000452	0.000987	0.065639	0.026092	0.588209
ASV2857	0.008167	0.376434	0.001448	4.92E-06	0.00912	0.004475	0.600351

ASV2893	0.003721	0.648915	0.001104	0.000244	0.010092	0.002626	0.333299
ASV2946	0.002249	0.370423	0.005774	0.000281	0.018882	0.005346	0.597045
ASV2981	5.21E-13	0.094382	0.000717	0.000318	0.008986	0.004153	0.891444
ASV3002	0	0.492704	0.000145	0.002024	0.023159	0.007881	0.474087
ASV3005	9.89E-17	0.711479	0.001907	0.000708	0.032864	0.047326	0.205716
ASV3026	0.060972	0.252662	0.065085	0.004818	0.001785	0.015889	0.598788
ASV3029	0.015269	0.583287	0.005571	0.00058	3.12E-05	0.000778	0.394485
ASV3042	0.004556	0.696777	0.004609	0.000127	0.006527	0.002988	0.284416
ASV3075	0.011675	0.093888	0.116683	0.000923	0.115629	0.010845	0.650357
ASV3092	4.10E-17	0.029475	0.106825	0.015517	0.156051	0.028955	0.663178
ASV3114	0.03109	0.265265	0.289789	1.23E-05	0.022779	0.000475	0.39059
ASV3131	0.005249	0.3925	0.000493	0.001542	0.000124	0.099864	0.500228
ASV3133	0.030393	0.194998	6.69E-06	7.78E-06	6.03E-05	0.040585	0.73395
ASV3164	0.032886	0.20089	0.084275	0.011069	0.029052	0.026894	0.614934
ASV3203	0.009295	0.446467	0.002099	0.000159	0.004076	0.009354	0.528551
ASV3243	0.002079	0.41849	0.002414	0.000501	0.022343	0.009347	0.544826
ASV3246	0.000972	0.937918	0.003841	0.001148	0.007824	0.001293	0.047004
ASV3258	0.00073	0.152413	0.012884	0.000118	0.024227	0.000587	0.809041
ASV3273	0.023383	0.246005	0.000141	0.001733	0.006326	0.001408	0.721003
ASV3297	0.003369	0.617397	0.00097	6.44E-05	0.003315	0.003452	0.371431
ASV3331	0.040954	0.387953	0.061602	0.000911	0.001984	0.000115	0.506482
ASV3428	0.002716	0.635075	8.36E-05	0.000687	0.000639	0.001334	0.359465
ASV3445	0.024015	0.676969	0.016749	0.0077	0.049784	0.015783	0.209
ASV3461	0.023156	0.111912	0.026657	0.008364	0.098428	0.004386	0.727097
ASV3472	0.015472	0.336503	0.237718	0.007015	0.111467	0.041993	0.249832
ASV3505	9.74E-13	0.168293	3.38E-05	0.001178	0.000275	0.063872	0.766348
ASV3519	0.00125	0.754153	0.001151	6.06E-05	0.017232	0.000745	0.225409
ASV3550	0.003386	0.083575	0.006763	0.007068	0.133217	0.010095	0.755896
ASV3573	1.33E-17	0.969488	2.26E-05	5.86E-05	0.001106	0.000159	0.029165
ASV3580	0.029438	0.351795	0.016756	0.000632	0.004596	0.000186	0.596597
ASV3642	0	0.127615	4.72E-06	7.11E-05	0.000118	0.000424	0.871767
ASV3673	0.00116	0.762753	0.002302	6.98E-06	0.003206	0.000448	0.230125
ASV3686	0.030387	0.244765	0.075216	0.006376	0.015906	0.014095	0.613255
ASV3716	0.000732	0.533622	0.001448	0.000617	0.015366	2.11E-05	0.448194
ASV3740	0.002654	0.752991	0.000466	0.000281	0.002397	0.000135	0.241076
ASV3772	0.000323	0.977319	0.00012	0.000144	0.001166	0.000196	0.020732
ASV3819	0.003526	0.782042	0.087051	0.000252	0.012453	0.003864	0.110812
ASV3821	0.001131	0.049212	0.008171	3.30E-07	0.123598	0.001253	0.816635
ASV3852	0	0.930173	7.56E-05	1.53E-06	0.00297	0.000413	0.066366
ASV3876	0.012848	0.565482	0.000328	0.000229	0.008827	0.028107	0.384179
ASV3895	0.00875	0.674548	0.000509	0.000238	0.000679	0.007237	0.308039

ASV3940	0.011816	0.495832	0.000139	0.005092	0.104403	0.034763	0.347955
ASV3950	2.77E-18	0.811712	0.000397	0.00016	0.004497	9.01E-05	0.183144
ASV3955	0.008288	0.876777	0.001209	0.000112	0.011424	0.010182	0.092009
ASV3961	0.001502	0.434348	0.002463	0.007711	0.017812	0.000111	0.536053
ASV3974	0.00398	0.538144	0.000752	0.000284	0.010254	0.001918	0.444669
ASV3975	0.022147	0.35561	0.024028	0.004475	0.034365	0.095314	0.464061
ASV4031	0.006541	0.541284	0.067891	0.001967	0.038449	0.000928	0.34294
ASV4120	0.002453	0.888525	0.001834	0.000956	0.009982	0.001885	0.094364
ASV4140	0.014056	0.176954	6.72E-05	0.001959	0.009657	0.023849	0.773458
ASV4145	0.00782	0.911319	7.15E-05	0.000815	7.81E-05	0.004367	0.07553
ASV4179	0.002207	0.4214	0.088005	0.008317	0.003733	0.075243	0.401095
ASV4181	0.00645	0.346244	0.011	0.000444	0.035078	0.005502	0.595282
ASV4237	0.01597	0.204296	0.000502	0.000128	6.97E-05	0.000529	0.778505
ASV4326	1.05E-14	0.253901	0.000406	5.20E-05	0.009617	0.030144	0.70588
ASV4363	0.002897	0.354202	0.000633	0.000101	0.008014	0.006822	0.627331
ASV4374	0.011298	0.571862	0.169402	0.002585	0.034535	0.007594	0.202724
ASV4388	0.035949	0.177615	0.001204	0.006629	0.080376	0.001688	0.696538
ASV4458	0.030816	0.315929	0.003673	0.000272	0.043192	0.008362	0.597756
ASV4608	2.71E-16	0.313673	0.052405	0.000695	0.046132	0.007776	0.579319
ASV4633	0.017317	0.44709	0.314201	0.000125	0.025175	0.014232	0.181861
ASV4644	0.000105	0.260814	0.043002	0.000198	0.091989	0.002801	0.60109
ASV4660	0.002042	0.543196	0.001724	0.000152	0.090242	0.029694	0.332949
ASV4682	0.009255	0.320907	0.00863	0.001463	0.01109	8.15E-05	0.648574
ASV4789	0.010742	0.801387	0.015616	4.17E-05	0.073917	0.014489	0.083807
ASV4839	5.01E-12	0.143699	0.016585	0.000135	0.073417	0.00327	0.762894
ASV4863	0.056556	0.712157	0.014661	0.000387	0.016016	0.016361	0.183861
ASV4867	0.00887	0.279819	0.009334	0.000281	0.000464	0.000216	0.701015
ASV4882	0.000458	0.917764	0.000369	0.000583	0.005881	0.000215	0.07473
ASV4891	0.022272	0.190885	0.048436	0.000353	0.087371	0.001298	0.649384
ASV4906	0.009786	0.436589	3.51E-05	0.001157	0.012167	3.60E-05	0.54023
ASV4925	5.01E-15	0.771484	0.000183	0.000994	2.40E-05	0.000395	0.22692
ASV4986	1.92E-15	0.242451	0.01786	0.01409	0.179185	0.038445	0.507968
ASV5024	1.31E-11	0.13714	0.000142	0.000433	2.58E-09	0.004312	0.857974
ASV5053	0.010439	0.467134	0.000794	6.02E-05	0.005007	0.001908	0.514657
ASV5078	0.017517	0.372517	0.000132	0.007513	0.177661	0.036347	0.388313
ASV5093	0.011004	0.585748	0.001288	0.000259	0.002279	0.000188	0.399234
ASV5118	0.001752	0.4053	0.000674	0.000879	0.0029	0.007689	0.580807
ASV5143	0.025152	0.196387	0.053497	0.000759	0.002952	0.033933	0.687321
ASV5156	0.000764	0.796704	0.000622	0.000244	0.007628	0.003762	0.190276
ASV5215	0	0.915478	4.92E-06	4.66E-05	0.000279	7.31E-05	0.084118
ASV5235	0.009267	0.236259	0.00162	0.000956	0.000185	0.020533	0.731181

ASV5254	0.029938	0.091081	0.000682	0.007086	0.00354	0.01633	0.851344
ASV5326	0.010739	0.615716	0.000931	0.000525	0.013253	0.013566	0.34527
ASV5337	0.006363	0.561848	0.005622	1.54E-05	0.048756	0.00396	0.373435
ASV5395	2.43E-12	0.430431	5.10E-05	0.016727	0.06955	0.027261	0.455979
ASV5497	0.005233	0.415595	0.001992	0.004477	0.021937	0.001484	0.549283
ASV5533	0.005967	0.896567	0.00111	3.27E-05	0.014634	0.007587	0.074102
ASV5594	0.002093	0.756638	0.001666	9.54E-05	0.002702	0.00277	0.234036
ASV5621	0.008113	0.699957	4.93E-05	0.004264	0.00172	0.037875	0.248021
ASV5643	0.000295	0.435187	0.016103	0.000192	0.015962	0.008078	0.524183
ASV5669	0.006581	1.17E-16	2.10E-05	0.006219	4.75E-07	0.005538	0.98164
ASV5727	0	0.858375	0.000254	0.000327	0.001441	0.003801	0.135801
ASV5743	0.000459	0.969202	3.40E-05	0.000392	6.43E-05	0.000743	0.029106
ASV5754	0.00435	0.18936	0.001219	0.006638	0.013055	3.21E-06	0.785375
ASV5764	0.003593	0.502899	0.01369	0.000788	0.002176	0.002688	0.474166
ASV5887	0.002161	0.833268	0.052632	0.000245	0.001325	0.01357	0.096799
ASV5906	0.012775	0.331757	0.004131	0.000764	0.034672	0.023679	0.592221
ASV5919	0.007862	0.460306	0.011121	0.00031	0.008193	0.003729	0.508479
ASV5997	0.013466	1.28E-11	0.001071	0.000167	0.043908	0.013098	0.92829
ASV6019	0.00943	0.530268	0.000448	0.006679	0.01292	0.051822	0.388433
ASV6041	3.01E-17	0.903417	9.77E-05	5.72E-05	0.002784	0.000475	0.093169
ASV6099	0.000621	0.037131	0.000251	0.001734	0.010424	0.03038	0.919459
ASV6105	0.023538	0.355021	0.002021	0.002219	0.014754	0.009977	0.59247
ASV6128	5.34E-12	0.266437	0.002047	0.001598	0.001311	0.003112	0.725495
ASV6149	0.000806	0.787867	0.001536	7.49E-06	0.018159	3.19E-08	0.191625
ASV6200	0	0.936694	9.66E-05	0.000401	0.002904	0.000163	0.059743
ASV6211	0.004038	0.084558	0.000994	0.006296	0.021792	0.004603	0.877718
ASV6222	0.0383	0.582392	0.008522	0.001712	0.015109	0.037995	0.31597
ASV6236	0.013706	0.753648	0.001979	5.26E-07	0.031286	0.004949	0.19443
ASV6238	0.010974	0.451819	5.59E-06	0.005748	0.057428	0.055016	0.41901
ASV6350	0.013046	0.165748	0.015295	0.012134	0.257732	0.010173	0.525873
ASV6363	0.001793	0.475246	0.001824	7.38E-05	0.007825	0.160275	0.352963
ASV6479	0.023902	0.528761	0.176791	0.001534	0.097371	0.00382	0.167821
ASV6499	0.004631	0.914599	0.001055	6.45E-06	0.007973	0.002152	0.069583
ASV6513	0.048664	0.536237	0.010982	0.000444	0.051275	0.057312	0.295087
ASV6569	0.009258	0.492028	0.005493	0.000642	0.007735	0.127464	0.357381
ASV6613	0.000561	0.89859	8.17E-05	0.000672	0.002317	0.000179	0.0976
ASV6622	4.95E-05	0.984012	1.04E-05	0.000168	0.000404	0.000334	0.015021
ASV6649	0.05094	0.012809	0.045941	0.006489	0.074607	0.025166	0.78405
ASV6683	0.000713	0.055634	0.008552	0.000103	0.003174	0.017771	0.914053
ASV6703	0.023539	0.368672	0.001218	0.000376	0.011998	0.007434	0.586764
ASV6773	7.04E-11	0.008983	0.030879	0.000771	0.107007	0.020741	0.83162

ASV6783	0	0.979575	7.72E-06	4.96E-05	0.000521	0.000395	0.019452
ASV6823	0.012612	0	8.47E-06	0.00102	0.067759	0.007584	0.911017
ASV6866	4.55E-15	0.416642	0.003397	5.45E-05	0.080661	0.000576	0.49867
ASV6876	0.014621	0.66125	0.06745	0.000724	0.057022	0.015989	0.182944
ASV6886	0.015128	0.199268	0.015919	0.002136	0.080415	0.004734	0.682399
ASV6895	0.027279	0.186258	0.003716	0.000731	0.0126	0.001397	0.768018
ASV6930	0.018398	0.159665	0.013754	0.00669	0.018797	0.031928	0.750769
ASV6955	1.03E-11	0.0534	0.022418	0.008917	0.056696	0.015825	0.842745
ASV7001	0.006519	0.585992	0.007183	2.44E-07	0.032238	0.009849	0.358219
ASV7037	0.000409	0.926511	0.001886	2.10E-06	0.018138	0.000693	0.052361
ASV7039	0.005501	0.634075	0.01777	1.25E-05	0.004337	0.000174	0.338131
ASV7040	0.001666	0.732845	0.000122	0.000681	0.003325	0.000337	0.261025
ASV7059	0.001655	0.805288	0.00011	9.39E-05	0.001538	0.001925	0.189391
ASV7072	0.011188	0.20683	0.005954	0.000229	0.059075	0.008582	0.708141
ASV7088	0.019667	0.242157	0.004216	0.00013	0.008139	0.005266	0.720426
ASV7123	0	0.577764	0.000386	0.000166	0.000132	0.006059	0.415493
ASV7192	0.012931	0.529759	0.115756	2.25E-05	0.001219	0.005063	0.33525
ASV7271	0.006477	0.551809	0.002321	0.000361	0.017932	0.012285	0.408816
ASV7277	5.77E-12	0.674548	0.000484	1.87E-06	0.004631	0.00593	0.314404
ASV7293	0.011385	0.74197	0.002508	5.82E-05	0.001389	0.018872	0.223818
ASV7301	7.41E-15	0.779972	0.000149	0.000187	0.001682	0.003614	0.214396
ASV7320	6.63E-05	0.428955	0.003191	0.00066	0.00579	0.000292	0.561046
ASV7361	0.006576	0.59881	0.002645	4.72E-05	0.018606	0.032039	0.341277
ASV7368	0.006544	0.469635	0.001397	1.28E-05	0.064786	0.002249	0.455376
ASV7376	5.21E-17	0.079822	0.000429	0.002352	0.029049	2.87E-05	0.888321
ASV7397	0.01006	0.577438	0.000313	0.002	0.047077	0.081504	0.281608
ASV7489	0.001918	0.312796	0.149606	0.011083	0.027397	5.50E-05	0.497146
ASV7506	0.005781	0.302606	0.019172	0.000236	0.12255	0.013923	0.535732
ASV7510	0.003215	0.477252	0.059752	0.000859	0.009191	0.047907	0.401824
ASV7602	0.018586	0.324538	0.002823	2.04E-06	0.048781	0.000971	0.604299
ASV7644	2.42E-13	0.367868	0.00466	0.002858	0.030417	0.008034	0.586163
ASV7658	0.009115	0.520752	0.003339	0.001121	0.041233	0.006764	0.417678
ASV7843	0.016274	0.411141	0.020342	0.003573	0.017756	0.012376	0.518538
ASV7846	0.018902	0.27188	0.021874	0.006223	0.058771	0.036674	0.585676
ASV7904	0.022534	0.398994	0.003254	0.000507	0.064957	0.140902	0.368852
ASV7905	0.011038	0.660754	0.000521	0.000127	0.002536	0.003861	0.321165
ASV7910	0.01397	0.064808	0.008245	0.001487	0.032641	0.002568	0.87628
ASV7961	2.36E-12	0.086095	0.009266	0.006627	0.021219	0.000578	0.876215
ASV7965	0	0.729566	2.98E-05	0.000753	0.003246	0.002365	0.264041
ASV7966	0.001192	0.885798	0.009264	0.000112	0.014904	0.001796	0.086935
ASV7982	5.95E-12	0.701546	0.000159	0.001381	0.000773	0.001788	0.294352

ASV8001	0.009807	0.254557	0.000212	0.000131	0.024097	0.005806	0.70539
ASV8003	0.009123	0.122142	0.001661	0.002346	0.080113	9.98E-05	0.784515
ASV8033	0	0.237233	0.001854	4.98E-05	9.87E-08	0.0481	0.712763
ASV8055	0.001961	0.577054	0.000657	0.001867	0.011906	0.02625	0.380306
ASV8079	0.016849	0.486026	0.035978	0.002188	0.030127	0.000649	0.428182
ASV8091	0.002205	0.297531	0.000488	0.008469	0.041994	0.021228	0.628085
ASV8098	0.029726	0.445189	0.010003	4.69E-05	0.107367	0.007262	0.400406
ASV8126	0.002863	0.29197	0.001189	0.001571	0.009281	0.043531	0.649595
ASV8267	0.019715	0.103962	0.007646	0.000603	0.022152	0.039603	0.806318
ASV8290	0.000138	0.394587	0.000368	0.00511	0.005613	0.001964	0.59222
ASV8293	0.02978	0.030381	0.085472	0.009781	0.081499	0.181838	0.581248
ASV8294	1.54E-13	0.228582	0.016666	0.001421	0.081725	0.025629	0.645976
ASV8314	0.004231	0.822347	0.052218	0.00111	0.000136	0.029544	0.090414
ASV8325	0.007402	0.430557	0.01066	0.00012	0.008608	0.024828	0.517823
ASV8375	0.010851	0.40852	0.000606	0.002739	1.67E-07	0.008219	0.569065
ASV8389	0.0008	0.920401	0.002305	5.42E-05	0.000135	0.001212	0.075092
ASV8391	0	0.964206	9.84E-06	0.000199	0.000229	0.000414	0.034942
ASV8402	0.00638	0.422025	0.007949	0.00184	0.180201	0.038789	0.342816
ASV8450	0.00372	0.450056	0.002757	0.000218	0.044971	5.92E-05	0.498219
ASV8470	0.038654	0.113029	0.016046	0.001113	0.002733	0.01389	0.814535
ASV8486	0.002517	0.807553	0.001077	0.003014	0.001706	0.012682	0.17145
ASV8513	0.004012	0.431436	0.00024	0.000435	0.023758	2.68E-05	0.540092
ASV8518	0.00216	0.770301	0.019758	0.000593	0.00197	2.28E-05	0.205195
ASV8525	4.83E-11	0.035102	0.055178	0.005302	0.022089	0.000599	0.881731
ASV8550	0.004461	0.480956	4.50E-05	1.27E-05	6.14E-05	0.000514	0.51395
ASV8553	0.002215	0.51113	0.000143	2.81E-06	0.000926	0.001265	0.484318
ASV8566	0.036831	0.147865	0.005003	0.004575	0.004434	0.05285	0.748442
ASV8590	0.021537	0.676928	0.003822	0.002535	0.025726	0.008084	0.261368
ASV8751	0.031169	0.541262	0.051045	2.59E-05	0.062483	0.001289	0.312726
ASV8799	0.086671	0.189585	0.01901	0.011348	0.224563	0.003845	0.464979
ASV8834	0.018611	0.644373	0.007007	0.000551	0.027741	0.026473	0.275244
ASV8887	6.74E-12	0.565626	0.001312	1.22E-06	0.013176	0.006223	0.413661
ASV8909	0.009484	0.914634	1.72E-05	0.000275	0.004009	0.001623	0.069958
ASV8929	0.047882	0.28048	0.037977	0.004865	0.115654	0.012594	0.500548
ASV8945	0.002443	0.823314	0.002972	0.000382	0.02372	0.012471	0.134698
ASV8988	0.006467	0.702042	0.000327	7.72E-05	0.00371	0.001993	0.285384
ASV8991	0.007322	0.89543	0.003659	0.000281	0.005774	6.71E-05	0.087466
ASV9019	0.012542	0.414304	0.00071	4.91E-09	0.067976	0.247008	0.25746
ASV9073	0.007744	0.702198	1.96E-05	2.98E-05	0.002161	0.001256	0.286592
ASV9099	6.46E-05	0.58925	0.001643	6.61E-05	0.103069	0.026154	0.279752
ASV9115	0.015846	0.518413	0.002459	6.35E-05	0.024168	0.007373	0.431676

ASV9127	0.00563	0.250768	0.002802	0.000115	0.000843	0.000812	0.739029
ASV9135	0	0.594389	0.00085	0.003223	0.004659	0.035987	0.360892
ASV9143	1.27E-12	0.363287	0.002128	0.00172	0.008217	0.025563	0.599086
ASV9170	0.002695	0.44453	0.019816	0.000189	0.248802	0.00381	0.280158
ASV9188	0.000492	0.946499	0.000127	0.000209	0.002305	5.28E-05	0.050316
ASV9198	0.004944	0.359226	0.000957	0.000653	0.000227	0.00105	0.632943
ASV9221	0.012018	0.328148	0.000326	0.000206	0.006747	0.001183	0.651372
ASV9226	9.15E-18	0.599721	0.003224	0.006119	0.011172	0.000885	0.378878
ASV9228	0.006232	0.303445	0.006171	0.002513	0.026539	0.03106	0.62404
ASV9266	0.024393	0.279811	0.015332	0.000217	0.012679	0.026194	0.641373
ASV9293	8.34E-09	0.417811	0.000219	9.13E-05	0.009566	0.008265	0.564047
ASV9313	0.015062	0.538677	0.08479	0.000366	0.016118	0.012768	0.332219
ASV9334	0.030998	0.125286	0.00725	0.001169	0.006121	0.00959	0.819585
ASV9354	0.011963	0.813811	4.46E-05	0.000185	0.003231	0.004799	0.165967
ASV9368	0.002398	0.561323	0.003961	0.002345	0.028669	0.00201	0.399293
ASV9414	0.000507	0.169836	0.009026	0.002276	0.078251	0.078354	0.66175
ASV9453	0.007785	0.4752	0.003103	5.22E-05	0.113686	0.005241	0.394933
ASV9499	0.007014	0.536985	0.000983	3.72E-05	0.000576	0.001239	0.453166
ASV9509	0	0.578067	0.002563	4.53E-06	0.037063	1.93E-05	0.382283
ASV9557	0.012717	0.208201	0.002177	1.85E-06	0.100107	0.000571	0.676225
ASV9617	0.0361	0.408928	0.001748	0.011695	0.009175	0.004587	0.527766
ASV9806	0.004225	0.087026	0.060797	0.001226	0.112717	0.001312	0.732697
ASV9875	0.000357	0.973363	0.000188	0.000117	0.001812	5.99E-05	0.024103
ASV9904	0.016005	0.121387	0.003556	0.000119	0.00403	0.002813	0.852091
ASV9919	0.001422	0.942671	4.92E-05	2.86E-05	9.49E-05	0.000739	0.054995
ASV9950	0.01446	0.270892	0.092345	0.000578	0.003061	0.001968	0.616696
ASV10004	0.009103	0.757827	0.001497	9.01E-09	0.005487	0.004414	0.221671
ASV10017	0.011876	0.664385	0.103555	0.000331	7.67E-05	0.005083	0.214693
ASV10021	1.25E-08	0.215064	0.02319	0.007738	0.00882	0.045619	0.699569
ASV10067	0	0.867161	0.00231	0.001699	0.036743	0.007459	0.084628
ASV10073	0.0165	0.062843	0.001483	2.69E-05	0.000375	0.052549	0.866222
ASV10123	0.028254	0.022844	0.010605	0.004652	0.004858	0.00863	0.920157
ASV10137	0.039122	0.404091	0.005748	0.002672	0.063463	0.002195	0.482709
ASV10140	0.000757	0.738711	0.000332	0.000112	0.010143	9.87E-07	0.249943
ASV10153	0.009364	0.781143	0.000117	0.002995	0.015926	0.00236	0.188095
ASV10170	0.002847	0.549609	6.51E-05	0.002396	0.042298	0.104851	0.297934
ASV10179	0.024957	0.369216	0.003083	0.00544	0.043903	0.035212	0.518188
ASV10181	0	0.008317	0.001122	0.000774	0.022508	0.013601	0.953677
ASV10192	0.019872	0.436312	0.009346	0.000795	0.021255	0.053583	0.458838
ASV10221	1.12E-16	0.282651	0.00549	5.44E-05	0.267939	0.094556	0.349309
ASV10248	0.035337	0.092348	0.036646	0.000309	0.006247	0.122611	0.706502

ASV10300	0.021086	0.199285	0.014639	0.000904	0.285303	0.000613	0.478171
ASV10374	0.001999	0.786762	5.83E-05	7.63E-05	0.000596	0.000464	0.210044
ASV10402	0.008766	0.425593	0.008805	0.011343	0.063631	0.000645	0.481216
ASV10409	0.020625	0.608905	0.114911	8.02E-05	0.0063	0.005232	0.243947
ASV10461	0.003648	0.130703	0.004852	0.000355	0.122054	0.015215	0.723173
ASV10480	0.006766	0.569351	0.000644	2.56E-05	0.008058	0.017587	0.397568
ASV10502	0.076112	0	0.026525	0.00107	0.034658	0.04099	0.820645
ASV10504	0.011573	0.522425	0.00562	6.49E-05	0.011563	0.004446	0.444308
ASV10521	0.005752	0.38485	0.015744	2.10E-05	0.039971	0.004445	0.549217
ASV10542	0.001042	0.621242	0.000816	0.002356	0.015297	0.000572	0.358674
ASV10559	0.028703	0.77338	0.001545	5.74E-05	0.037801	0.018087	0.140427
ASV10560	0.007713	0.202062	0.009129	0.004635	0.084633	0.024426	0.667403
ASV10562	0.007482	0.747617	0.016425	0.002282	0.003862	0.013295	0.209037
ASV10565	0.001381	0.906197	0.000543	6.88E-05	1.03E-05	0.016635	0.075165
ASV10589	0.000317	0.760542	0.008947	0.000166	0.000239	0.000525	0.229264
ASV10604	0.011288	0.637232	0.001925	0.002975	0.005567	0.000281	0.340732
ASV10625	0.008674	0.186111	0.004677	0.001518	0.067414	0.014955	0.71665
ASV10674	0	0.077819	0.022375	1.55E-06	0.009685	0.000723	0.889396
ASV10683	0.007638	0.214116	0.003482	0.000381	1.83E-06	0.024716	0.749665
ASV10736	0.001511	0.127937	0.001004	0.000512	0.002279	0.00045	0.866307
ASV10747	0.001375	0.631182	0.00033	1.94E-05	0.001424	0.004281	0.361389
ASV10749	0.020371	0.437851	2.36E-05	0.00333	0.000471	0.001463	0.536491
ASV10755	0.042955	0.582902	0.015904	0.009022	0.003781	0.022954	0.322483
ASV10795	7.04E-14	0.79783	0.001075	3.89E-08	0.005133	0.00748	0.188482
ASV10799	0	0.355731	0.001035	0.003617	0.186476	0.05447	0.398671
ASV10878	0.000818	0.827591	0.003534	0.001749	0.024615	0.001261	0.140432
ASV10899	2.46E-19	0.134952	2.98E-05	0.009044	0.073155	0.013491	0.769328
ASV10924	0.008215	0.512581	7.98E-05	1.38E-06	0.005336	0.000714	0.473072
ASV10928	0.005503	0.462342	0.002293	0.002756	0.000396	0.00946	0.51725
ASV10935	3.51E-10	0.403893	3.56E-05	0.004643	0.012275	0.01125	0.567904
ASV11001	0.004486	0.359921	0.008749	0.000589	0.075261	0.001304	0.54969
ASV11035	0.005681	0.639138	0.008732	0.002925	7.20E-05	0.013793	0.329658
ASV11058	0.014415	0.39766	0.000439	1.03E-05	0.010054	0.024536	0.552886
ASV11067	0	0.497662	0.000381	0.001974	5.29E-07	0.000202	0.499781
ASV11090	0.005233	0.084804	0.010455	0.01534	0.025129	0.089618	0.769422
ASV11103	0.092436	0.28017	0.015776	0.020448	0.012082	0.000292	0.578796
ASV11126	0.013757	0.67862	5.92E-05	0.001952	2.30E-06	0.009381	0.296229
ASV11146	9.09E-06	0.952595	0.000153	0.001332	0.004879	0.003934	0.037097
ASV11162	0.043188	0.144573	0.050025	0.001826	0.066513	0.088044	0.605829
ASV11242	0.002374	0.161259	0.01212	0.012162	0.118805	0.000778	0.692502
ASV11258	0.000882	0.439052	0.006835	0.000175	0.021943	0.003977	0.527136

ASV11395	0.007012	0	0.007012	0.00064	0.026174	0.02796	0.931201
ASV11472	0.000154	0.97278	5.71E-06	0.000328	0.000167	0.000334	0.026232
ASV11509	0.002026	0.52122	0.007864	1.53E-05	0.037972	0.000154	0.430748
ASV11546	0.029546	0.438393	0.003535	0.000519	0.002461	0.004512	0.521035
ASV11577	0.031221	0.540633	0.000137	0.000114	0.003713	0.0081	0.41608
ASV11594	0.008749	0.497525	0.010183	0.00675	0.043885	0.002849	0.43006
ASV11614	0.018228	0.303871	0.003394	0.006869	0.000125	0.015056	0.652457
ASV11665	0.004855	0.365184	0.006535	0.004027	0.136465	0.001137	0.481797
ASV11716	0.014971	0.528166	0.001923	0.007048	0.019596	0.003122	0.425174
ASV11731	0.002448	0.112297	0.002682	0.005263	0.030085	0.030928	0.816297
ASV11739	0.001913	0.54841	0.002343	0.00025	0.039995	0.0025	0.404589
ASV11744	0.00379	0.36034	0.000199	0.000774	0.033445	0.028035	0.573417
ASV11752	0	0.034639	0.000243	0.00341	0.04669	0.00571	0.909307
ASV11763	0.017379	0.321262	0.001247	0.004376	0.029966	0.000204	0.625565
ASV11824	0.001577	0.672327	0.002087	0.000572	0.01759	0.004114	0.301733
ASV11848	0.053732	0.069532	0.026911	0.016606	3.02E-08	0.019878	0.813341
ASV11890	0.026132	0.435628	0.311472	0.004838	0.000497	0.001503	0.21993
ASV11958	0.001771	0.725594	0.00129	0.001388	0.004642	0.005922	0.259392
ASV11975	0.001833	0.409415	0.000486	4.34E-08	0.004399	0.000255	0.583612
ASV11984	0.001003	0.533191	0.001082	0.000102	0.038084	0.001276	0.425263
ASV12012	0.138927	0.420144	0.038904	0.003092	0.005501	0.016766	0.376665
ASV12022	0.002616	0.124577	0.049459	0.000383	0.021583	0.000459	0.800923
ASV12034	0.000142	0.978087	9.01E-06	0.000461	0.000129	9.40E-05	0.021078
ASV12053	0.003526	0.352304	0.007921	0.000995	0.080698	0.001391	0.553166
ASV12072	0.014722	5.03E-15	0.00543	0.001165	0.053691	0.0273	0.897691
ASV12177	0.02814	0.209693	0.004086	5.02E-07	0.131056	0.105784	0.521241
ASV12199	0.014434	0.190561	0.005767	0.002818	0.02324	0.029402	0.733779
ASV12232	0.004718	0.154306	0.010877	0.000468	0.049415	0.006708	0.773508
ASV12251	0.004566	0.381705	0.001898	0.000121	0.012486	0.009937	0.589287
ASV12301	1.16E-16	0.484368	0.00069	0.001072	0.001097	0.000832	0.51194
ASV12316	0.033186	0.167116	0.000542	1.56E-05	0.003988	0.007417	0.787735
ASV12330	0.002483	0.292886	0.000338	0.000187	0.00534	0.004444	0.694322
ASV12349	0.000345	0.912412	0.000479	0.002876	0.006733	0.01278	0.064375
ASV12403	0.019875	0.465276	0.012505	0.001824	0.073885	0.002447	0.424188
ASV12441	0	0.417285	0.000124	3.86E-05	0.003681	0.00109	0.577782
ASV12477	0.004211	0.075917	0.001932	0.000676	0.001413	0.029087	0.886764
ASV12496	6.73E-16	0.657438	0.000388	0.000565	0.010669	0.013059	0.317882
ASV12498	7.20E-05	0.921615	0.000241	0.000144	0.007151	0.005316	0.065461
ASV12524	0	0.697815	4.63E-05	0.001474	0.002252	0.002776	0.295637
ASV12560	0.077402	0.409006	0.010839	0.000535	0.023823	0.022911	0.455485
ASV12613	0.027666	0.390188	0.383457	0.001425	0.021703	5.78E-06	0.175556

ASV12647	0.006243	0.63622	0.0011	0.001047	0.002412	0.025074	0.327906
ASV12683	0.00149	0.312722	0.000302	8.65E-06	0.001981	0.000896	0.6826
ASV12711	0.01128	0.436522	0.130101	2.85E-05	0.014959	0.03195	0.37516

APPENDIX C

ADDITIONAL FIGURES AND TABLES FOR CHAPTER FOUR

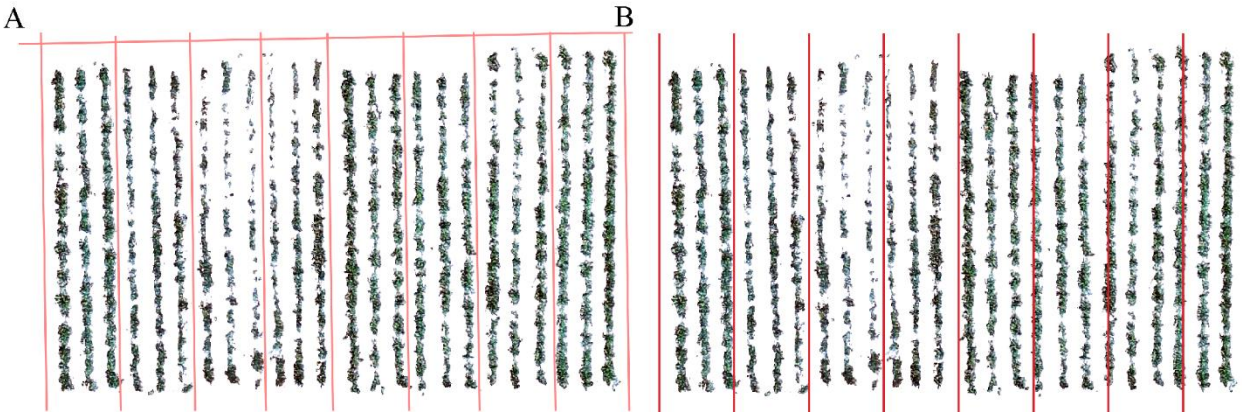

Figure A4.1: Example of how automated plot layouts can cause frameshift. (A) The correctly designated plots account for varying plot spacing to maintain accurate delineation. (B) Automated plot boundaries based on a single plot size and spacing metric lose accuracy across plots.

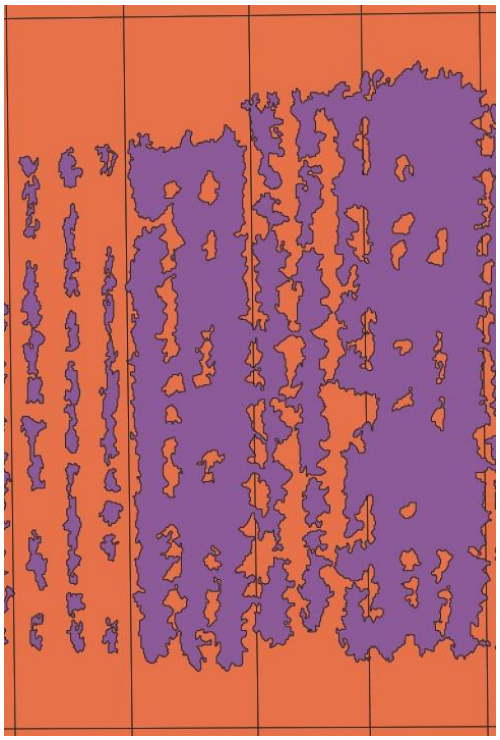

Figure A4.2: Example of testing canopy cover to delineate plots from plants 90 DAP. The red background polygons represent semi-automated plot boundaries for reference, while the purple polygons define plots based on connected canopy cover. Low density plots like the left-most are designated as many plots in one as there is significant space between plants. Due to no plot boundaries, dense plots are unable to delineate between plants of different plots, leading to multiple plots being defined as one, as seen on the two right-most plots.

Table A4.1: Basic sensor and flight metrics.

Image dimensions	5472 x 3648 pixels
Sensor Dimensions	1 inch
Focal Length	28 millimeters
Flight Altitude	30 meters

Table A4.2. Pearson correlation between indices and plant traits at each flight, days after planting.

Index DAP	Heading Date	Maturity Date	Grain Fill	Plant Height	Yield
	Pearson correlation coefficient				
EGI 51	-0.0851	-0.2759	-0.1171	0.1662	0.2137
VARI 51	0.0279	-0.1733	-0.1365	0.2125	0.3985
NExG 51	-0.0540	-0.2959	-0.1544	0.1835	0.3246
RGBVI 51	-0.0733	-0.3093	-0.1484	0.1619	0.2899
GLI 51	-0.0542	-0.2947	-0.1535	0.1823	0.3246
EGI 56	-0.0348	-0.1653	-0.0827	0.1521	0.2230
VARI 56	0.1050	-0.1432	-0.1762	0.2663	0.4059
NExG 56	0.0585	-0.2542	-0.2139	0.2369	0.3250
RGBVI 56	0.0477	-0.2650	-0.2126	0.2195	0.2999
GLI 56	0.0586	-0.2528	-0.2129	0.2355	0.3252
EGI 66	0.1283	-0.0759	-0.1497	0.2697	0.2922
VARI 66	0.3164	-0.0781	-0.2966	0.4031	0.5257
NExG 66	0.2115	-0.1553	-0.2666	0.3356	0.4244
RGBVI 66	0.1901	-0.1609	-0.2538	0.3173	0.3995
GLI 66	0.2120	-0.1546	-0.2665	0.3359	0.4251
EGI 77	0.2400	0.0253	-0.1723	0.3585	0.2656
VARI 77	0.3863	0.2093	-0.1665	0.2081	0.2547
NExG 77	0.2451	0.0859	-0.1365	0.1231	0.1839
RGBVI 77	0.2276	0.0746	-0.1301	0.1115	0.1745
GLI 77	0.2458	0.0869	-0.1363	0.1228	0.1848
EGI 80	0.1693	0.1330	-0.0428	0.0252	0.1279
VARI 80	0.4228	0.3786	-0.0760	0.0262	0.1879
NExG 80	0.2334	0.2961	0.0157	-0.1337	0.1269
RGBVI 80	0.1939	0.2704	0.0293	-0.1462	0.1104
GLI 80	0.2327	0.2968	0.0168	-0.1329	0.1268
EGI 84	0.4456	0.0359	-0.3210	0.2469	0.3505
VARI 84	0.5158	0.3019	-0.1989	0.3483	0.4003
NExG 84	0.4307	0.1856	-0.2102	0.2302	0.3496
RGBVI 84	0.4031	0.1614	-0.2048	0.2047	0.3304
GLI 84	0.4322	0.1878	-0.2099	0.2310	0.3510
EGI 86	0.3049	-0.1897	-0.3617	0.1774	0.0285
VARI 86	0.6062	0.1273	-0.3846	0.3549	0.2732
NExG 86	0.4825	0.0617	-0.3325	0.2424	0.2010

RGBVI 86	0.4748	0.0591	-0.3282	0.2371	0.1992
GLI 86	0.4841	0.0628	-0.3329	0.2435	0.2033
EGI 90	0.5019	0.1020	-0.3207	0.3403	0.2942
VARI 90	0.5673	0.3317	-0.2190	0.3492	0.3772
NExG 90	0.4864	0.3943	-0.1149	0.2251	0.3409
RGBVI 90	0.4589	0.4054	-0.0862	0.1930	0.3296
GLI 90	0.4873	0.3975	-0.1135	0.2251	0.3428
EGI 92	0.4996	0.3002	-0.1875	0.3267	0.3684
VARI 92	0.5168	0.4133	-0.1258	0.3409	0.3932
NExG 92	0.4876	0.4851	-0.0556	0.2158	0.3708
RGBVI 92	0.4716	0.4990	-0.0340	0.1850	0.3641
GLI 92	0.4881	0.4876	-0.0543	0.2174	0.3732
EGI 101	0.1445	0.7365	0.3766	-0.1089	0.3236
VARI 101	0.1132	0.5499	0.2771	-0.0293	0.2268
NExG 101	0.1156	0.7328	0.3965	-0.0970	0.3081
RGBVI 101	0.1052	0.7218	0.3973	-0.1035	0.3009
GLI 101	0.1157	0.7333	0.3968	-0.0967	0.3089
EGI 104	0.0626	0.5404	0.3100	0.0691	0.3356
VARI 104	0.0640	0.3409	0.1765	0.0582	0.2002
NExG 104	0.0569	0.5394	0.3137	0.0631	0.3107
RGBVI 104	0.0433	0.5423	0.3261	0.0545	0.3080
GLI 104	0.0573	0.5398	0.3136	0.0627	0.3111